LAMINAR HEAT TRANSFER IN NON-NEWTONIAN PLANE POISEUILLE-COUETTE FLOW

June, 2003

Graduate School of Science and Technology
Nagasaki University

Ganbat Davaa

Contents

Nomenclature iv

1 INTRODUCTION **1**

1.1 Research Background 1

1.2 Poiseuille-Couette Flow 3

1.3 Research Coverage 4

1.3.1 Objective 4

1.3.2 Scope 5

1.4 Research Applications 7

1.5 Outline of the Dissertation 9

2 LITERATURE SURVEY **12**

2.1 Heat Transfer Related to Moving Boundary 12

2.1.1 Viscous Dissipation 13

2.1.2 Thermal Entrance Region 14

2.1.3 Thermally Fully Developed Region 16

2.2 Effects of Viscous Dissipation and Axial Heat Conduction 16

2.2.1 Newtonian Fluids 16

2.2.2 Non-Newtonian Fluids 17

2.3 Viscous Dissipation Effect 19

2.3.1 Newtonian Fluids 19

2.3.2 Non-Newtonian Fluids 19

2.4 Axial Heat Conduction Effect 20

2.4.1 Newtonian Fluids 20

2.4.2 Non-Newtonian Fluids 22

3 POISEUILLE-COUETTE FLOW **23**

3.1 Fluid Behaviors 23

3.2 Problem Description 26

3.3 Newtonian Fluid Flow 27
3.4 Non-Newtonian Fluid Flow 29
3.4.1 Power-Law Model 29
3.4.2 Modified Power-Law Model 38
3.5 Summary 44

4 THERMALLY DEVELOPING POISEUILLE-COUETTE FLOW 45
4.1 Problem Formulation 45
4.2 Solution Method 52
4.2.1 Additional Condition 52
4.2.2 Infinite Domain and Mesh System 54
4.3 Effects of Viscous Dissipation and Axial Heat Conduction 58
4.3.1 (T) Thermal Boundary Condition 59
4.3.2 The First Kind Thermal Boundary Condition 65
(a) The Case of Moving Plate Heated 65
(b) The Case of Stationary Plate Heated 74
4.3.3 The Second Kind Thermal Boundary Condition 78
(a) The Case of Moving Plate Heated 78
(b) The Case of Stationary Plate Heated 86
4.4 Effect of Viscous Dissipation for $Pe \to \infty$ 88
4.4.1 The First Kind Thermal Boundary Condition 88
(a) The Case of Moving Plate Heated 88
(b) The Case of Stationary Plate Heated 94
4.4.2 The Second Kind Thermal Boundary Condition 97
(a) The Case of Moving Plate Heated 97
(b) The Case of Stationary Plate Heated 103
4.5 Effect of Axial Heat Conduction for $Br = 0$ 104
4.5.1 The First Kind Thermal Boundary Condition 105
(a) The Case of Moving Plate Heated 105
(b) The Case of Stationary Plate Heated 110
4.5.2 The Second Kind Thermal Boundary Condition 112
(a) The Case of Moving Plate Heated 112
(b) The Case of Stationary Plate Heated 117
4.6 Effects of Thermal Boundary Conditions 119
4.7 Summary 130

5 THERMALLY DEVELOPED POISEUILLE-COUETTE FLOW 133

5.1 Newtonian Fluid 133

5.2 Non-Newtonian Fluid 138

5.2.1 Power-Law Model 138

5.2.2 Modified Power-Law Model 141

5.3 Summary 148

6 CONCLUSIONS 150

ACKNOWLEDGEMENT 153

APPENDICES 155

A. Tables 155

A.1 Comparisons with the Available Data 155

A.2 Numerical Values of Nusselt Numbers 157

B. Analytical Results 161

B.1 Heat Transfer of Newtonian Fluids (The second kind thermal boundary condition) 161

B.2 Heat Transfer of Power-Law Fluids (The second kind thermal boundary condition) 162

BIBLIOGRAPHY 166

NOMENCLATURE

A	: area normal to the flow direction	[m^2]
Br	: Brinkman number	
C	: integration constant, Eqs.(3.41) and (3.52)	
c_{p}	: specific heat at constant pressure	[kJ/(kg·K)]
D_{h}	: hydraulic diameter $\equiv 2L$	[m]
D_{j1}	: coefficients, Eq.(B.11) or Eq.(B.18)	
D_{j2}	: coefficients, Eq.(B.12) or Eq.(B.19)	
E	: constant of the axial transformation, Eq.(4.35)	
f	: friction factor	
F	: dimensionless parameter, Eq.(3.14)	
h	: heat transfer coefficient	[W/(m^2 ·K)]
k	: thermal conductivity	[W/(m·K)]
L	: channel width	[m]
L_{max}	: location of the maximum velocity	[m]
L^*_{max}	: dimensionless location of the maximum velocity	
m	: consistency index	[N · s^n/m^2]
n	: flow index	
Nu	: Nusselt number	
P	: pressure	[Pa]
Pe	: Peclet number $\equiv RePr$, or $\equiv Re_{\mathrm{M}}Pr_{\mathrm{M}}$	
Pr	: Prandtl number $\equiv c_{\mathrm{p}}\mu/k$	
Pr_{M}	: modified Prandtl number $\equiv c_{\mathrm{p}}\eta/k$	
q	: wall heat flux	[W/m^2]
Re	: Reynolds number $\equiv \rho u_{\mathrm{m}} D_{\mathrm{h}}/\nu$	
Re^*	: generalized Reynolds number $\equiv \rho u_{\mathrm{m}}^{2-n} D_{\mathrm{h}}^n/m$	
Re_{M}	: modified Reynolds number $\equiv \rho u_{\mathrm{m}} D_{\mathrm{h}}/\eta$	
S_{j1}	: coefficients, Eq.(B.9) or Eq.(B.16)	
S_{j2}	: coefficients, Eq.(B.10) or Eq.(B.17)	
T	: temperature	[K]
u	: axial velocity of the flow	[m/s]
u_{m}	: average velocity of the flow	[m/s]

u^*	: dimensionless velocity $\equiv u/u_{\mathrm{m}}$	
U	: axial velocity of the moving boundary	[m/s]
U^*	: dimensionless relative velocity of the moving boundary $\equiv U/u_{\mathrm{m}}$	
V	: dimensionless parameter, Eq.(4.32) or Eq.(5.32)	
y	: coordinate normal to the plate	[m]
y^*	: dimensionless coordinate $\equiv y/D_{\mathrm{h}}$	
z	: axial coordinate	[m]
z^*	: dimensionless axial coordinate $= z/(PeD_{\mathrm{h}})$	
z_t^*	: transformed axial coordinate	

Greek symbols

β	: dimensionless shear rate parameter	
η	: reference viscosity based on D_{h}	[N·s/m^2]
η_a	: apparent viscosity	[N·s/m^2]
η_a^*	: dimensionless apparent viscosity $\equiv \eta_a/\eta$	
η_0	: viscosity at zero shear rate	[N·s/m^2]
μ	: dynamic viscosity	[N·s/m^2]
ν	: kinematic viscosity $\equiv \mu/\rho$	[m^2 / s]
ρ	: density	[kg/m^3]
τ	: shear stress	[Pa]
θ	: dimensionless temperature	

Subscripts

b	: bulk
e	: entrance or inlet
fd	: fully developed
j	: j = L for Case A, $j = 0$ for Case B
L	: lower plate
0	: upper plate
w	: wall

Abbreviation words

B.C.	boundary condition
N	Newtonian
nN	non-Newtonian
MPL	modified power-law
PL	power-law
T.B.C.	thermal boundary condition
Ⓣ T.B.C.	constant temperatures at the walls

Chapter 1

INTRODUCTION

1.1 Research Background

The present research obtains the results leading to a better understanding of the basic heat transfer processes associated with a continuously moving boundary and providing insights into process in the systems related to manufacturing applications. Problems of fluid flow and heat transfer involving a moving boundary of solid body or liquid in a passage can be found in many manufacturing processes. The heat transfer results for plane Poiseuille-Couette flow, which will be particularized later in Section 1.2, are of considerable practical and theoretical importance as the parallel plates channel is one of the basic channel configurations.

The present fundamental study is concerned with heat transfer for laminar plane Poiseuille-Couette flow of non-Newtonian fluids and it is part of a continuing study on the fluid flow and heat transfer in annuli with axially moving cores [1] - [5]. In the below, the review of the papers [1] - [5] is given.

In the previous studies [1] - [2] the problem of fully developed turbulent flow and heat transfer in concentric annuli with moving cores were treated. The velocity profiles and temperature distributions in annuli with cores moving at various velocities were predicted for the conditions of (a) a constant heat flux at the inner core with the outer wall insulated, (b) outer wall heated with the inner core insulated and (c) both of the walls heated at any heat flux ratio. The study showed that for equal conditions, increasing the relative velocity of the core causes a decrease in friction factor and an increase in Nusselt number. Also it was observed that the relative velocity effect diminishes with a decreasing value of the radius ratio. This diminishing effect in the relative velocity was more pronounced for the case of the

outer wall heated and the inner core insulated.

In [3] an analytical investigation of a fully developed laminar fluid flow and heat transfer in concentric annuli with moving cores has been carried out for two cases of (a) the inner wall heated with the outer wall insulated and (b) the outer wall heated with the inner wall insulated. The assumptions made in this reference were concentric annulus, smooth wall surfaces, incompressible flow and negligible viscous dissipation. It was shown that for equal conditions, increasing the relative velocity results in (1) a decrease in friction factor, (2) an increase in Nusselt number for the inner wall heated case and (3) a decrease in Nusselt number for the outer wall heated case.

Laminar heat transfer in the thermal entrance regions of concentric annuli with moving heated cores was analytically studied in [4] for four kinds of the thermal boundary conditions. The assumptions made in this reference were steady and hydrodynamically fully developed flow, constant physical properties and negligible effects of viscous dissipation and fluid axial heat conduction. It was observed that for equal conditions, increasing relative velocity results in (1) an increase in Nusselt numbers at the inner core while Nusselt numbers at the outer tube decrease for all cases and (2) an increase in the value of the thermal entrance length, $X_{th,d}$, with a maximum at a given relative velocity of the core, $U^* > 0$. The maximum value of $X_{th,d}$ increases with increasing values of $U^* > 0$ for smaller values of radius ratio.

In a recent paper [5], fully developed laminar forced convection in an eccentric annulus with a moving core has been analyzed under the assumptions of negligible viscous dissipation and fluid axial heat conduction.

As discussed in the previous works related to the forced convection in annuli with axially moving cores, the effects of the relative velocity of the core cylinder and the radius ratio on the heat transfer have been studied. In general, in these previous analyses the following assumptions and conditions were used.

- Newtonian fluids with constant physical properties.
- Hydrodynamically fully developed flow in annuli with axially moving cores.
- Negligible viscous dissipation.
- Negligible fluid axial heat conduction.

1.2 Poiseuille-Couette Flow

Poiseuille-Couette flows exhibit semi-parabolic velocity profiles. When the fluid film is sheared by a moving boundary in addition to pressure forces, a semi-parabolic velocity profiles are established. The limiting cases of such profiles are parabolic velocity profile and linear velocity profile. The parabolic velocity profiles are referred as Poiseuille flow and this type of flow is due to a pressure gradient. On the other hand the linear velocity profiles correspond to the flow due to a relative motion of one of the surfaces and such flow is called a Couette flow. Poiseuille-Couette flow is a flow that both Poiseuille flow and Couette flow are superimposed. In Fig.1-1, the velocity profiles of these flows are shown.

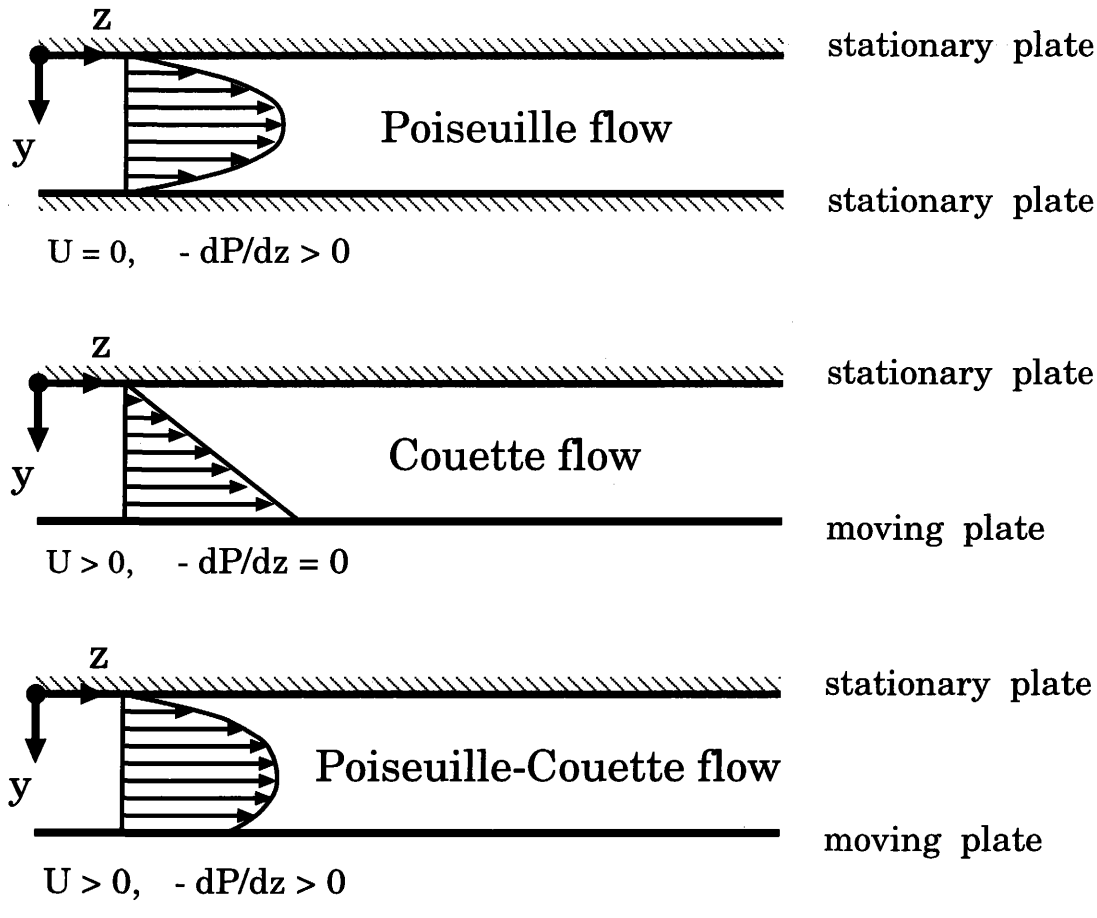

Fig.1-1 Velocity profiles

1.3 Research Coverage

1.3.1 Objective

The present research extends the works [1] - [5] described in Section 1.1 to plane Poiseuille-Couette flow of non-Newtonian fluids and treats the heat transfer problem associated with moving boundary in a view of removing the assumptions of negligible viscous dissipation and fluid axial heat conduction.

To the author's knowledge, the analyses of fluid flow and heat transfer with moving boundary that considered the effects of both viscous dissipation and fluid axial heat conduction are not available in the open literature. The intention of the present work is to provide a comprehensive treatment of the laminar heat transfer problem associated with moving boundary and to clarify the effects of viscous dissipation and fluid axial heat conduction. The research objectives can be summarized as below.

1. Obtaining accurate velocity distribution for plane Poiseuille-Couette flow of non-Newtonian fluids.

2. Investigation of the effects of viscous dissipation on the heat transfer for plane Poiseuille-Couette flow of non-Newtonian fluids.

3. Investigation of the effects of axial heat conduction on the heat transfer for plane Poiseuille-Couette flow of non-Newtonian fluids.

Objective 1 is to predict the velocity field for plane Poiseuille-Couette flow of non-Newtonian fluids accurately. As already stated, a literature survey revealed that there is no information for plane Poiseuille-Couette flow of non-Newtonian fluids. The fluid considered in the previous works [1] - [5] was a Newtonian fluid with constant physical properties. In the present research dealing with the heat transfer associated with a moving boundary, non-Newtonian fluids of viscosity changing with shear rate are under consideration. In general, the areas of application of non-Newtonian fluids are wide and non-Newtonian fluid behaviors are encountered in almost all the chemical and allied processing industries. Non-Newtonian flow and rheology are interdisciplinary in their nature and the factors which determine the rheological characteristics are highly complex [6]. The modified power-law model, MPL, is chosen to describe the shear stress-shear rate relationship of the non-Newtonian fluids, as this model has an advantage providing accurate solutions even for lower shear rates including zero [7] and it will be discussed in more detail in Sections 3.1 and 3.4.2.

Objectives 2 and 3 are to study the heat transfer for plane Poiseulle-Couette flow of non-Newtonian fluids in a view of removing the assumptions made in the previous works [1] - [5], which are negligible viscous dissipation and fluid axial heat conduction. Giving a special emphasis to the effects of viscous dissipation and fluid axial heat conduction leads to gain insights into the heat transfer involving moving boundaries and yields new solution data for the related heat transfer problems. The special attention is given to the heat generation due to viscous dissipation because the moving wall deforms the fluid velocity profile near the wall region, resulting changes in the velocity gradient there. Thus, viscous dissipation may not be neglected in heat transfer involving moving boundaries and it is necessary to verify the viscous dissipation effects. As stated above, one of the major objectives of this research has been to determine the effect of axial heat conduction within the flow on heat transfer for plane Poiseuille-Couette flow. There is no information on fluid axial heat conduction effects on heat transfer involved moving boundaries.

1.3.2 Scope

In the present research, the problem related to the forced convection in plane Poiseuille-Couette flow of non-Newtonian fluids has been investigated further including the effects of viscous dissipation and fluid axial heat conduction. The considered flow field is assumed to be steady, laminar and hydrodynamically fully developed and the physical properties are constant except viscosity.

The governing parameters for the problem are found to be in

- the dimensionless relative velocity of the moving plate, U^*, which is the ratio of the moving plate velocity to the average velocity of the fluid
- the rheological parameters such as the flow index, n, and the dimensionless shear rate parameter, β
- the Brinkman number, Br, which represents the ratio of overall dissipation to heat conduction from the wall and
- the Peclet number, Pe, which characterizes the ratio of heat convection to heat conduction.

Figure 1-2 illustrates the details of the coverage of the present work. The heat transfer for the plane Poiseuille-Couette flow has been studied in both thermally

developing and fully developed regions. The threefold objectives of the present research have been achieved by studying the heat transfer in the thermal entrance region. However, the heat transfer in the fully developed region was also studied. Because the study for the effects of viscous dissipation on the heat transfer associated with a moving boundary brings forth some interesting results for the second kind of thermal boundary condition, T.B.C. 2, in the thermally fully developed region. The analytical method was applicable for the study on heat transfer to Newtonian

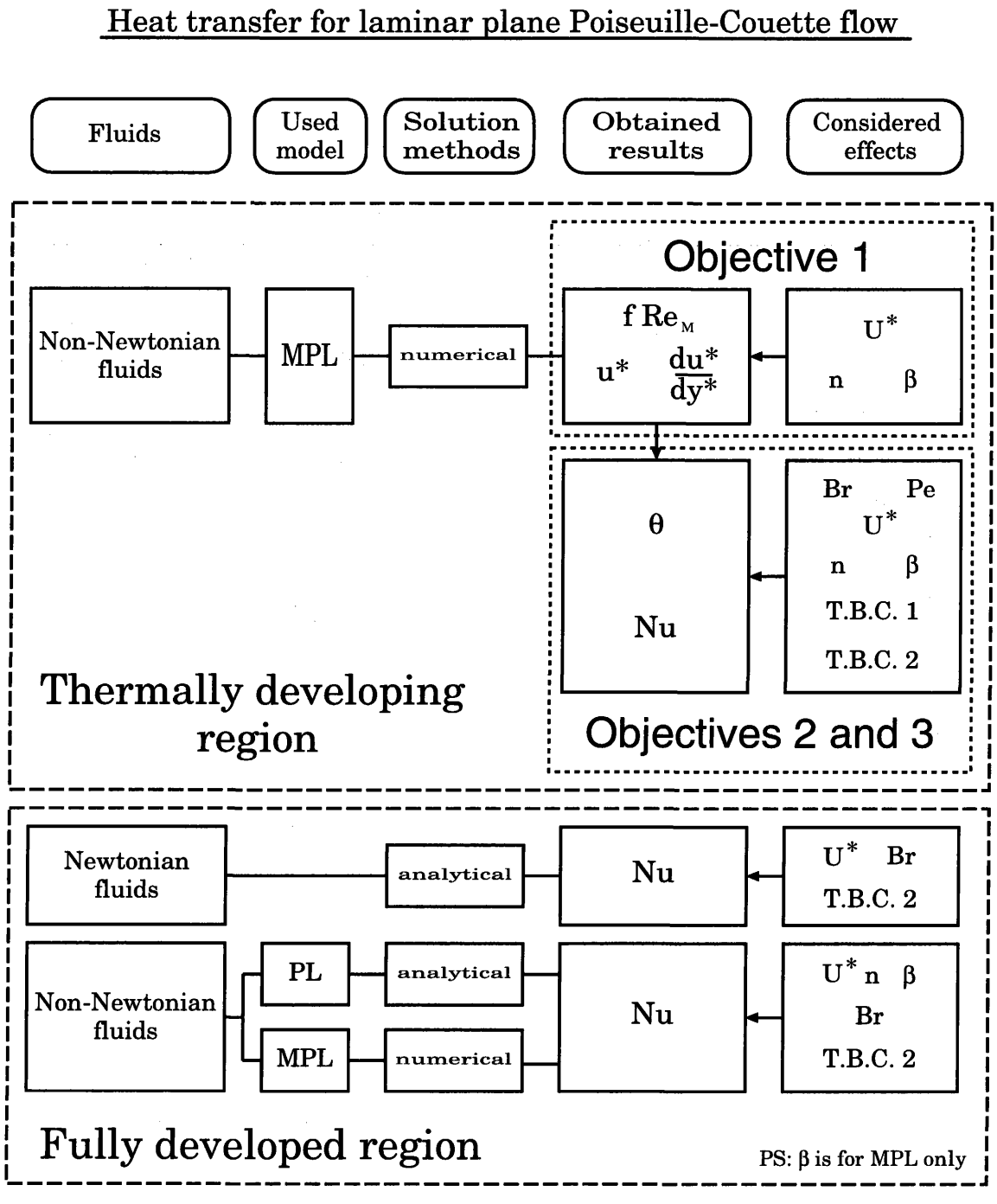

Fig.1-2 Details and coverage of the research

and power-law fluids in the fully developed region. The results of the heat transfer for Newtonian and non-Newtonian fluids in the fully developed region were also useful for checking the corresponding solutions obtained by studying the heat transfer in thermally developing region.

Having achieved Objective 1, the effects of the moving plate velocity, U^*, rheological parameters such as flow index, n, and dimensionless shear rate parameter, β, on friction factor in terms of fRe_{M}, velocity distribution, u^*, and velocity gradient, du^*/dy^*, were studied. With an aim of obtaining the accurate velocity field the modified power law (MPL) model was employed. As a result of achievement of Objective 1, it became possible to pay attention to the heat transfer.

The overall focus of Objectives 2 and 3 are to obtain quantitative information about the heat transfer for the plane Poiseuille-Couette flow of non-Newtonian fluids with the emphasis to the effects of viscous dissipation in terms of Brinkman number and fluid axial heat conduction in terms of Peclet number for the different thermal boundary conditions. Since the flow involves the moving boundary, the effects of the moving plate velocity, U^*, was considered. Also as the fluid is non-Newtonian, the effects of rheological parameters such as, n and β, are considered.

1.4 Research Applications

The areas of the application of the research are broad and diverse because the study is fundamental. In considering the applicability of the research work, it is hoped that the obtained results of the research is not only be of fundamental interest, but also will advance the qualitative understanding of the aspects of heat transfer in industrial processes and also will provide appropriate design parameters of the systems related to manufacturing applications. The fluid flow and heat transfer for the plane Poiseuille-Couette flow of non-Newtonian fluids represent an idealization of many industrial processes and various engineering situations.

There exist many industrial processes involving fluid flow and heat transfer with a moving boundary of solid body or liquid. In such processes, continuous surfaces move steadily through either a quiescent or a moving ambient environment and examples include

- continuous casting
- hot rolling

- extrusion of metals, plastic sheets or food materials
- drawing of wire and glass fiber
- wire and tube coating
- metal forming
- crystal growing
- cooling of an infinite metallic plate in a cooling bath
- the boundary layer along material handling conveyers
- the boundary layer along a liquid film in condensation processes, etc.

The speed at which the heated surface moves in these manufacturing processes can be as low as a few centimeters per hour as in the case of the Czochralski crystal growth process, or as high as a few meters per second as in the case of hot rolling or drawing [8]. In these manufacturing processes a very commonly encountered circumstance is that a moving boundary continuously exchanges heat with the surrounding environment. For such cases, the fluid involved may be Newtonian or non-Newtonian and the flow situations encountered can be either laminar or turbulent.

In most of the listed manufacturing processes such as hot rolling, plastic extrusion, metal forming, glass fiber drawing and contiguous casting [9], the moving boundary induces a flow in the otherwise quiescent ambient medium and thus loses energy to the fluid. When the moving boundary emerges from the die or the rollers, it is at a temperature higher than that of the surroundings and in many practical circumstances, the extruded material passes through a cooling bath or trough. For example, in wire coating process, the metal wire is coated with a plastic sheath from an extruder and then the insulated wire passes through a cooling system. The cooling troughs are nowadays of the order of 30 m [10]. As one of the research application, it is possible to save space and to ensure the uniform thermal stress along the wire by establishing a passage as a cooling through with steadily moving ambient fluids. Since the present research is concerned with the forced convection, it produces the results applicable for the configuration of the engineering applications with the ambient fluid is steadily in motion.

In the present research, the surrounding environment is a non-Newtonian fluid and the flow situation is laminar. Many important industrial fluids are non-Newtonian

in the flow characteristics. Indeed non-Newtonian fluid behavior is encountered in almost all the chemical and allied processing industries [6]. In a broad variety of chemical and industrial processes, non-Newtonian fluids have to be heated or cooled and examples related with the heat transfer characteristics or non-Newtonian fluid flows appear very common in heat exchangers.

In most practical problems, interest lies mainly in the heat transfer rate on the surface, because it affects the thermal stresses and quality of the product and the control of the heat rate is very important in obtaining a desired structure. For the configuration, it is important to know how much the heat transfer rate is influenced by viscous dissipation of the flowing fluid and by axial heat conduction within the fluid, how one can change the temperature field through geometry and, through the thermal boundary conditions and moving wall velocity. For a thorough understanding of the heat transfer characteristics, temperature solutions obtained including the viscous dissipation and the fluid axial heat conduction are important and as a result of the present study the new solution data have been obtained for the heat transfer associated with a surface movement.

1.5 Outline of the Dissertation

Chapter 1 describes the background of the research, it specifies the objectives and scope of the research and it sets out the parameters of the theoretical problem, and it identifies the areas in engineering in which the solutions to the problem can be applied. The present research is part of a continuing study on the fluid flow and heat transfer in annuli with axially moving cores. The aim of the research is to provide a theoretical framework for a quantitative analysis of heat transfer for the plane Poiseuille-Couette flow of non-Newtonian fluids including the effects of viscous dissipation and fluid axial heat conduction and the present research objectives are threefold. The present research will advance the quantitative understanding of the aspects of heat transfer associated with the movement of a surface.

Chapter 2 reviews the relevant studies of the heat transfer associated with moving boundary and also those considered the effects of viscous dissipation and fluid axial heat conduction. The papers reviewed in this chapter are restricted to those which are particularly relevant to the present work for one of the following three reasons. The first reason is that they (the papers reviewed) consider heat transfer associated with moving boundaries. The second and third reasons are that they

consider the viscous dissipation effect and the fluid axial heat conduction effect, respectively. The cited papers are classified by the involved fluids whether Newtonian or non-Newtonian and by the considered regions of the thermally developing or fully developed. The literature survey reveals that data on heat transfer corresponding to the situations encountered in the present research are apparently not available.

In Chapter 3, the general behaviors of fluids have been reviewed and the coverage of the fluid flow study is outlined. In this chapter, Objective 1 has been achieved as the accurate velocity field of the plane Poiseuille-Couette flow of non-Newtonian fluids was obtained by employing the modified power-law model. The inclusion of the Newtonian and power-law fluids in the study intends to provide the data for exact solutions of the problem and the analytical method has been employed for all applicable situations. The exact solutions are given for the Newtonian and power-law fluids in Sections 3.3 and 3.4.1. With the valid exact solutions in hand, different numerical solutions for the modified power-law fluids were validated since the modified power-law model covers the behavior of Newtonian fluid at low shear rate and it tends to a power-law functionality at high shear rate. Thus in this chapter, the analyses for the hydrodynamically fully developed steady laminar flow of the Newtonian, power-law and modified power-law fluids in the plane Poiseuille-Couette flow are discussed.

The two chapters that follow are devoted to the heat transfer analyses. Chapter 4 presents analyses of the laminar heat transfer for the plane Poiseuille-Couette flow in the thermally developing region. In this chapter Objectives 2 and 3 have been achieved as the effects of viscous dissipation and fluid axial heat conduction on the heat transfer for plane Poiseuille-Couette flow were clarified. The study on the effect of fluid axial heat conduction is directed to solve an elliptic type differential equation. A numerical method to solve the governing elliptic type energy equation is proposed in this chapter. The results demonstrating the effects of viscous dissipation and fluid heat conduction are presented for three sets of thermal boundary conditions. The Ⓣ thermal boundary condition (constant, uniform, and equal temperatures on both walls) was examined first in order to do comparison of the results with the available data sets and to give explanation for this simple case. As the feasible conditions at the walls, the first kind (constant, uniform but different temperatures at the walls) and second kind (one wall insulated with the other heated constantly) thermal boundary conditions are examined for two cases at each wall. The results for the typical situations are compared with the available data by the previous

researchers in order to demonstrate that the consistent results were produced in this work.

Chapter 5 presents the thermally fully developed plane Poiseuille-Couette flow of Newtonian and non-Newtonian fluids with an emphasis on the effects of viscous dissipation. This chapter is designated for the explanation of the results in the thermally fully developed region for a wide range of values of the moving wall velocity. Also the results obtained in this chapter were used to check the corresponding results from the previous chapter. The exact solutions were obtained for the Newtonian and power-law fluids. For the modified power-law fluids, a numerical calculation was carried out.

Chapter 2

LITERATURE SURVEY

The present research is motivated by the fact that few studies have been performed to determine the heat transfer characteristics in Poiseuille-Couette flow inside ducts. For laminar internal flows an extensive literature review is given by Shah and London [11] and by Kakac et al. [7]. As a result of the author's careful literature survey for the papers concerned heat transfer associated with moving boundaries and the effects of viscous dissipation and fluid axial heat conduction, this chapter provides the review of the papers relevant to the present research. The cited papers will be restricted to those which are particularly relevant to the present research on heat transfer associated with moving surfaces, with an emphasis to the effects of viscous dissipation and fluid axial heat conduction. The papers concerned the heat transfer analyses associated with moving boundary are reviewed first. Then the papers considering viscous dissipation effect and fluid axial heat conduction effect are reviewed.

2.1 Heat Transfer Related to Moving Boundary

The papers concerning the heat transfer between steadily moving rod and free quiescent medium can be found in [12] - [26] and an extensive literature survey has been given by [26]. In this section the review of the papers treated Poiseuille-Couette flows is presented as the present research is involved with the heat transfer for inlet flows.

As far as is known to the author, there has been no work in the literature that studied heat transfer involved moving boundaries which considered the fluid axial heat conduction effect. There are a few papers that treated heat transfer

problem involved with moving boundaries including the effect of viscous dissipation and the reviews of these papers are given first. The other papers related to heat transfer associated with moving boundaries are classified by whether they treated heat transfer in the thermal entrance region or in the fully developed region.

2.1.1 Viscous Dissipation

El-Ariny and Aziz [27] numerically studied entrance region heat transfer in plane Poiseuille-Couette flow including the effect of viscous dissipation for the thermal boundary conditions of (a) the fixed wall temperature is maintained at the entering fluid temperature with the moving wall is kept at a temperature differing from the entering fluid temperature and (b) the moving wall insulated with the fixed one is kept at a constant temperature. They noted that for the thermal boundary condition (b) the effect of viscous dissipation is to reduce the Nusselt number and it is pronounced if pressure gradient is high.

Laminar entrance region heat transfer to plane Poiseuille-Couette flow of non-Newtonian fluids was numerically studied by Lin [28] for two types of boundary conditions as El-Ariny and Azis [27] applied. In this reference the power-law model was applied. It was noted that the flow index, n, ranging from 0.2 to 1 covers a large number of non-Newtonian fluids including liquid foods, polymer melts and lubrication oils. For larger n the dimensionless bulk temperature was larger. The results for bulk temperature and Nusselt number development in the thermal entrance region were presented graphically for $n = 0.2$, 0.6 and 1.

Heat transfer to non-Newtonian Couette flow in an annulus with a moving core was studied by Lin and Hsieh [29] and with a moving outer cylinder by Lin [30]. They [29] noted that the polymer flow in the coating problem takes place between two concentric cylinders in which the outer cylinder is motionless while the inner cylinder moves in the flow direction. In such process the wire surface is to be coated with a layer of polymer and the thickness of the fluid layer is assumed (radius ratio of the annuli) to be small compared to the inner core radius so that the problem becomes identical to a Couette flow with uniform pressure in the flow direction. In this reference, they developed the velocity distribution equations including the two driving forces, namely, the axial pressure and the moving inner cylinder. In their study the fluid was described by the power-law model and the viscous dissipation term was included in the energy equation while axial conduction was assumed to be negligible. They considered cooling process subject to the boundary conditions

of the outer stationary cylinder is kept at a constant temperature equal to the entering fluid temperature with the core is kept at a constant temperature. In the reference [30], heat transfer in a concentric annulus with a moving outer cylinder was considered as the problem simulates the polymer coating inside a tube and the velocity distribution had been presented by applying the power law model. The core is kept at a constant temperature of the entering fluid and the outer moving tube is kept at a constant temperature different from the entering fluid temperature. He has extended solutions for different pseudoplastic fluids and considered viscous dissipation effects on the heat transfer in the thermally developing region.

2.1.2 Thermal Entrance Region

Heat transfer to thermally developing plane Poiseuille-Couette flow has been studied analytically by Hudson and Bankoff [31] for the boundary conditions of constant and equal temperatures specified at the walls. Their solutions were obtained for negligible viscous dissipation and axial heat conduction.

Šesták and Rieger [32] have investigated analytically laminar heat transfer to plane Couette flow in the thermally entrance region for four different boundary conditions under the assumptions of constant pressure gradient along the duct and negligible body forces, axial heat conduction and viscous dissipation. It was noted that the heat transfer rate expressed in terms of the dimensionless Nusselt group exhibit higher values at the moving wall. The limiting values for Nusselt number were tabulated for the different boundary conditions and the results were presented in a graphical form.

A conjugate problem of laminar Poiseuille-Couette flow was studied analytically and experimentally by Davis and Gill [33] including axial heat conduction in the wall.

The results for Nusselt numbers at the walls for Poiseuille, Couette and Poiseuille-Couette flows in the thermally developing range were presented graphically by Davis [34] for Newtonian fluids between parallel-plates. In reference [34], both viscous dissipation and fluid axial heat conduction were considered to be negligible and the thermal boundary conditions were (a) constant and different temperatures at the walls and (b) one wall insulated while the other is heated constantly.

Unsteady temperature field in plane Couette flow was investigated by Winter [35] and he pointed out that the viscosity of a fluid in Couette flow system can not be measured isothermally because viscous dissipation generates heat. This reference

deals with developing temperature and velocity fields for a Newtonian fluid with a temperature dependent viscosity for constant wall temperature condition.

Bruin [36] has studied temperature distributions in the thermal entrance region of plane Couette flow with and without additional pressure gradient. The parallel-plates were considered as kept at different temperatures. It was noted that this reference was designated to study pasteurization systems. The results were given in a graphical form.

Payvar and Majumdar [37] have studied numerically heat transfer to flow between parallel-plates of finite length for situations in which the flow is induced by the continuous motion for the condition of the moving wall is kept at a constant temperature with the stationary wall insulated. They presented Nusselt numbers for different values of the induced flow rate.

Kang and Jaluria [38] have numerically investigated conjugate heat transport from a continuously moving heated plate in a parallel channel flow. A flat plate or sheet moving vertically and horizontally in a wide channel was considered. The fluids were air and water. The results obtained in this reference indicated that the thermal boundary layer is thinner when a plate is moving vertically than when it moves horizontally. It was also found that the rate of heat removal from the heated plate largely depends on the local velocity near the plate surface, rather than the velocity level over much of the cross section channel. Thus, they concluded that the plate speed affects the heat transfer rate significantly.

Forced transient convective heat transfer from a continuously moving cylindrical rod was studied numerically by Choudhury and Jaluria [39] for opposing and aiding flows. In this reference the flow was induced by the moving rod. They considered the effects of several physical and process parameters like rod speed, material, fluid velocity, channel width and fluid on the local Nusselt number, the centerline temperature decay, the radial variation in temperature and on the flow field.

The extrusion of viscoplastic fluids was studied analytically and experimentally by Lawal and Kalyon [40] and Couette flow was used as the flow model. It was noted an occurrence of wall slip behavior of a concentrated suspension and therefore they used the Herschel-Bulkley model. The applied thermal boundary conditions were (a) isothermal barrel, adiabatic screw (b) isothermal barrel and screw (c) adiabatic screw and barrel and (d) arbitrary heat transfer coefficients.

2.1.3 Thermally Fully Developed Region

Heat transfer to fully developed non-Newtonian creeping flow in a rectangular channel with a top wall moving was studied numerically by Syrjälä [41] for the conditions of the moving wall maintained at a constant velocity with the other three walls insulated.

Demirel [42] has studied the entropy generation in laminar, fully developed Couette flows in parallel-plates and in concentric annuli with asymmetric wall temperatures for an incompressible fluid with temperature dependent viscosity and thermal conductivity. In this reference, the outer tube rotates and Newtonian fluid (unused engine oil) was considered. It was found that the entropy generation depends on the pressure gradient and viscous dissipation, and without the pressure gradient the entropy generation is relatively small for the plane Couette flow. For annuli, the effect of Brinkman number on the entropy generation is minimal for high Reynolds numbers.

2.2 Effects of Viscous Dissipation and Axial Heat Conduction

As the present research is involved in studying the effects of viscous dissipation and fluid axial heat conduction, a careful survey of the papers concerning these effects has been conducted. The review of the papers considered the effects of both viscous dissipation and fluid axial heat conduction is presented in this section.

2.2.1 Newtonian Fluids

Deavours [43] investigated analytically the heat transfer to Newtonian fluids in the thermally developing region in a parallel-plates duct. In his study the effect of axial heat conduction in laminar Newtonian fluid flow was considered for the boundary condition of that the walls were divided into two parts left half and right half. Temperatures at the walls were equal but they were taken as different in the two parts. He decomposed the eigenvalue problem into a system of ordinary differential equations, for which he proved the orthogonality of the eigenfunctions by assuming at the axial infinity the temperature is a some function independent of the axial coordinate. In this reference, first six positive and negative eigenvalues for $Pe = 1$ and, the numbers of series terms needed to obtain error of less than 0.01 at

various downstream axial locations were tabulated. He presented the results of axial temperature profiles and center-line temperature distributions in right half channel for Poiseuille flow for a range of Peclet numbers.

2.2.2 Non-Newtonian Fluids

Magneto-hydrodynamic (MHD) entrance region heat transfer in parallel-plates has been studied by LeCroy and Eraslan [44] including Joule heating, viscous dissipation and fluid axial heat conduction. The associated problem was solved by the Galerkin method and their results were presented for boundary conditions of (a) the walls maintained at an equal temperature and (b) walls subjected to constant heat flux. The eigenvalues for different Hartmann number and Peclet number (∞, 100, 10 and 1) values were tabulated and the modified dimensionless temperatures and the Nusselt numbers were presented graphically for Brinkman number 0.1 and 1.

Heat transfer in the thermally developing region including fluid axial heat conduction within a non-Newtonian (power-law model) fluid in tube with internal heat generation due to compression work has been studied by Dang [45]. Later in another reference [46] he presented a study on the steady state heat transfer of power-law fluids at low Peclet number flow for the cooling process in parallel-plates and cylinders. He applied two semi infinite regions under two thermal boundary conditions (a) temperature at one wall is kept at a constant value equal to the entering fluid temperature at $z < 0$ while for $z \geq 0$ it is maintained at a constant value less than the entering temperature and (b) for $z < 0$ one wall is insulated while $z \geq 0$ heat is removed with a constant heat flux at that wall. In both of these cases the other wall is insulated. Viscous dissipation effect was considered in the downstream region ($z < 0$) but was neglected in the upstream region ($z \geq 0$).

Liou and Wang [47] have studied the thermally developing heat transfer of power-law fluids with three different entrance conditions assuming the fluid flowing from an adiabatic well-stirred reserviour into a conduit. The three inlet conditions were (a) uniform inlet temperature (b) continuous axial energy flux or Dankwerts entrance condition and (c) both the temperature and total axial energy flux are continuous at the inlet. They included the fluid axial heat conduction term and the viscous dissipation term in their formulation.

Laminar Hartmann flow in the thermally developing region of a parallel-plate channel has been studied analytically by Lahjomri et al. [48] by including viscous dissipation, Joule heating and axial heat conduction with a step change in the wall

temperature. These authors pointed out that the nonorthogonal eigenfunctions in upstream and downstream regions correspond to Mathieu's functions and presented examples for MHD flow of liquid metals. The liquid metals considered were sodium liquid and lithium liquid and, radial temperature profiles for the fluids were shown graphically for $Pe = 5$ and $Pe = 100$. It was pointed out that the effect of axial heat conduction decreases for $Pe = 100$. Since for the liquid metals Prandtl number is very small, the viscous dissipation was not considerable.

Laminar heat transfer of a Bingham plastic in a circular pipe has been studied by Min et al. [49] for uniform wall temperature condition and by Min and Yoo [50] for uniform wall heat flux condition. In reference [49], for Bingham plastic fluids they obtained a correlation formula between Nusselt number and Peclet number in the thermally developed region and studied the effects of viscous dissipation and fluid axial heat conduction in the thermally developing region. In reference [50], heat transfer in the thermally developing and fully developed regions for Bingham plastics was studied numerically including both viscous dissipation and fluid axial heat conduction.

Thermally developing heat transfer for a porous medium in parallel-plates channel at uniform temperature was studied by Nield et al. [51]. In this reference the effects of viscous dissipation and fluid axial heat conduction are considered. It was noted that the assumption of temperature at a great distance is independent of the axial coordinate is questionable if viscous dissipation is considered.

By solving the energy equation including the terms of viscous dissipation and axial heat conduction, Wei and Zhang [52] have showed that both the parabolic and the elliptic problem are well posed and the solutions to both problems on a cross section of the pipe converge exponentially of to the same steady state solution as the cross section moves far away from the entrance of the pipe.

2.3 Viscous Dissipation Effect

In this section the studies on forced laminar convection in parallel plates those considered the effects of viscous dissipation are reviewed.

2.3.1 Newtonian Fluids

Hwang et al. [53] have numerically studied the viscous dissipation effect on heat transfer to Newtonian fluids in the thermally developing region of parallel-plates under the assumptions of hydrodynamically fully developed flow and negligible body forces and axial heat conduction. In this reference the thermal boundary conditions were one wall insulated with the other heated constantly.

Ou and Cheng [54] have investigated the effects of pressure work and viscous dissipation on heat transfer in the thermally developing region for gas flows in parallel-plate channels under the assumptions of fully developed laminar steady flow and negligible effects of free convection, axial heat conduction, and variable physical properties for two thermal boundary conditions of (a) one wall insulated with the other maintained at a constant temperature and (b) one wall heated constantly with the other insulated. It was pointed out that the effects of pressure work and viscous dissipation on heat transfer are completely different for the different thermal boundary conditions and pressure work has no effects on Nusselt number results.

2.3.2 Non-Newtonian Fluids

Laminar heat transfer in the thermally developing region for a cooling process of power-law fluids in parallel-plates has been investigated numerically by Vlachopoulos and Keung [55]. They included the viscous dissipation effect and the considered boundary conditions were the walls maintained at a constant and equal temperature. The bulk temperature and local Nusselt number results in the thermally developing range for the neglected viscous dissipation case were tabulated for flow index of $n = 1/4$, $1/2$, 1 and 2. The flow was assumed to be fully developed hydrodynamically.

Laminar heat transfer to power-law fluids in the thermal entrance region of parallel plates was studied Lin and Hsu [56] including the viscous dissipation effect for both cooling and heating processes by considering temperature dependent viscosity.

Etemad et al. [57] have investigated numerically viscous dissipation effects on heat transfer for a power-law fluid in the entrance region of parallel plates and reported that the Nusselt number distribution along the walls is affected appreciably

by the variation of the fluid viscosity with temperature, viscous dissipation, the magnitude of the power-law index as well as the fluid Prandtl number and thermal boundary conditions. They considered four different thermal boundary conditions and the considered flow was simultaneously developing, steady and laminar. The authors of this reference pointed out that the results were markedly different from those obtained assuming temperature independent viscosity. Their numerical study was carried out for $n = 0.5$, 1 and 1.25; $Re = 500$, $Pr = 1$ and 10.

Laminar forced convection to non-Newtonian fluids in parallel-plate ducts and circular tubes with prescribed wall heat flux was studied analytically by Cotta and Özisik [58] under the assumptions of the thermally developing, hydrodynamically fully developed flow with negligible axial heat conduction and free convection, while viscous dissipation effect included. The power-law model was applied and the results of Nusselt number for the values of flow index, $n = 1/3$, 1, 3 were presented in a tabular form for constant wall heat flux condition. The above work was extended in reference [59] for prescribed wall temperature boundary conditions.

Barletta has been studying the effects of viscous dissipation on forced, free and mixed convections. In his paper [60], fully developed laminar forced convection in circular ducts for power-law fluids was studied by considering the viscous dissipation effect. The applied thermal boundary condition was axially changing heat flux at the duct wall. Fluid axial heat conduction was assumed to be negligible.

2.4 Axial Heat Conduction Effect

In this section the studies on laminar forced convection in parallel plates those considered the fluid axial heat conduction are reviewed.

2.4.1 Newtonian Fluids

Heat transfer in the thermal entrance regions of parallel-plate and cylinder ducts has been studied by Nguyen [61] under the assumptions of hydrodynamically fully developed flow, negligible body forces and viscous dissipation. In this reference the local Nusselt number were presented for Peclet number ranging from 1 to 1000.

Laminar heat transfer with axial conduction was studied by Telles et al. [62] for the thermal boundary conditions of (a) prescribed wall temperatures (b) prescribed wall heat flux and (c) prescribed convective heat transfer to the surroundings. Additionally the specified wall conditions were allowed to vary with the axial coordinate.

Their solution was based on Gram-Charlier basis or the Hibert space of square integrable functions of a real variable which depends upon the determination of the asymptotic solution at large axial coordinates, z. For large axial coordinates or for $z \rightarrow \infty$, they substituted the first derivative of the dimensionless temperature with respect to z by its asymptotic constant value, β_∞. For the cases of specified wall temperature and convective boundary conditions this limit of β_∞ was set zero. But for the case of specified wall heat flux, the value of β_∞ was a constant. The solutions were presented for the flows inside a circular pipe, an annular space between pipes, and between parallel plates. They considered fully developed flow of a Newtonian fluid and viscous dissipation and other forms of energy generation were neglected.

Jones [63] studied the heat transfer in the thermal entrance region by including fluid axial heat conduction for the prescribed heat flux boundary conditions at the walls of a parallel plates channel. The heat fluxes were represented as delta functions and a mathematical approach to solve the energy equation was presented.

Laminar heat transfer in parallel plates has been studied by Deavours [64]. The problem was treated in two regions and with discontinuous boundary conditions with a jump at the origin. The two solutions for the two divided domain were matched at the origin by the requirement of continuity.

Agrawal [65] studied laminar heat transfer by considering the effect of fluid axial heat conduction. His solution method was to solve the energy equation for two regions of $z \leq 0$ and $0 \leq z$, and then to impose the continuity condition.

Pahor and Strnad [66] obtained the asymptotic value expression for Nusselt number as a function of Peclet number for the parallel-plates at equal and constant temperatures. They neglected viscous dissipation effect.

Laminar heat transfer for flow in a tube and between parallel plates has been studied by Schmidt and Zeldin [67]. For tube the boundary condition was uniform wall temperature and for parallel-plates one wall insulated with the other is at uniform wall temperature. In this reference the effect of fluid axial heat conduction is studied by using a finite difference technique and the solution domain stretched axially in $0 \leq z < \infty$.

Hsu [68] studied the fluid axial heat conduction effect on heat transfer in the thermal entrance region of circular and parallel-plates ducts by considering two semi-infinite regions of $-\infty < z \leq 0$ and $0 \leq z < \infty$. He determined first 20 eigen constants for the adiabatic ($-\infty < z \leq 0$) and heated ($0 \leq z < \infty$) regions separately.

An integral method was used to study the fluid axial heat conduction effect by Taitel and Tamir [69] for tube and parallel plates channels. They noted that third order polynomial for temperature profiles is recommendable as the expected accuracy was better than 12 percent.

Heat transfer with fluid axial heat conduction effect has been studied for the thermally developing region by Lahjomri and Oubarra [70] and the solutions for uniform wall temperature boundary conditions were obtained by the method of separation of variables. They determined the temperature field in two semi infinite regions, an upstream region ($-\infty < z \leq 0$) and a downstream region ($0 \leq z < \infty$) and the two solutions were matched at $z = 0$.

Weigand et al. [71] have studied heat transfer in the thermal entrance regions of laminar and turbulent flows in a pipe or a parallel plate channel taking into account axial heat conduction effects for piecewise uniform wall heat flux boundary conditions. In this reference the energy equation was decomposed into a pair of first order partial differential equations.

2.4.2 Non-Newtonian Fluids

Olek [72] has studied heat transfer to laminar non-Newtonian fluids in the thermally developing region of circular and parallel-plate ducts including axial heat conduction, where (a) one wall insulated and the other convect heat and (b) constant temperature at the pipe wall. The results for Nusselt number and bulk temperature were tabulated for $n = 1/3$, 1 and 3 and compared with those who neglected the axial heat conduction effects. Also the results of Newtonian fluid for $Pe = 1$ was tabulated for a pipe duct subject to a constant wall temperature.

Chapter 3

POISEUILLE-COUETTE FLOW

3.1 Fluid Behaviors

Fluids may be classified either according to their response to the effects produced under the action of a shear stress or according to the externally applied pressure. The extensive description of the classification of fluid behaviors is given in [6], [7], [73] and etc.

In this fundamental study of the steady laminar heat transfer problem, time-independent or purely viscous fluids are considered. The most common type of time-independent non-Newtonian fluid behavior observed is pseudo-plasticity or shear-thinning characterized by an apparent viscosity which decreases with increasing shear rate. Shear thickening or dilatant fluid behavior is less widespread in chemical and processing industries, except in systems with high solids loading. For dilatant fluids, their apparent viscosity increases with increasing shear rate. The power-law model is frequently used in fluid flow and heat transfer analyses for pseudoplastic and dilatant fluids. This mathematical expression to model shear stress and shear rate relationship is plotted by a straight line in the log-log plot for viscosity and shear rate. Figure 3-1 shows a qualitative graph which is indicative of the behavior of many pseudoplastic fluids. As it is shown schematically, both at very low and at very high shear rates, $\dot{\gamma}$ ($\dot{\gamma} = du/dy$), most shear-thinning or pseudoplastic fluids exhibit Newtonian behavior, i.e. the values of apparent viscosity, η_a, become constant. The apparent viscosity, η_a, values at very low and very high shear rates, $\dot{\gamma}$, are η_0 and η_∞, respectively. It is seen, the power-law model does not predict the zero and infinite shear rate viscosities as shown by the dotted lines and the correct velocity field is not ensured if the power-law model is applied

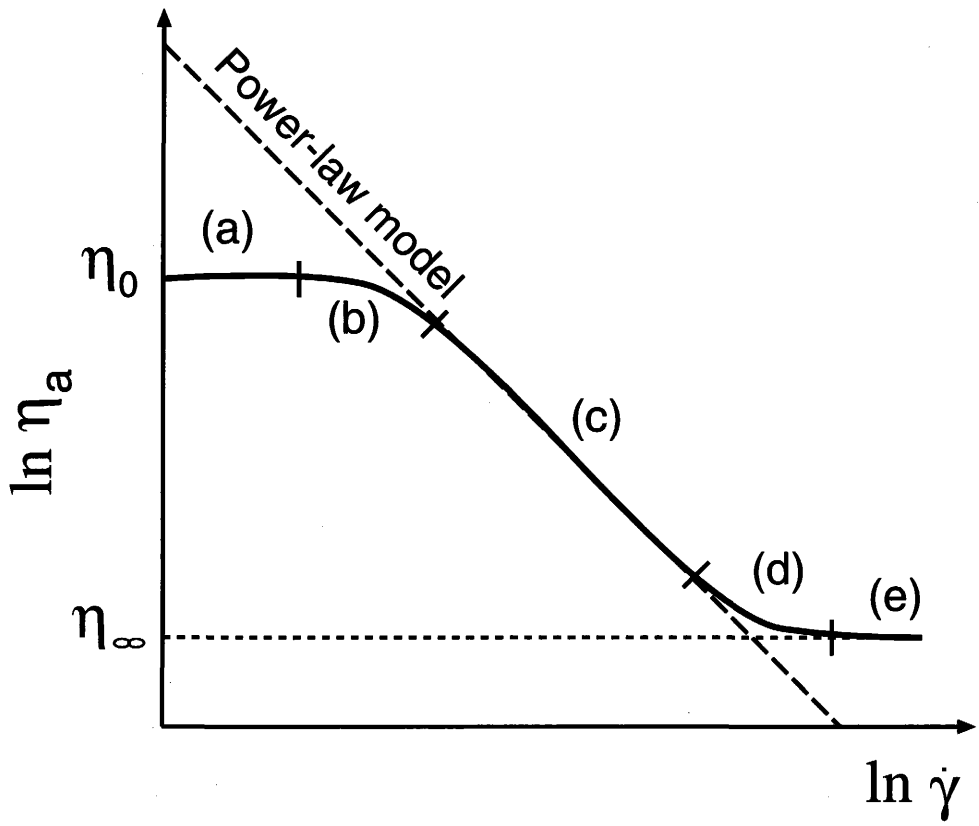

Fig.3-1 Illustrative flow curve for a pseudoplastic fluid

to the regions of low (a), medium (b), higher (d) and very high (e) shear rates. In order to accurately calculate the velocity field, the modified power-law model described by Dunleavy and Middleman [74] is applied in this study. The modified power-law model was first used by Brewster and Irvine [75] in the analysis of laminar flows within circular ducts and by Capobianchi and Irvine [76] for concentric annular ducts. More recently Luelf and Burmeister [77] applied this model for the study on viscous dissipation effect on pressure gradient to bridge the region between the two extremes of a Newtonian and a power-law fluid.

The modified power-law model has advantages in permitting the calculation at very low (a), medium (b) and high (c) shear rates. Carreau model [6], which has four parameters predicts the whole region of shear rates but from Fig.3-2, it is seen the modified power-law model can accurately describe real fluid behaviors. These examples showing the shear stress-shear rate behaviors of three pseudoplastic polymer solutions are taken from reference [6]. Also experimental data on apparent viscosity and other physical properties of fluids for which the modified power-law model may be applicable, can be found in [7] for tap water with addition of 1000 wppm

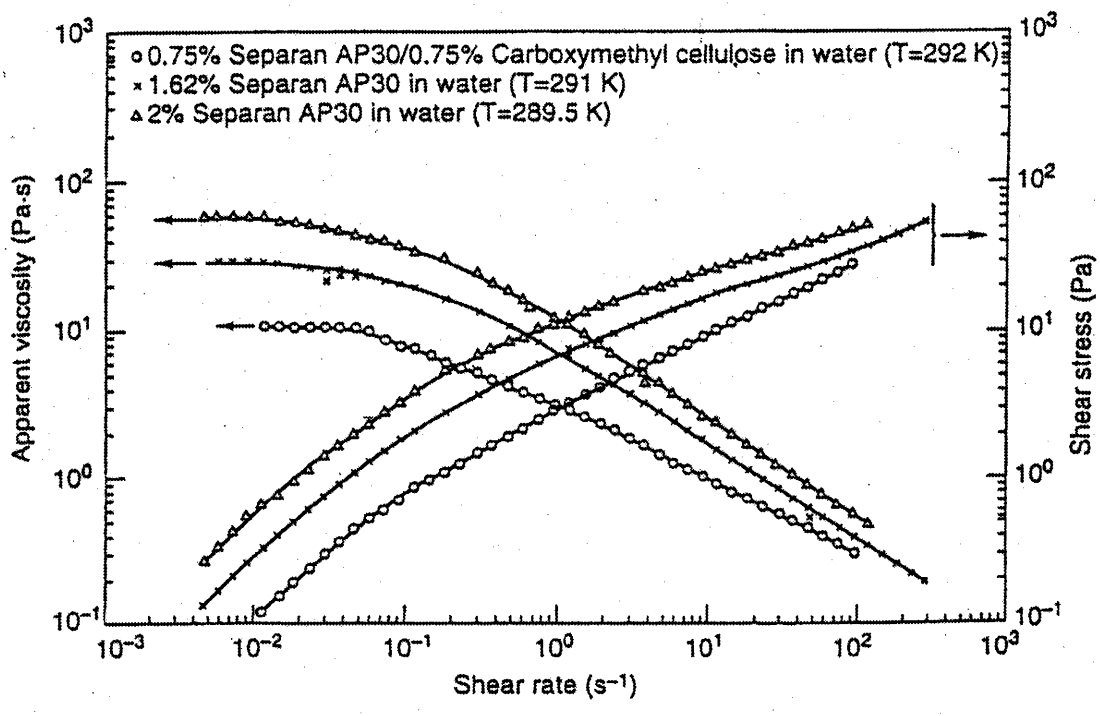

Fig.3-2 Representative shear stress and apparent viscosity plots for three pseudoplastic polymer solutions (cited from [6] p.8)

(parts per million by weight) of sodium carboxymethyl cellulose (CMC), and in [78] and [79] for polymer melts.

By applying the modified power-law model, accurate information about the fluid in plane Poiseuille-Couette flow is assured. The following sections provide exact solutions for the Newtonian and power-law fluids and numerical solutions for the modified power-law fluids. The aim of acquiring the exact solutions for the Newtonian and power-law fluids was to check the validity of the numerical solutions for the modified power-law fluids. It will be discussed in more detail in Section 3.4.2, that the modified power-law model covers the Newtonian fluid behavior at very small shear rate and the power-law fluid behavior at high shear rate values.

3.2 Problem Description

Throughout this study the following physical model is applied.

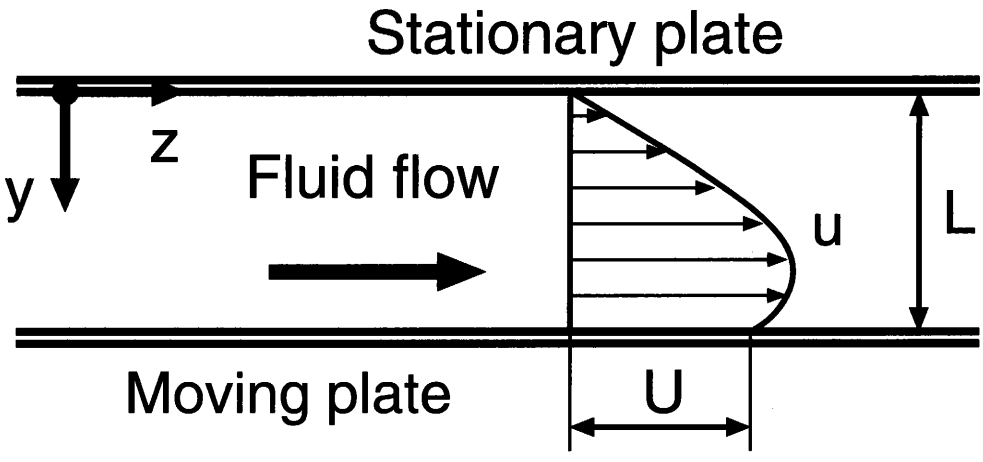

Fig.3-3 Schematic of parallel-plates with the lower plate moving

The assumptions and conditions used in the analysis are:

Passage

- The fluid flows between parallel-plates.
- The upper plate is stationary.
- The lower plate moves at a constant velocity, U.
- The distance between the stationary and moving plates is, L.

Flow

- steady laminar,
- fully developed hydrodynamically.
- No fluid slip at the walls.
- The pressure is uniform in y direction.

Fluid

- Non-Newtonian or Newtonian
- The physical properties, density, ρ, thermal conductivity, k, and specific heat at constant pressure, c_p, are constant.

- Viscosity changes with shear rate (or the magnitude of velocity gradient perpendicular to the direction of flow) and the shear stress can be written as $\tau = -\eta_a \frac{du}{dy}$.

3.3 Newtonian Fluid Flow

The purpose of this section is to obtain an exact solution for the plane Poiseuille-Couette flow of Newtonian fluids. For the Newtonian fluids the apparent viscosity is $\eta_a = \mu$. Then with the assumptions described above the momentum equation for the Newtonian fluids is

$$\mu \frac{d^2u}{dy^2} = \frac{dP}{dz} \tag{3.1}$$

The boundary conditions are:

$$\begin{cases} u = 0 \quad \text{at} \quad y = 0 \\ u = U \quad \text{at} \quad y = L \end{cases} \tag{3.2}$$

By solving the momentum equation with the boundary conditions, the following expression for the flow velocity is obtained.

$$u = \frac{1}{2\mu}\left(\frac{dP}{dz}\right)\left(y^2 - Ly\right) + \frac{U}{L}y \tag{3.3}$$

The average velocity of the flow, u_{m}, is defined as

$$u_{\mathrm{m}} \equiv \frac{1}{L}\int_0^L u dy \tag{3.4}$$

Substituting u and solving Eq.(3.4) gives

$$u_{\mathrm{m}} = \frac{1}{12\mu}\left[-\frac{dP}{dz}\right]L^2 + \frac{1}{2}U \tag{3.5}$$

Then the exact solution for the Newtonian fluid velocity is presented in the dimensionless form as

$$u^* \equiv \frac{u}{u_{\mathrm{m}}} = 4y^*[3\left(1 - 2y^*\right) + \left(3y^* - 1\right)U^*] \tag{3.6}$$

The dimensionless velocity gradient, du^*/dy^*, is obtained as

$$\frac{du^*}{dy^*} = 4[3\left(1 - 4y^*\right) + \left(6y^* - 1\right)U^*] \tag{3.7}$$

Dimensionless velocity profiles and square of the velocity gradient of the Newtonian fluid for different values of the relative velocity ($-1 \leq U^* \leq 3$) are presented in Fig.3-4. It is seen clear that the fluid velocity profile is deformed by the moving plate. Bearing in mind that, this characteristic would also be retained for non-Newtonian fluids, from these velocity profiles three assumptions of the velocity profile shape for an analysis of the power-law fluid flows were made. They are discussed in the next section (see Fig.3-5). The square of velocity gradient is used to clarify the viscous dissipation effects. Close to the walls, if the wall moves to the opposite direction of the fluid flow, or for opposing flows the square of velocity gradient is seen to be higher.

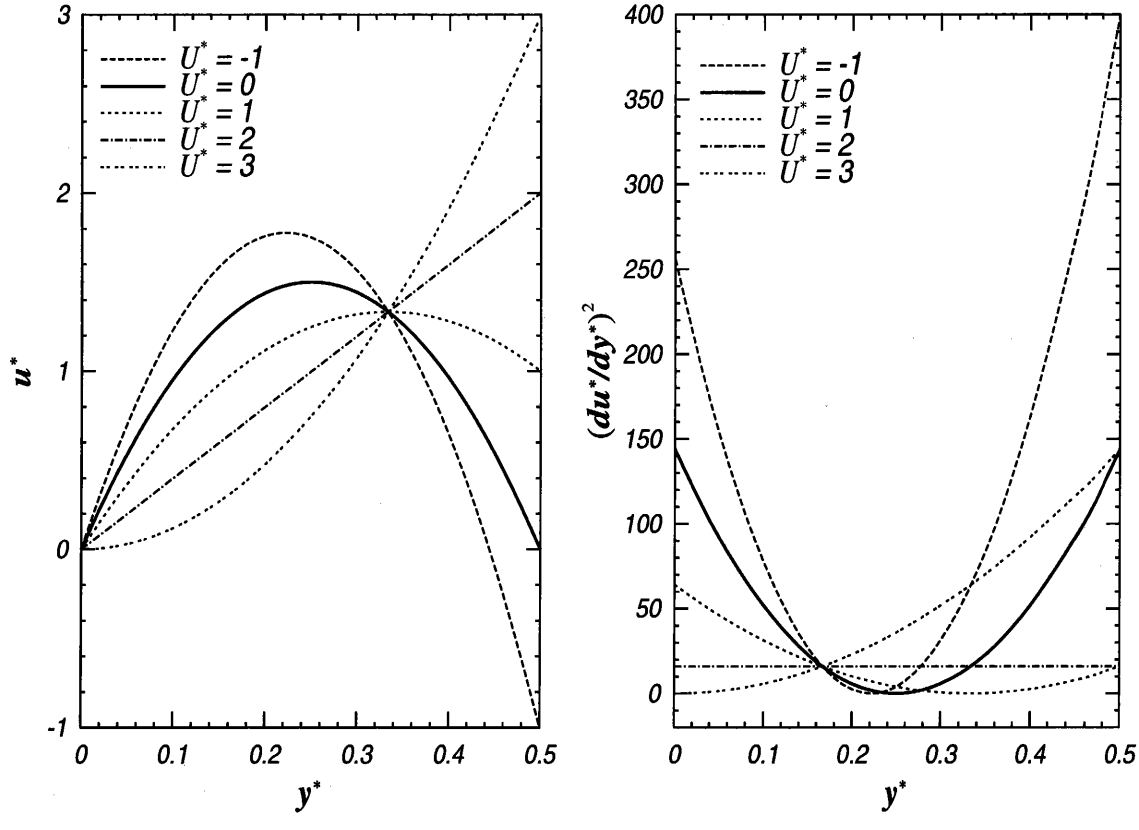

Fig.3-4 Velocity profile and square of velocity gradient for a Newtonian fluid

Further detail is available in [80].

3.4 Non-Newtonian Fluid Flow

With the assumptions discussed in Section 3.2, a simple momentum balance of the flow yields

$$\frac{d\tau}{dy} = -\frac{dP}{dz} \tag{3.8}$$

The boundary conditions are:

$$\begin{cases} u = 0 \quad \text{at} \quad y = 0 \\ u = U \quad \text{at} \quad y = L \end{cases} \tag{3.9}$$

3.4.1 Power-Law Model

In this subsection, exact solutions for the velocity distribution of the plane Poiseuille-Couette flow of non-Newtonian fluids are obtained by applying the power-law model. The shear stress, τ, given by the power-law model is:

$$\tau = -m\left|\frac{du}{dy}\right|^{n-1}\frac{du}{dy} \tag{3.10}$$

It is seen for $n = 1$, the described fluid is a Newtonian fluid and fluid consistency, m, coincides with the ordinary viscosity, μ. In Eq.(3.10), the sign of the velocity gradient is seen to be important for the prediction of the velocity field distribution. For consideration of the sign, the velocity profiles of the power-law fluid flows are assumed to be inherent in the flow patterns of the Newtonian fluid flows that were obtained in Section 3.3. It was observed from the analysis for the Newtonian fluid flows that there may be three kinds of typical patterns of velocity profiles of the plane Poiseuille-Couette flow exist. In the analysis for the non-Newtonian fluids, these three typical patterns of velocity profiles are assumed. The three patterns are respectively referred to as Pattern I, Pattern II and Pattern III. These are illustrated in Fig.3-5.

- Pattern I: The maximum velocity of the flow is between the stationary plate and the moving plate.
- Pattern II: The largest fluid velocity is always on the moving plate (velocity profiles change from a convex form to a linear form).
- Pattern III: Velocity profiles have concave forms (velocity profiles change from a linear form to a concave form).

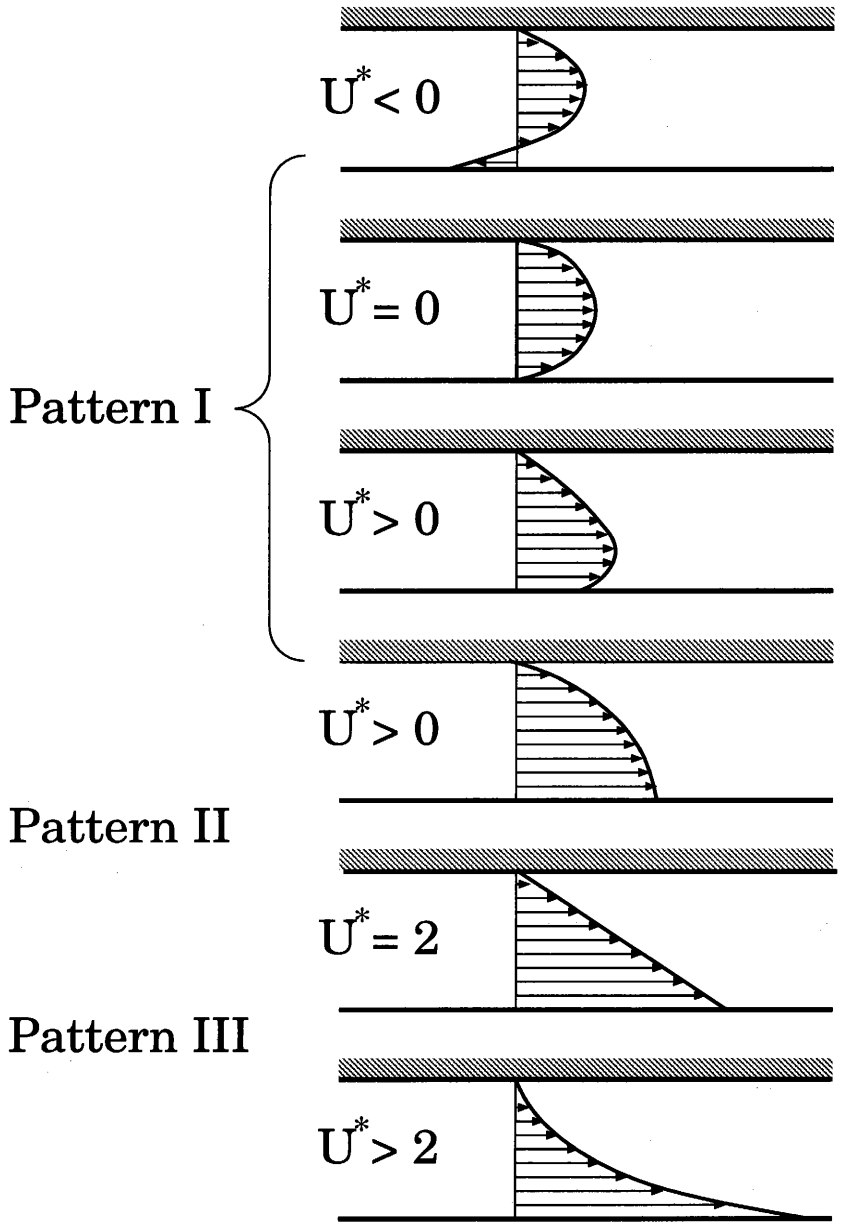

Fig.3-5 Assumed velocity profiles

In these figures showing the assumed patterns for velocity profiles, U^* is dimensionless relative velocity of the moving lower wall. The dimensionless relative velocity is defined as

$$U^* = \frac{U}{u_{\mathrm{m}}} \tag{3.11}$$

Besides, the dimensionless relative velocity, U^*, in determining the velocity field the following dimensionless quantities are applied. Friction factor, f, and generalized Reynolds number, Re^*, are defined as

$$f \equiv \frac{D_{\mathrm{h}}}{2\rho u_{\mathrm{m}}^2}\left(-\frac{dP}{dz}\right) \tag{3.12}$$

$$Re^* \equiv \frac{\rho u_{\mathrm{m}}^{2-n} D_{\mathrm{h}}^n}{m} \tag{3.13}$$

Here D_{h} is the hydraulic diameter, ρ is the fluid density, n is flow index and m is consistency index. The definition of u_{m} is given by Eq.(3.4). For the convenience of the later manipulation a dimensionless parameter, F, is introduced.

$$F = 2fRe^* = \frac{D_{\mathrm{h}}^{n+1}}{m \cdot u_{\mathrm{m}}^n}\left(-\frac{dP}{dz}\right) \tag{3.14}$$

Pattern I

The velocity profiles of Pattern I correspond to moderate values of U^*, which may be reasonable for laminar flow with non-slip boundary conditions. In Fig.3-6, the assumed velocity profile form is shown along with the velocity gradient. In this case, the sign of the velocity gradient, du/dy, changes its sign from positive to negative.

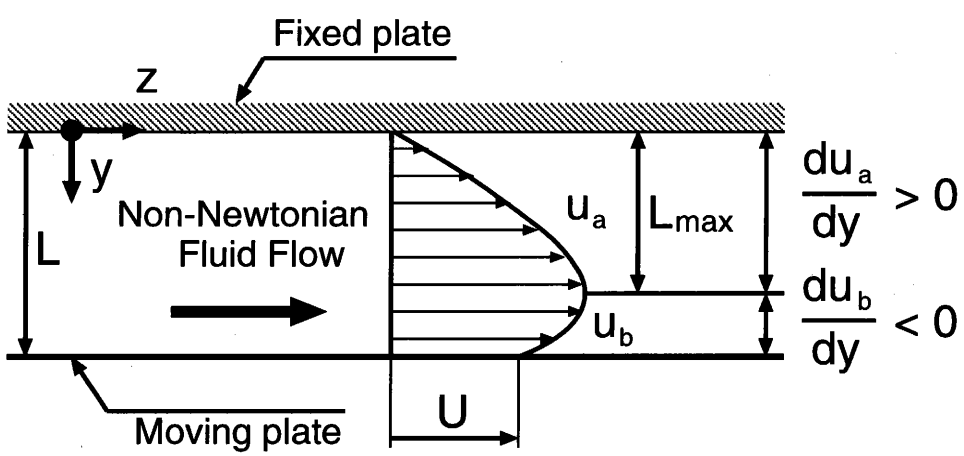

Fig.3-6 Velocity profile assumed in the analysis (Pattern I)

The flow channel is then divided into two sectors:

- Sector with positive velocity gradient ($0 \leq y \leq L_{max}$). The velocity there is referred as u_{a}.
- Sector with negative velocity gradient ($L_{max} \leq y \leq L$). The velocity there is referred as u_{b}.

Where L_{max} is the location of the maximum fluid flow velocity.
Then the shear stresses in the two sectors can be expressed as below

$$\tau = -m\left(\frac{du_a}{dy}\right)^n \qquad (0 \leq y \leq L_{max}) \tag{3.15}$$

$$\tau = m\left(-\frac{du_b}{dy}\right)^n \qquad (L_{max} \leq y \leq L) \tag{3.16}$$

The momentum equation in the two sectors are

$$-m\frac{d}{dy}\left(\frac{du_a}{dy}\right)^n = -\frac{dP}{dz} \qquad (0 \leq y \leq L_{max}) \tag{3.17}$$

$$m\frac{d}{dy}\left(-\frac{du_b}{dy}\right)^n = -\frac{dP}{dz} \qquad (L_{max} \leq y \leq L) \tag{3.18}$$

The following dimensionless parameters:

$$y^* = \frac{y}{D_\mathrm{h}}, \qquad L^*_{max} = \frac{L_{max}}{D_\mathrm{h}}, \qquad u^*_a = \frac{u_a}{u_\mathrm{m}}, \qquad u^*_b = \frac{u_b}{u_\mathrm{m}} \tag{3.19}$$

are introduced to Eqs.(3.17) and (3.18) and they are solved as follows.

(a) The sector with positive velocity gradient, $0 \leq y^* \leq L^*_{max}$

The momentum equation and its boundary conditions are reduced as

$$\frac{d}{dy^*}\left(\frac{du^*_a}{dy^*}\right)^n = -2fRe^* = -F \qquad (F > 0) \tag{3.20}$$

$$\begin{cases} u^*_a = 0 \quad \text{at} \quad y^* = 0 \\ \dfrac{du^*_a}{dy^*} = 0 \quad \text{at} \quad y^* = L^*_{max} \end{cases} \tag{3.21}$$

The integration of Eq.(3.20) together with Eq.(3.21) gives

$$u^*_a = F^{\frac{1}{n}}\left(\frac{n}{n+1}\right)\left[L^{*\frac{n+1}{n}}_{max} - (L^*_{max} - y^*)^{\frac{n+1}{n}}\right] \tag{3.22}$$

(b) The sector negative velocity gradient, $(L^*_{max} \leq y^* \leq 1/2)$

The momentum equation and its boundary conditions are:

$$\frac{d}{dy^*}\left(-\frac{du^*_b}{dy^*}\right)^n = 2fRe^* = F \qquad (F > 0) \tag{3.23}$$

$$\begin{cases} u^*_b = U^* \quad \text{at} \quad y^* = \dfrac{1}{2} \\ \dfrac{du^*_b}{dy^*} = 0 \quad \text{at} \quad y^* = L^*_{max} \end{cases} \tag{3.24}$$

The integration of Eq.(3.23) together with Eq.(3.24) gives

$$u^*_b = U^* + F^{\frac{1}{n}}\left(\frac{n}{n+1}\right)\left[\left(\frac{1}{2} - L^*_{max}\right)^{\frac{n+1}{n}} - (y^* - L^*_{max})^{\frac{n+1}{n}}\right] \tag{3.25}$$

The unknown values of F and L^*_{max} are determined as follows. From the continuity of the velocities at the location of the maximum velocity

$$u^*_a = u^*_b \quad \text{at} \quad y^* = L^*_{max} \tag{3.26}$$

we get a relationship between F and L^*_{max}.

$$F = \left[\frac{U^*}{\left(\frac{n}{n+1}\right)\left\{ L^{*\frac{n+1}{n}}_{max} - \left(\frac{1}{2} - L^*_{max}\right)^{\frac{n+1}{n}} \right\}} \right]^n \tag{3.27}$$

From the mass balance:

$$\int_0^{\frac{1}{2}} u^* dy^* = \int_0^{L^*_{max}} u^*_a dy^* + \int_{L^*_{max}}^{\frac{1}{2}} u^*_b dy^* = \frac{1}{2} \tag{3.28}$$

another relationship between F and L_{max} can be found.

$$F = \left[\frac{1 - 2\left(\frac{1}{2} - L^*_{max}\right) U^*}{2\left(\frac{n}{2n+1}\right)\left\{ L^{*\frac{2n+1}{n}}_{max} + \left(\frac{1}{2} - L^*_{max}\right)^{\frac{2n+1}{n}} \right\}} \right]^n \tag{3.29}$$

Combining Eq.(3.27) and Eq.(3.29), we have the following relationship among U^*, L^*_{max} and n.

$$U^* = \frac{L^{*\frac{n+1}{n}}_{max} - \left(\frac{1}{2} - L^*_{max}\right)^{\frac{n+1}{n}}}{L^{*\frac{n+1}{n}}_{max} - 2\left(\frac{n}{2n+1}\right)\left\{ L^{*\frac{2n+1}{n}}_{max} + \left(\frac{1}{2} - L^*_{max}\right)^{\frac{2n+1}{n}} \right\}} \tag{3.30}$$

The dimensionless location of the maximum velocity, L^*_{max}, is calculated by using the Newton method and the results are given in [81] for wide ranges of the flow index ($0.1 \leq n \leq 2$) and the relative velocity of the moving plate ($-2 \leq U^* \leq 1.6$). When the maximum velocity of the flow coincides with the relative velocity of the moving plate or, in other words if L^*_{max} is at the moving plate, the velocity profile form is referred to the border between Pattern I and Pattern II. From Eq.(3.30) with L^*_{max} = 1/2 the corresponding relative velocity is found

$$U^*_{\text{I, II}} = \frac{2n+1}{n+1} \tag{3.31}$$

In Fig.3-7, the friction factors in term of fRe^* are presented as a function of flow index, n, and the relative velocity of the moving plate, U^*, as a parameter. The values of U^* range from -1 to 1.5. Friction factor in terms of fRe^* is higher for higher flow index fluids for the same relative velocity. For a given fluid, fRe^* increases with a decrease in U^*. The numerical values of fRe^* are given in [81].

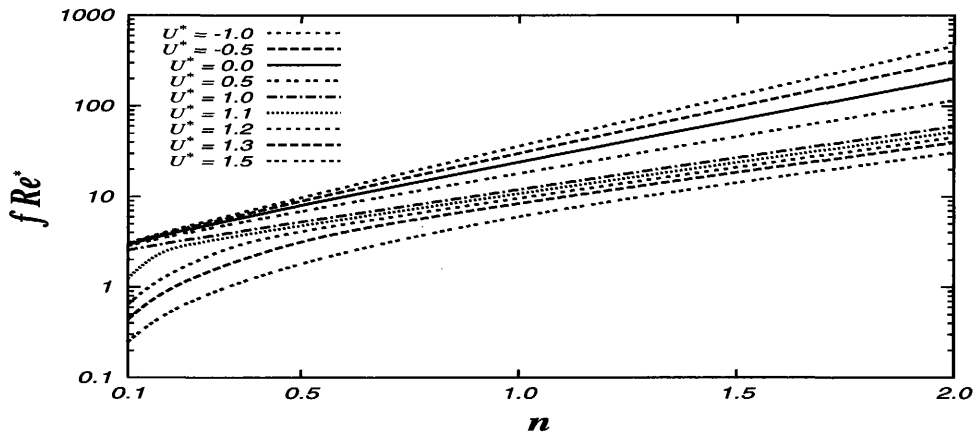

Fig.3-7 Friction factor

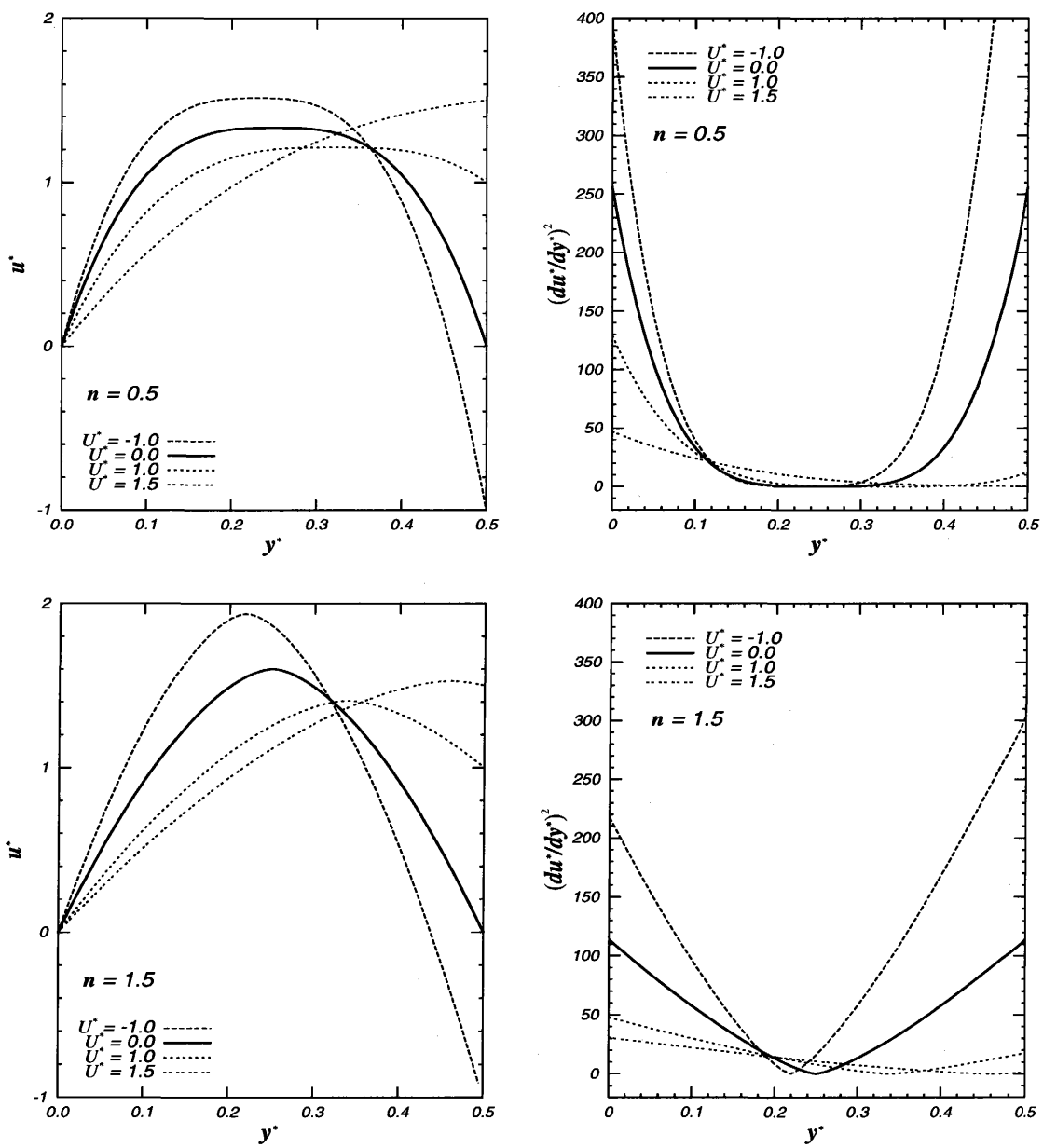

Fig.3-8 Velocity profiles and square of velocity gradient for power-law fluids ($n = 0.5$ and $n = 1.5$)

The effect of the variable relative velocity on the velocity profile across the parallel-plate channel is clearly seen from the computed results and they are given graphically in Fig.3-8 for a pseudoplastic fluid of $n = 0.5$, and for a dilatant fluid of $n = 1.5$. These velocity profiles and square of velocity gradients are presented for various relative velocity of the moving plate. As it is seen from Fig.3-8, near to the stationary wall, the square of velocity gradient of a pseudoplastic fluid ($n = 0.5$) is higher than that of a dilatant fluid ($n = 1.5$) at the same value of the relative velocity U^*.

Pattern II

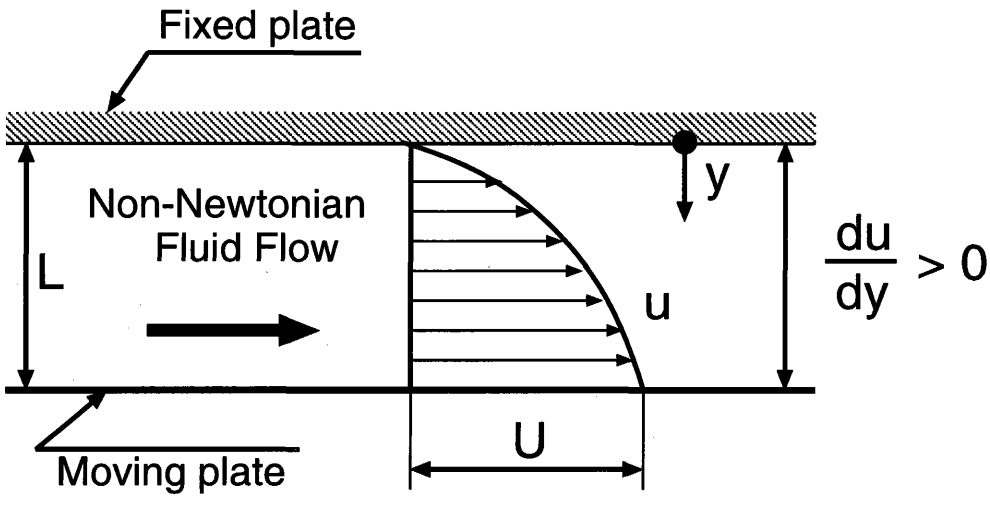

Fig.3-9 Velocity profile assumed in the analysis (Pattern II)

In this case, in between the plates the velocity gradient of the flow is positive. The shear stress is determined as

$$\tau = -m\left(\frac{du}{dy}\right)^n \qquad (0 \le y \le L) \tag{3.32}$$

Then the momentum equation and its boundary conditions are reduced to

$$\frac{d}{dy^*}\left(\frac{du^*}{dy^*}\right)^n = -2fRe^* = -F \qquad (F \ge 0) \tag{3.33}$$

$$\begin{cases} u^* = 0 \quad \text{at} \quad y^* = 0 \\ u^* = U^* \quad \text{at} \quad y^* = \dfrac{1}{2} \end{cases} \tag{3.34}$$

The integration of Eq.(3.33) gives

$$u^* = F^{\frac{1}{n}}\left(\frac{n}{n+1}\right)\left[C^{\frac{n+1}{n}} - (C - y^*)^{\frac{n+1}{n}}\right] \tag{3.35}$$

where C is an integral constant.

Applying the boundary conditions of Eq.(3.34) to Eq.(3.35), we have

$$U^* = F^{\frac{1}{n}}\left(\frac{n}{n+1}\right)\left[C^{\frac{n+1}{n}} - \left(C - \frac{1}{2}\right)^{\frac{n+1}{n}}\right] \tag{3.36}$$

We have the first relationship between F and C as

$$F = \left[\frac{U^*}{\left(\frac{n}{n+1}\right)\left\{C^{\frac{n+1}{n}} - \left(C - \frac{1}{2}\right)^{\frac{n+1}{n}}\right\}}\right]^n \tag{3.37}$$

From the mass balance across the plates:

$$\int_0^{\frac{1}{2}} u^* dy^* = \int_0^{\frac{1}{2}} \left[F^{\frac{1}{n}}\left(\frac{n}{n+1}\right)\left\{C^{\frac{n+1}{n}} - (C - y^*)^{\frac{n+1}{n}}\right\}\right] dy^* = \frac{1}{2} \tag{3.38}$$

From Eq.(3.38), we have

$$F^{\frac{1}{n}}\left(\frac{n}{n+1}\right)\left[\frac{1}{2}C^{\frac{n+1}{n}} + \left(\frac{n}{2n+1}\right)\left\{\left(C - \frac{1}{2}\right)^{\frac{2n+1}{n}} - C^{\frac{2n+1}{n}}\right\}\right] = \frac{1}{2} \tag{3.39}$$

The parameter, F, is calculated as

$$F = \left[\frac{1}{2\left(\frac{n}{n+1}\right)\left[\frac{1}{2}C^{\frac{n+1}{n}} + \left(\frac{n}{2n+1}\right)\left\{\left(C - \frac{1}{2}\right)^{\frac{2n+1}{n}} - C^{\frac{2n+1}{n}}\right\}\right]}\right]^n \tag{3.40}$$

Combining Eq.(3.37) and Eq.(3.40), we have the following relationship among U^*, C, and n.

$$U^* = \frac{\frac{1}{2}\left\{C^{\frac{n+1}{n}} - \left(C - \frac{1}{2}\right)^{\frac{n+1}{n}}\right\}}{\frac{1}{2}C^{\frac{n+1}{n}} + \left(\frac{n}{2n+1}\right)\left\{\left(C - \frac{1}{2}\right)^{\frac{2n+1}{n}} - C^{\frac{2n+1}{n}}\right\}} \tag{3.41}$$

C is calculated by using the Newton method and the results are listed in [81]. Further detail is also available in [82].

The condition at $F = 0$ may be considered as the bordering condition between the two forms of Pattern II and Pattern III.

Solving Eq.(3.33) with Eq.(3.34) for $F = 0$, one obtains the value of the velocity corresponding to the bordering condition.

$$u^* = 2\, U^* y^* \tag{3.42}$$

It is seen, the linear velocity profile is at the border of Patterns II and III.

Pattern III

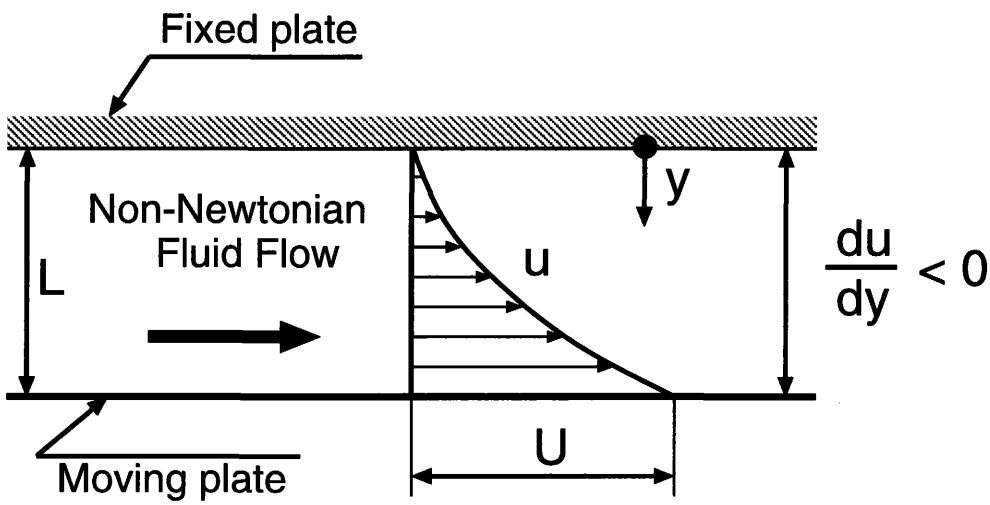

Fig.3-10 Velocity profile assumed in the analysis (Pattern III)

In this case, the shear stress is given as

$$\tau = m\left(\frac{du}{dy}\right)^n \qquad (0 \le y \le L) \tag{3.43}$$

The momentum equation and its boundary conditions are reduced to

$$\frac{d}{dy^*}\left(\frac{du^*}{dy^*}\right)^n = F \qquad (F < 0) \tag{3.44}$$

$$\begin{cases} u^* = 0 \quad \text{at} \quad y^* = 0 \\ u^* = U^* \quad \text{at} \quad y^* = \dfrac{1}{2} \end{cases} \tag{3.45}$$

Integrating Eq.(3.44), we have

$$u^* = F^{\frac{1}{n}}\left(\frac{n}{n+1}\right)\left[(C+y^*)^{\frac{n+1}{n}} - C^{\frac{n+1}{n}}\right] \tag{3.46}$$

where C is an integral constant.

Applying the boundary conditions of Eq.(3.45) to Eq.(3.46), we have

$$U^* = F^{\frac{1}{n}}\left(\frac{n}{n+1}\right)\left[\left(C+\frac{1}{2}\right)^{\frac{n+1}{n}} - C^{\frac{n+1}{n}}\right] \tag{3.47}$$

We have the first relationship between F and C.

$$F = \left[\frac{U^*}{\left(\frac{n}{n+1}\right)\left\{\left(C+\frac{1}{2}\right)^{\frac{n+1}{n}} - C^{\frac{n+1}{n}}\right\}}\right]^n \tag{3.48}$$

From the mass balance between the plates:

$$\int_0^{\frac{1}{2}} \left[F^{\frac{1}{n}} \left(\frac{n}{n+1} \right) \left\{ (C+y^*)^{\frac{n+1}{n}} - C^{\frac{n+1}{n}} \right\} \right] dy^* = \frac{1}{2} \tag{3.49}$$

From Eq.(3.49), one obtains

$$F^{\frac{1}{n}} \left(\frac{n}{n+1} \right) \left[\left(\frac{n}{2n+1} \right) \left\{ \left(C + \frac{1}{2} \right)^{\frac{2n+1}{n}} - C^{\frac{2n+1}{n}} \right\} - \frac{1}{2} C^{\frac{n+1}{n}} \right] = \frac{1}{2} \tag{3.50}$$

where the parameter, F, is calculated as

$$F = \left[\frac{1}{2\left(\frac{n}{n+1} \right) \left[\left(\frac{n}{2n+1} \right) \left\{ \left(C + \frac{1}{2} \right)^{\frac{2n+1}{n}} - C^{\frac{2n+1}{n}} \right\} - \frac{1}{2} C^{\frac{n+1}{n}} \right]} \right]^n \tag{3.51}$$

Combining Eq.(3.48) and Eq.(3.51), we have the following relationship among U^*, n, and C.

$$U^* = \frac{\left(C + \frac{1}{2} \right)^{\frac{n+1}{n}} - C^{\frac{n+1}{n}}}{2\left(\frac{n}{2n+1} \right) \left\{ \left(C + \frac{1}{2} \right)^{\frac{2n+1}{n}} - C^{\frac{2n+1}{n}} \right\} - C^{\frac{n+1}{n}}} \tag{3.52}$$

C is calculated by using the Newton method and the results are listed in [81]. Further detail is also available in [82].

3.4.2 Modified Power-Law Model

In this subsection, the velocity distribution of plane Poiseuille-Couette flow of non-Newtonian fluids are obtained by applying the modified power-law model. This modified power-law model overcomes the drawback of the power-law model as the modified power-law model ensures a correct velocity field even in the of lower shear rates including zero shear rate. The shear stress in the momentum equation, Eq.(3.8), is described the modified power-law model as

$$\tau = -\eta_a \frac{du}{dy}. \tag{3.53}$$

Here the apparent viscosity, η_a, is defined as

$$\eta_a = \eta_0 \Big/ \left(1 + \frac{\eta_0}{m} \left| \frac{du}{dy} \right|^{1-n} \right) \qquad \text{for} \quad n < 1, \tag{3.54}$$

$$\eta_a = \eta_0 \left(1 + \frac{m}{\eta_0} \left| \frac{du}{dy} \right|^{n-1} \right) \qquad \text{for} \quad n > 1. \tag{3.55}$$

Where η_0 is viscosity at zero shear rate (see Fig.3-1). As it is seen from Eqs.(3.54) and (3.55) the modified power-law model gives representation of the gradual change in the shear stress versus shear rate relationship from a linear one at low shear rate to a power law one at a high shear rate. It is seen that the relationship (between shear stress and shear rates) expressed by the modified power-law model is convenient to use as it has a Newtonian range at low shear rates and tends to a power-law functionality at high shear rates. In the following this relationship is used to provide results that bridge the region between the two extremes of the Newtonian fluid region and the power-law fluid region.

The momentum equation and its boundary conditions in dimensionless form are:

$$\frac{d}{dy^*}\left(\eta_a^* \frac{du^*}{dy^*}\right) = -2\, f Re_{\mathrm{M}}, \tag{3.56}$$

$$\begin{cases} u^* = 0 \quad \text{at} \quad y^* = 0 \\ u^* = U^* \quad \text{at} \quad y^* = \dfrac{1}{2}. \end{cases} \tag{3.57}$$

Where f is the friction factor and its definition is given by Eq.(3.12). The definition of modified Reynolds number is

$$Re_{\mathrm{M}} \equiv \frac{\rho u_{\mathrm{m}} D_{\mathrm{h}}}{\eta}. \tag{3.58}$$

The dimensionless apparent viscosity η_a^* is defined as

$$\eta_a^* \equiv \frac{\eta_a}{\eta} = \frac{1+\beta}{1+\beta\left|\dfrac{du^*}{dy^*}\right|^{1-n}}, \qquad \text{for} \quad n < 1, \tag{3.59}$$

$$\eta_a^* \equiv \frac{\eta_a}{\eta} = \frac{\beta + \left|\dfrac{du^*}{dy^*}\right|^{n-1}}{\beta+1}, \qquad \text{for} \quad n > 1. \tag{3.60}$$

where the reference viscosity, η, and dimensionless shear rate parameter, β, are

$$\eta = \eta_0 \big/ (1+\beta) \qquad \text{for} \quad n < 1, \tag{3.61}$$

$$\eta = \eta_0 \left(1 + \frac{1}{\beta}\right) \qquad \text{for} \quad n > 1, \tag{3.62}$$

$$\beta = \frac{\eta_0}{m}\left(\frac{u_{\mathrm{m}}}{D_{\mathrm{h}}}\right)^{1-n}. \tag{3.63}$$

The parameter, β, represents the dimensionless average shear rate under the specified fluid flow condition. As stated above, for pseudoplastic fluids ($n < 1$) the extreme at $\beta \rightarrow 0$ corresponds to a Newtonian fluid behaviour and that at $\beta \rightarrow \infty$ a power law fluid behaviour. For dilatant fluids ($n > 1$) the extreme at $\beta \rightarrow \infty$ corresponds to a Newtonian fluid behaviour and that at $\beta \rightarrow 0$ to a power law fluid behaviour. When the rheological parameters of a non-Newtonian fluid, η_0, n and m, are prescribed, β represents the effects of the average velocity, u_{m}, and the hydraulic diameter, D_{h}. β increases with an increase in u_{m} or with a decrease in D_{h} for $n < 1$ and vice versa for $n > 1$.

For obtaining the velocity field besides the dimensionless momentum equation, Eq.(3.56), the dimensionless continuity equation was also applied. The continuity equation in dimensionless form is

$$\int_0^{\frac{1}{2}} u^* dy^* = \frac{1}{2}, \tag{3.64}$$

The dimensionless velocity, u^*, was determined by the finite difference method. Along the vertical axis, y^*, the calculation zone was divided evenly and u^* was calculated from Eqs.(3.56), (3.57) and (3.64). First, we assume the value of fRe_{M} for a given set of parameters: n, β and U^* to solve Eq.(3.56) with Eq.(3.57). Then, Eq.(3.64) is checked by substituting the obtained velocity distribution, u^*, into it. Unless Eq.(3.64) is satisfied within the accuracy of 10^{-5}, a new value of fRe_{M} is assumed. This process is repeated until the correct value of fRe_{M} is obtained. The detailed analysis and results are given in reference [83].

The predictions of friction factor in terms of fRe_{M} are graphically presented as a function of the dimensionless shear rate parameter, β, in Fig.3-11 taking the flow index, n, as a parameter. In these figures the relative velocity of the moving plate, U^*, is -1, 0 and 1, and the effect of parameter β on friction factor is seen. The values of fRe_{M} at the extremes of $\beta \rightarrow 0$ and $\beta \rightarrow \infty$ correspond respectively, to the values of Newtonian fluid and power law fluid. It is seen that the values of fRe_{M} become greater with a decrease in U^*.

The present results corresponding to Newtonian fluids are checked against the available data reported in references [3], [11], [57] and [76], and to power-law fluids are checked against the available data reported in references [57] and [76]. The comparison is given in tabular form in Tables 1.1-1.2 (see Appendix A.1) and the solutions are in excellent agreement within the error of 0.1%.

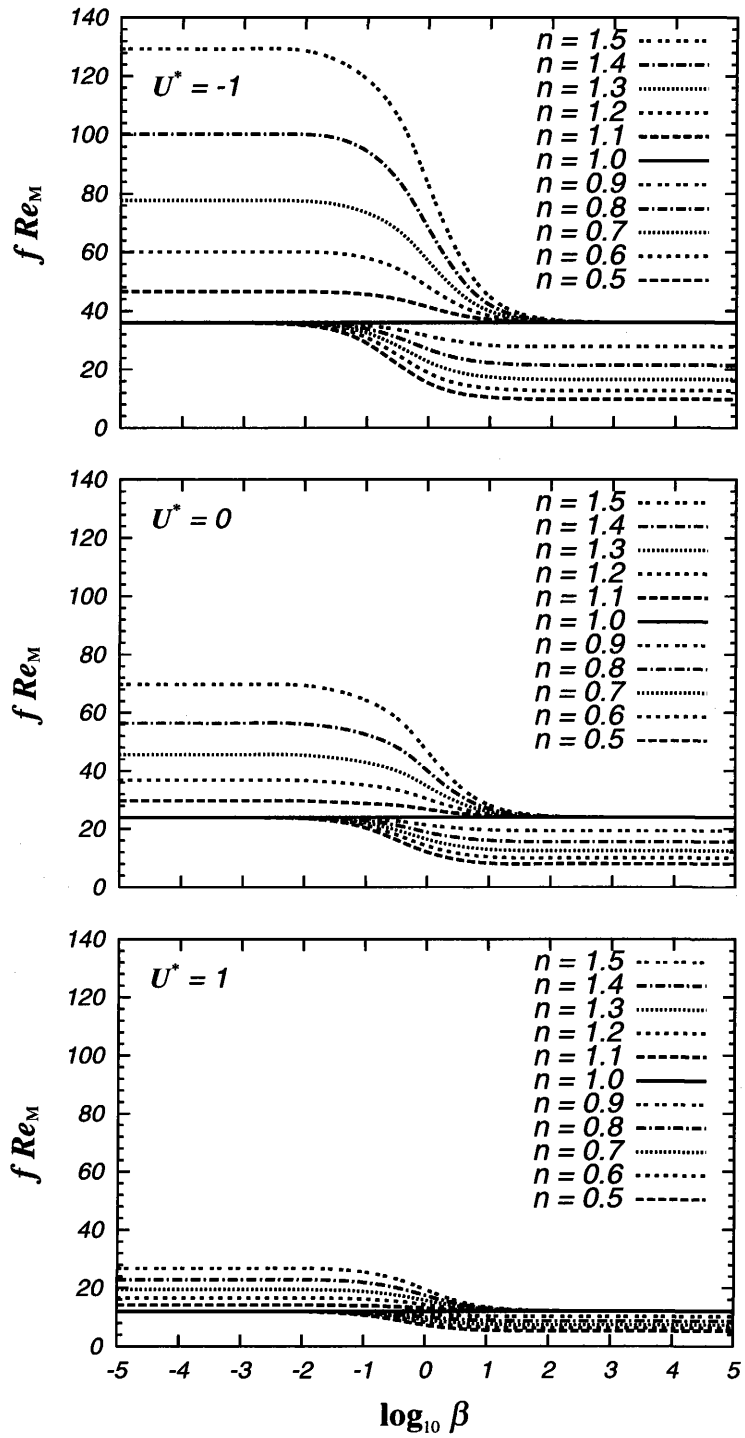

Fig.3-11 Friction factor

Figure 3-12 shows the effect of parameter β on velocity profile, u^*, across the channel for the six combinations of n = 0.5, 1.5 and U^* = -1, 0, 1. For n = 0.5 and n = 1.5 the velocity profiles are different depending on the magnitudes of β and U^*.

In Fig.3-13, the predictions for square of velocity gradient, $(du^*/dy^*)^2$, are presented graphically and these would provide velocity field effects on heat transfer with respect to viscous dissipation.

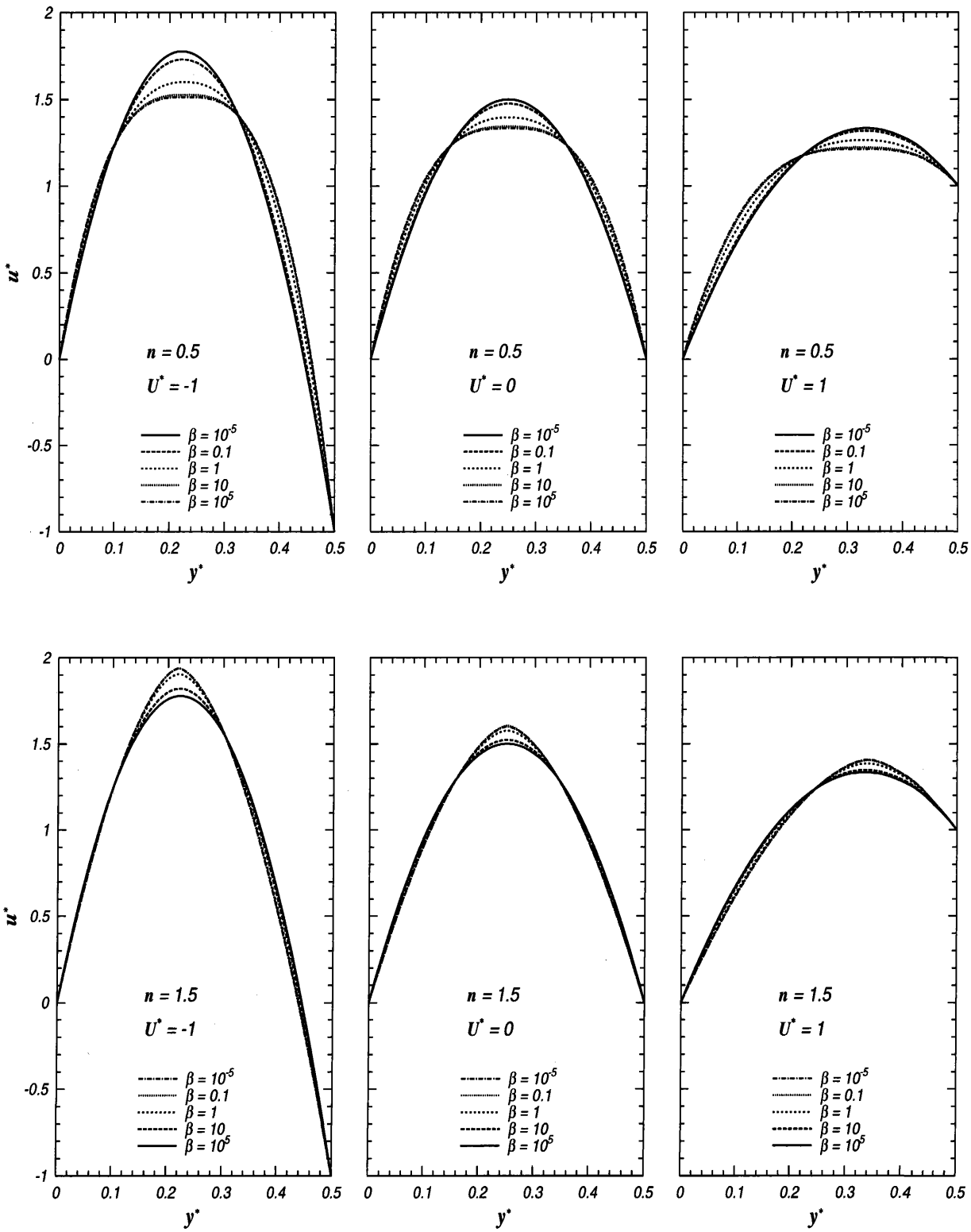

Fig.3-12 Velocity profiles

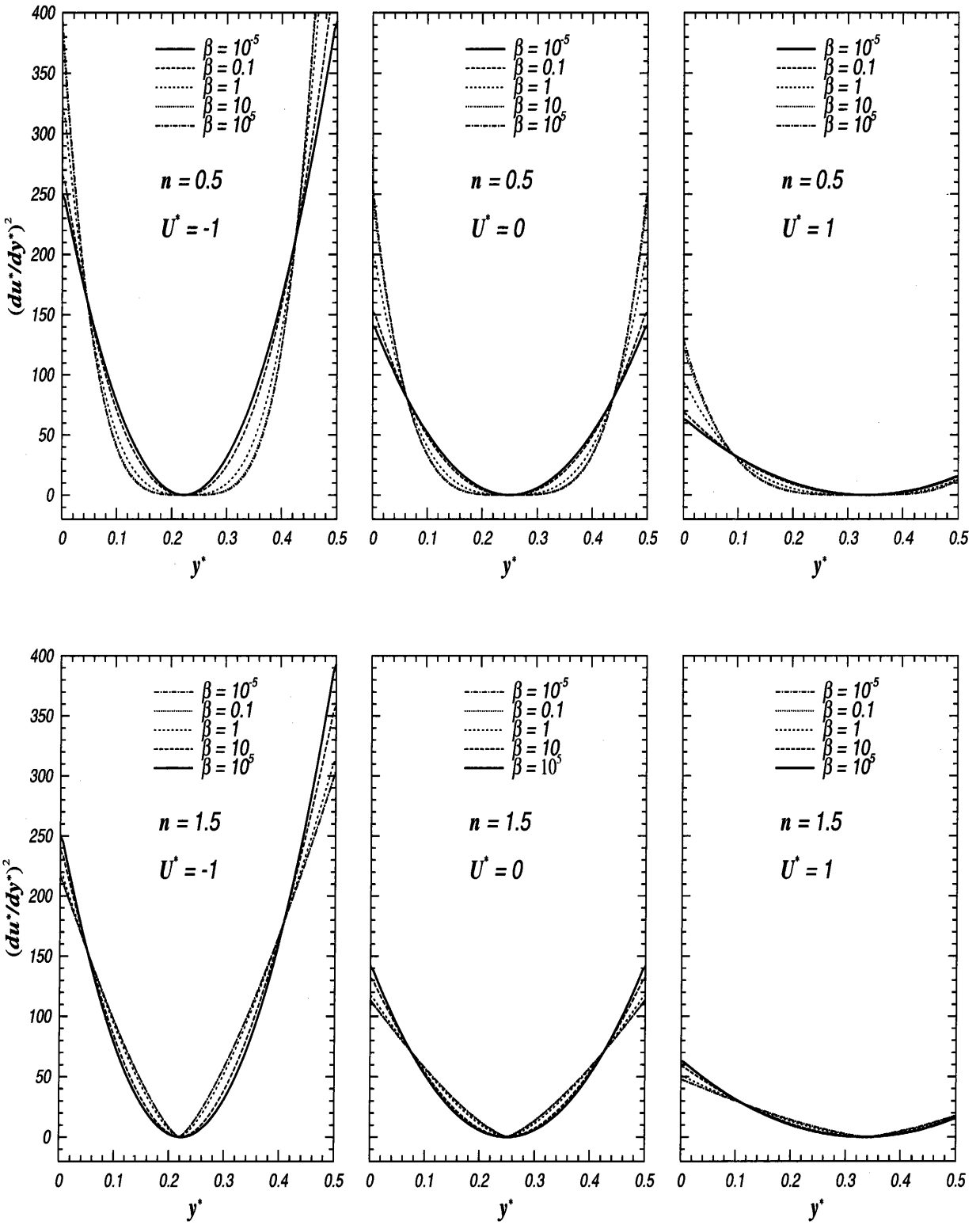

Fig.3-13 Square of velocity gradient

3.5 Summary

The predictions of steady state, hydrodynamically fully developed velocity fields in plane Poiseuille-Couette flow have been obtained for various values of the moving plate velocity. The analytical method has been employed for the flows of Newtonian and power-law fluids and the exact solutions for the velocity distributions are derived. The solutions for the modified power-law fluids, those were obtained by the finite difference method, have been checked against the corresponding exact solutions of the Newtonian fluid and the power-law fluid in this chapter and in literature, and they are in excellent agreement.

The computed variations of the dimensionless velocity profiles across the channel and friction factor are plotted in graphics. The effects of the relative velocity of the moving plate and the rheological parameters of the fluid on the velocity field and on the friction factor are considered.

From the results on the fluid flow study, the following observations can be made.

- The velocity profiles across the channel are greatly affected by the relative velocity of the moving plate.
- The velocity profiles of the different fluids that are the fluids described with different flow index, n, are greatly differ for opposing flows, that is if the plate moves to the opposite direction of the flow. However, for aiding flows, that is if their directions are the same, the effect of n on the velocity profiles is small.
- The friction factor in terms of fRe^* or fRe_{M} decreases with increasing values of the relative velocity, U^*.
- fRe^* is higher for the fluids of higher flow index.

Chapter 4

THERMALLY DEVELOPING POISEUILLE-COUETTE FLOW

The aim of this chapter is to clarify the effects of viscous dissipation and fluid axial heat conduction on the heat transfer in the thermally developing region of plane Poiseuille-Couette flow and Objectives 2 and 3 of the present research are achieved in this chapter. By applying the velocity field obtained in Section 3.4.2, the effects of viscous dissipation and fluid axial heat conduction on the heat transfer are studied numerically. This chapter provides the solutions for the Ⓣ thermal boundary condition and also for the first and second kinds of thermal boundary conditions.

4.1 Problem Formulation

The purpose of this section is to formulate the problem of the heat transfer in the thermally developing region of the plane Poiseuille-Couette flow by including the viscous dissipation and the fluid axial heat conduction. The descriptions of the passage and fluid flow are given in Section 3.2. The physical model for the heat transfer analysis is shown in Figs.4-1, 4-2 and 4-3. Two semi-infinite regions of $-\infty < z \leq 0$ and $0 < z < \infty$ are considered in order to investigate the fluid axial heat conduction effect as the temperature profile at $z = 0$ (where the heating at the wall commences) is affected by the fluid axial heat conduction from downstream. The following assumptions and conditions are applied in the analysis.

- The body forces are neglected.
- The fluid is a modified power-law fluid.

- The entering fluid temperature, T_e, at $z \to -\infty$ is constant.
- Three types of thermal boundary conditions were examined.

Ⓣ **T.B.C.:** Axially symmetric thermal boundary conditions along the walls, in which the walls are kept at the entering fluid temperature in $z \leq 0$, while they are at a constant temperature of T_w in $0 < z$.

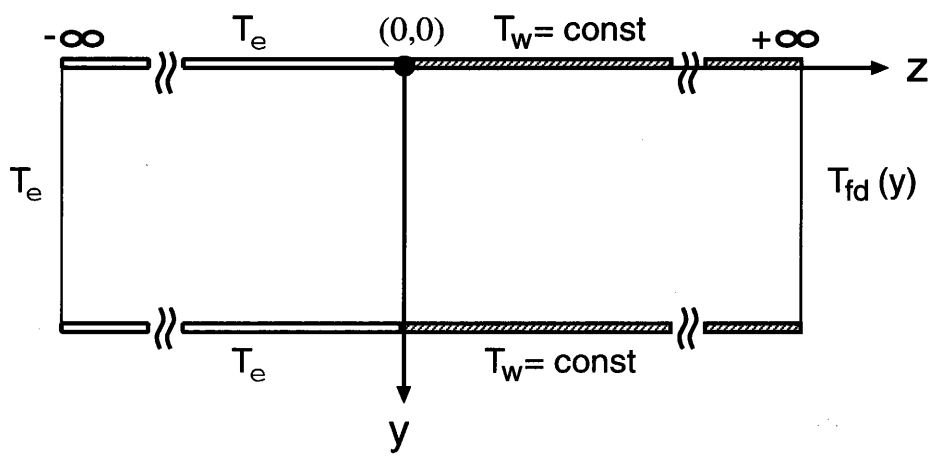

Fig.4-1 Ⓣ thermal boundary condition

The first kind T.B.C.: Within this type of thermal boundary condition, two different cases are examined.

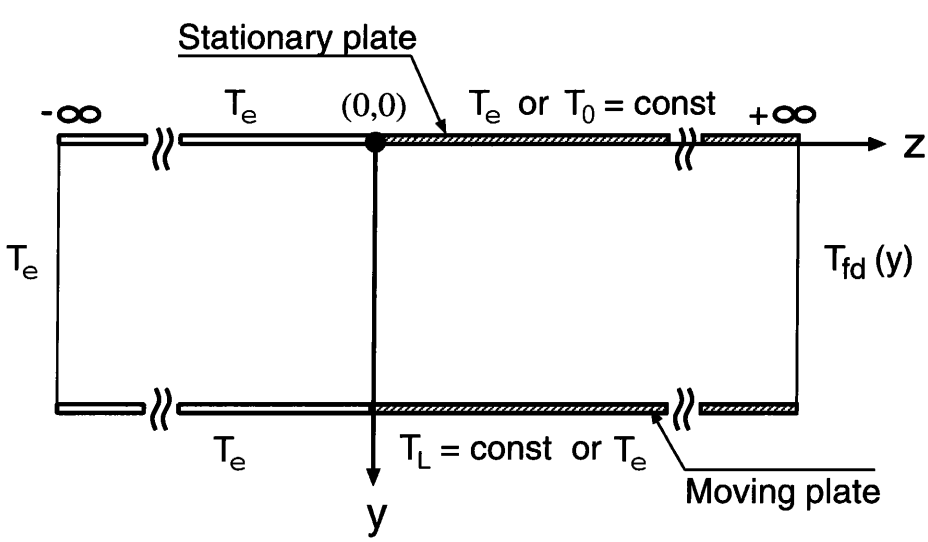

Fig.4-2 The first kind thermal boundary condition

The case of moving plate heated: This case is also referred to Case A. In this case the lower wall is heated at a constant temperature of T_L in $0 < z$. The upper wall temperature is equal to the entering fluid temperature, T_e, everywhere and the lower wall temperature is at T_e in $z \leq 0$.

The case of stationary plate heated: This case is also referred to Case B. In this case the upper wall is heated at a constant temperature of T_0 in $0 < z$. The lower wall temperature is equal to the entering fluid temperature, T_e, everywhere and the upper wall temperature is at T_e in $z \leq 0$.

The second kind T.B.C: Within this type of thermal boundary condition, two different cases were examined.

The case of moving plate heated: This case is also referred to Case A. In this case the lower wall is heated at a constant heat flux, q_L in $0 < z$. The upper wall is insulated everywhere, while the lower wall is insulated in $z \leq 0$.

The case of stationary plate heated: This case is also referred to Case B. In this case the upper wall is heated at a constant heat flux, q_0 in $0 < z$. The lower wall is insulated everywhere, while upper wall is insulated in $z \leq 0$.

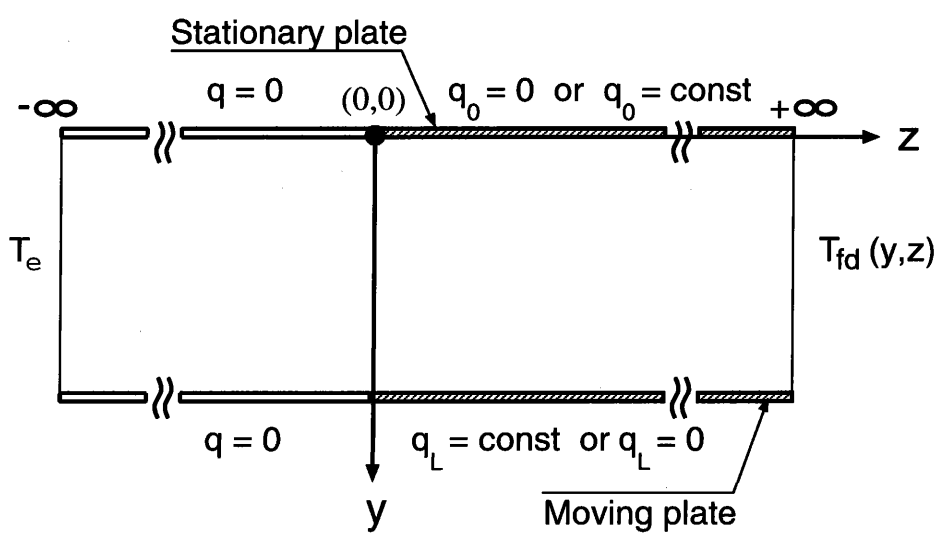

Fig.4-3 The second kind thermal boundary condition

For a detailed explanation about the thermal boundary conditions, the monograph by Lundberg et al. [84] and, Shah and London [11] may be consulted.

The energy equation for the steady laminar flow of a modified power-law fluid with the assumptions above is written as

$$k\left(\frac{\partial^2 T}{\partial y^2}+\frac{\partial^2 T}{\partial z^2}\right)+\eta_a\left(\frac{du}{dy}\right)^2=\rho c_{\mathrm{p}} u\frac{\partial T}{\partial z} \tag{4.1}$$

$$\text{in} \quad 0\le y\le L \quad \text{and} \quad -\infty<z<\infty$$

where k is the thermal conductivity, η_a the fluid apparent viscosity, ρ the fluid density, c_{p} the specific heat, u the fluid velocity, and y and z are coordinates. It is assumed that k, ρ and c_{p} are all constants.

The inclusion of the viscous dissipation alone into the analysis amounts to adding a heat generation term and the governing equation is a parabolic differential equation. However, the incorporation of the effect of the axial heat conduction is directed in an elliptic type equation and requires a major change in solution method. The solution method for the elliptic type energy equation is proposed in Section 4.2.

As it was described above, three types of thermal boundary conditions were examined.

(1) (T) T.B.C.

$$\begin{cases} T=T_e & \text{at} \quad y=0 & \text{for} \quad 0\le z \\ T=T_{\mathrm{w}} & \text{at} \quad y=0 & \text{for} \quad 0<z \\ T=T_e & \text{at} \quad y=L & \text{for} \quad z\le 0 \\ T=T_{\mathrm{w}} & \text{at} \quad y=L & \text{for} \quad 0<z \\ T=T_e & \text{at} \quad 0<y<L & \text{for} \quad z\to-\infty \\ T=T_{fd}(y) & \text{at} \quad 0<y<L & \text{for} \quad z\to+\infty \end{cases} \tag{4.2}$$

(2) The first kind T.B.C.

$$\text{Case A} \quad \begin{cases} T=T_e & \text{at} \quad y=0 & \text{for} \quad -\infty<z<\infty \\ T=T_e & \text{at} \quad y=L & \text{for} \quad z\le 0 \\ T=T_{\mathrm{L}} & \text{at} \quad y=L & \text{for} \quad 0<z \\ T=T_e & \text{at} \quad 0<y<L & \text{for} \quad z\to-\infty \\ T=T_{fd}(y) & \text{at} \quad 0<y<L & \text{for} \quad z\to+\infty \end{cases} \tag{4.3}$$

$$\text{Case B} \quad \begin{cases} T = T_e & \text{at} \quad y = L & \text{for} \quad -\infty < z < \infty \\ T = T_e & \text{at} \quad y = 0 & \text{for} \quad z \leq 0 \\ T = T_0 & \text{at} \quad y = 0 & \text{for} \quad 0 < z \\ T = T_e & \text{at} \quad 0 < y < L & \text{for} \quad z \to -\infty \\ T = T_{fd}(y) & \text{at} \quad 0 < y < L & \text{for} \quad z \to +\infty \end{cases} \tag{4.4}$$

(3) The second kind T.B.C.

$$\text{Case A} \quad \begin{cases} \dfrac{\partial T}{\partial y} = 0 & \text{at} \quad y = 0 & \text{for} \quad -\infty < z < \infty \\ \dfrac{\partial T}{\partial y} = 0 & \text{at} \quad y = L & \text{for} \quad z \leq 0 \\ k\dfrac{\partial T}{\partial y} = q_{\mathrm{L}} & \text{at} \quad y = L & \text{for} \quad 0 < z \\ T = T_e & \text{at} \quad 0 < y < L & \text{for} \quad z \to -\infty \\ T = T_{fd}(y, z) & \text{at} \quad 0 < y < L & \text{for} \quad z \to +\infty \end{cases} \tag{4.5}$$

$$\text{Case B} \quad \begin{cases} \dfrac{\partial T}{\partial y} = 0 & \text{at} \quad y = L & \text{for} \quad -\infty < z < \infty \\ \dfrac{\partial T}{\partial y} = 0 & \text{at} \quad y = 0 & \text{for} \quad z \leq 0 \\ -k\dfrac{\partial T}{\partial y} = q_0 & \text{at} \quad y = 0 & \text{for} \quad 0 < z \\ T = T_e & \text{at} \quad 0 < y < L & \text{for} \quad z \to -\infty \\ T = T_{fd}(y, z) & \text{at} \quad 0 < y < L & \text{for} \quad z \to +\infty \end{cases} \tag{4.6}$$

The bulk temperature, T_{b}, is defined as

$$T_{\mathrm{b}} \equiv \frac{\int_0^L uT dy}{\int_0^L u dy} \tag{4.7}$$

Nusselt number at the walls are calculated as:

$$Nu \equiv \frac{hD_{\mathrm{h}}}{k} \tag{4.8}$$

where the heat transfer coefficients at the walls are

$$h_0 = \frac{q_0}{T_0 - T_{\mathrm{b}}}, \qquad h_{\mathrm{L}} = \frac{q_{\mathrm{L}}}{T_{\mathrm{L}} - T_{\mathrm{b}}} \tag{4.9}$$

$$q_0 = -k\frac{\partial T}{\partial y}\bigg|_{y=0}, \qquad q_{\mathrm{L}} = k\frac{\partial T}{\partial y}\bigg|_{y=L} \tag{4.10}$$

The following dimensionless quantities are introduced

$$z^* = \frac{z}{Pe \cdot D_\mathrm{h}}, \qquad Pe \equiv \frac{\rho c_\mathrm{p} u_\mathrm{m} D_\mathrm{h}}{k} = Re_\mathrm{M} \cdot Pr_\mathrm{M} \tag{4.11}$$

$$\theta^{(1)} = \frac{T^{(1)} - T_e}{T_\mathrm{j}^{(1)} - T_e}, \qquad \theta^{(2)} = \frac{k(T^{(2)} - T_e)}{q_\mathrm{j} D_\mathrm{h}} \tag{4.12}$$

$$Br^{(1)} = \frac{\eta\, u_\mathrm{m}^2}{k(T_\mathrm{j}^{(1)} - T_e)}, \qquad Br^{(2)} = \frac{\eta\, u_\mathrm{m}^2}{q_\mathrm{j} D_\mathrm{h}} \tag{4.13}$$

where $j = \mathrm{L}$ for Case A and $j = 0$ for Case B. The superscripts: (1) and (2) indicate the first kind T.B.C. and the second kind T.B.C., respectively. For (T) thermal boundary condition, the definitions of θ and Br are the same as those for the first kind T.B.C. except that the subscript $j = \mathrm{w}$.

With the substitution of the above quantities into the dimensional formulations, the dimensionless energy equation and boundary conditions are reduced to

$$\frac{\partial^2 \theta}{\partial y^{*2}} + \frac{1}{Pe^2}\frac{\partial^2 \theta}{\partial z^{*2}} + Br\, \eta_a^* \left(\frac{du^*}{dy^*}\right)^2 = u^* \frac{\partial \theta}{\partial z^*} \tag{4.14}$$

$$\text{in} \quad 0 \le y^* \le \frac{1}{2} \quad \text{and} \quad -\infty < z^* < \infty$$

(1) (T) T.B.C

$$\begin{cases} \theta = 0 & \text{at} \quad y^* = 0 & \text{for} \quad 0 \le z^* \\ \theta = 1 & \text{at} \quad y^* = 0 & \text{for} \quad 0 < z^* \\ \theta = 0 & \text{at} \quad y^* = \frac{1}{2} & \text{for} \quad z^* \le 0 \\ \theta = 1 & \text{at} \quad y^* = \frac{1}{2} & \text{for} \quad 0 < z^* \\ \theta = 0 & \text{at} \quad 0 < y^* < \frac{1}{2} & \text{for} \quad z^* \to -\infty \\ \theta = \theta_{fd}(y^*) & \text{at} \quad 0 < y^* < \frac{1}{2} & \text{for} \quad z^* \to +\infty \end{cases} \tag{4.15}$$

(2) The first kind T.B.C.

$$\text{Case A} \quad \begin{cases} \theta = 0 & \text{at} \quad y^* = 0 & \text{for} \quad -\infty < z^* < \infty \\ \theta = 0 & \text{at} \quad y^* = \frac{1}{2} & \text{for} \quad z^* \leq 0 \\ \theta = 1 & \text{at} \quad y^* = \frac{1}{2} & \text{for} \quad 0 < z^* \\ \theta = 0 & \text{at} \quad 0 < y^* < \frac{1}{2} & \text{for} \quad z^* \to -\infty \\ \theta = \theta_{fd}(y^*) & \text{at} \quad 0 < y^* < \frac{1}{2} & \text{for} \quad z^* \to +\infty \end{cases} \tag{4.16}$$

$$\text{Case B} \quad \begin{cases} \theta = 0 & \text{at} \quad y^* = \frac{1}{2} & \text{for} \quad -\infty < z^* < \infty \\ \theta = 0 & \text{at} \quad y^* = 0 & \text{for} \quad z^* \leq 0 \\ \theta = 1 & \text{at} \quad y^* = 0 & \text{for} \quad 0 < z^* \\ \theta = 0 & \text{at} \quad 0 < y^* < \frac{1}{2} & \text{for} \quad z^* \to -\infty \\ \theta = \theta_{fd}(y^*) & \text{at} \quad 0 < y^* < \frac{1}{2} & \text{for} \quad z^* \to +\infty \end{cases} \tag{4.17}$$

(3) The second kind T.B.C.

$$\text{Case A} \quad \begin{cases} \frac{\partial \theta}{\partial y^*} = 0 & \text{at} \quad y^* = 0 & \text{for} \quad -\infty < z^* < \infty \\ \frac{\partial \theta}{\partial y^*} = 0 & \text{at} \quad y^* = \frac{1}{2} & \text{for} \quad z^* \leq 0 \\ \frac{\partial \theta}{\partial y^*} = 1 & \text{at} \quad y^* = \frac{1}{2} & \text{for} \quad 0 < z^* \\ \theta = 0 & \text{at} \quad 0 < y^* < \frac{1}{2} & \text{for} \quad z^* \to -\infty \\ \theta = \theta_{fd}(y^*, z^*) & \text{at} \quad 0 < y^* < \frac{1}{2} & \text{for} \quad z^* \to +\infty \end{cases} \tag{4.18}$$

$$\text{Case B} \quad \begin{cases} \frac{\partial \theta}{\partial y^*} = 0 & \text{at} \quad y^* = \frac{1}{2} & \text{for} \quad -\infty < z^* < \infty \\ \frac{\partial \theta}{\partial y^*} = 0 & \text{at} \quad y^* = 0 & \text{for} \quad z^* \leq 0 \\ \frac{\partial \theta}{\partial y^*} = -1 & \text{at} \quad y^* = 0 & \text{for} \quad 0 < z^* \\ \theta = 0 & \text{at} \quad 0 < y^* < \frac{1}{2} & \text{for} \quad z^* \to -\infty \\ \theta = \theta_{fd}(y^*, z^*) & \text{at} \quad 0 < y^* < \frac{1}{2} & \text{for} \quad z^* \to +\infty \end{cases} \tag{4.19}$$

Information on the fluid flow which is required in solving the energy equation: η_a^*, du^*/dy^*, and u^* were obtained in Section 3.4.2. By applying them the energy equation (Eq.4.14) is solved and the temperature distribution in an infinite axial domain is obtained. Nusselt numbers at the walls are:

(1) Ⓣ T.B.C.

$$Nu_{\mathrm{w}} = -\frac{1}{(\theta_{\mathrm{w}} - \theta_{\mathrm{b}})}\frac{\partial\theta}{\partial y^*}\bigg|_{y^*=0} \quad \text{or} \quad Nu_{\mathrm{w}} = \frac{1}{(\theta_{\mathrm{w}} - \theta_{\mathrm{b}})}\frac{\partial\theta}{\partial y^*}\bigg|_{y^*=1/2} \tag{4.20}$$

(2) The first kind T.B.C.

$$Nu_0^{(1)} = -\frac{1}{\theta_0^{(1)} - \theta_{\mathrm{b}}^{(1)}}\frac{\partial\theta^{(1)}}{\partial y^*}\bigg|_{y^*=0} \qquad Nu_{\mathrm{L}}^{(1)} = \frac{1}{\theta_{\mathrm{L}}^{(1)} - \theta_{\mathrm{b}}^{(1)}}\frac{\partial\theta^{(1)}}{\partial y^*}\bigg|_{y^*=1/2} \tag{4.21}$$

(3) The second kind T.B.C.

$$Nu_j^{(2)} = \frac{1}{\theta_j^{(2)} - \theta_{\mathrm{b}}^{(2)}} \tag{4.22}$$

Where, θ_{b}, the bulk temperature in the dimensionless form is

$$\theta_{\mathrm{b}}^{(\mathrm{k})} \equiv 2\int_0^{1/2} u^*\theta^{(\mathrm{k})}dy^* \qquad (\mathrm{k} = 1 \text{ or } 2) \tag{4.23}$$

4.2 Solution Method

In this section, the method to solve the elliptic type energy equation is proposed and the associated numerical procedure is outlined. Two complexities arise for solving the energy equation as an elliptic type problem. One is related with the semi-infinite domain and the other is the necessity of an additional boundary condition.

4.2.1 Additional Condition

For solving elliptic type equations the boundary conditions are needed on all of the boundaries [85]. The boundary conditions at the inlet and at the walls are already specified. However one more boundary condition is needed at the downstream infinity.

Ⓣ T.B.C. and the first kind T.B.C.

For infinitely large values of the axial distance ($z^* \to \infty$), thermally fully developed region is reached. For Ⓣ T.B.C. and for the first kind T.B.C., in the fully developed region the dimensionless temperature is a function of y^* alone [44], [46],

[52] and [62]. According to this limitation the dimensionless temperature θ_{fd} was determined as the particular solution of the following equation.

$$\frac{\partial^2 \theta_{fd}}{\partial y^{*2}} = -Br\ \eta_a^* \left(\frac{du^*}{dy^*}\right)^2 \tag{4.24}$$

(1) (T) T.B.C.

$$\begin{cases} \theta_{fd} = 1 \text{ at } y^* = 0 \\ \theta_{fd} = 1 \text{ at } y^* = \dfrac{1}{2} \end{cases} \tag{4.25}$$

(2) The first kind T.B.C.

$$\text{Case A} \quad \begin{cases} \theta_{fd} = 0 \text{ at } y^* = 0 \\ \theta_{fd} = 1 \text{ at } y^* = \dfrac{1}{2} \end{cases} \tag{4.26}$$

$$\text{Case B} \quad \begin{cases} \theta_{fd} = 1 \text{ at } y^* = 0 \\ \theta_{fd} = 0 \text{ at } y^* = \dfrac{1}{2} \end{cases} \tag{4.27}$$

The second kind T.B.C.

For the second kind of T.B.C., since the thermal boundary condition is different, the fully developed temperature profile is calculated differently from the first kind of T.B.C. To seek the expression of θ_{fd}, a solution of the following form is assumed on the fact that in the thermally fully developed region, the constant heat flux through the wall will result in a rise of the fluid temperature linearly with the axial coordinate [44], [46] and [50].

$$\theta_{fd} = Cz^* + \psi(y^*) \tag{4.28}$$

Substitution of Eq.(4.28) into Eq.(4.14) yields

$$\frac{d^2\psi}{dy^{*2}} = Cu^* - V \tag{4.29}$$

$$\text{Case A} \quad \begin{cases} \dfrac{d\psi}{dy^*} = 0 \text{ at } y^* = 0 \\ \dfrac{d\psi}{dy^*} = 1 \text{ at } y^* = \dfrac{1}{2} \end{cases} \tag{4.30}$$

$$\text{Case B} \quad \begin{cases} \dfrac{d\psi}{dy^*} = -1 \quad \text{at} \quad y^* = 0 \\ \dfrac{d\psi}{dy^*} = 0 \quad \text{at} \quad y^* = \dfrac{1}{2} \end{cases} \tag{4.31}$$

where

$$V = Br\ \eta_a^* \left(\frac{du^*}{dy^*}\right)^2 \tag{4.32}$$

On the other hand, as it will be discussed in Section 5.2.2 (see Eq.(5.29)) in the thermally fully developed region

$$\frac{\partial^2 \theta_{fd}}{\partial y^{*2}} = 2u^* \left(1 + \int_0^{0.5} V dy^*\right) - V \tag{4.33}$$

From Eqs.(4.28) and (4.33), the coefficient C in Eq.(4.29) is obtained as

$$C = 2\left(1 + \int_0^{0.5} V dy^*\right) \tag{4.34}$$

$\psi(y^*)$ was calculated from Eq.(4.29) with Eq.(4.30) by the finite difference method. The calculation results of θ_{fd} for (T) T.B.C. and the first and second kinds T.B.C. were used as the boundary conditions at downstream infinity.

4.2.2 Infinite Domain and Mesh System

As stated previously in Section 4.1 that the two semi-infinite regions are necessary for the investigation of the fluid axial heat conduction. Of particular importance to apply the two semi-infinite region was the need to ensure a domain that is placed upstream of any regions where the fluid axial heat conduction from downstream to upstream would occur. However, the appropriate extension length is not known a prior and this length can be adjusted by applying the following transform for the dimensionless axial coordinate, z^*.

$$z^* = E \tan(\pi z_t^*) \qquad \text{or} \qquad z_t^* = \frac{1}{\pi} \arctan \frac{z^*}{E} \tag{4.35}$$

The above tangent transverse transform was employed also by Fuller and Samuels [85], Verhoff and Fisher [86], Ku and Hatziavramidis [87] and by Campo and Auguste [88] those studied the fluid axial heat conduction effects. By applying the above transformation, upstream infinity at $z^* \to -\infty$ and downstream infinity at $z^* \to \infty$ are converted to z_t^* = -0.5 and z_t^* = 0.5, respectively. The locations at the upstream and downstream infinities or the length of the two semi-infinite regions are justified

by changing the constant of the axial transformation, E, in Eq.(4.35). Larger values of E correspond to larger solution zone and it will be discussed later in this section.

By introducing the transformed coordinate z_t^*, the energy equation becomes

$$l_1 \frac{\partial \theta}{\partial z_t^*} = \frac{\partial^2 \theta}{\partial y^{*2}} + l_2 \frac{\partial^2 \theta}{\partial z_t^{*2}} + \eta_a^* Br \left(\frac{du^*}{dy^*} \right)^2 \tag{4.36}$$

$$\text{in} \quad 0 \leq y^* \leq \frac{1}{2} \quad \text{and} \quad -0.5 \leq z_t^* \leq 0.5$$

where

$$l_1 = \frac{\cos^2(\pi z_t^*)}{\pi E} \left[u^* + \frac{1}{Pe^2} \frac{\sin(2\pi z_t^*)}{E} \right] \qquad \text{and} \qquad l_2 = \frac{1}{Pe^2} \left[\frac{\cos^2(\pi z_t^*)}{\pi E} \right]^2 \tag{4.37}$$

The solution zone for the transformed energy equation is now a finite domain of $0 \leq y^* \leq 0.5$ and $-0.5 \leq z_t^* \leq +0.5$ and the boundary conditions become:

(1) (T) T.B.C.

$$\begin{cases} \theta = 0 & \text{at} \quad y^* = 0 & \text{for} \quad 0 \leq z^* \\ \theta = 1 & \text{at} \quad y^* = 0 & \text{for} \quad 0 < z^* \\ \theta = 0 & \text{at} \quad y^* = \frac{1}{2} & \text{for} \quad z^* \leq 0 \\ \theta = 1 & \text{at} \quad y^* = \frac{1}{2} & \text{for} \quad 0 < z^* \\ \theta = 0 & \text{at} \quad 0 < y^* < \frac{1}{2} & \text{for} \quad z_t^* = -0.5 \\ \theta = \theta_{fd}(y^*) & \text{at} \quad 0 < y^* < \frac{1}{2} & \text{for} \quad z_t^* = 0.5 \end{cases} \tag{4.38}$$

(2) The first kind T.B.C.

$$\text{Case A} \quad \begin{cases} \theta = 0 & \text{at} \quad y^* = 0 & \text{for} \quad -0.5 < z_t^* < 0.5 \\ \theta = 0 & \text{at} \quad y^* = \frac{1}{2} & \text{for} \quad z_t^* \leq 0 \\ \theta = 1 & \text{at} \quad y^* = \frac{1}{2} & \text{for} \quad 0 < z_t^* \\ \theta = 0 & \text{at} \quad 0 < y^* < \frac{1}{2} & \text{for} \quad z_t^* = -0.5 \\ \theta = \theta_{fd}(y^*) & \text{at} \quad 0 < y^* < \frac{1}{2} & \text{for} \quad z_t^* = 0.5 \end{cases} \tag{4.39}$$

$$\text{Case B} \quad \begin{cases} \theta = 0 & \text{at} \quad y^* = \frac{1}{2} & \text{for} \quad -0.5 < z_t^* < 0.5 \\ \theta = 0 & \text{at} \quad y^* = 0 & \text{for} \quad z_t^* \leq 0 \\ \theta = 1 & \text{at} \quad y^* = 0 & \text{for} \quad 0 < z_t^* \\ \theta = 0 & \text{at} \quad 0 < y^* < \frac{1}{2} & \text{for} \quad z_t^* = -0.5 \\ \theta = \theta_{fd}(y^*) & \text{at} \quad 0 < y^* < \frac{1}{2} & \text{for} \quad z_t^* = 0.5 \end{cases} \tag{4.40}$$

(3) The second kind T.B.C.

$$\text{Case A} \quad \begin{cases} \frac{\partial \theta}{\partial y^*} = 0 & \text{at} \quad y^* = 0 & \text{for} \quad -0.5 < z_t^* < 0.5 \\ \frac{\partial \theta}{\partial y^*} = 0 & \text{at} \quad y^* = \frac{1}{2} & \text{for} \quad z_t^* \leq 0 \\ \frac{\partial \theta}{\partial y^*} = 1 & \text{at} \quad y^* = \frac{1}{2} & \text{for} \quad 0 < z_t^* \\ \theta = 0 & \text{at} \quad 0 < y^* < \frac{1}{2} & \text{for} \quad z_t^* = -0.5 \\ \theta = \theta_{fd} & \text{at} \quad 0 < y^* < \frac{1}{2} & \text{for} \quad z_t^* = 0.5 \end{cases} \tag{4.41}$$

$$\text{Case B} \quad \begin{cases} \frac{\partial \theta}{\partial y^*} = 0 & \text{at} \quad y^* = \frac{1}{2} & \text{for} \quad -0.5 < z_t^* < 0.5 \\ \frac{\partial \theta}{\partial y^*} = 0 & \text{at} \quad y^* = 0 & \text{for} \quad z_t^* \leq 0 \\ \frac{\partial \theta}{\partial y^*} = -1 & \text{at} \quad y^* = 0 & \text{for} \quad 0 < z_t^* \\ \theta = 0 & \text{at} \quad 0 < y^* < \frac{1}{2} & \text{for} \quad z_t^* = -0.5 \\ \theta = \theta_{fd} & \text{at} \quad 0 < y^* < \frac{1}{2} & \text{for} \quad z_t^* = 0.5 \end{cases} \tag{4.42}$$

The solutions for the temperature field of the plane Poiseuille-Couette flow are acquired by solving Eq.(4.36) along with the associated boundary conditions Eqs.(4.38) - (4.42).

The solution domain was divided with a mesh system proposed by the author and the numerical approach employed for the system equations was based on Gauss-

Seidel method. The proposed mesh system was consisted of denser grids near $z_t^* = 0$ to allow more accurate representation of the fluid axial heat conduction effect. The finest mesh was used next to $z_t^* = 0$ and as the location of the node goes farther from the origin, the mesh size was increased with a ratio

$$\sigma = \Delta z_{t,n}^* / \Delta z_{t,n-1}^* \tag{4.43}$$

Where $\Delta z_{t,n}^*$ and $\Delta z_{t,n-1}^*$ are the mesh sizes along the axial coordinate in the vicinity. Mesh system was built as mesh spacing continually decreases with the degree of σ in the upstream region as it approaches to $z_t^* = 0$, while it increases from $z_t^* = 0$ at each node by ratio of σ in the downstream part of the calculation zone. But along the vertical axis the solution zone was divided evenly.

The calculation has been carried out with two steps in order to get the results with high accuracy. First, the temperature at every node in the whole region of $-0.5 \leq z_t^* \leq 0.5$ and $0 \leq y^* \leq 0.5$ has been calculated. Then by using the calculation results of the temperature at the axial coordinates of $z^* = 0$ and $z^* = 1.001$, more accurately calculated temperature profiles at the thermally developing region have been obtained. In the first step the finest mesh spacing was $\Delta z_t^* = 1.059 \times 10^{-7}$ and, mesh size was changed with the ratio $\Delta z_{t,n-1}^* / \Delta z_{t,n}^* = 1.33$ for $z_t^* < 0$ and $\Delta z_{t,n}^* / \Delta z_{t,n-1}^* = 1.33$ for $0 < z_t^*$. In the second step, the finest mesh spacing was $\Delta z_t^* = 4.93 \times 10^{-7}$ and the ratio was $\Delta z_{t,n}^* / \Delta z_{t,n-1}^* = 1.02$. Subdividing in this manner yielded a more closely spaced mesh in terms of the physical coordinates z^* in the thermal entrance region.

Constant of the axial transformation, E, was chosen as 4.62 for the first kind T.B.C. in both calculation steps. For the second kind T.B.C., E was chosen as unity. For $E = 4.62$, the calculation zone was within $-7.5 \times 10^{16} \leq z^* \leq 7.5 \times 10^{16}$ and for $E = 1$ it was $-1.6 \times 10^{16} \leq z^* \leq 1.6 \times 10^{16}$.

In order to decide on the values of σ and E, a numerical experiment has been performed. Then the obtained results for the limiting special cases of negligible viscous dissipation and fluid axial heat conduction were checked against the exact solutions by Shah and London in reference [11]. It was found that the accuracy of the solution does not depend on the value E, however for smaller σ and the agreement was superior.

4.3 Effects of Viscous Dissipation and Axial Heat Conduction

In order to study the effects of viscous dissipation and fluid axial heat conduction on the heat transfer for the plane Poiseuille-Couette flow, the computations were carried out for the values of the independent governing parameters of:

Relative velocity of the moving lower wall, U^*:

$U^* = 0$ (Poiseuille flow) and $U^* = 1$ (Poiseuille-Couette flow)

Brinkman number, Br:

$Br = 0$ (negligible viscous dissipation); $Br = 0.05$, 0.1, 0.5 and 1

Peclet number, Pe:

$Pe = 5$, 10, 20, 50, 100 and $Pe \rightarrow \infty$ (negligible fluid axial heat conduction)

Flow index, n:

$n = 1$ (Newtonian fluid), $n = 0.5$ (pseudoplastic fluid), $n = 1.5$ (dilatant fluid)

Dimensionless shear rate parameter, β:

$\beta \rightarrow 0$, $\beta \rightarrow \infty$ (asymptotes showing Newtonian or power-law fluid behaviors) and $\beta = 1$.

The temperature field throughout the region of $-\infty < z^* < \infty$ and $0 \leq y^* \leq 1/2$ has been calculated with the above parameters. In this section, the results are presented and discussed in terms of the temperature profiles across the channel and of the axial developments of bulk temperature and Nusselt number. The axial developments of bulk temperature and Nusselt number are depicted for the heated wall region or for $0 < z^*$, since the thermally developing region, namely, the region in $0 < z^*$ is of interest.

The problem as stated in Eq.(4.14) is completely described by 7 parameters (θ, Br, Pe, u^*, η_a^*, y^* and z^*) together with the boundary conditions. The investigation of the results for this numerical study on the forced convection in the plane Poiseuille-Couette flow is presented by considering the factors that affect the heat transfer such as the relative velocity of the lower plate, the rheological parameters, the viscous dissipation, the fluid axial heat conduction and the thermal boundary conditions.

In order to verify the accuracy of the present solutions, the results for special case studies are compared with the data sets published in the open literature. As it was

noted in Chapter 2, there are no data on the thermally developing Poiseuille-Couette flow of modified power law fluids, the corresponding fully developed heat transfer study results in Chapter 5.2.2 were applied to check the validity of the solutions in this chapter.

Various relevant results and figures have been discussed from the view point of viscous dissipation and fluid axial heat conduction phenomena in the plane Poiseuille flow. Brinkman number is proposed to serve as a controlling index that indicates the relative importance of viscous dissipation. Peclet number is proposed to serve as a controlling index that indicates the relative importance of fluid axial heat conduction. Since the thermal boundary conditions influence the heat transfer in a large extent, the results are discussed for each boundary condition separately.

4.3.1 Ⓣ Thermal Boundary Condition

In this subsection, the effects of viscous dissipation and fluid axial heat conduction on the heat transfer are discussed for the Poiseuille flows with Ⓣ thermal boundary condition. There exist appreciable amount of data for this thermal boundary condition and comparisons were made with the available data by other researchers.

The variations of local temperature profiles with Br and Pe are shown in Fig.4-4 for a Newtonian fluid ($n = 1$). The upper two figures, Figs.4-4(a) and 4-4(b), are for the case where the viscous dissipation term is neglected ($Br = 0$) and the lower two figures are for $Br = 0.1$. By scanning each row one would observe the fluid axial heat conduction effect (in terms of Pe) on the developing temperature distributions. If one scans each column of these figures the effect of viscous dissipation (in terms of Br) would be observed.

$y^* = 0$ corresponds to the upper wall and $y^* = 0.5$ is the lower wall. In these figures the solid lines stand for the local temperature development at $z^* = 0$. At $z^* = 0$, there is a step change in the wall temperature. The other axial locations of z^* in these figures were chosen arbitrarily without any special criteria. For example, the local temperature profiles at $z^* = -5.8 \times 10^{-3}$ and $z^* = -1.4 \times 10^{-3}$ just represent local developing temperature profiles in the fluid before it reaches the heated walls. The local temperature profiles at the three locations namely, $z^* = 5.8 \times 10^{-3}$, $z^* = 2.4 \times 10^{-2}$ and $z^* = 5.7 \times 10^{-2}$ are representatives of the temperature distributions in the thermal entrance range. The local temperature profile at $z^* = 1.8$ is one of the local temperature profiles in the fully developed region.

Figures 4-4(a) and 4-4(b) show the case of $Br = 0$, that is, the fluid experiences

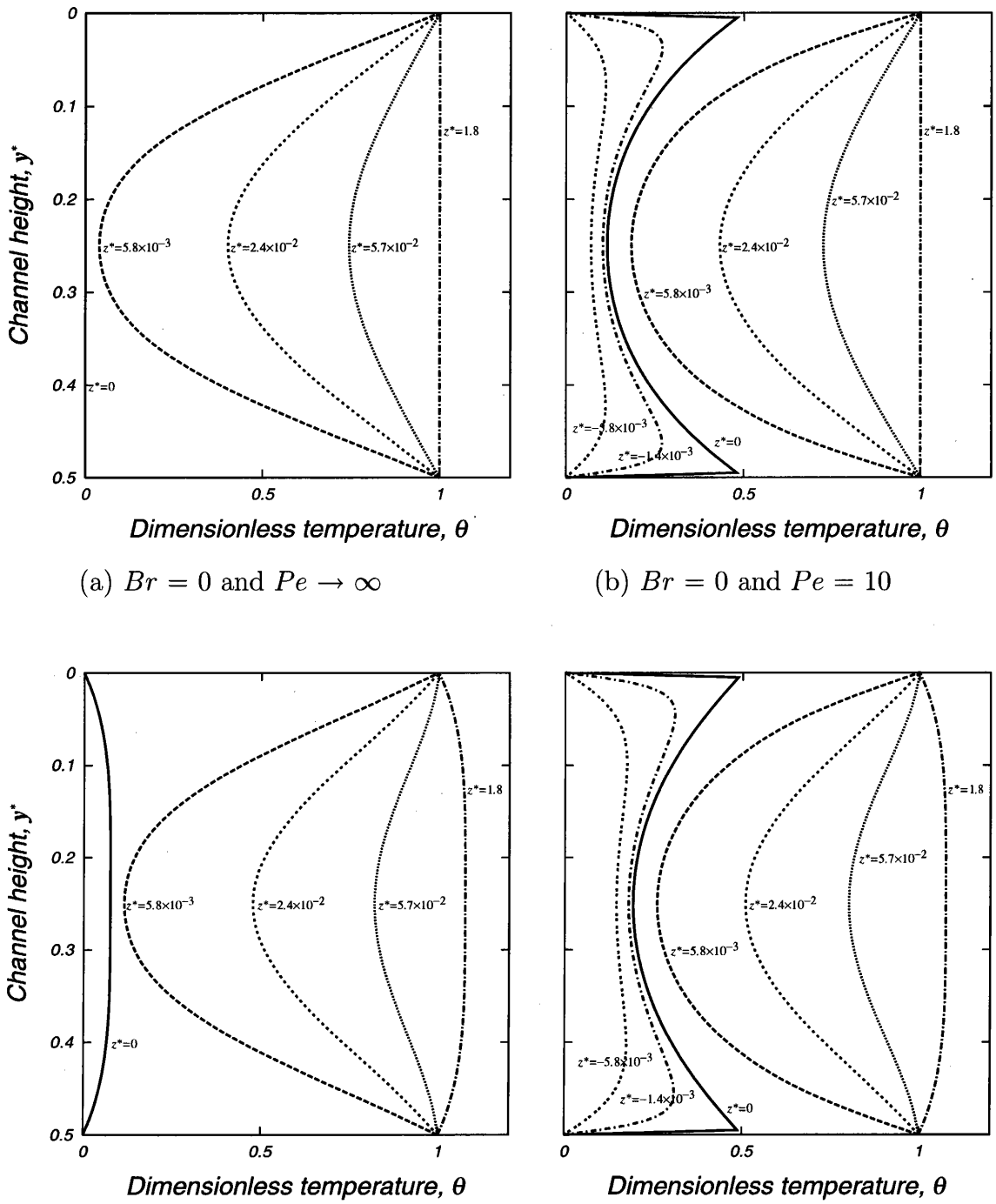

(a) $Br = 0$ and $Pe \to \infty$

(b) $Br = 0$ and $Pe = 10$

(c) $Br = 0.1$ and $Pe \to \infty$

(d) $Br = 0.1$ and $Pe = 10$

Fig.4-4 Developing temperature profiles ($n = 1$) for (T) thermal boundary condition. (a) Negligible viscous dissipation and fluid axial heat conduction: $Br = 0$ and $Pe \to \infty$. (b) Negligible viscous dissipation and considerable fluid axial heat conduction: $Br = 0$ and $Pe = 10$. (c) Considerable viscous dissipation and negligible fluid axial heat conduction: $Br = 0.1$ and $Pe \to \infty$. (d) Both viscous dissipation and fluid axial heat conduction are considerable: $Br = 0.1$ and $Pe = 10$.

no gain of heat due to viscous dissipation. In Fig.4-4(a), for $Pe \to \infty$ and $Br = 0$, at $z^* = 0$ $(0 \leq y^* \leq 0.5)$ the dimensionless temperature of the fluid, θ, is zero. But for $Pe = 10$ and $Br = 0$ in Fig.4-4(b) the fluid temperature increase is occurred for negative values of z^*. This indicates that the temperature increase is due to the fluid axial heat conduction and that the influence of axial heat conduction in the fluid for $z^* \leq 0$ vanishes with an increasing Peclet number. From Figs.4-4(c) and 4-4(d) for $Br = 0.1$, it can be seen that the dimensionless temperature of the fluid for $z^* \leq 0$ deviates definitely from zero. In Fig.4-4(c), the increase of the fluid temperature in $z^* \leq 0$ is due to the contribution of viscous dissipation in the flowing fluid. As the viscous dissipation effect builds up, heat is transferred to the main body of the fluid flow and heat generation due to viscous dissipation behaves like a heat source, increasing the fluid temperature as it is seen. Also by comparing the local temperature profiles at the fully developed region ($z^* = 1.8$) in Figs.4-4(a) and 4-4.(c), it is seen that the corresponding linear profile for $Br = 0$ is distorted by the viscous dissipation effect for $Br = 0.1$. Scanning the figures in the second row, it can be observed from the temperature developments that the fluid temperature increases before the fluid reaches the heated wall region because of the heat generated by viscous dissipation and the heat conducted from downstream into the region of $z \leq 0$.

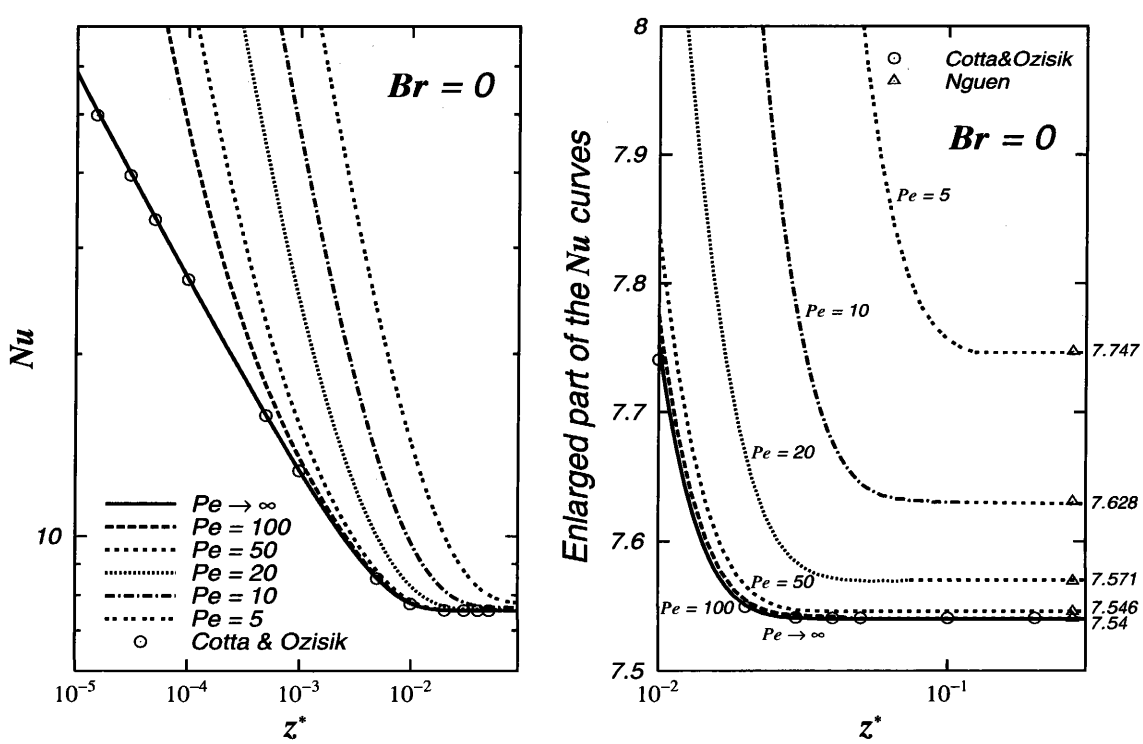

Fig.4-5 Nusselt number for different Peclet numbers ($n = 1$, $Br = 0$)

In the above figures the heat transfer results are illustrated in terms of the conventional Nusselt number at the wall. Figure 4-5 presents the results in the thermally developing range for a Newtonian fluid. In this figure, the Nusselt number is shown as a function of the axial coordinate with Peclet number as a parameter. These Nusselt curves are for the case of the neglected viscous dissipation term by setting the Brinkman number value as zero. It is worthwhile to compare the present results with those reported by Cotta and Ozisik [59] who presented the results for the limiting case of neglected viscous dissipation and fluid axial heat conduction. Even at small values of z^*, the agreement is excellent. In the figure on the right side, the Nusselt number curves are enlarged. The circles show the results by Cotta and Ozisik [59] and the triangles are the results by Nguyen [61].

The effects of both Peclet number and Brinkman number on the Nusselt number are demonstrated in figures from Fig.4-6 to Fig.4-8 for Newtonian ($n = 1$), pseudo-plastic ($n = 0.5$) and dilatant ($n = 1.5$) fluids, respectively. The solid lines stand for the case of negligible viscous dissipation. The dashed lines are the Nusselt curves for non-zero Brinkman numbers. In this study, according to the Brinkman number definition, for minus Brinkman numbers the fluid is considered as being cooled and

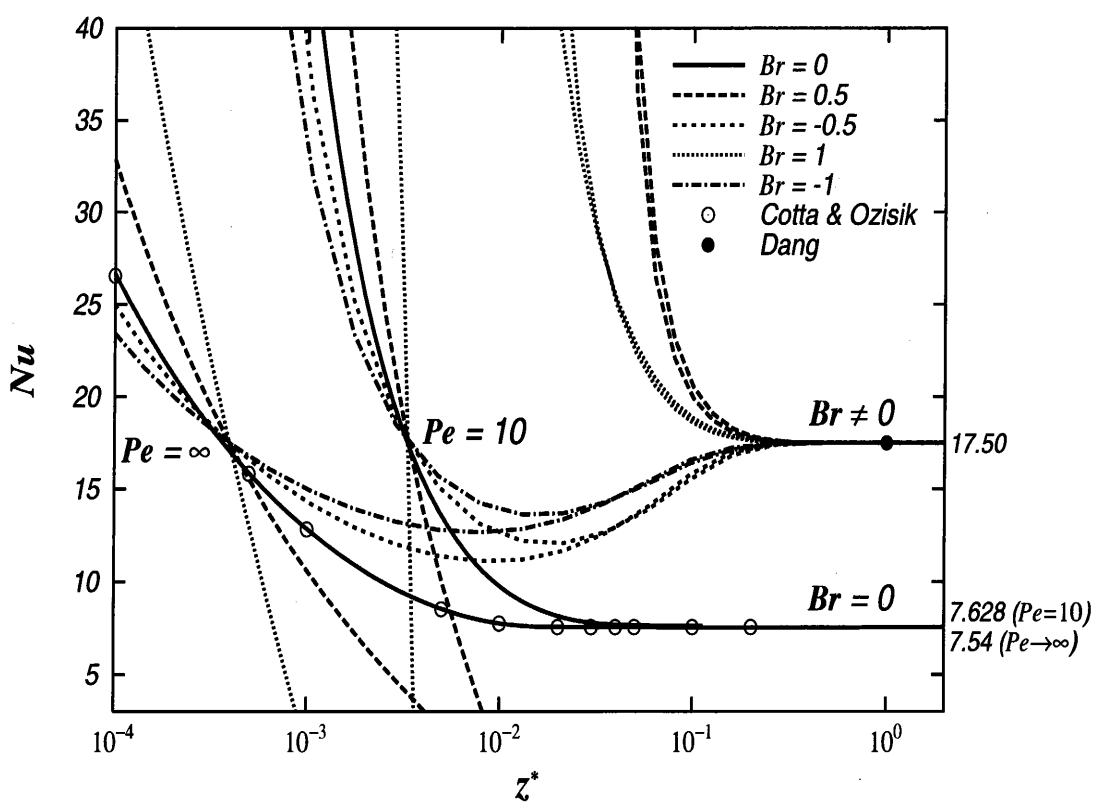

Fig.4-6 Effects of Br and Pe on Nusselt number for $n = 1$

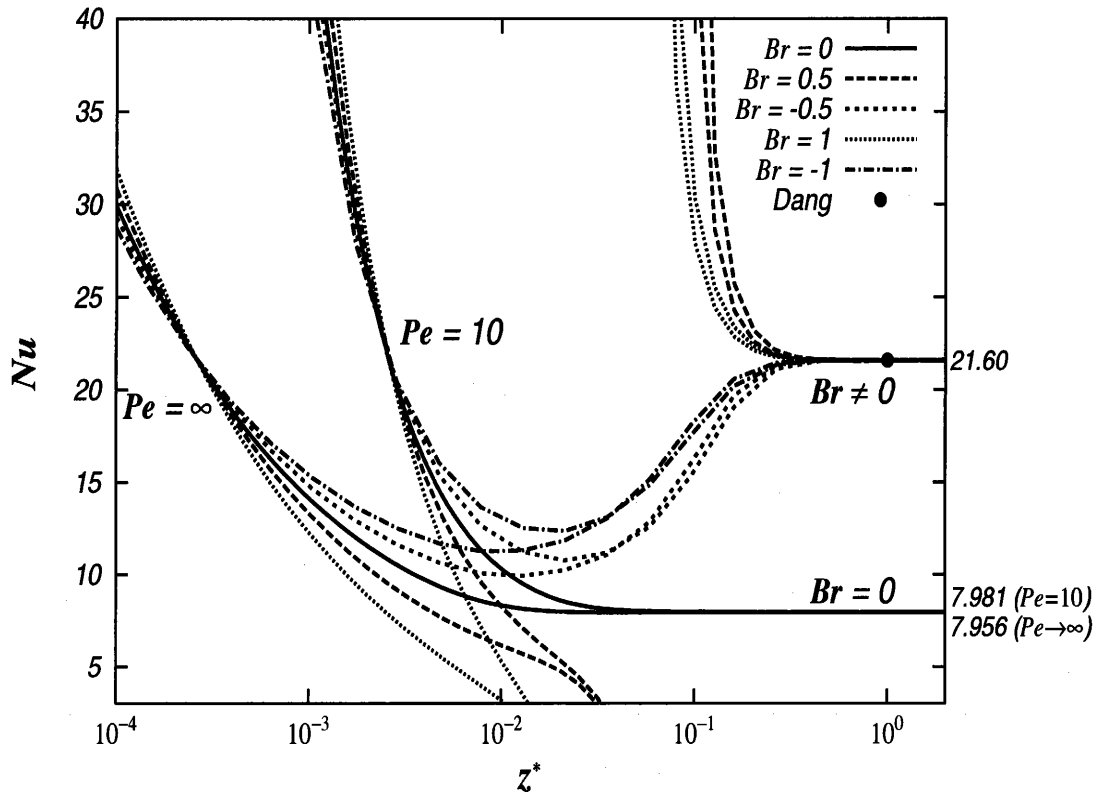

Fig.4-7 Effects of Br and Pe on Nusselt number for $n = 0.5$

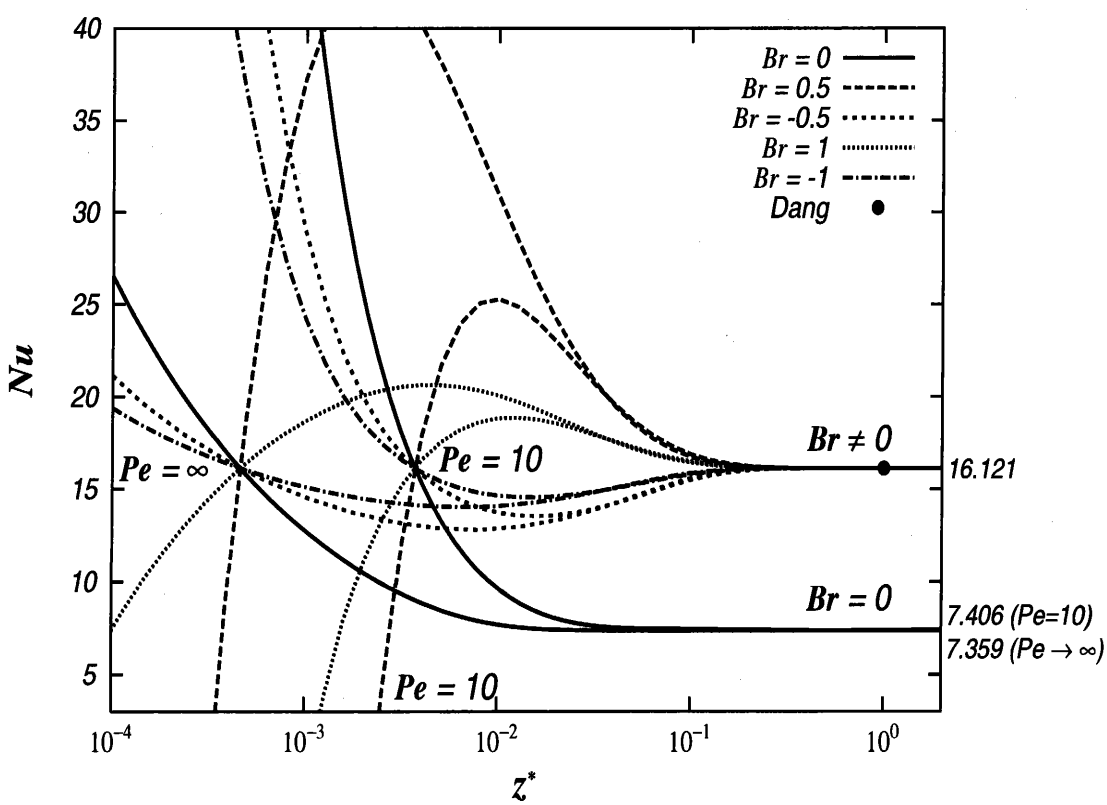

Fig.4-8 Effects of Br and Pe on Nusselt number for $n = 1.5$

positive Brinkman numbers show that the fluid is being heated from the wall. The results for the Nusselt numbers in the fully developed range were in excellent agreement with those of by Dang [46].
Further detail is available in [89] and the main trends of the temperature development and of the Nusselt curves with different degrees of viscous dissipation and fluid axial heat conduction are described in the below.

Discussion

θ, temperature profile

The fluid temperature increases at $z \leq 0$ due to the fluid axial heat conduction and due to the viscous dissipation before the fluid enters the heated wall region.

Nu_{L}, Nusselt number at the walls ($T_{\mathrm{L}} > T_e$, $z > 0$)

For a given fluid, the asymptotic value of Nusselt number at the wall is a single value for different non-zero values of Brinkman number.

For non-zero Brinkman numbers, the asymptotic Nusselt number does not depend on the Peclet number values.

However, for zero Brinkman numbers, the asymptotic Nusselt numbers depend on Peclet number values and with a decrease in Peclet number the asymptotic Nusselt number values increase slightly.

4.3.2 The First Kind Thermal Boundary Condition

(a) The Case of Moving Plate Heated

Newtonian fluid

Some representative developing temperature profiles are given for plane Poiseuille-Couette flow ($U^* = 1$) of Newtonian fluids ($n = 1$) in Fig.4-9 for the case of the moving wall heated (Case A). The description of this thermal boundary condition is given in Section 4.1. $y^* = 0$ corresponds to the upper stationary wall and $y^* = 0.5$ is the lower moving wall. The upper two figures are for the case where the viscous dissipation term is neglected ($Br = 0$) and the two figures at the bottom are for Br

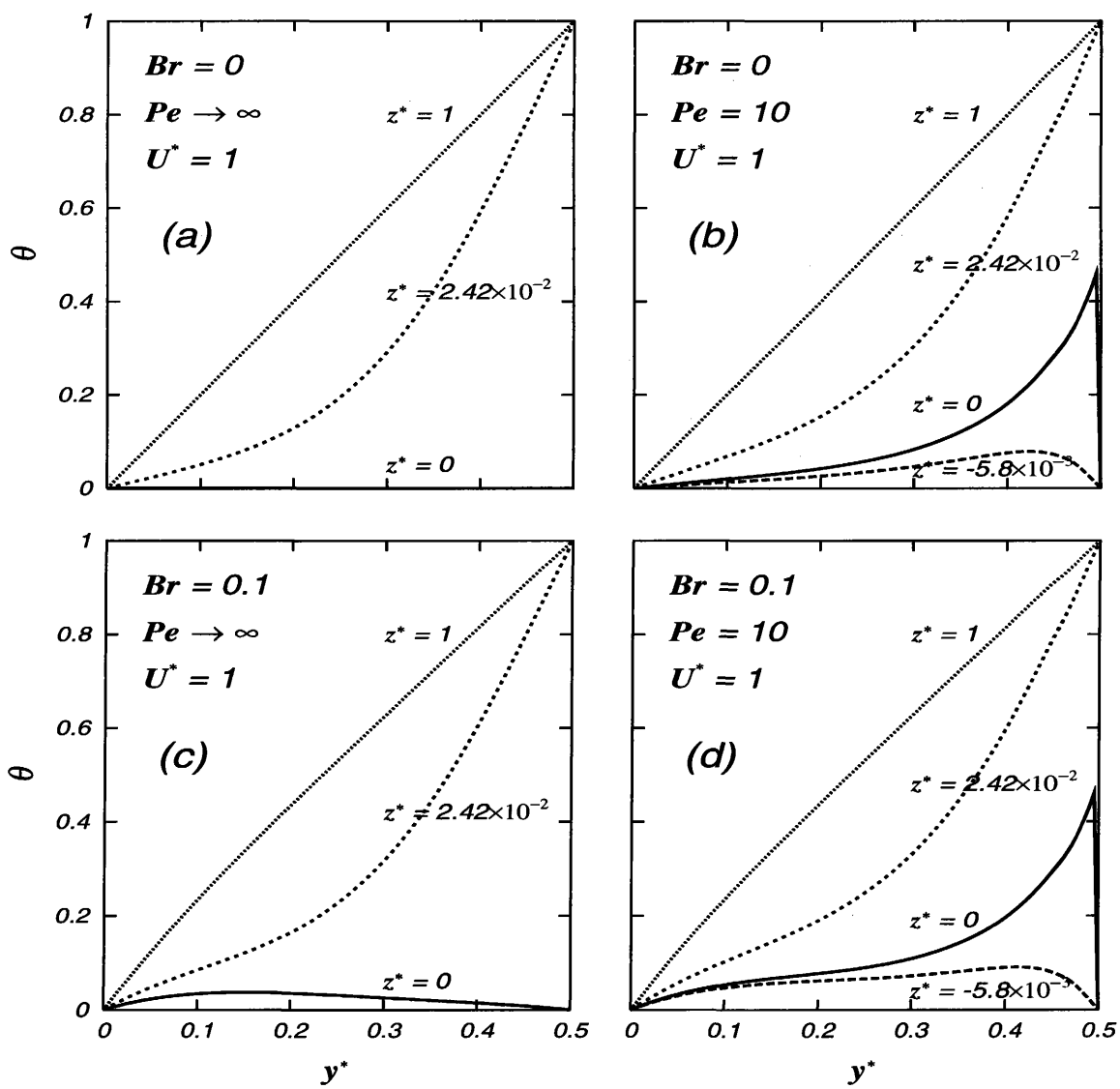

Fig.4-9 Developing temperature profiles for Case A, $U^* = 1$.
(Newtonian fluid, $n = 1$)

$= 0.1$. By scanning each row of the figures one can observe the effect of the fluid axial heat conduction on the developing temperature distributions. If one compares these figures by scanning each column, then the effect of the viscous dissipation on the temperature distribution in the thermal entrance region is observed. In these figures the solid lines stand for the local temperature development profile at $z^* = 0$, which is the location of a step change in the wall temperature. The other axial locations of z^* corresponding to the local temperature development profiles in these figures were chosen arbitrarily without any special criteria. For example, the temperature profile at the location of $z^* = 2.42 \times 10^{-2}$ just represents temperature profiles in the thermally developing range. The profile at the location of $z^* = -5.8 \times 10^{-3}$ represents one of the local temperature profiles existing in the fluid before it reaches the heated wall and $z^* = 1$ represents one of the fully developed local temperature profiles. In Fig.4-9(a), the case of the neglected viscous dissipation ($Br = 0$) and fluid axial heat conduction ($Pe \rightarrow \infty$) is shown. In this case, at $z^* = 0$ the dimensionless temperature is zero. At $z^* = 2.42 \times 10^{-2}$ the dimensionless temperature has been increased due to the heat from wall and due to the convection. When the fluid reaches the location of $z^* = 1$, the temperature profile is already fully established and it is linear. In Fig.4-9(b), the local temperature profile development is presented for the case of considerable fluid axial heat conduction ($Pe = 10$) while the viscous dissipation term is neglected ($Br = 0$). It is seen in Fig.4-9(b) the fluid temperature at $z^* = 0$ is definitely deviates from zero even there is no heat from the wall. In fact it is seen the temperature increase is occurred at $z^* = -5.8 \times 10^{-3}$. This increase is due to the contribution of the fluid axial heat conduction. By comparing Figs.4-9(a) and 4-9(c) the viscous dissipation effect on the developing temperature profiles is observed in two ways. First, the dimensionless temperature profile at $z^* = 0$ is not zero for $Br = 0.1$. The second one is related to the fully developed temperature profile. For the negligible viscous dissipation case in Fig.4-9(a) the fully developed temperature profile is linear. But this linear fully developed profile is distorted by the viscous dissipation effect specially near the stationary upper wall at $y^* = 0$. In Fig.4-9(d), the local temperature development is shown for the case of considerable viscous dissipation ($Br = 0.1$) and fluid axial heat conduction $Pe = 10$. It is seen the fluid axial heat conduction is more pronounced near the heated wall ($y^* = 0.5$), while the viscous dissipation effect is strong near the stationary wall ($y^* = 0$). Because the highest shear rate occurs near the stationary wall as it was seen in Fig.3-13, the viscous dissipation effect is more pronounced near the stationary wall.

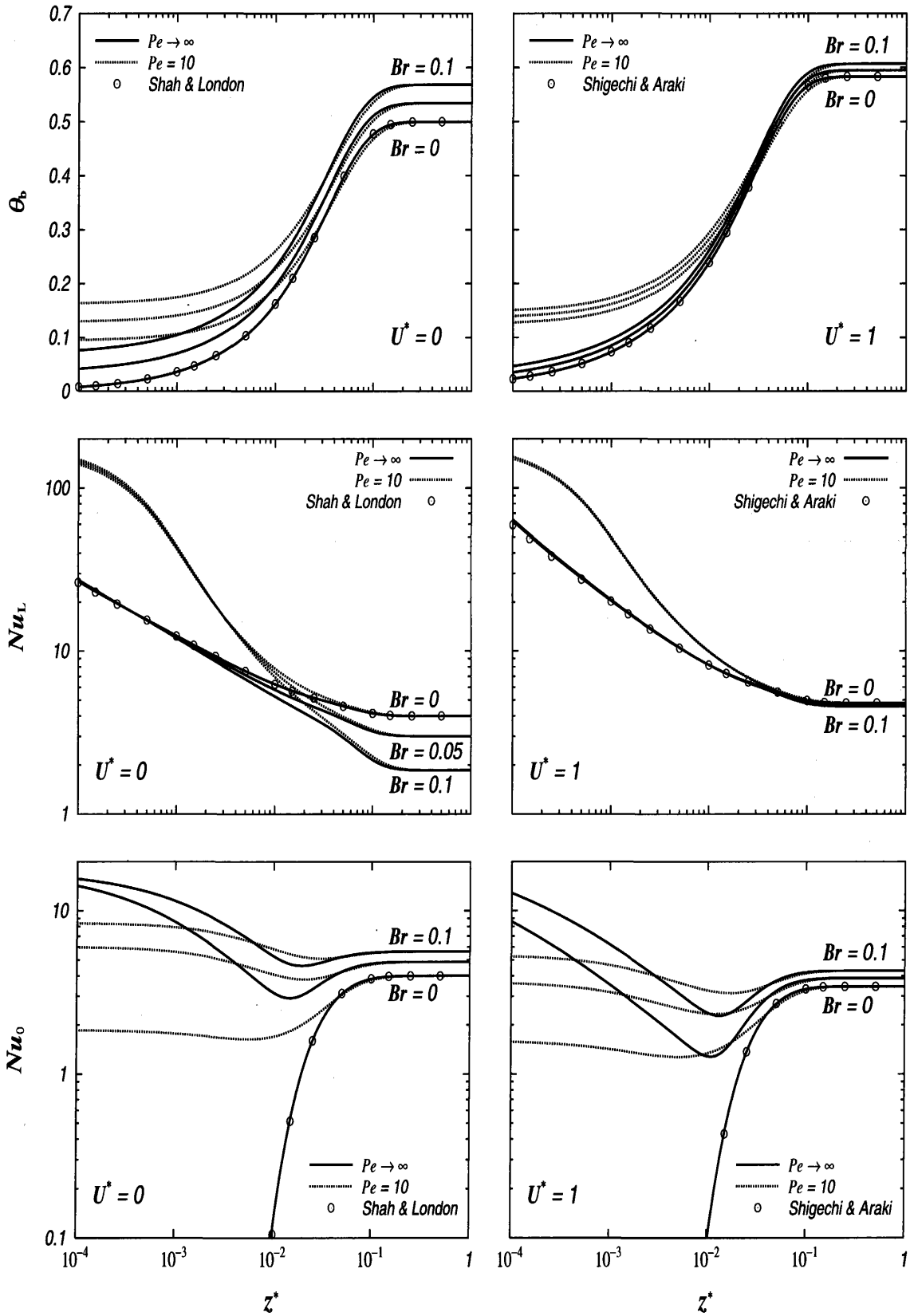

Fig.4-10 Effects of Br and Pe on θ_b and Nu at walls for Case A, $U^* = 0$, 1. (Newtonian fluid, $n = 1$)

The comparison of the developing temperature profiles for the Newtonian fluid with those of pseudoplastic and dilatant fluids will be made later at the end of this subsection.

In Fig.4-10, the axial developments of the bulk temperature and Nusselt number at the walls are presented in comparison them with the relative velocity, U^*. The presented results are given in a pair in the rows of the figures. The figures on the left side show the results for pure Poiseuille flow ($U^* = 0$), while the other ones are for Poiseuille-Couette flow ($U^* = 1$). In these figures the parameters are the Peclet number and the Brinkman number. The values of the Peclet number are 10 and ∞. The Brinkman numbers are 0, 0.05 and 0.1. The solid lines in these figures show the result for the case when the fluid axial heat conduction term is neglected ($Pe \rightarrow \infty$). The dashed lines are for $Pe = 10$. The special case study results or the case of negligible viscous dissipation ($Br = 0$) and negligible fluid axial heat conduction ($Pe \rightarrow \infty$) are compared with the available data sets. The circles show the results by Shah and London [11] for $U^* = 0$ and by Shigechi and Araki [4] for $U^* = 1$. The course of heat transfer is conveniently expressed by the change in bulk temperature with the axial coordinate z^* in the upper two figures. For the case of negligible viscous dissipation ($Br = 0$) and negligible fluid axial heat conduction ($Pe \rightarrow \infty$), the fluid temperature increases due to the heat conducted from the wall and to the axial convection. The largest bulk temperature value at the given location in the thermally developing range corresponds to the case with considerable viscous dissipation ($Br = 0.1$) and fluid axial heat conduction ($Pe = 10$). In the following figures Nusselt number values in the thermally developing range are shown. From these figures one can see the effects of both Brinkman number and Peclet number. Scanning each row of the figures, the relative velocity effect is seen.

Further detail is also available in [90].

Pseudoplastic fluid

The following figures present the results for a pseudoplastic fluid ($n = 0.5$ and $\beta = 1$) in the same way of illustration as done for the Newtonian fluid above. In Fig.4-11, the developing temperature profiles are shown for a Poiseuille-Couette flow of the pseudoplastic fluid. It is seen the general qualitative behavior of the axial development of temperature is quite similar to the trends observed for the Newtonian fluid.

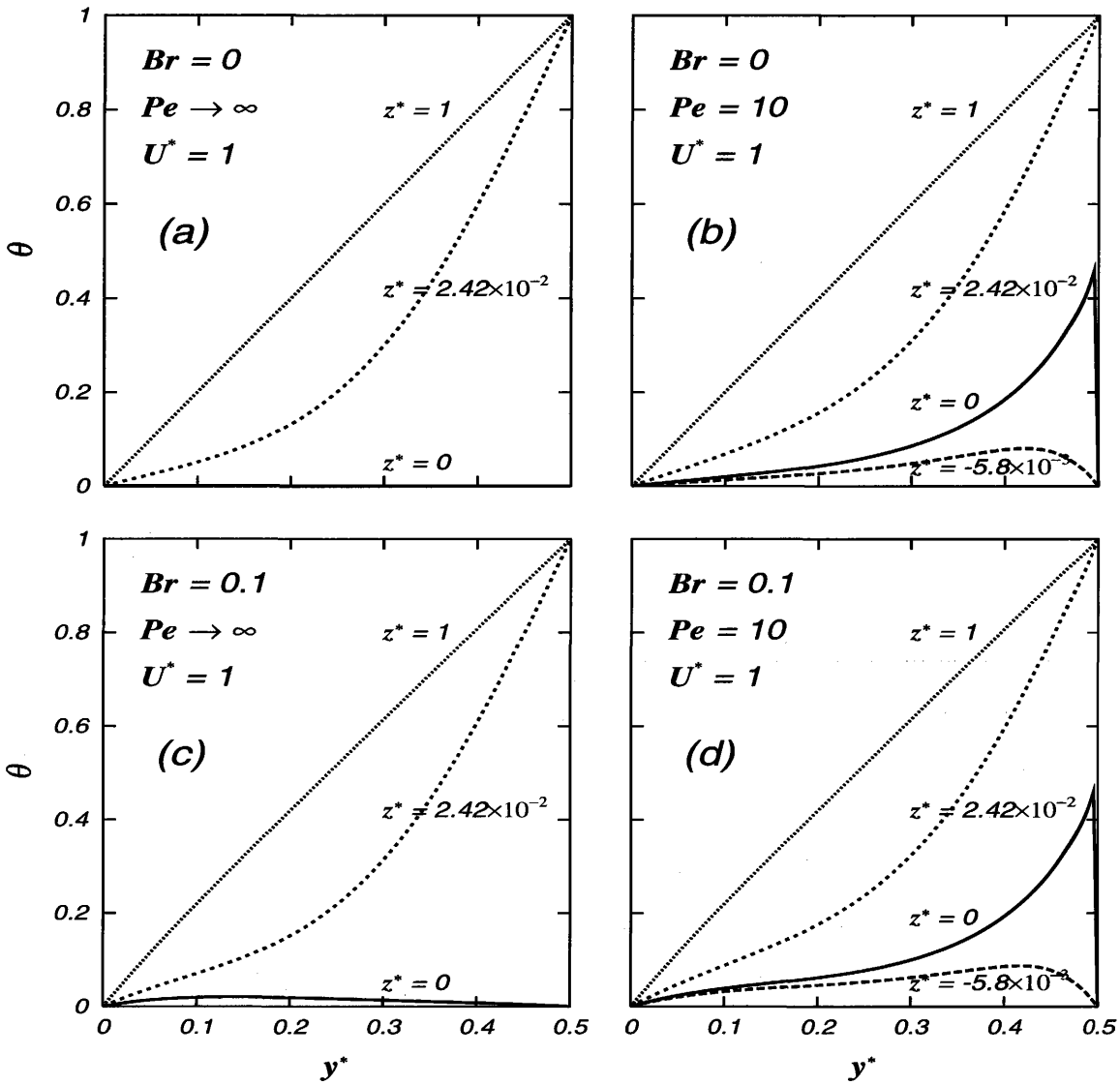

Fig.4-11 Developing temperature profiles for Case A, $U^* = 1$.
(pseudoplastic fluid, $n = 0.5$, $\beta = 1$)

The course of the heat transfer for the pseudoplastic fluid ($n = 0.5$ and $\beta = 1$) is expressed by the axial development of bulk temperature and Nusselt numbers at the walls in Fig.4-12. As it was mentioned above, the general qualitative behavior of the course of the heat transfer is similar to the trend of the Newtonian fluids. However for the pseudoplastic fluid the effect of viscous dissipation is seen to be less than for the Newtonian fluid.

Further detail is also available in [90].

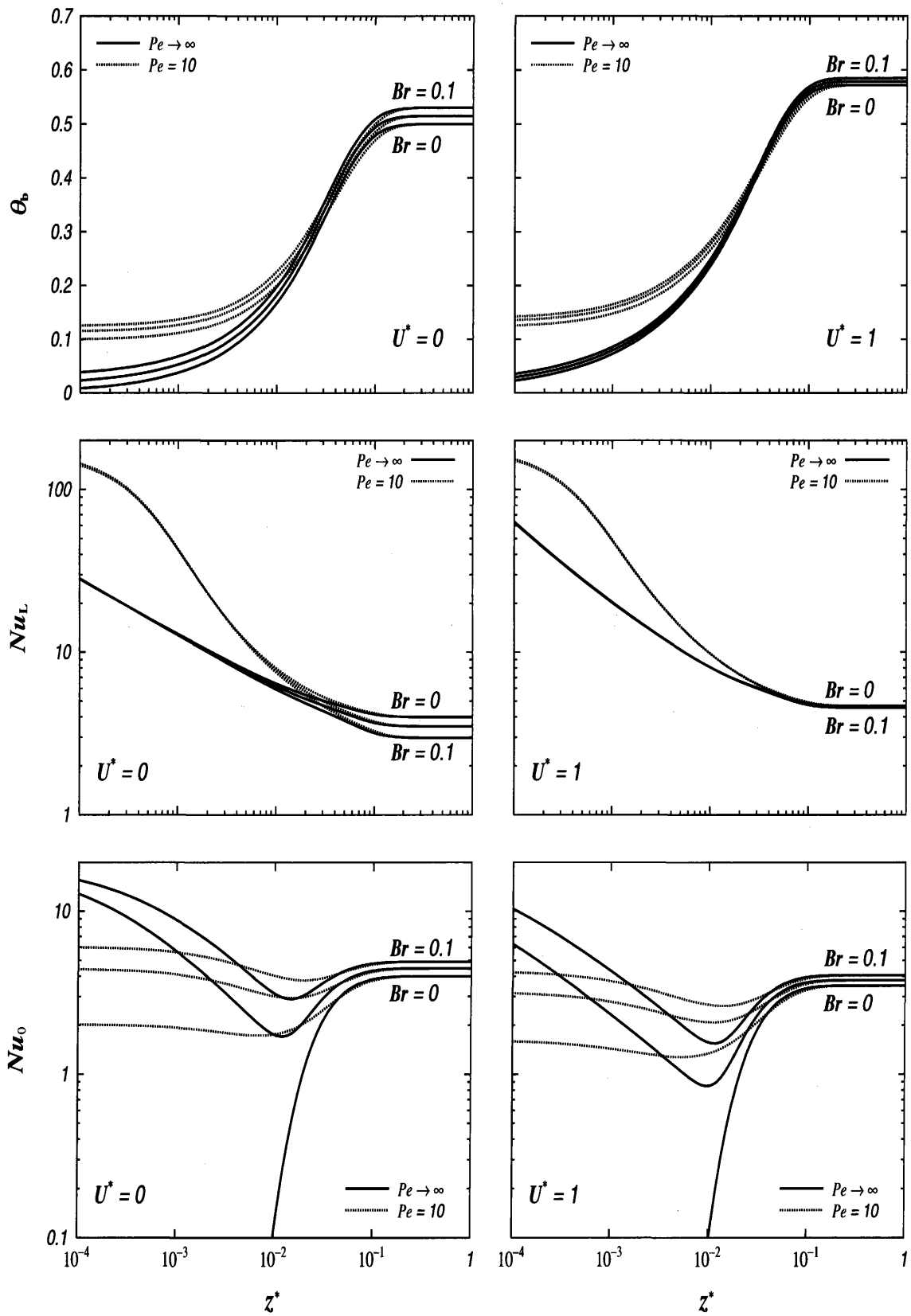

Fig.4-12 Effects of Br and Pe on θ_b and Nu at walls for Case A, $U^* = 0$, 1. (pseudoplastic fluid, $n = 0.5$, $\beta = 1$)

Dilatant fluid

The following figures present the results for a dilatant fluid ($n = 1.5$ and $\beta = 1$) in the same way of illustration as done for the Newtonian and pseudoplastic fluids above. In Fig.4-13, the developing temperature profiles are shown for a Poiseuille-Couette flow ($U^* = 1$) of the dilatant fluid. It is seen the general qualitative behavior of the axial development of temperature is quite similar for the different fluid behaviors. From Figs.4-13(c) and 4-13(d), the viscous dissipation effect is seen more pronounced for the dilatant fluid than for the Newtonian and pseudoplastic fluids.

The course of the heat transfer for the dilatant fluid ($n = 1.5$ and $\beta = 1$) is expressed by the axial developments of bulk temperature and Nusselt numbers at

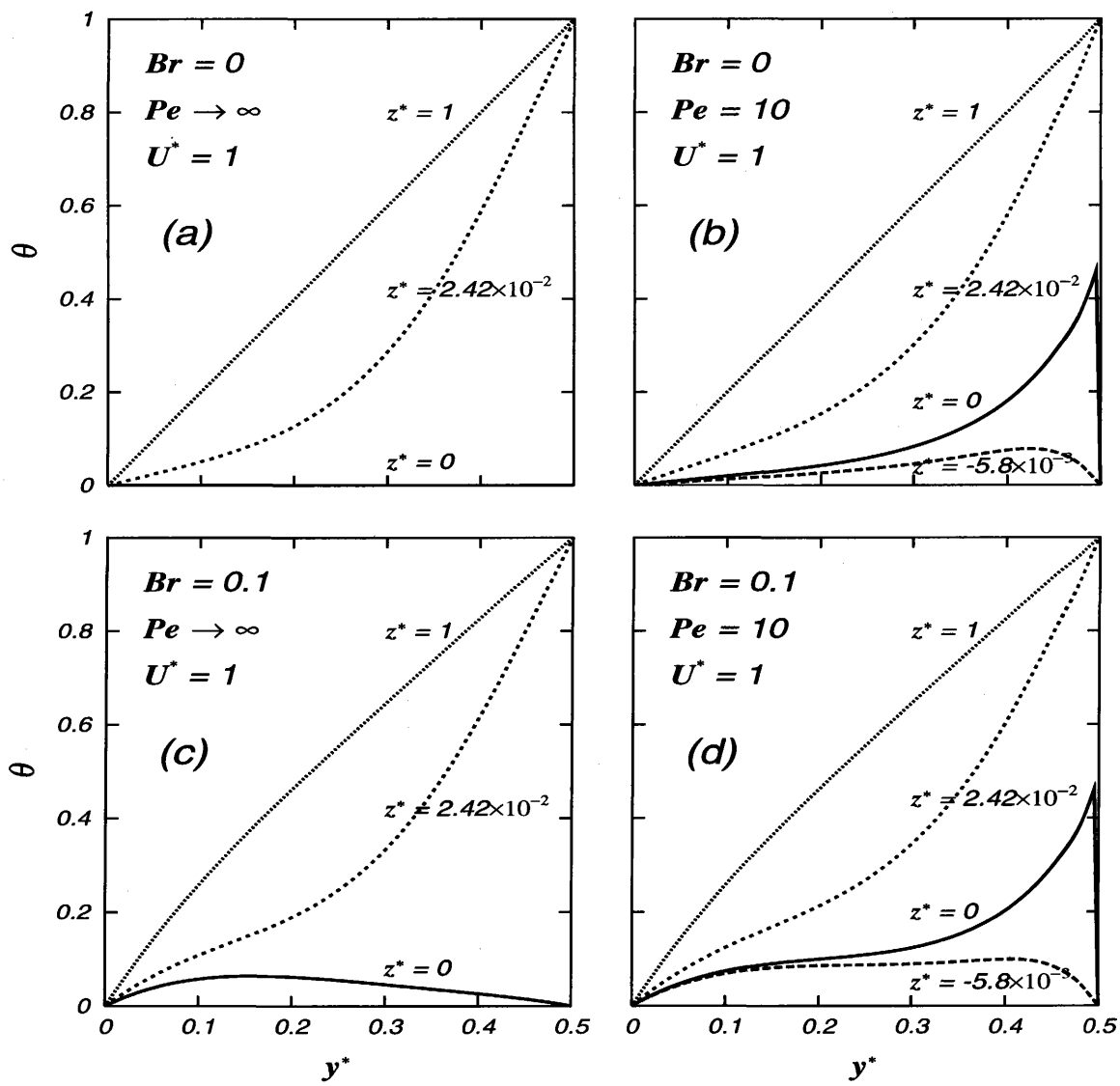

Fig.4-13 Developing temperature profiles for Case A, $U^* = 0$, 1.
(dilatant fluid, $n = 1.5$, $\beta = 1$)

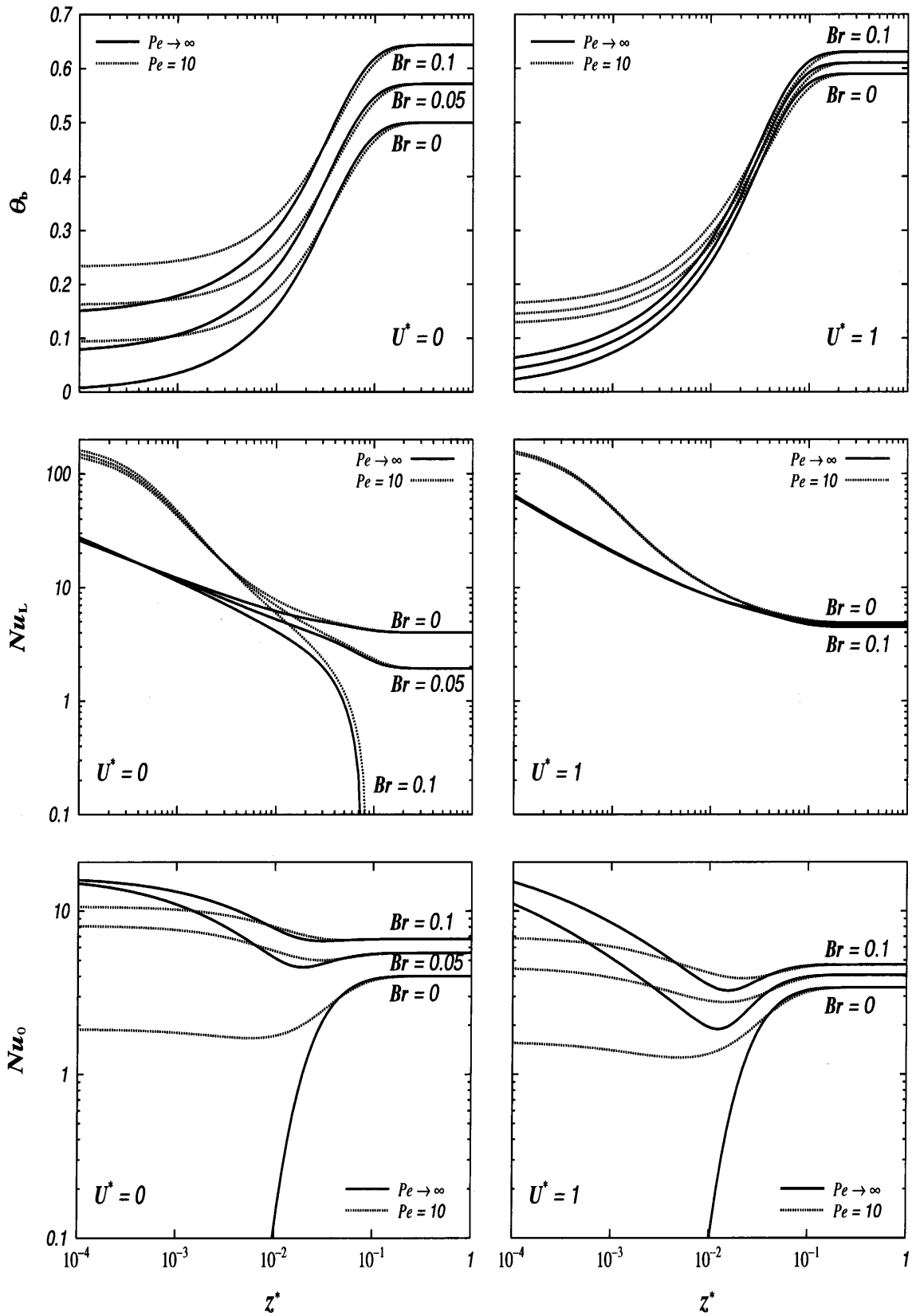

Fig.4-14 Effects of Br and Pe on Nu at walls for Case A, $U^* = 0$, 1.
(dilatant fluid, $n = 1.5$, $\beta = 1$)

the walls in Fig.4-14. It is observed more pronounced effect of the viscous dissipation in the dilatant fluid. Unlike for the Newtonian and pseudoplastic fluids, for the dilatant fluid the heat transfer direction is changed in the fully developed region for $Br = 0.1$ if both of the plates are stationary ($U^* = 0$) or if the flow is the pure Poiseuille flow. However for $U^* = 1$ or for Poiseuille-Couette flows, the viscous dissipation effect is not important for the different fluid behaviors.

Discussion

θ, temperature profile

The general qualitative behavior of the axial development of the temperature field is quite similar for the different fluids. The viscous dissipation effect is more pronounced for the dilatant fluid and less remarkable for the pseudoplastic fluid.

θ_{b}, bulk temperature

The bulk temperature data show a more pronounced effect of viscous dissipation for $U^* = 0$, while for $U^* = 1$ this effect is weak.

The effect of fluid axial heat conduction is strong only in the thermally developing range.

The moving plate at the relative velocity $U^* = 1$ causes an increase in bulk temperature due to the convection in the fully developed region. However for non-zero Brinkman numbers, close to the origin or near $z^* = 0$, the bulk temperature for $U^* = 1$ shows less value than for $U^* = 0$ due to the viscous dissipation.

Nu_{L}, Nusselt number at the lower wall ($T_{\mathrm{L}} > T_e$, $0 < z$)

As a consequence of inclusion of the viscous dissipation and fluid axial heat conduction effects in the study, Nusselt number decreases in the fully developed region and increases in the thermally developing region from that special case with negligible viscous dissipation and fluid axial heat conduction. Decreasing of Nu_{L} in the fully developed region is caused by viscous dissipation. The fluid temperature becomes closer to the wall temperature θ_{L} as the flow proceeds and when we include viscous heating, the fluid temperature takes higher values, which decreases the temperature difference between the fluid and the wall.

For the dilatant fluid the heat transfer direction is changed in the fully developed range for $Br = 0.1$ if both of the plates are stationary ($U^* = 0$). Including the fluid axial heat conduction accounts for the bulk temperature increase (as it is seen from the bulk temperature development) in the thermally developing region. An increase in the bulk temperature attributes the denominator decrease in Eq.(4.21) and in turn this accounts the change in the curve shape in the thermally developing region.

The heat transfer rate in terms of Nusselt number exhibit higher values at the moving plate.

The viscous dissipation effect on the Nusselt number at the moving wall ($U^* = 1$) is very weak.

The trend for the Nusselt curves indicate that the axial heat conduction effect prevails at the thermally developing region for both $U^* = 0$ and 1, and the viscous dissipation effect dominates the heat transfer in the fully developed region if $U^* = 0$. But the viscous dissipation effect is diminished for $U^* = 1$.

Nu_0, Nusselt number at the upper wall ($T_0 = T_e$)

The Nusselt curves show a more pronounced effect of the Brinkman number and the Peclet number on the Nusselt number at the upper wall, whose temperature is kept equal to the entering fluid temperature.

As a consequence of inclusion of the viscous dissipation and fluid axial heat conduction effects in the study, in the thermally developing region the Nusselt number increases from 0 (which is the Nu_0 value for negligible viscous dissipation and fluid axial heat conduction in the thermally developing range). The effect of the Brinkman number is strong in both of the thermally developing and fully developed regions.

(b) The Case of Stationary Plate Heated

The following figures illustrate the results for the case of the stationary wall heated (Case B). In this study as described in Section 3.2, the stationary wall is the upper wall. Since the heat transfer study results of Case B for Poiseuille flow or for $U^* = 0$ would not give some additional insights into the heat transfer (as the bulk temperatures are identical for Cases A and B. Also the Nusselt number values at the upper wall for Case A are identical to those of the Nusselt numbers at the lower

wall for Case B), only the results for $U^* = 1$ are presented in this subsection. The axial development of the bulk temperature is not included.

In Fig.4-15, the developing temperature profiles of a pseudoplastic fluid ($n = 0.5$ and $\beta = 1$) in the Poiseuille-Couette flow of $U^* = 1$ are portrayed. $y^* = 0$ corresponds to the upper stationary wall and $y^* = 0.5$ is the lower moving wall. Here the upper wall at $y^* = 0$ is kept $\theta_0 = 1$ in $0 < z^*$, while the lower wall temperature is $\theta_L = 0$. The upper two figures are for the case where the viscous dissipation term is neglected ($Br = 0$) and the two figures at the bottom are for $Br = 0.1$. By comparing the figures in the same row one can observe the effect of the fluid axial heat conduction on the developing temperature distributions. If one compares the

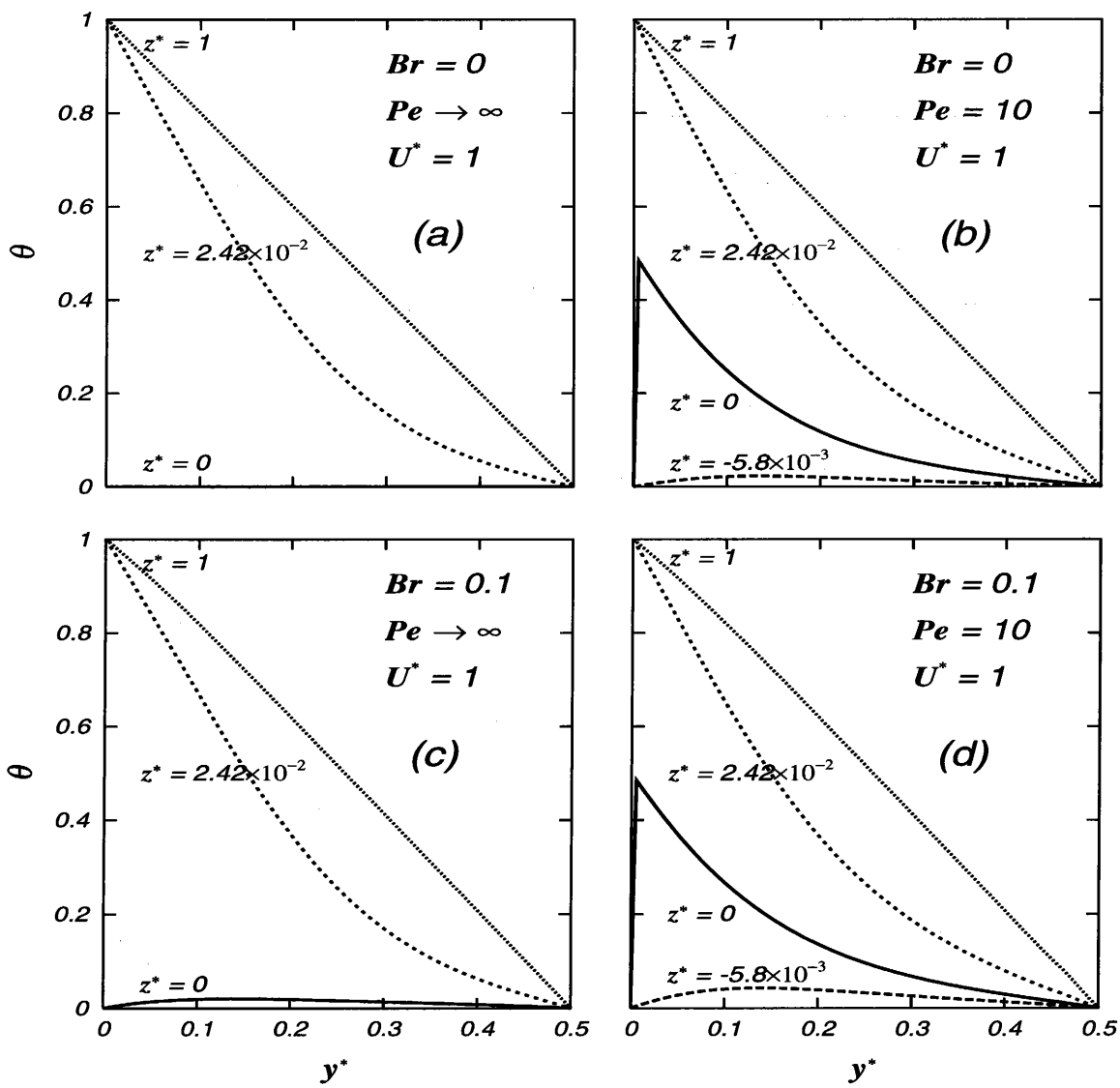

Fig.4-15 Developing temperature profiles for Case B, $U^* = 1$.
(pseudoplastic fluid, $n = 0.5$, $\beta = 1$)

figures in the same column then the effect of the viscous dissipation on the temperature distribution in the thermal entrance region is observed. In these figures the solid lines stand for the local temperature development profile at $z^* = 0$, which is the location of a step change in the stationary wall temperature. In Fig.4-15(a), the case of the neglected viscous dissipation ($Br = 0$) and fluid axial heat conduction ($Pe \rightarrow \infty$) is shown. In this case, at $z^* = 0$ the dimensionless temperature is zero. At $z^* = 2.42\times10^{-2}$ the dimensionless temperature has been increased due to the heat from the wall and due to the convection. When the fluid reaches the location of $z^* = 1$, the temperature profile is already fully established and becomes linear. In Fig.4-15(b), the local temperature profile development is presented for the case of considerable fluid axial heat conduction ($Pe = 10$) while the viscous dissipation term is neglected ($Br = 0$). It is seen in Fig.4-15(b) the fluid temperature at $z^* = 0$ is definitely deviates from zero even there is no heat from the wall. In fact it is seen the temperature increase is occurred at $z^* = -5.8\times10^{-3}$. This increase is due to the contribution of the fluid axial heat conduction. By comparing Figs.4-15(a) and 4-15(c) the viscous dissipation effect on the developing temperature profiles is observed in two ways. First, the dimensionless temperature profile at $z^* = 0$ is not zero for $Br = 0.1$. The second one is related to the fully developed temperature profile. For the negligible viscous dissipation case in Fig.4-15(a) the fully developed temperature profile is linear. But this linear fully developed profile is distorted slightly in Fig.4-15(c). In Fig.4-15(d) the local temperature development is shown for the case of considerable viscous dissipation ($Br = 0.1$) and fluid axial heat conduction $Pe = 10$. It is seen the fluid axial heat conduction is more pronounced near the heated wall ($y^* = 0$).

The effects of the Brinkman number and the Peclet number on the Nusselt numbers at the walls are displayed in Fig.4-16 for Case B in the case of the three different fluid behaviors such that pseudoplastic ($n = 0.5$ and $\beta = 1$), Newtonian ($n = 1$) and dilatant ($n = 1.5$ and $\beta = 1$). The figures to the left show the Nusselt number at the heated stationary wall. The other figures are for the Nusselt number at the moving wall kept at the entering fluid temperature. The Peclet number values in these figures are $Pe = 10$ and $Pe \rightarrow \infty$. The Brinkman numbers are $Br = 0$, 0.05 and 0.1. The solid lines stand for the case of the neglected fluid axial heat conduction term ($Pe \rightarrow \infty$). The dashed lines are for the case of considerable fluid axial heat conduction $Pe = 10$. By comparing the figures in Fig.4-16 one can observe the difference of the different flow indices.

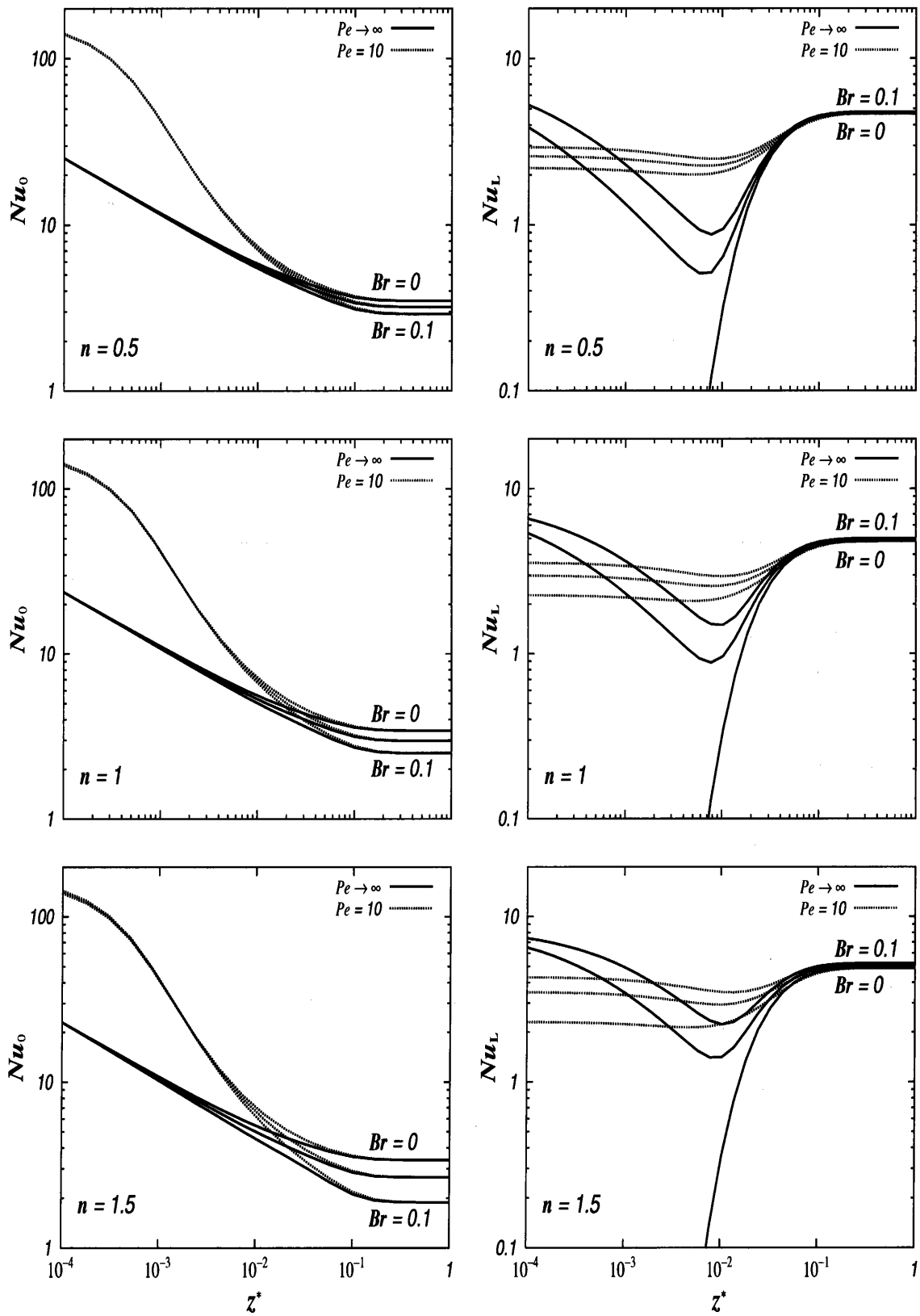

Fig.4-16 Effects of Br and Pe on Nu at walls for Case B, $U^* = 1$.
(pseudoplastic, $n = 0.5$, Newtonian, $n = 1$, and dilatant, $n = 1.5$, fluids, $\beta = 1$)

Discussion

Nu_0, Nusselt number at the upper wall ($T_0 > T_e$, $0 < z$) for the case of the moving lower wall at a velocity $U^* = 1$

As a consequence of inclusion of the viscous dissipation and fluid axial heat conduction effects in the study, the Nusselt number decreases in the fully developed region and increases in the thermally developing region from that special case with negligible the viscous dissipation and fluid axial heat conduction. The explanation of these trends can be made just as done for Nu_L for Case A. The trends for Nu_0 indicate that the fluid axial heat conduction effect prevails in the thermally developing region, while the viscous dissipation effect dominates in the thermally fully developed range.

Nu_L, Nusselt number at the lower wall ($T_L = T_e$) moving at a velocity $U^* = 1$

The Nusselt curves at the moving wall which is kept at the entering fluid temperature show a more pronounced effect of the Brinkman number and the Peclet number on the Nusselt number. As a consequence of inclusion of the viscous dissipation and fluid axial heat conduction effects in the study, in the thermally developing region the Nusselt number increases from 0 (which is the Nu_L value for negligible viscous dissipation and fluid axial heat conduction in the thermally developing range).

The trend for Nu_L indicate that both of the axial heat conduction effect and the viscous dissipation effect dominate in the thermally developing region.

4.3.3 The Second Kind Thermal Boundary Condition

(a) The Case of Moving Plate Heated

Newtonian fluid

The description for the thermal boundary condition of Case A of the second kind T.B.C. is given in Section 4.1. In Fig.4-17, some representative developing temperature profiles are given. The figures in the first row show the case of the neglected viscous dissipation ($Br = 0$). The second row figures are for $Br = 0.1$. The figures on the left side are for pure Poiseuille flow or for $U^* = 0$. In the figures on the right side, the local temperature development is shown for the Poiseuille-Couette

flow of $U^* = 1$. By scanning each row of the figures in Fig.4-17 one can observe the relative velocity, U^*, effect on the temperature distribution in the thermal entrance region. If one compares the figures in the same column then the viscous dissipation effect is observed. $y^* = 0$ corresponds to the upper wall and $y^* = 0.5$ is the lower wall. At $z^* = 0$, there is a step change in the lower wall heat flux. The solid lines stand for the case of neglected fluid axial heat term or $Pe \rightarrow \infty$ and the dashed lines are for $Pe = 10$. The axial locations of z^* for the presented temperature profiles

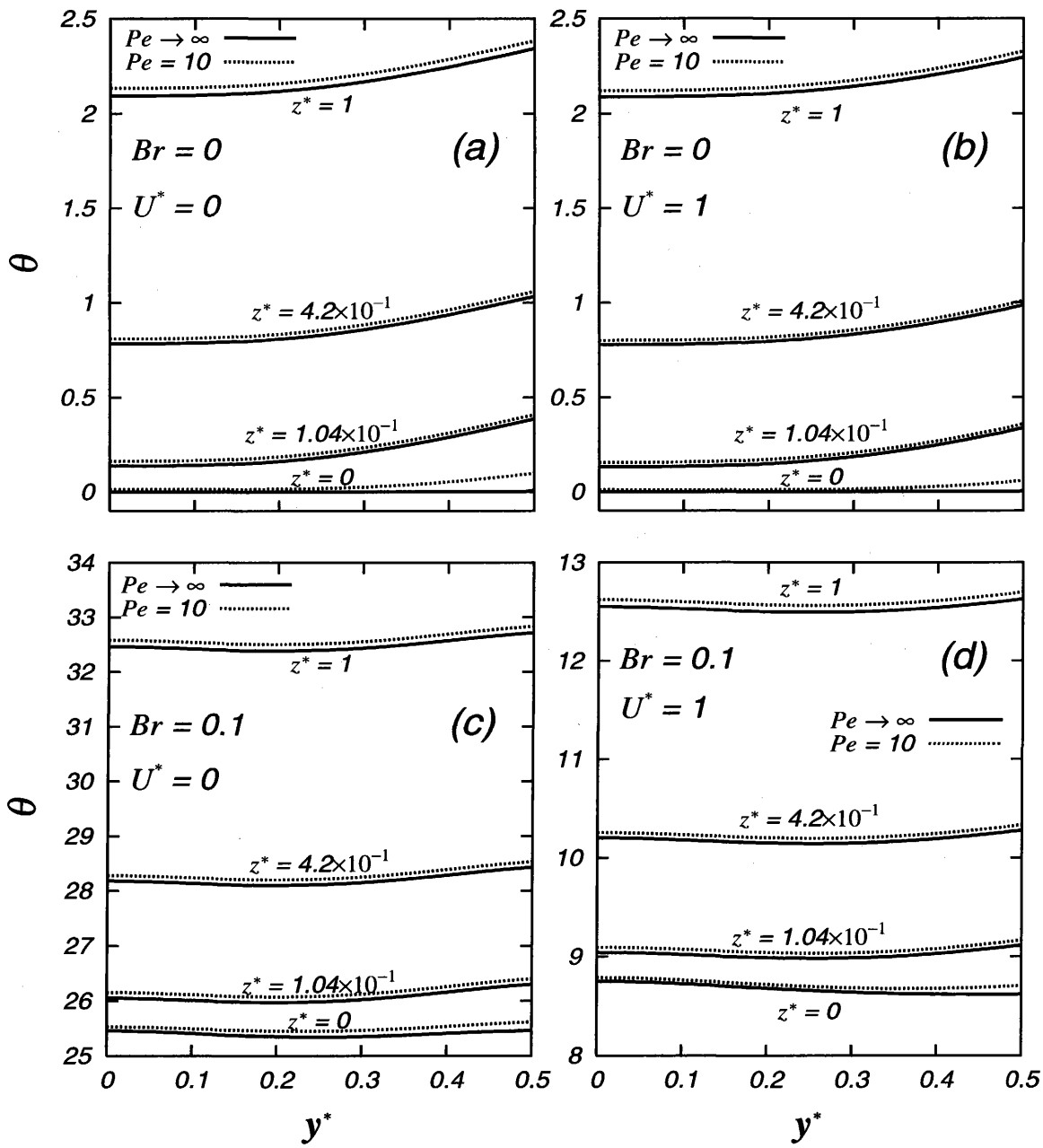

Fig.4-17 Developing temperature profiles for Case A, $U^* = 1$ (Newtonian fluid, $n = 1$)

were chosen arbitrarily. In Figs.4-17(a) and 4-17(b) for $Br = 0$ and $Pe \rightarrow \infty$, at $z^* = 0$ the dimensionless fluid temperature is zero. The temperature for $Pe = 10$ is seen to be deviated from zero at $z^* = 0$. This temperature increase is due to the fluid axial heat conduction. For $Br = 0.1$, as it is seen in Figs.4-17(c) and 4-17(d) the fluid temperature at $z^* = 0$ is definitely deviates from zero even there is no heat flux from the wall. This increase is due to the contribution of viscous dissipation in the flowing fluid. Since the highest shear rate occurs near the stationary wall as it was seen in Fig.3-13, the effect of viscous dissipation is significant for $U^* = 0$ than for $U^* = 1$. In fact, it can be seen from Figs.4-17(c) and 4-17(d) that the fluid temperature increases significantly before the fluid reaches the heated wall because of the heat generated by viscous dissipation. Viscous dissipation is large in the case of stationary wall as seen in Fig.4-17(c). As this effect builds up, heat is transferred to the main body of the fluid flow and heat generation due to viscous dissipation behaves like a heat source. Also from the developing temperature profiles, it is seen for the 2nd kind thermal boundary condition, the wall-to-fluid temperature difference is small whereas the effect of viscous dissipation is more significant. The comparison of the developing temperature profiles for the Newtonian fluid with those of pseudoplastic and dilatant fluids will be discussed later in this subsection.

In order to study the effects of viscous dissipation and fluid axial heat conduction, the heat transfer results are shown in the following figures. In Fig.4-18, the axial developments of the bulk temperature, θ_b, and Nusselt number at the lower wall, Nu_{L}, are presented in comparison them with the relative velocity, U^*. The results are given in pair of figures for $U^* = 0$ and $U^* = 1$. The figures to the left show the results for the Poiseuille flow ($U^* = 0$), while the other ones are for the Poiseuille-Couette flow ($U^* = 1$). In these figures the parameters are the Peclet number and the Brinkman number. The values of the Peclet number are 10 and ∞. The Brinkman numbers are 0, 0.05 and 0.1. The solid lines in these figures show the results for the case when the fluid axial heat conduction term is neglected ($Pe \rightarrow \infty$). The dashed lines are for $Pe = 10$. The special case study results or the case of negligible viscous dissipation ($Br = 0$) and fluid axial heat conduction ($Pe \rightarrow \infty$) are compared with the available data sets. The circles show the results by Shah and London [11] for $U^* = 0$ and by Shigechi and Araki [4] for $U^* = 1$. The course of heat transfer is expressed by the change of bulk temperature with the axial coordinate z^* in log-log scale. The upper two figures show the bulk temperature development. For the case of negligible viscous dissipation ($Br = 0$) and negligible fluid axial heat

conduction ($Pe \rightarrow \infty$), the fluid temperature increases due to the heat conducted from the wall and due to the axial convection. The bulk temperature profiles show that the viscous dissipation increases the bulk temperature for $Br = 0.05$ and $Br = 0.1$. The following two figures show the Nusselt number values in the thermally developing region. Scanning this row of the figures one can see the relative velocity effects on the heat transfer. The results are discussed in more detail at the end of this subsection.

Further detail is also available in [90].

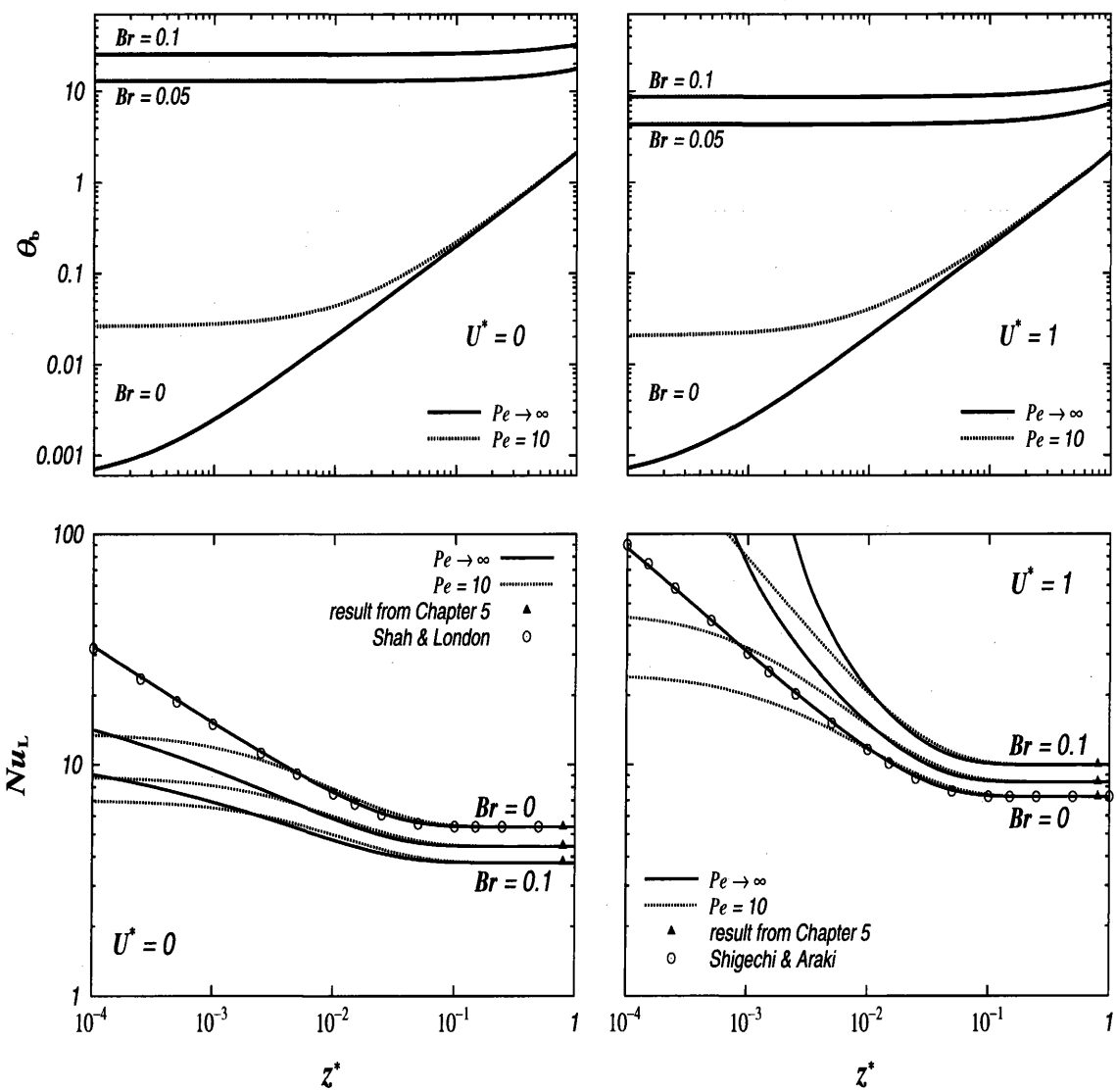

Fig.4-18 Nu for various Br and Pe for Case A, $U^* = 0$, 1.
(Newtonian fluid, $n = 1$)

Pseudoplastic fluid

The following figures present the results for a pseudoplastic fluid ($n = 0.5$ and $\beta = 1$) in the same way of illustration as done for the Newtonian fluid above. In Fig.4-19, the developing temperature profiles are shown for the pseudoplastic fluid for $U^* = 0$ and 1. It is seen the general qualitative behavior of the axial development of temperature is quite similar to the trends observed for the Newtonian fluid.

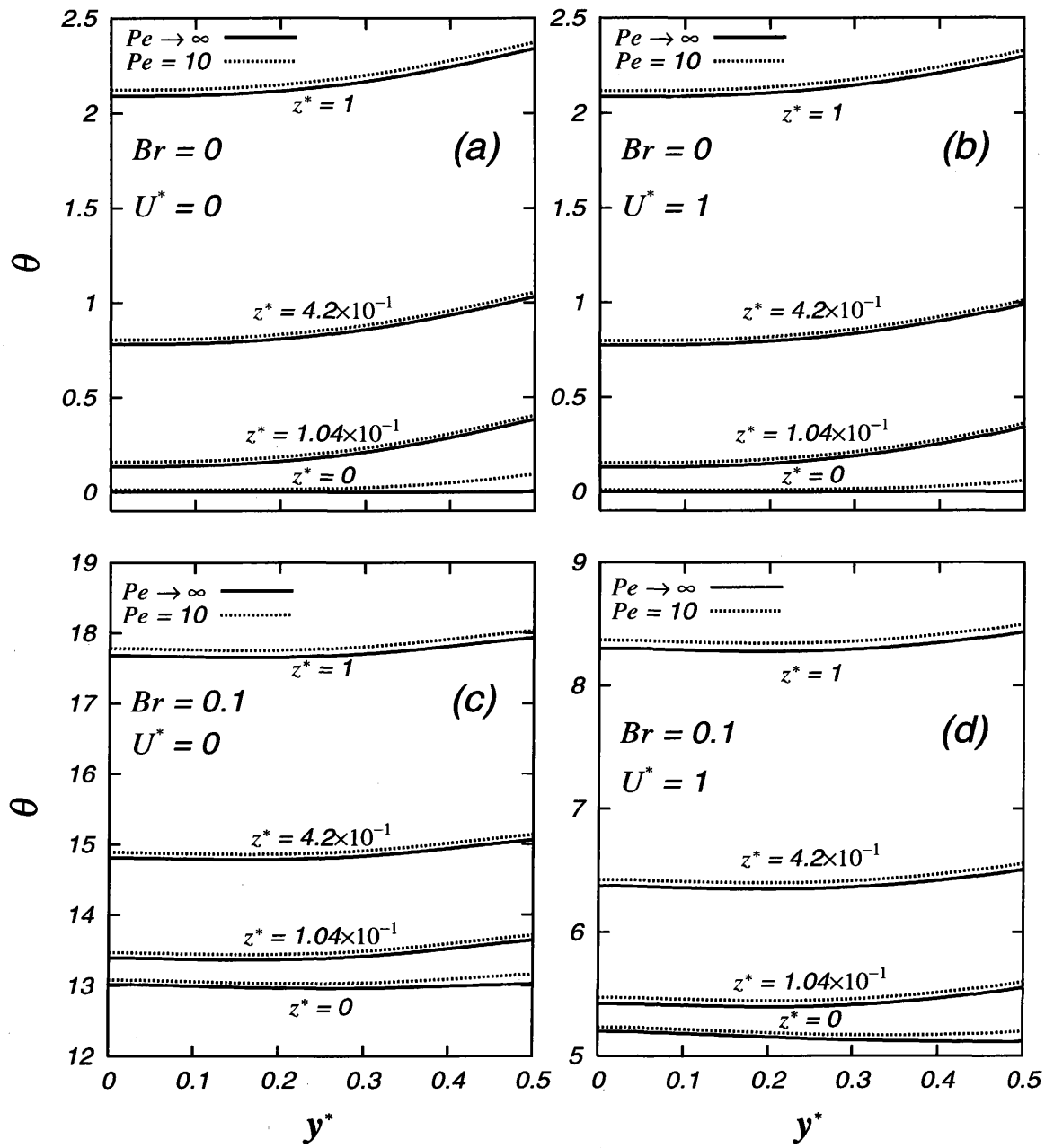

Fig.4-19 Developing temperature profiles for Case A, $U^* = 0$, 1.
(pseudoplastic fluid, $n = 0.5$, $\beta = 1$)

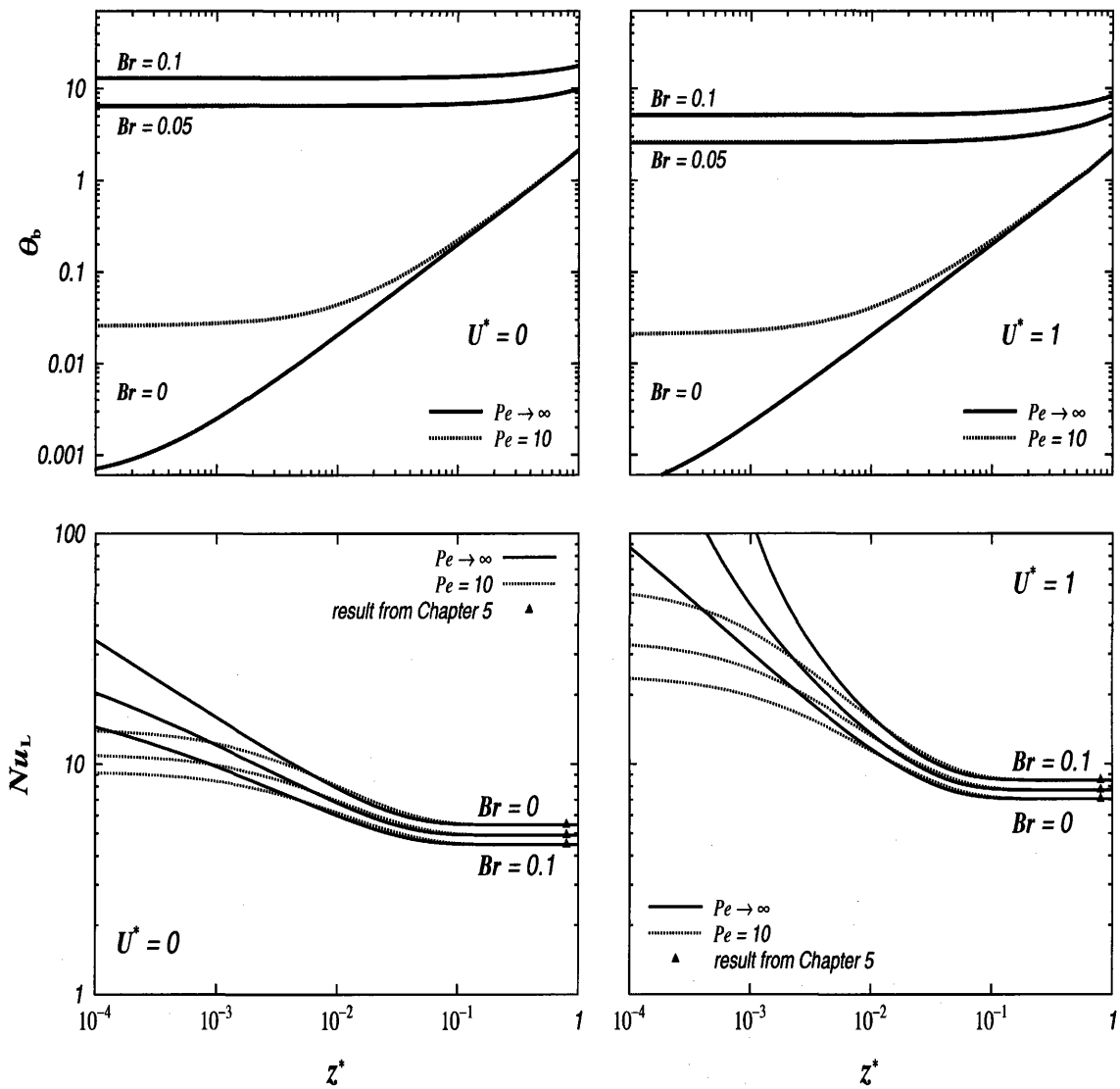

Fig.4-20 Nu for various Br and Pe for Case A, $U^* = 0$, 1.
(pseudoplastic fluid, $n = 0.5$, $\beta = 1$)

The course of the heat transfer for the pseudoplastic fluid ($n = 0.5$ and $\beta = 1$) is expressed by the axial developments of bulk temperature and Nusselt number at the wall in Fig.4-20. As it was mentioned above, the general qualitative behavior of the course of the heat transfer is similar to the trend of the Newtonian fluids. However for the pseudoplastic fluid the effect of viscous dissipation is seen to be weaker than for the Newtonian fluid. Further detail is also available in [90].

Dilatant fluid

The following figures present the results for a dilatant fluid ($n = 1.5$ and $\beta = 1$) in the same way of illustration as done for the Newtonian and pseudoplastic fluids

above. In Fig.4-21, the developing temperature profiles are shown for the dilatant fluid for $U^* = 0$ and 1. It is seen the general qualitative behavior of the axial development of temperature is quite similar for the different fluid behaviors. From Figs.4-21(c) and 4-21(d), the viscous dissipation effect is seen more pronounced for the dilatant fluid than for the Newtonian and pseudoplastic fluids. The course of the heat transfer for the dilatant fluid is expressed by the axial developments of bulk temperature and Nusselt number at the heated wall in Fig.4-22. It is observed more pronounced effect of viscous dissipation in the dilatant fluid.

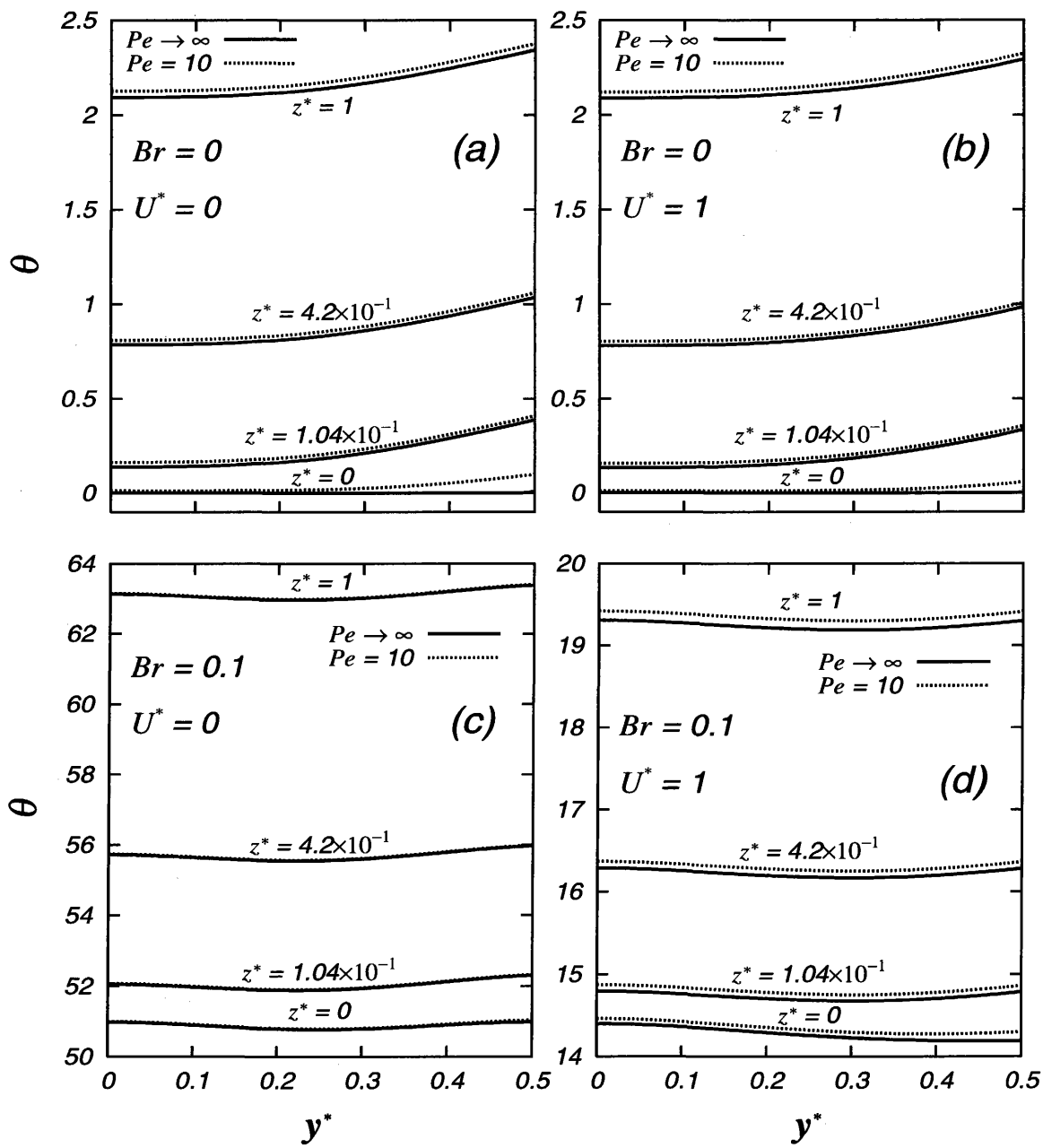

Fig.4-21 Developing temperature profiles for Case A, $U^* = 0$, 1.
(dilatant fluid, $n = 1.5$, $\beta = 1$)

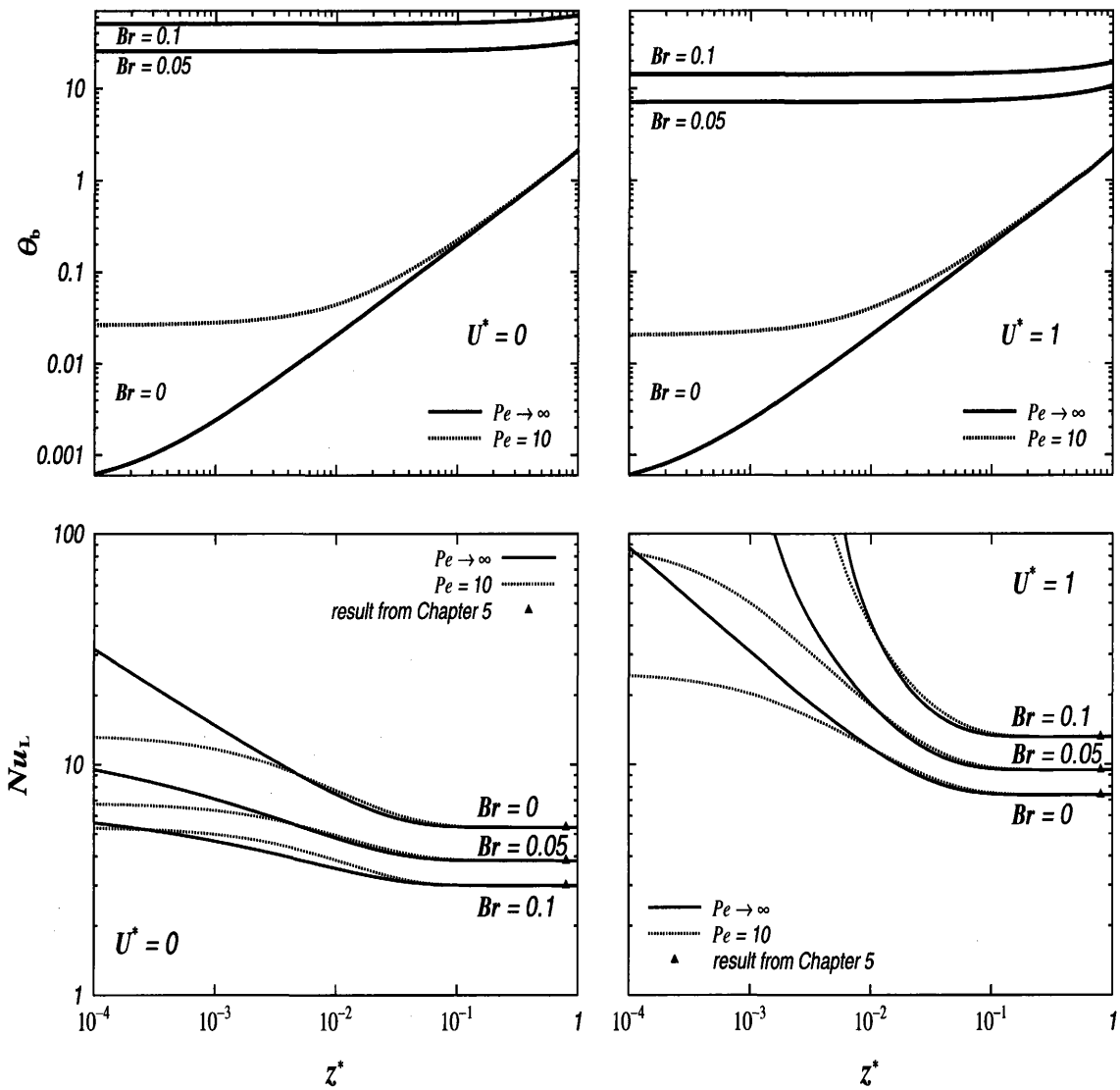

Fig.4-22 Nu for various Br and Pe for Case A, $U^* = 0$, 1.
(dilatant fluid, $n = 1.5$, $\beta = 1$)

Discussion

θ, temperature profile

The general qualitative behavior of the axial development of temperature is quite similar for the different fluids. However the viscous dissipation effect is more pronounced for the dilatant fluid.

θ_b, bulk temperature

The bulk temperature data show a more pronounced effect of viscous dissipation for $U^* = 0$. In the thermally fully developed region the bulk temperature

values do not change with the Peclet numbers. But in the thermally developing region the bulk temperature increases with a decrease in Peclet number slightly. Unlike the 1st kind thermal boundary condition, the moving plate at $U^* = 1$, causes a decrease in the bulk temperature. It may be explained as follows. The moving plate causes more fluid flow. The more flow is heated in less extent from the wall at constant heat flux.

Nu_L, Nusselt number at the lower heated wall (q_L = const, $z > 0$)

As a consequence of inclusion of the viscous dissipation and fluid axial heat conduction effects in the study, Nusselt number decreases in the thermally developing region from that the special case with negligible viscous dissipation and fluid axial heat conduction for Poiseuille flows ($U^* = 0$). Unlike the first kind T.B.C case, the Brinkman number effect is specific depending on the relative velocity of the wall. The explanation of this trend with Br is covered in Sections 4.4.2 and 5.2.2. Even the fluid axial heat conduction accounts for the bulk temperature increase in the thermally developing region, the wall temperature also increases. As Eq.(4.22) suggests, in the thermally developing region in terms of increments of θ_L and θ_b due to the fluid axial heat conduction, the increment of θ_L is larger than that of θ_b and in turn this accounts the change in the curve shape. The heat transfer rate in terms of Nusselt number exhibit higher values at the moving plate. The trend for the Nu curves indicate that the axial heat conduction effect prevails at the thermally developing region and viscous dissipation effect dominates in both the thermally developing and fully developed regions.

(b) The Case of Stationary Plate Heated

The following figures illustrate the combined effects of the Brinkman number and the Peclet number on the Nusselt number for Case B, in which the lower wall is insulated with the upper wall is heated constantly in $0 < z^*$. As it was noted previously in Section 4.3.2(b) that for $U^* = 0$ the values of the Nusselt number at the upper wall, Nu_0 are identical to those of Nu_L for Case A, the results are given for $U^* = 1$ only. The axial development of Nusselt number at the upper (stationary) wall is shown for the different fluid properties such as pseudoplastic, Newtonian and dilatant fluids. The developing temperature profiles and the axial development of bulk temperature are not included here since they would not give some additional

insights other than those obtained for Case A.

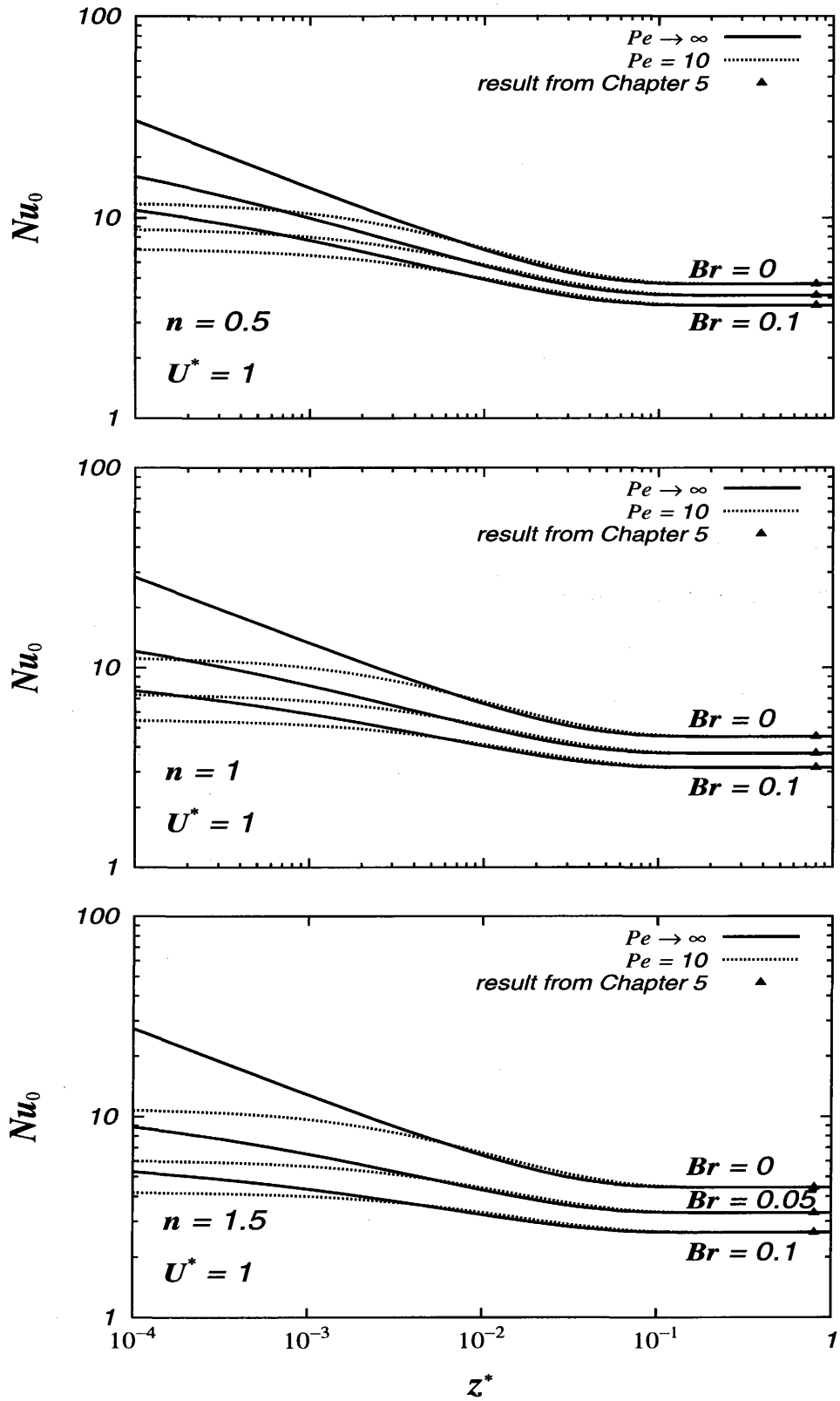

Fig.4-22 Effects of Br and Pe on Nu for Case B, $U^* = 1$. (pseudoplastic, n =0.5, Newtonian, $n = 1$, and dilatant, $n = 1.5$, fluids, $\beta = 1$)

Discussion

Nu_0, Nusselt number at the upper wall (q_0 = const, $0 < z$) for the case of the lower wall moves at a velocity $U^* = 1$

As a consequence of inclusion of the viscous dissipation and fluid axial heat conduction effects in the study, the Nusselt number becomes smaller than the special case of negligible viscous dissipation and fluid axial heat conduction. With the given Brinkman number and the Peclet number at a specified axial location, Nu_0 for the pseudoplastic fluid is higher than for those of the Newtonian and dilatant fluids. The trend for the Nusselt curves are found to be same as in Case A. The axial heat conduction effect prevails at the thermally entrance region while the viscous dissipation effect dominates in both the thermally developing and fully developed regions.

4.4 Effect of Viscous Dissipation for $Pe \rightarrow \infty$

Various relevant results and figures have been discussed from the view point of viscous dissipation phenomena in the plane Poiseuille-Couette flow. Brinkman number is proposed to serve as a controlling index that indicates the relative importance of viscous dissipation. Here the axial heat conduction effect is neglected by setting the Peclet number to an infinite value. In this study $Pe \rightarrow \infty$ corresponds to $Pe = 10^8$.

4.4.1 The First Kind Thermal Boundary Condition

(a) The Case of Moving Plate Heated

In the following figures the effects of the viscous dissipation and of the moving wall velocity are shown. The computed results for Case A, in which the lower wall is heated in $0 < z^*$ and the upper wall is specified at the inlet fluid temperature, are illustrated first.

Newtonian fluid

In Fig.4-23 the effect of viscous dissipation on the axial development of the bulk temperature and Nusselt number at the plates is portrayed for Newtonian fluids. The presented results in these figures are given in a pair at row for comparison them with the relative velocity. The figures on the left side are for $U^* = 0$ and the

other ones are for $U^* = 1$. The calculation results for the case of negligible viscous dissipation ($Br = 0$) of the present study are compared with the predictions by Shah and London [11] for stationary plates channel or pure Poiseuille flow ($U^* = 0$), and by Shigechi and Araki [4] for Poiseuille-Couette flow ($U^* = 1$), respectively. The circles show the results from [11] and [4]. Even at small values of z^*, it can be seen that the agreement is excellent. Since it was observed that the general qualitative behavior of the axial developments of bulk temperature and Nusselt number at the

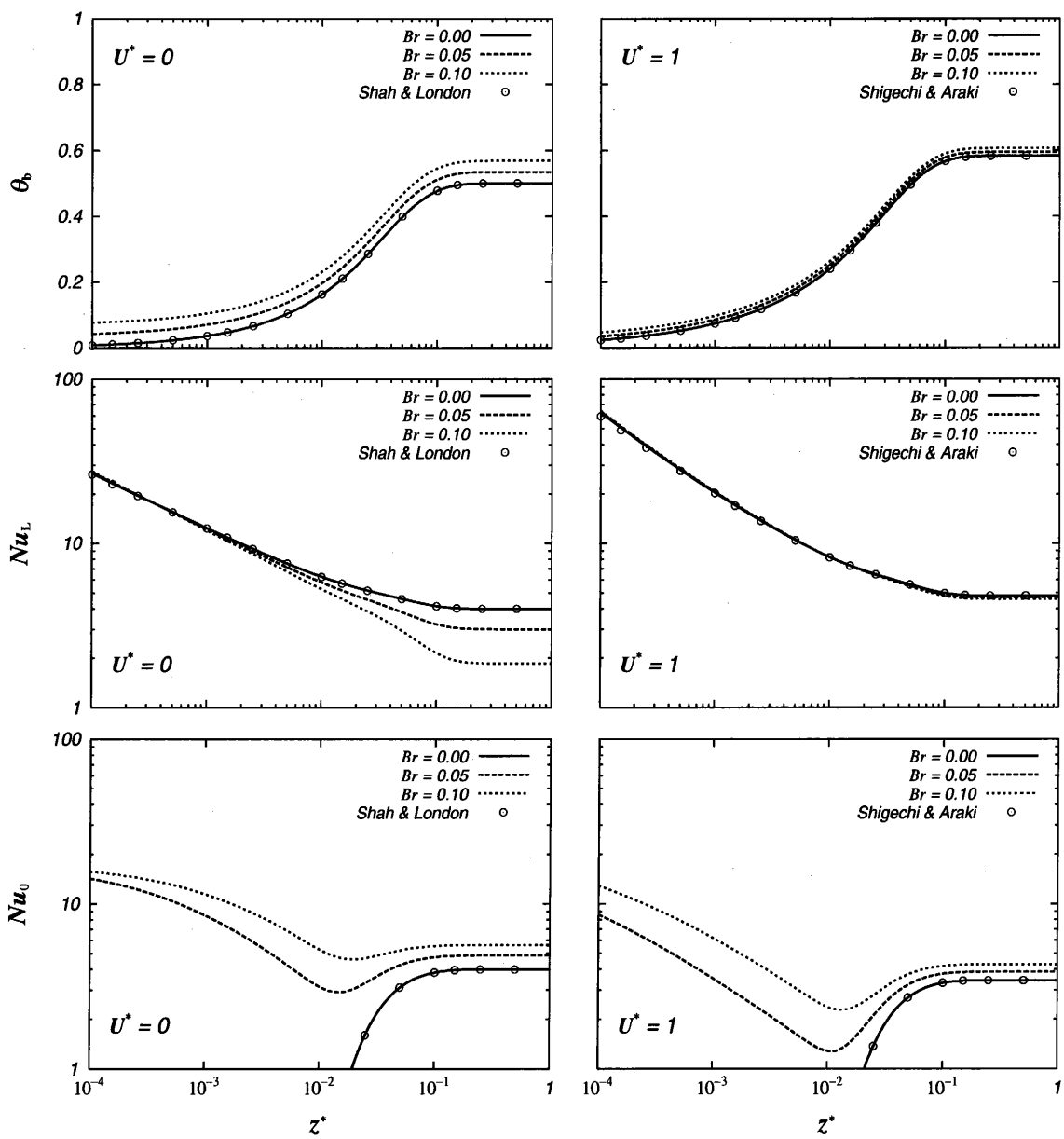

Fig.4-23 Bulk temperature and Nu at the walls for Case A, $U^* = 0$, 1 (Newtonian fluid, $n = 1$)

plates is quite similar for the different fluids, the Brinkman number effects on the bulk temperature, θ_b, Nusselt number at the lower plate, Nu_{L}, and Nusselt number at the upper plate, Nu_0, will be discussed in more detail at the end of this subsection.

Pseudoplastic fluid

As it was mentioned above, the general qualitative behavior of the axial development of temperature is quite similar for different fluids, sample developing temperature profiles are presented to illustrate viscous dissipation effect on developing temperature profiles only for a pseudoplastic fluid of $n = 0.5$ and $\beta = 1$. The local development of the temperature profiles during heating from the lower wall

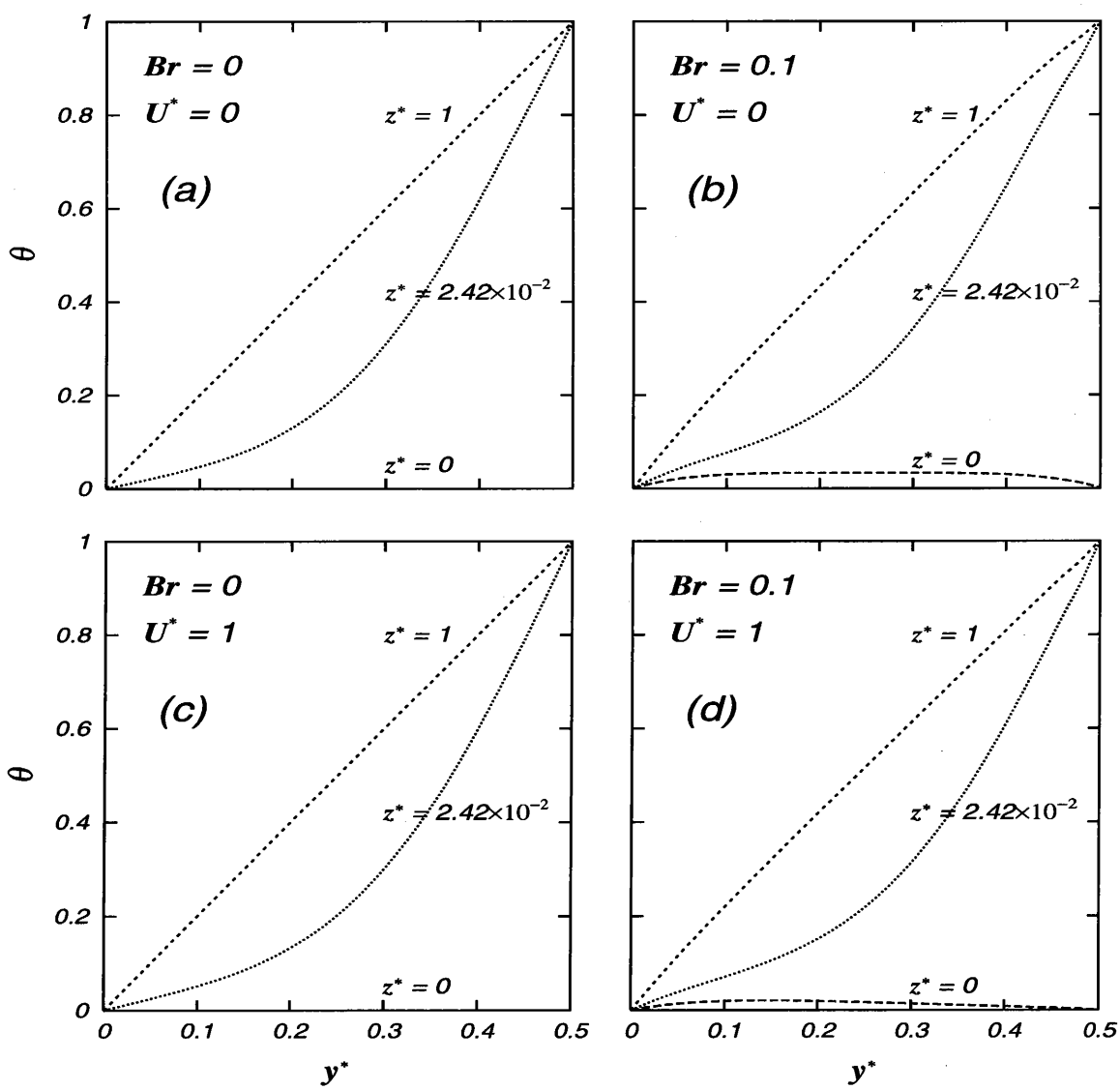

Fig.4-24 Developing temperature profiles for Case A, $U^* = 0$, 1.
(pseudoplastic fluid, $n = 0.5$, $\beta = 1$)

(Case A), of the pseudoplastic fluid ($n = 0.5$ and $\beta = 1$) is shown in Fig.4-24. $y^* = 0$ corresponds to the upper wall and $y^* = 0.5$ is the lower wall. The upper two figures are for $U^* = 0$ and the two figures at the bottom are for $U^* = 1$. By comparing the figures in the same row one can observe the viscous dissipation effect on the developing temperature distributions. If one compares the figures in the same column, then the relative velocity effect on the temperature distribution in the thermal entrance region is observed. At $z^* = 0$, there is a step change in the lower wall temperature. In Figs.4-24(a) and 4-24(c) for $Br = 0$, at $z^* = 0$ the

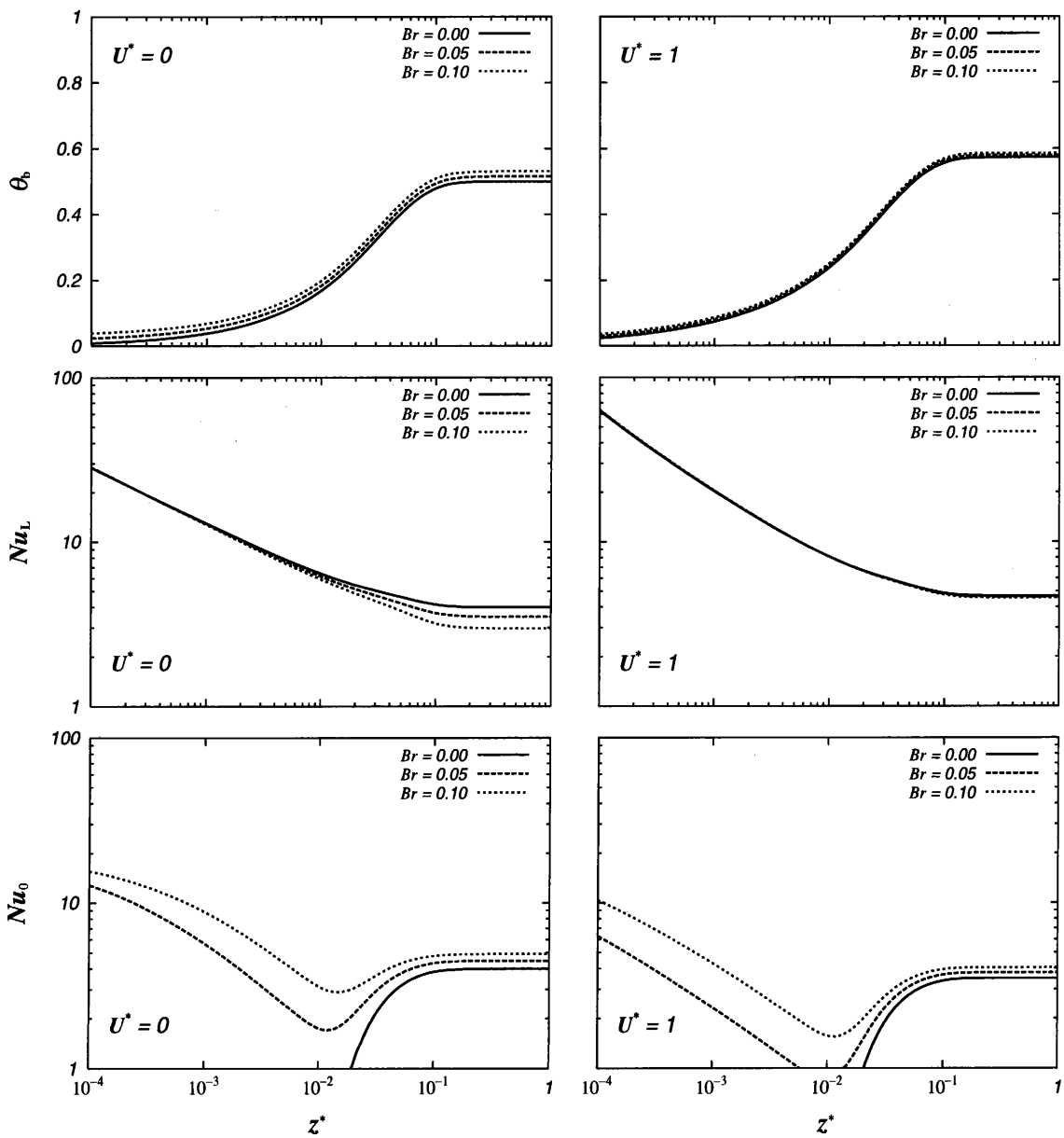

Fig.4-25 Bulk temperature and Nusselt numbers for Case A, $U^* = 0$, 1. (pseudoplastic fluid, $n = 0.5$, $\beta = 1$)

dimensionless fluid temperature is zero. But for $Br = 0.1$, as it is seen in Figs.4-24(b) and 4-24(d) the fluid temperature at $z^* = 0$ is definitely deviates from zero even there is no heat from the wall. This increase is due to the contribution of viscous dissipation in the flowing fluid. Since the highest shear rate occurs near the stationary wall as it was seen in Fig.3-13, the effect of viscous dissipation is most significant near the fixed wall ($y^* = 0$) as shown in Fig.4-24(b) and also it is seen the temperature increase due to viscous dissipation is greater for $U^* = 0$ than for $U^* = 1$.

In order to study the viscous dissipation effect, the heat transfer results for the bulk temperature and Nusselt numbers are shown for a pseudoplastic fluid ($n = 0.5$ and $\beta = 1$) in Fig.4-25. The corresponding heat transfer results are displayed for the three values of Brinkman number on these figures. Figure 4-25 presents the dimensionless bulk temperature and Nusselt number at the walls as functions of the axial distance z^*. The Brinkman number is the parameter in these figures. In these figures the solid lines show the case of negligible viscous dissipation, $Br = 0$. The way of illustration of the figures is given in the explanation for Fig.4-23. Scanning each row of the figures, the relative velocity effect is seen. The figures on the left side are for $U^* = 0$ or for Poiseuille flow case and the other ones are for $U^* = 1$ or for Poiseuille-Couette flow.

Dilatant fluid

The effect of viscous dissipation on heat transfer for a dilatant fluid ($n = 1.5$ and $\beta = 1$) is shown in Fig.4-26, in the same way of illustration as done in Figs.4-23 and 4-25. As it was noted the general qualitative behavior is quite similar to those of the Newtonian and pseudoplastic fluids. But it is seen that for the dilatant fluid the effect of Brinkman number on the dimensionless bulk temperature and on the Nusselt numbers is stronger than for the Newtonian and pseudoplastic fluids.

Discussion

θ, temperature profile

The effect of viscous dissipation is most significant near the fixed wall. The temperature increase due to the viscous dissipation is greater for $U^* = 0$ than for $U^* = 1$.

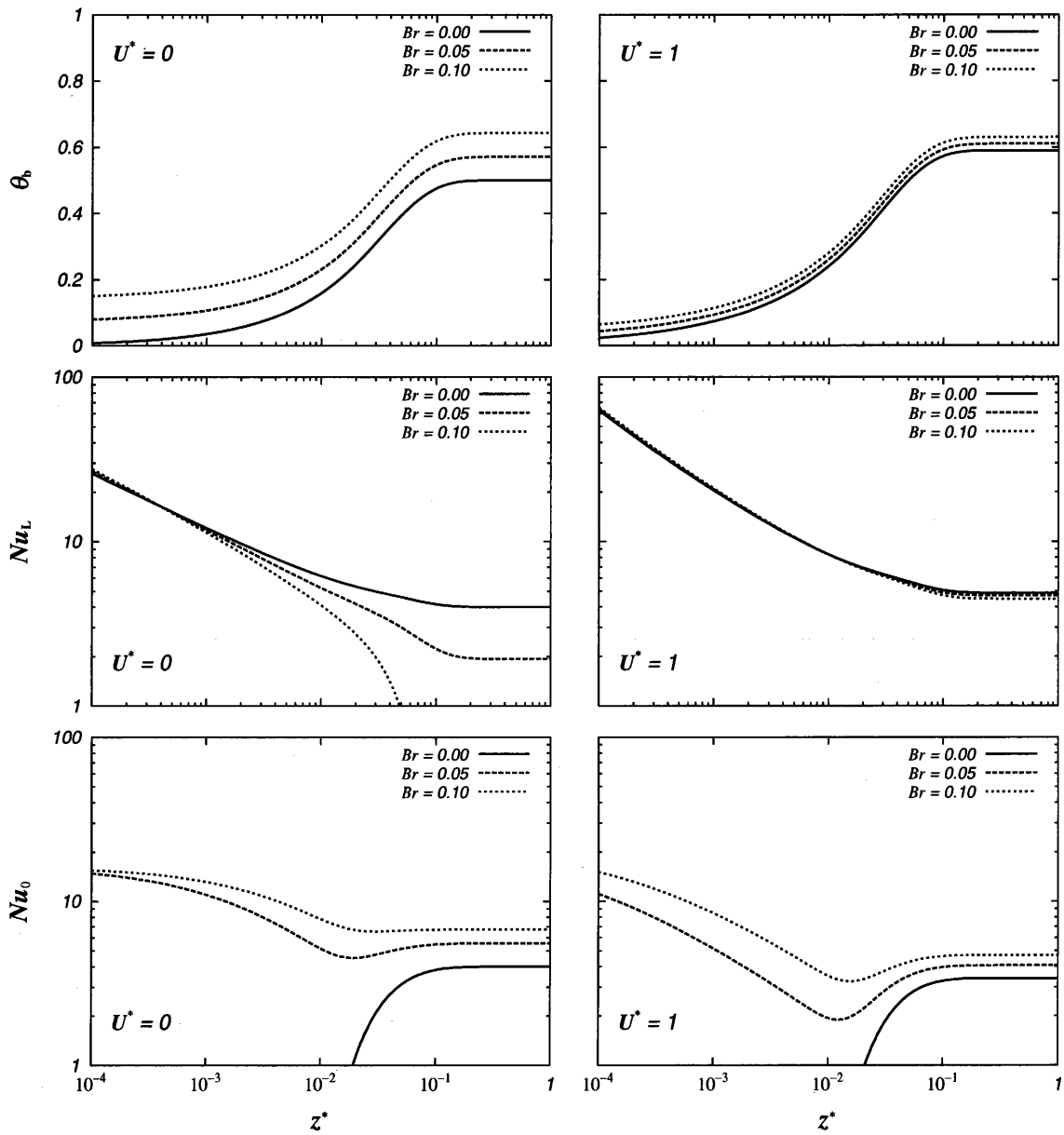

Fig.4-26 Bulk temperature and Nusselt numbers for Case A, $U^* = 0$, 1. (dilatant fluid, $n = 1.5$, $\beta = 1$)

θ_b, bulk temperature

The bulk temperature data show a more pronounced effect of viscous dissipation for $U^* = 0$. The effect of Br on the bulk temperature becomes weak if the lower wall moves with a velocity $U^* = 1$. The moving plate at $U^* = 1$, causes an increase in bulk temperature in the fully developed region.

Nu_L, Nusselt number at the lower wall ($T_L > T_e$)

In the thermal entrance region, the Nusselt numbers are almost identical for the three Brinkman numbers either the cases of the wall being stationary or

moving.

The data show a more pronounced effect of viscous dissipation in the fully developed region for the Poiseuille flow case or if the wall is fixed ($U^* = 0$). For $U^* = 0$, the Nusselt number at the lower wall decreases with an increase in Brinkman number in the fully developed region. However, they are identical for the three Brinkman numbers if the lower wall moves with a velocity $U^* = 1$ throughout both the thermally developing and fully developed regions.

For a specified position with a given Brinkman number, Nusselt number at the lower wall is larger if this wall moves at a velocity of $U^* = 1$ than the case of the wall is fixed.

Nu_0, Nusselt number at the upper, fixed wall ($T_0 = T_e$)

Viscous dissipation effect ($Br \neq 0$) has a strong effect on the Nusselt number at the upper wall.

Nusselt number at the upper wall whose temperature is kept equal to the entering fluid is larger in the case of $U^* = 0$ than in the case of $U^* = 1$.

Including the viscous dissipation causes an increase in Nusselt number at the upper wall. For $n = 0.5$ and $\beta = 1$, the fully developed Nusselt number at the upper wall changes from 4.0 to 4.903 for $U^* = 0$ and, from 3.495 to 4.051 for $U^* = 1$ if Br is increased from 0 to 0.1.

(b) The Case of Stationary Plate Heated

The following figures illustrate the results for Case B, in which the lower wall is kept at the inlet temperature and the upper wall is heated in $0 < z^*$. Since the heat transfer study results of Case B for the Poiseuille flow or for $U^* = 0$ would not give some additional insights into the heat transfer (as the Nusselt number values at the upper wall for Case A are identical to those of the Nusselt numbers at the lower wall for Case B), only the heat transfer results for $U^* = 1$ are presented. However the temperature development is illustrated for $U^* = 0$ and 1 for comparison. The axial development of the bulk temperature is not included.

Sample developing temperature profiles are presented in Fig.4-27 to illustrate the viscous dissipation effect in Case B. These figures show the development of temperature of a pseudoplastic fluid ($n = 0.5$ and $\beta = 1$) by comparing them with the viscous dissipation degree and with the moving lower wall velocity. Scanning each row of the figures, the viscous dissipation effect on the temperature development

is seen. The figures in the first row show the temperature profiles of the Poiseuille flow ($U^* = 0$). The second row figures are for $U^* = 1$ or the Poiseuille-Couette flow. $y^* = 0$ corresponds to the upper wall and $y^* = 0.5$ is for the lower wall. This temperature development is seen to be vice versa with the y^* to those illustrated in Fig.4-24 as the boundary conditions suggest.

Axial developments of Nusselt number at the walls are illustrated in Fig.4-28 for the three different fluid behaviors such that pseudoplastic ($n = 0.5$ and $\beta = 1$), Newtonian ($n = 1$) and dilatant ($n = 1.5$ and $\beta = 1$). The figures on the left side show the Nusselt number at the heated stationary wall. The other figures are for the Nusselt number at the moving wall whose temperature is kept at the entering

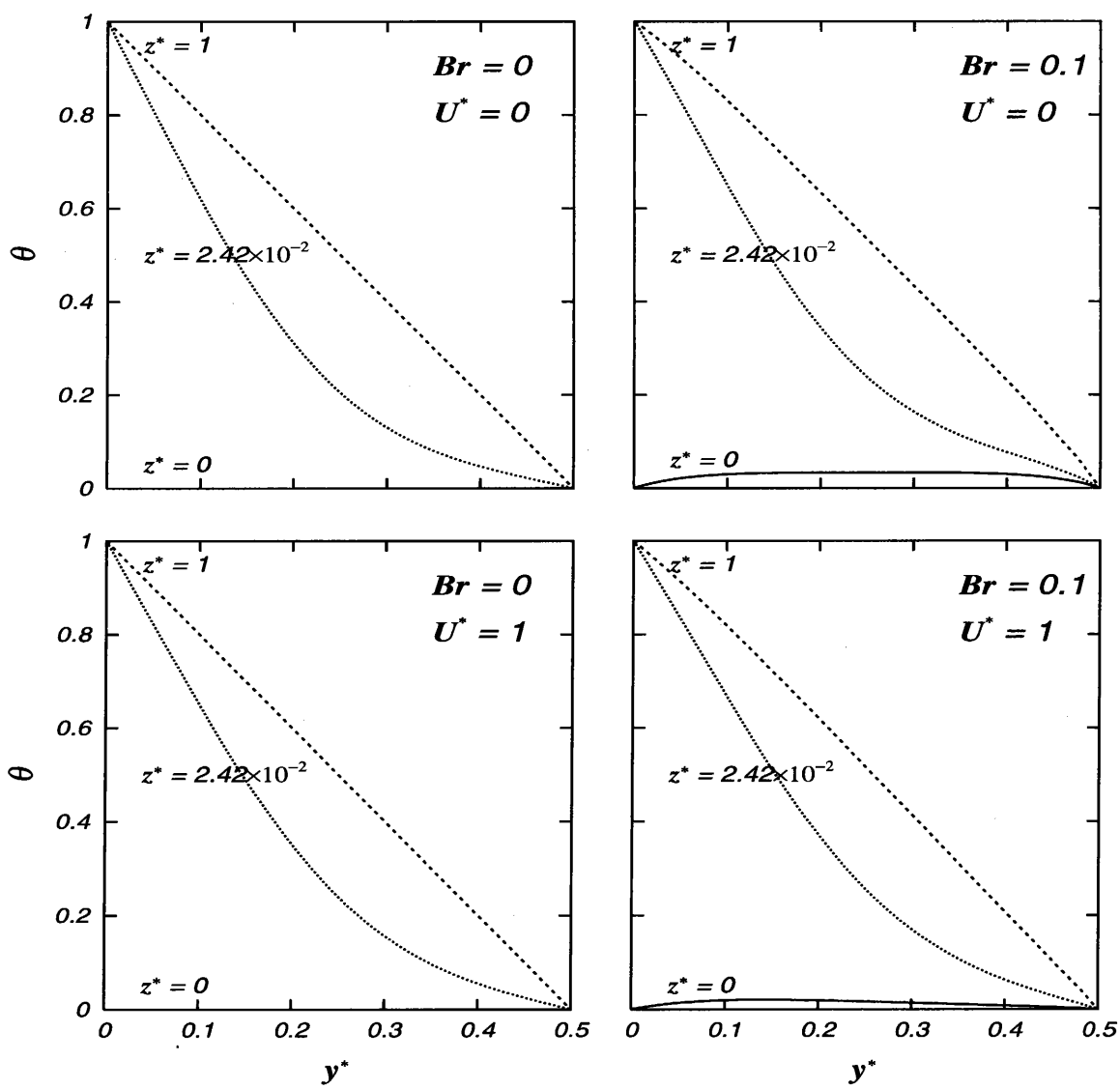

Fig.4-27 Developing temperature profiles for Case B, $U^* = 0$, 1.
(pseudoplastic fluid, $n = 0.5$, $\beta = 1$)

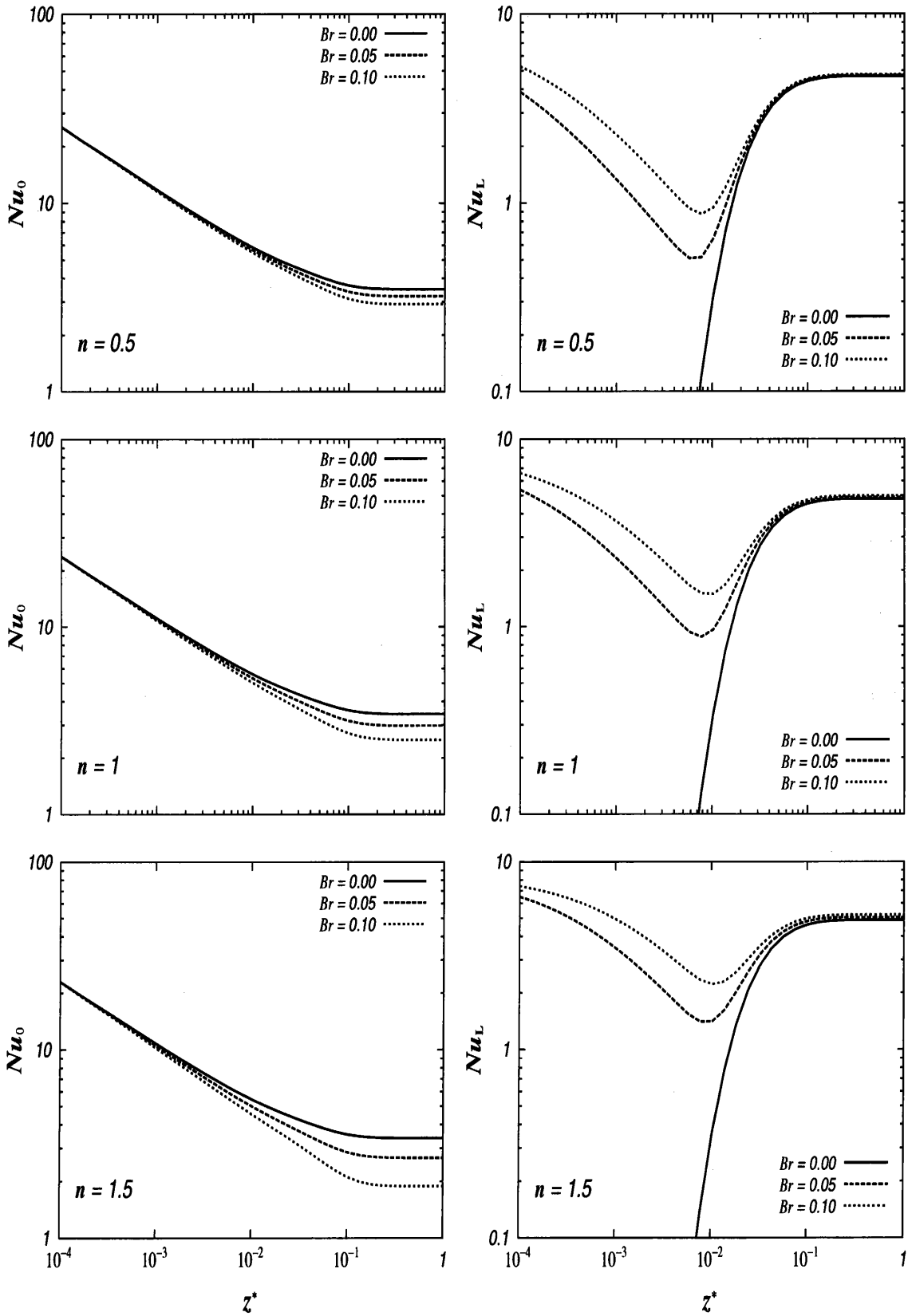

Fig.4-28 Nu at the walls for Case B, $U^* = 1$.

(pseudoplastic, $n = 0.5$, Newtonian, $n = 1$, and dilatant, $n = 1.5$, fluids, $\beta = 1$)

fluid temperature. The results are given with the three values of Brinkman number $Br = 0$, 0.05 and 0.1. The solid lines show the case of negligible viscous dissipation ($Br = 0$). It is seen the qualitative behavior of the heat transfer rate in terms of Nusselt number is similar for the three different fluids. By comparing the figures at the same column in Fig.4-28, one can observe the effect of the flow index, n, on the Nusselt numbers. As it was observed for Case A, the viscous dissipation effect is also stronger in the dilatant fluid than that in the Newtonian and pseudoplastic fluids.

Discussion

Nu_0, Nusselt number at the upper, fixed wall ($T_0 > T_e$) for the case of the lower wall moves at a velocity $U^* = 1$

Nu_0 is seen to be identical for the three Brinkman numbers in the thermal entrance region. But in the fully developed region, Nu_0 decreases with an increase in Br.

Nu_L, Nusselt number at the lower, moving wall ($T_L = T_e$) at a velocity $U^* = 1$

Including viscous dissipation effect in the analysis causes an increase in Nu_L in the thermally developing region. In the fully developed region, the values of Nu_L are almost identical for the three Brinkman number.

4.4.2 The Second Kind Thermal Boundary Condition

(a) The Case of Moving Plate Heated

In the following figures the effects of the viscous dissipation and of the moving wall velocity are shown for the second kind thermal boundary condition. The computed results for Case A, in which the constantly heated lower wall for $z^* > 0$ and the insulated upper wall are illustrated first.

Newtonian fluid

In Fig.4-29, the effects of viscous dissipation on the axial developments of temperatures at the walls, θ_0 and θ_L, and of Nusselt number at the heated lower plate are portrayed for the Newtonian fluid. The presented results in these figures are

given in pair of rows for comparison them with the relative velocity. The figures on the left side are for $U^* = 0$ and the other ones are for $U^* = 1$. The calculation results for the case of neglected viscous dissipation ($Br = 0$) of the present study are compared with the predictions by Shah and London [11] for stationary plates channel or for the Poiseuille flow ($U^* = 0$), and by Shigechi and Araki [4] for the Poiseuille-Couette flow ($U^* = 1$), respectively. The circles show the results from [11] and [4]. Even at small values of z^*, it can be seen that the agreement is excellent. Since it was observed that the general qualitative behaviors of the axial development of the temperature profiles and Nusselt number at the plate are quite similar for the different fluids, the Brinkman number effect on the temperature development and

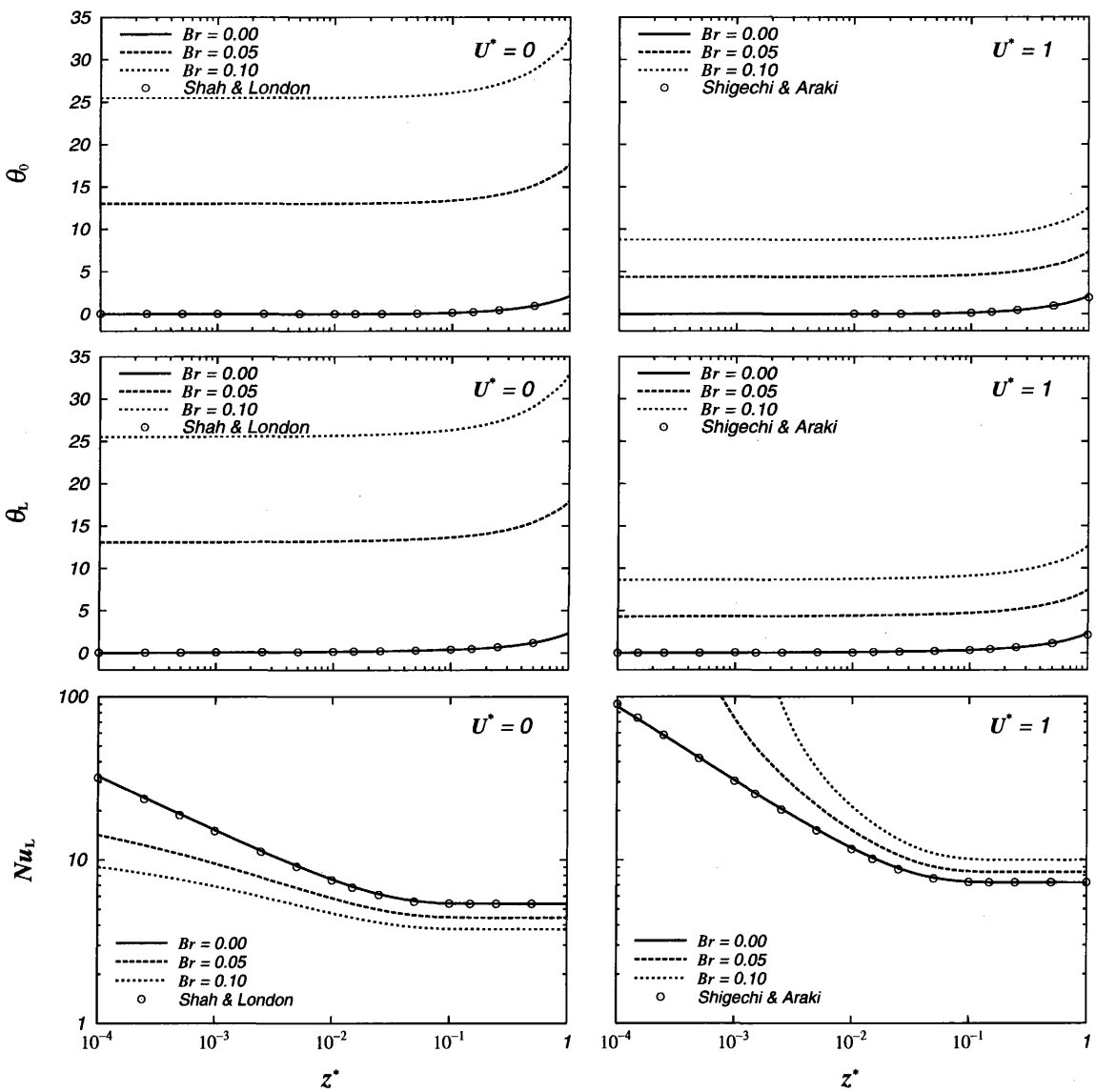

Fig.4-29 Wall temperatures and Nu for Case A, $U^* = 0$, 1.
(Newtonian fluid, $n = 1$)

Nusselt number at the heated plate, Nu_{L}, will be discussed in more detail at the end of this subsection.

Pseudoplastic fluid

As it was mentioned above, the general qualitative behavior of the axial developments of temperature is quite similar for the different fluids, sample developing temperature profiles are presented to illustrate viscous dissipation effect on the developing temperature profiles.

The local development of temperature profiles of a pseudoplastic fluid ($n = 0.5$ and $\beta = 1$) during heating from the lower wall (Case A) is shown in Fig.4-30. The upper two figures are for $U^* = 0$ and the two figures at the bottom are for $U^* = 1$. By comparing the figures in the same row one can observe the effect of viscous dissipation on the developing temperature distributions. If one compares the figures in the same column, then the relative velocity effect on the temperature distribution in the thermal entrance region is observed. $y^* = 0$ corresponds to the upper wall and $y^* = 0.5$ is the lower wall. At $z^* = 0$, there is a step change in heat flux at the lower wall. Figures 4-30(a) and 4-30(c) are for $Br = 0$ and there at $z^* = 0$ the dimensionless fluid temperature is zero. But for $Br = 0.1$, as it is seen in Figs.4-30(b) and 4-30(d) the fluid temperature at $z^* = 0$ is definitely deviates from zero even there is no heat flux from the wall. This increase is due to the contribution of the viscous dissipation in the flowing fluid. Since the highest shear rate occurs near the stationary wall as it was seen in Fig.3-13, the effect of viscous dissipation is most significant near the fixed wall ($y^* = 0$) as shown in Fig.4-30(b) and also it is seen the temperature increase due to viscous dissipation is greater for $U^* = 0$ than for $U^* = 1$. In fact, it can be seen from Figs.4-30(b) and 4-30(d) that the fluid temperature increases significantly before the fluid reaches the heated wall because of the heat generated by the viscous dissipation effect. As this effect builds up, heat is transferred to the main body of the fluid flow and heat generation due to viscous dissipation behaves like a heat source. Also from the developing temperature profiles, it is seen for the boundary condition of constant wall heat flux, the wall-to-fluid temperature difference is small whereas the effect of viscous dissipation is more significant.

In order to study the viscous dissipation effect, the heat transfer results are shown for a pseudoplastic fluid ($n = 0.5$ and $\beta = 1$) in Fig.4-31. The heat transfer results for the bulk temperature and for the Nusselt number at the heated wall are

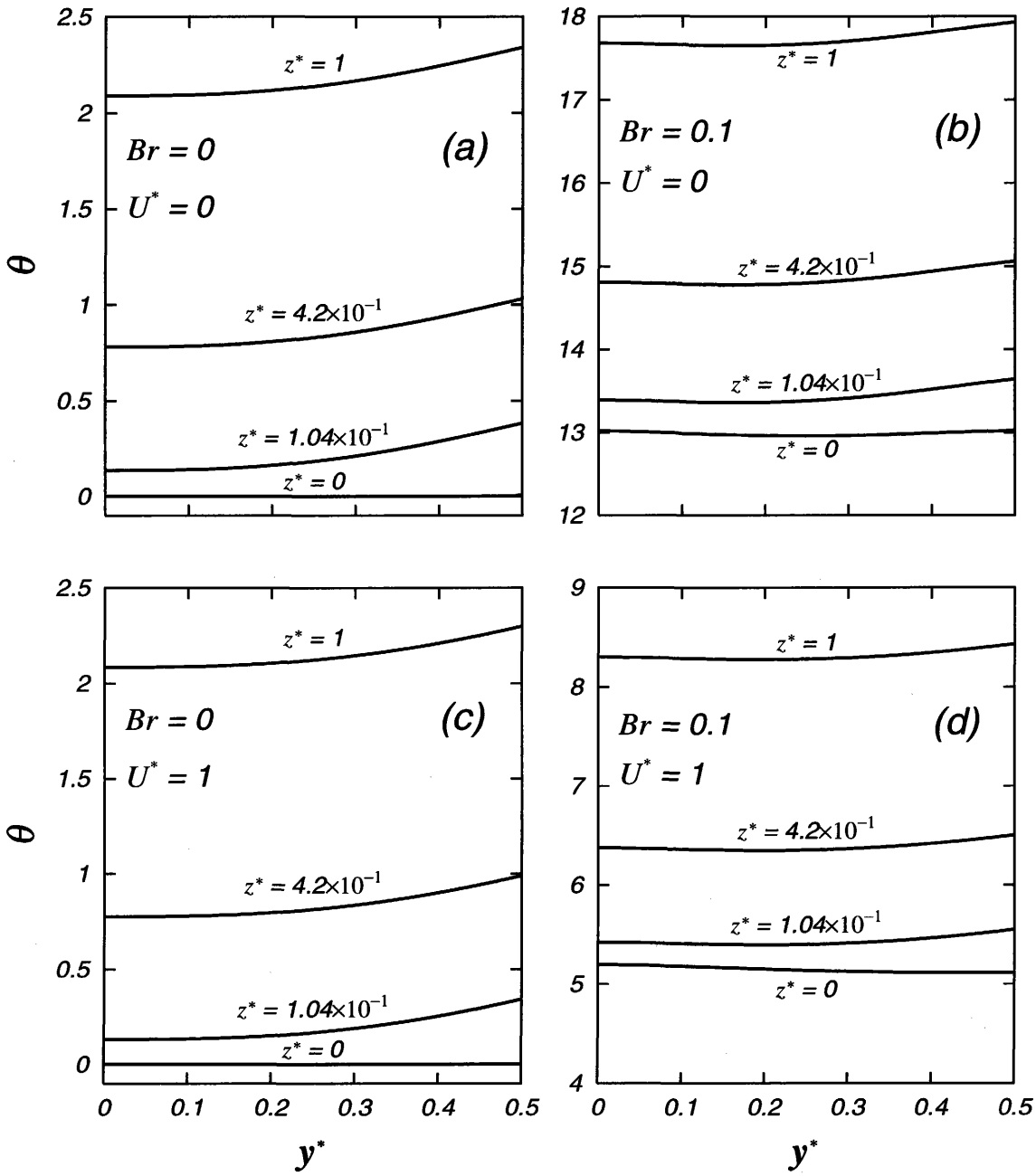

Fig.4-30 Developing temperature profiles for Case A, $U^* = 0$, 1.
(pseudoplastic fluid, $n = 0.5$, $\beta = 1$)

displayed for the three values of Brinkman number on these figures. Figure 4-31 displays θ_b and Nu_L as functions of the axial distance z^*. The Brinkman number is the parameter in these figures. In these figures the solid lines show the case of negligible viscous dissipation $Br = 0$. The way of illustration of the figures is given in the explanation for Fig.4-29. Scanning each row of the figures, the relative velocity effect is seen. The figures on the left side are for $U^* = 0$ or for the Poiseuille flow and the other ones are for $U^* = 1$ or for the Poiseuille-Couette flow.

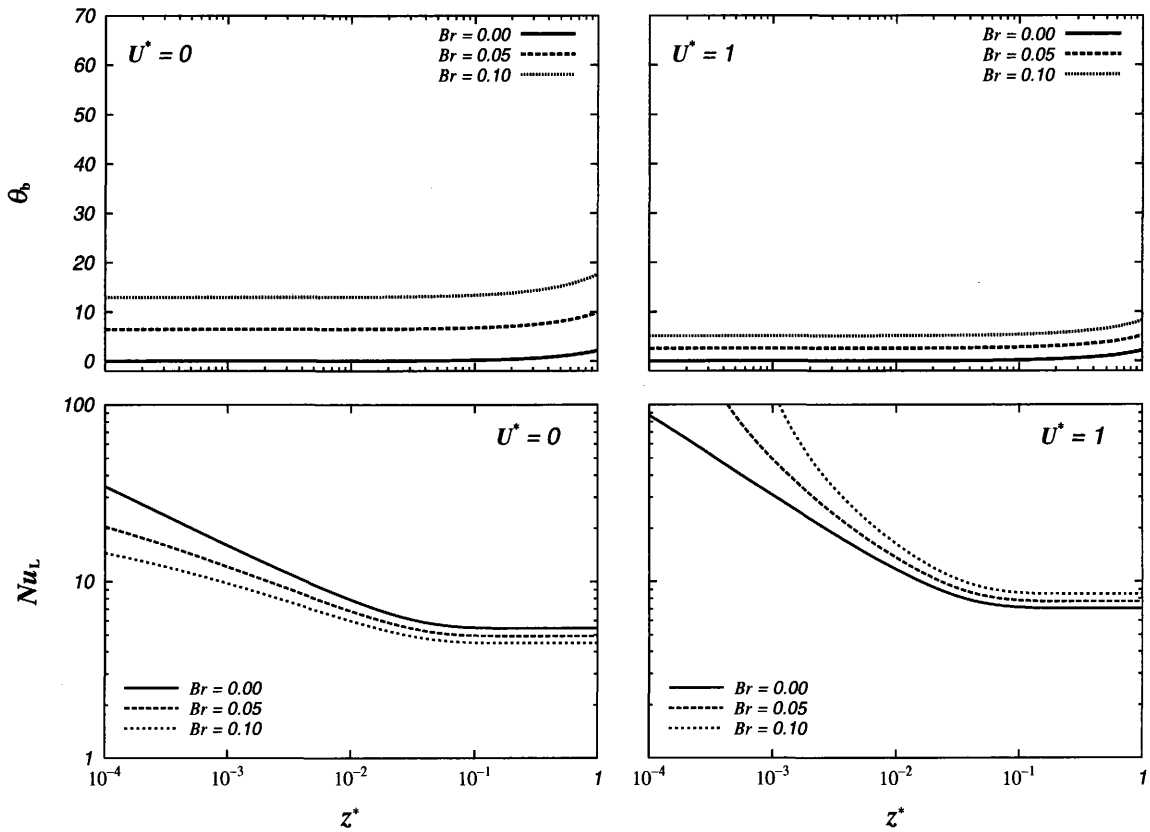

Fig.4-31 Bulk temperature and Nu for Case A, $U^* = 0$, 1.
(pseudoplastic fluid, $n = 0.5$, $\beta = 1$)

Dilatant fluid

The viscous dissipation effect on the heat transfer for a dilatant fluid ($n = 1.5$ and $\beta = 1$) is shown in the following figures in the same way of illustration as done in Figs.4-29 and 4-31. As it was noted the general qualitative behavior is quite similar to those of the Newtonian and pseudoplastic fluids. It is seen also that for the dilatant fluid the effect of Brinkman number on the dimensionless bulk temperature and on the Nusselt number is stronger than for the Newtonian and pseudoplastic fluids.

Discussion

θ, temperature profile

The temperature increase due to the viscous dissipation effect is greater for $U^* = 0$ than for $U^* = 1$.

For the boundary condition of constant wall heat flux, the wall-to-fluid temperature difference is small whereas the viscous dissipation effect is more sig-

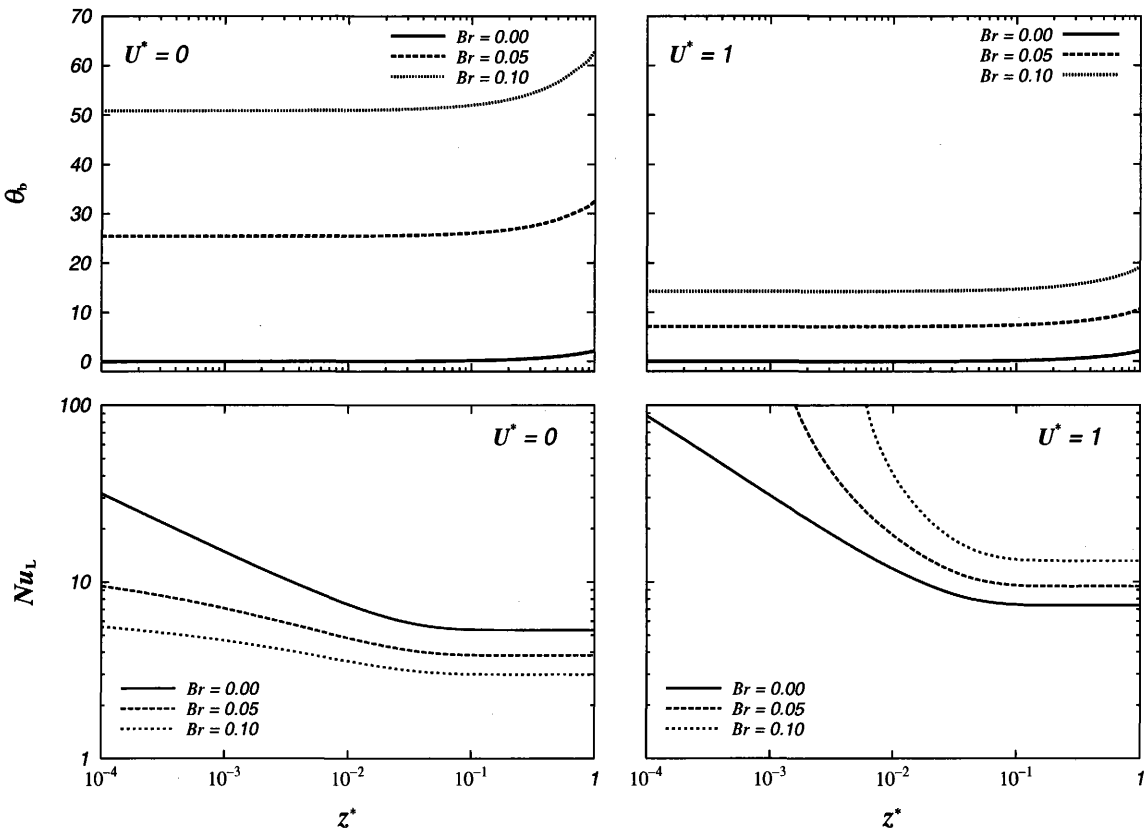

Fig.4-32 Wall temperatures and Nu for Case A, $U^* = 0$, 1.
(dilatant fluid, $n = 1.5$, $\beta = 1$)

nificant than the first kind of thermal boundary condition case.

θ_b, bulk temperature

The bulk temperature data show a more pronounced effect of viscous dissipation for $U^* = 0$. The moving plate at $U^* = 1$, causes a decrease in bulk temperature. It may be explained as follows. The moving plate at $U^* = 1$ induces more fluid flow. However the heat flux at the plate is constant. Then the temperature increase is less for $U^* = 1$ than $U^* = 0$.

Nu_L, Nusselt number at the lower heated wall (q_L = const, $0 < z^*$)

Unlike the first kind T.B.C., the Nusselt number at the heated wall is greatly affected by Br in both of the thermal entrance region and fully developed region.

The effect of Br on Nusselt number is different depending on the relative velocity, U^*. In the fully developed region, viscous dissipation has a definite effect for both cases of $U^* = 0$ and $U^* = 1$. Nusselt number decreases with

an increase in Br for the fixed walls case ($U^* = 0$) and vice versa for the case of the moving wall ($U^* = 1$). These behaviors of Nu due to the viscous dissipation are comprehended as follows. The value of Nu is calculated using the dimensionless temperature difference ($\theta_{\mathrm{L}} - \theta_{\mathrm{b}}$) as is given by Eq.(4.22). Both of θ_{L} and θ_b increase in the flow direction of z^* as it is illustrated in Fig.4-30 and Fig.4-31. In terms of the increments of θ_{L} and θ_{b} due to the viscous dissipation, the increment of θ_{L} is larger than that of θ_{b} for $U^* = 0$ and vice versa for $U^* = 1$.

(b) The Case of Stationary Plate Heated

The following figures illustrate the results for Case B, in which the lower wall is insulated with the upper wall is heated constantly in $0 < z^*$. Since the heat transfer study results of Case B for the Poiseuille flow or for $U^* = 0$ would not give some additional insights into the heat transfer (as the Nusselt number values at the upper wall for Case A are identical to those of the Nusselt numbers at the lower wall for Case B), only the results for $U^* = 1$ are presented. Also the axial development of the bulk temperature is not included. The axial development of the Nusselt number at the upper wall is illustrated in Fig.4-33 for the Newtonian, pseudoplastic and dilatant fluids in Poiseuille-Couette flow. The results are given with the three values of Brinkman number. The solid lines show the case of negligible viscous dissipation ($Br = 0$).

Discussion

Nu_0, Nusselt number at the upper, heated stationary wall (q_o = const, $0 < z$), for the case of the lower wall moves at $U^* = 1$

Nusselt number decreases with an increase in Brinkman number and including the viscous dissipation in the analysis causes a decrease in Nusselt number at that wall if the other moving wall is insulated.

As it was noted for Case A, the viscous dissipation has stronger effect in the dilatant fluid than that in the Newtonian and pseudoplastic fluids.

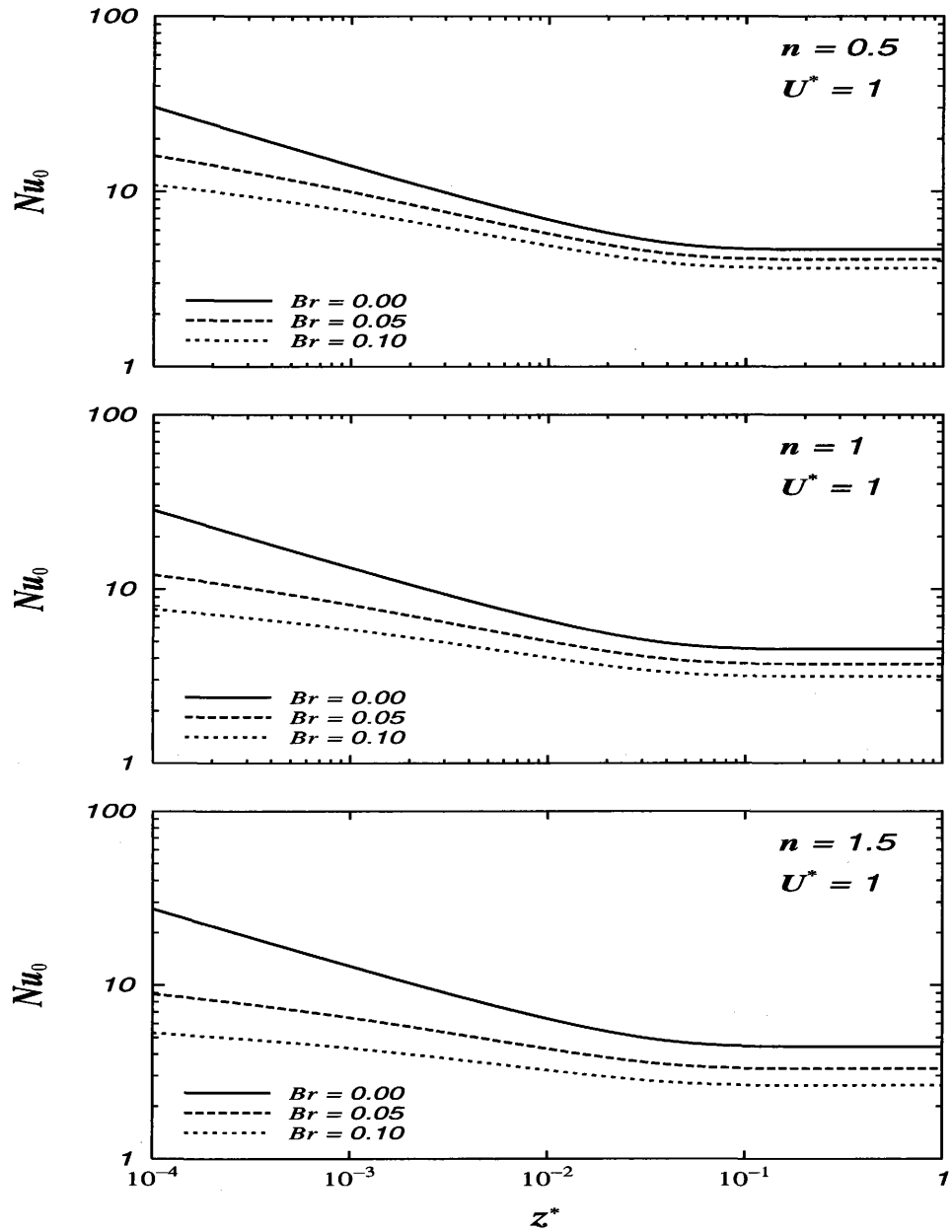

Fig.4-33 Nu for Case B, $U^* = 1$.

(pseudoplastic, $n = 0.5$, Newtonian, $n = 1$, and dilatant, $n = 1.5$, fluids, $\beta = 1$)

4.5 Effect of Axial Heat Conduction for $Br = 0$

Various relevant results and figures have been discussed from the view point of fluid axial heat conduction phenomena in the plane Poiseuille-Couette flow by neglecting the viscous dissipation term or by setting the Brinkman number value as zero. Peclet number is proposed to serve as a controlling index that indicates the relative importance of the fluid axial heat conduction.

4.5.1 The First Kind Thermal Boundary Condition

(a) The Case of Moving Plate Heated

In the following figures the effects of axial heat conduction combined with the moving wall velocity is shown. The computed results for Case A, in which the lower wall is heated in $0 < z^*$ and the upper wall is specified at the inlet fluid temperature, are illustrated first.

Newtonian fluid

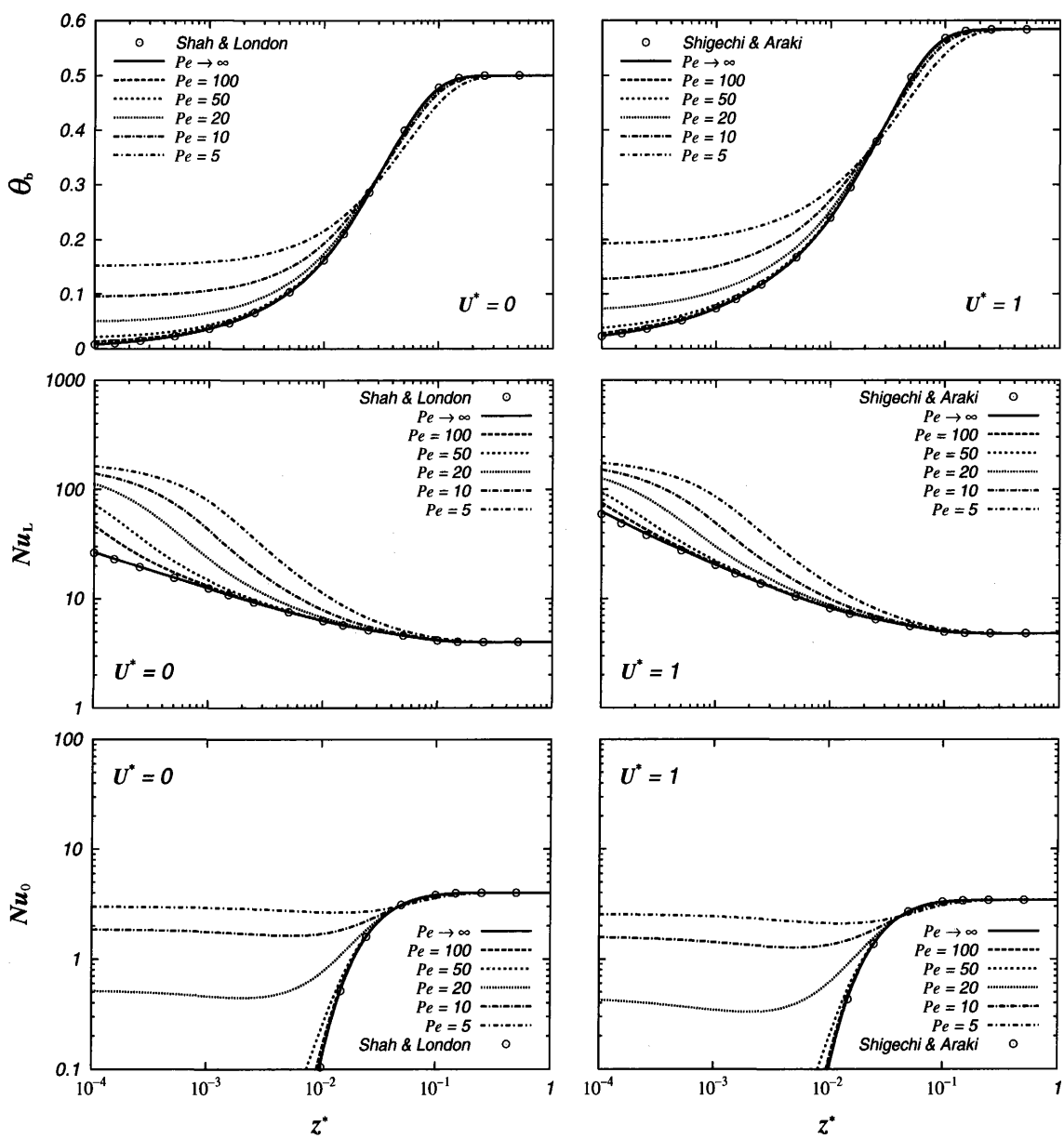

Fig.4-34 Bulk temperature and Nu at the walls for Case A, $U^* = 0$, 1 (Newtonian fluid, $n = 1$)

In Fig.4-34 the axial heat conduction effect on the axial developments of the bulk temperature and Nusselt number at the plates are portrayed for a Newtonian fluid. The presented figures are given in pair for comparison them with the relative velocity. The figures on the left side are for $U^* = 0$ and the other ones are for $U^* = 1$. The calculation results for the case of neglected fluid axial heat conduction ($Pe \rightarrow \infty$) of the present study are compared with the predictions by Shah and London [11] for stationary plates channel or for the Poiseuille flow ($U^* = 0$), and by Shigechi and Araki [4] for the Poiseuille-Couette flow ($U^* = 1$), respectively. The circles show the results from [11] and [4]. Even at small values of z^*, it can be seen that the agreement is excellent. Since it was observed that the general qualitative behaviors of the axial development of bulk temperature and Nusselt number at the plates are quite similar for the different fluids, the Peclet number effects on the bulk temperature, θ_b, Nusselt number at the lower plate, Nu_{L}, and Nusselt number at the upper plate, Nu_0, will be discussed in more detail later at the end of this subsection.

Pseudoplastic fluid

Sample developing temperature profiles are presented to illustrate the fluid axial heat conduction effect on the developing temperature profiles. The local development of temperature profiles during heating, from the lower wall (Case A), of a pseudoplastic fluid ($n = 0.5$ and $\beta = 1$) is shown in Fig.4-35. The upper two figures are for $U^* = 0$ and the two figures at the bottom are for $U^* = 1$. By comparing the figures in the same row one can observe the effect of fluid axial heat conduction on the developing temperature distributions. If one compares the figures in the same column, then the relative velocity effect on the temperature distribution in the thermal entrance region is observed. $y^* = 0$ corresponds to the upper wall and $y^* = 0.5$ is the lower wall. At $z^* = 0$, there is a step change in the lower wall temperature. In Figs.4-35(a) and 4-35(c) for $Pe \rightarrow \infty$, at $z^* = 0$ the dimensionless fluid temperature is zero. But for $Pe = 10$, as it is seen in Figs.4-35(b) and 4-35(d) the fluid temperature at $z^* = 0$ is definitely deviates from zero even there is no heat from the wall. This increase is due to the contribution of the axial heat conduction within the fluid. Scanning each row of the figures, one can observe that the influence of the fluid axial heat conduction in the fluid vanishes with an increasing Peclet number. From Figs.4-35(b) and 4-35(d), it is seen the temperature increase due to the fluid axial heat conduction is greater for $U^* = 0$ than for $U^* = 1$. This is because fluid

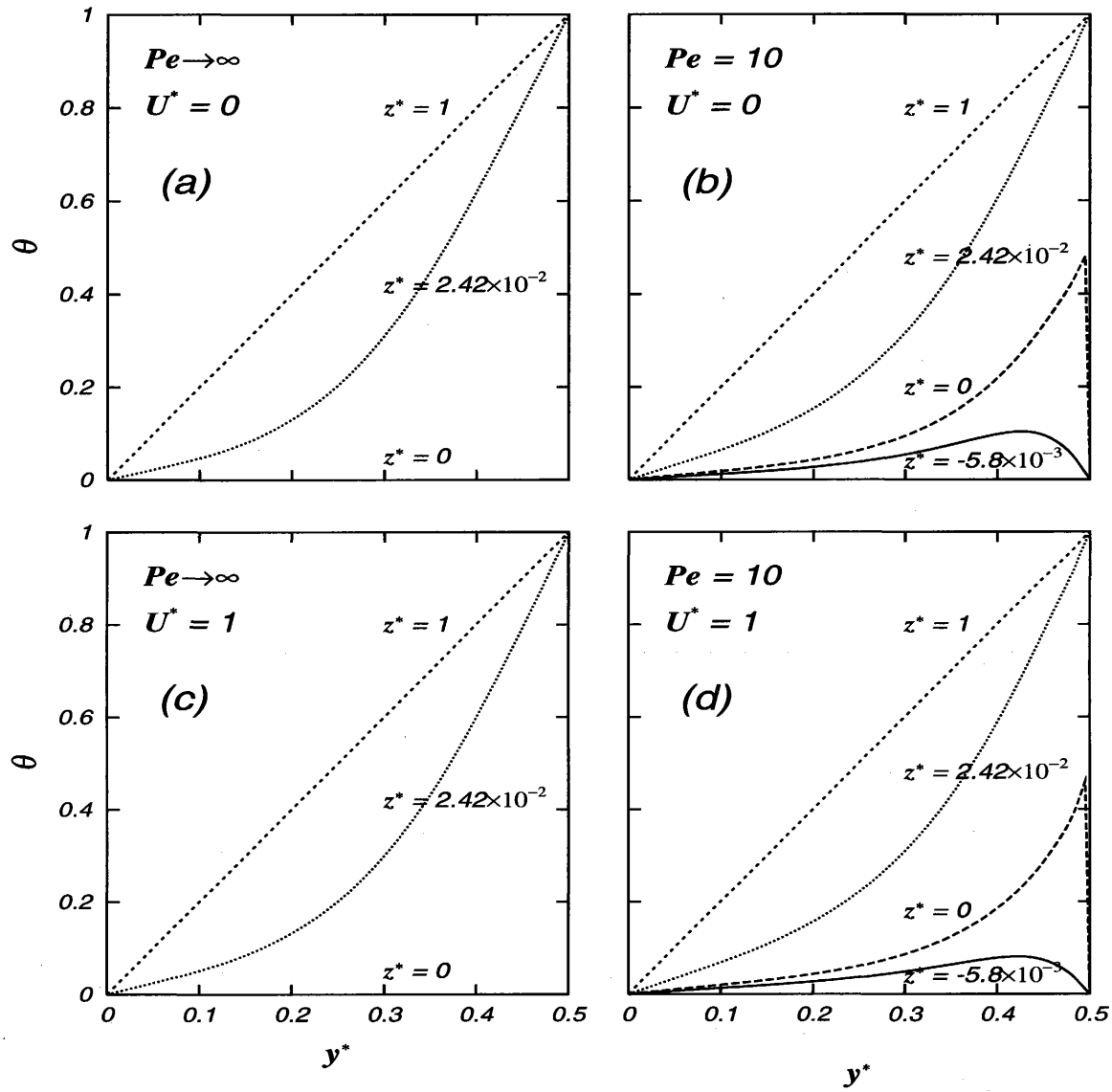

Fig.4-35 Developing temperature profiles for Case A, $U^* = 0$, 1.
(pseudoplastic fluid, $n = 0.5$, $\beta = 1$)

axial heat conduction is directed against the axial convection direction and for U^* = 1 the moving wall at $y^* = 0.5$ causes an increase in the flow velocity specially near the heated wall as it is shown in Fig.3-12.

In order to study the fluid axial heat conduction effect, the heat transfer results are shown for a pseudoplastic fluid ($n = 0.5$ and $\beta = 1$) in Fig.4-36. These figures display the dimensionless bulk temperature and Nusselt number at the walls as functions of the axial distance z^*. The corresponding heat transfer results are displayed for the six values of Peclet number on these figures. The Peclet number is the parameter in these figures. In these figures the solid lines show the case of negligible fluid axial heat conduction $Pe \to \infty$. The way of illustration of the fig-

ures is given in the explanation for Fig.4-34. Scanning each row of the figures, the relative velocity effect is seen. The figures on the left side are for $U^* = 0$ or for the Poiseuille flow and the other ones are for $U^* = 1$ or for the Poiseuille-Couette flow.

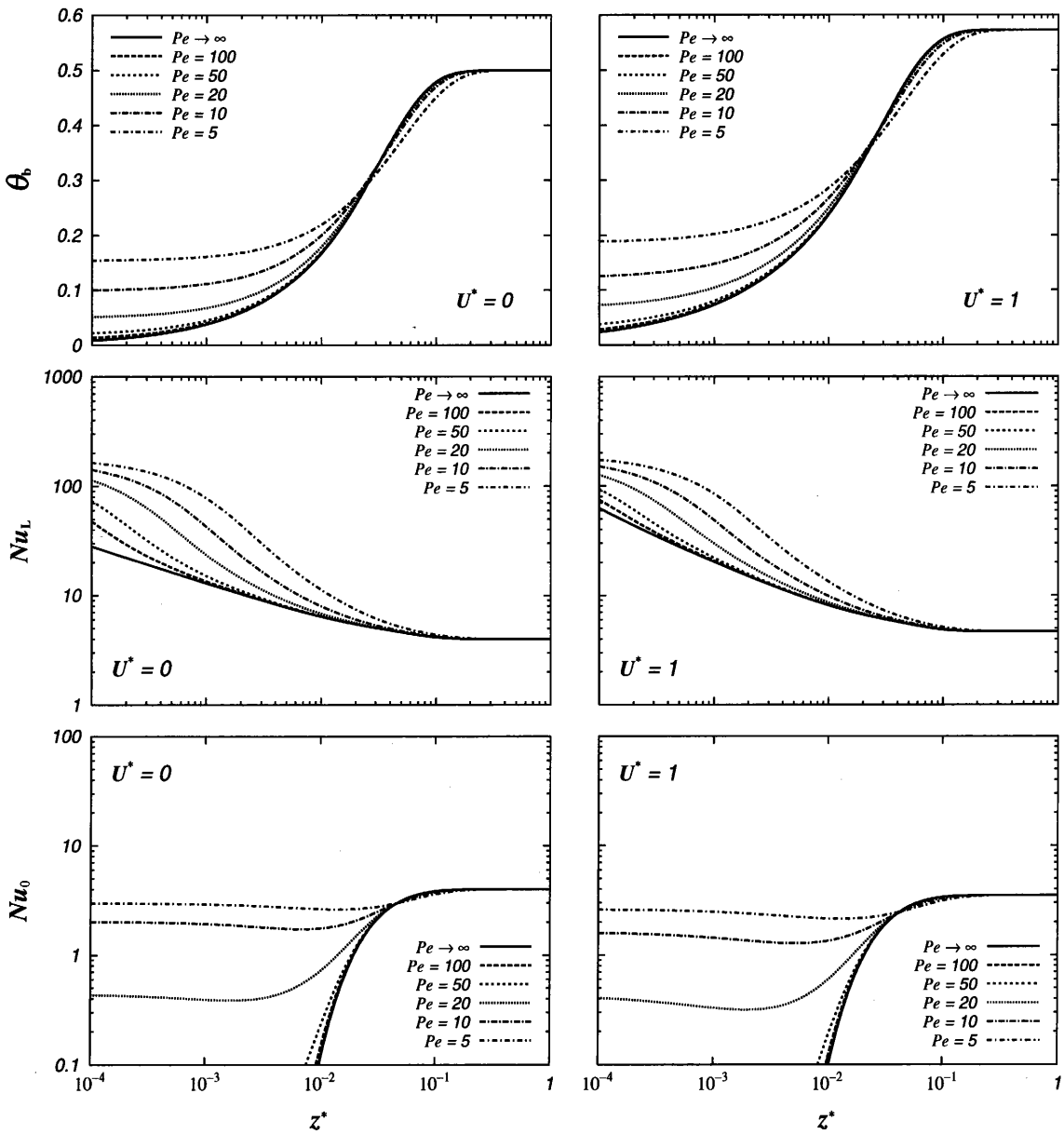

Fig.4-36 Bulk temperature and Nu at the walls for Case A, $U^* = 0$, 1 (pseudoplastic fluid, $n = 0.5$, $\beta = 1$)

Dilatant fluid

The fluid axial heat conduction effect on the heat transfer for a dilatant fluid ($n = 1.5$ and $\beta = 1$) is shown in the following figures in the same way of illustration as done in Figs.4-34 and 4-36. It was noted the general qualitative behaviors are quite

similar to those of the Newtonian and pseudoplastic fluids.

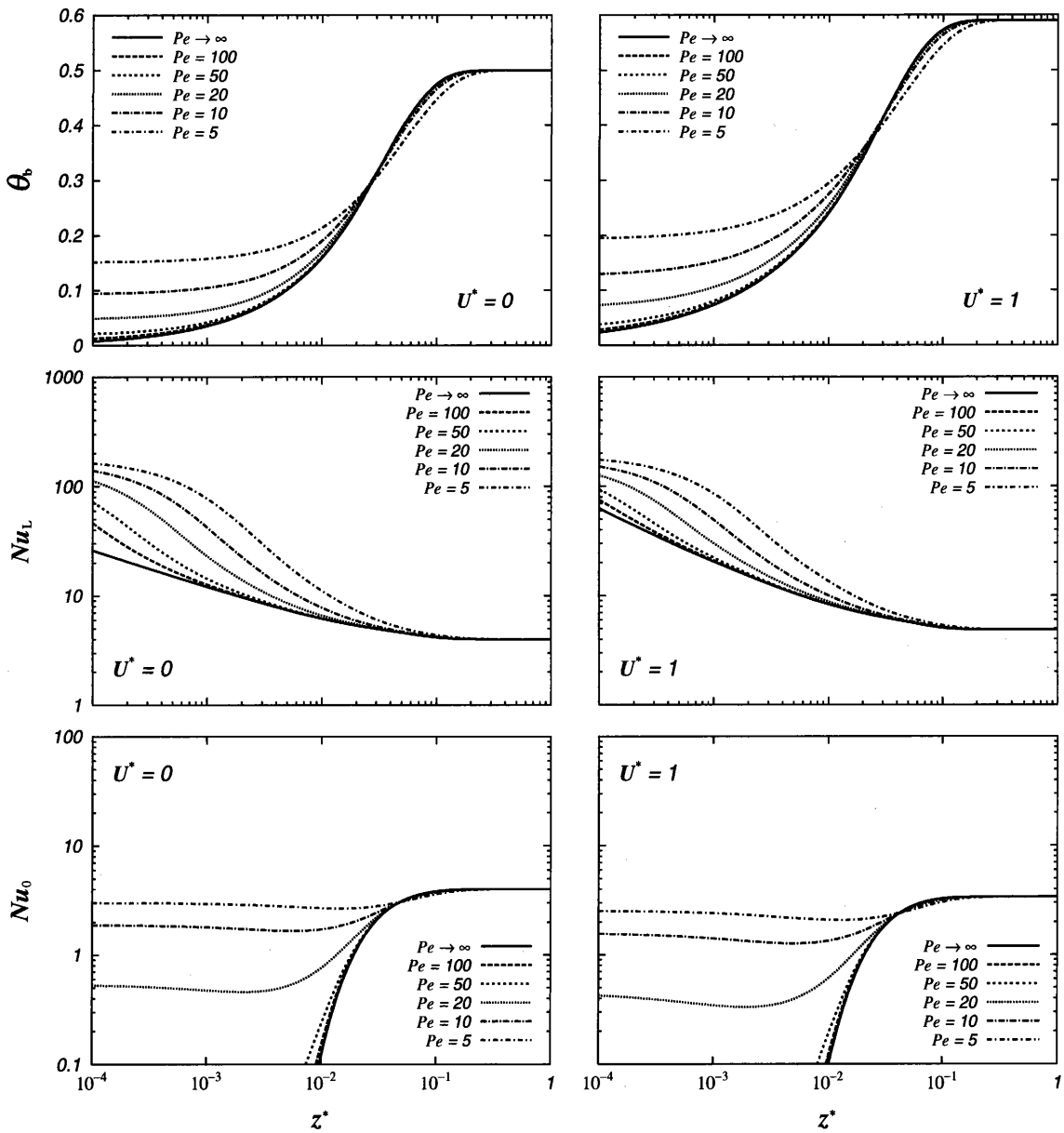

Fig.4-37 Bulk temperature and Nu at the walls for Case A, $U^* = 0$, 1 (dilatant fluid, $n = 1.5$, $\beta = 1$)

Discussion

θ, temperature profile

The temperature increase due to the fluid axial heat conduction is greater for $U^* = 0$ than for $U^* = 1$. This is because the fluid axial heat conduction is directed against the axial convection direction and for $U^* = 1$ the moving wall causes an increase in the flow velocity.

θ_b, bulk temperature

The dimensionless bulk temperature increases with decreasing Peclet number in the thermally developing region, while they are almost identical in the fully developed region.

The bulk temperature in both the thermal entrance region and the fully developed region is higher for the case of moving lower wall ($U^* = 1$) than in the case of $U^* = 0$. This increase is due to the convection.

Nu_L, Nusselt number at the lower wall ($T_L > T_e$, $0 < z^*$)

In the fully developed region, the Nusselt numbers at the wall are almost identical for the six Peclet numbers either the cases $U^* = 0$ and $U^* = 1$.

In the thermally developing region, Nusselt number increases with decreasing Peclet number. For a specified position with a given Peclet number, Nusselt number at the lower wall is larger if this wall moves at a velocity of $U^* = 1$ than the case of $U^* = 0$.

Nu_0, Nusselt number at the upper, fixed wall ($T_0 = T_e$)

In the thermally developing region, Nusselt number increases with decreasing Peclet number.

Nusselt number at the upper wall remains almost constant throughout the thermal entrance region if Pe is small. This behavior is attributed to that the fluid temperature increases due to the fluid axial heat conduction (for $z^* \leq 0$) before the fluid flow reaches the heated wall.

(b) The Case of Stationary Plate Heated

The following figures illustrate the results for Case B, in which the lower wall is kept at the inlet temperature and the upper wall is heated in $0 < z^*$. Since the heat transfer study results of Case B for the Poiseuille flow or for $U^* = 0$ would not give some additional insights into the heat transfer (as the Nusselt number values at the upper wall for Case A are identical to those of the Nusselt numbers at the lower wall for Case B), only the results for $U^* = 1$ are presented. Also the axial development of the bulk temperature is not included.

Newtonian fluid

Axial development of the Nusselt numbers at the walls is illustrated in Fig.4-38 for the Newtonian fluid in the Poiseuille-Couette flow. The solid lines show the case

of negligible fluid axial heat conduction ($Pe \to \infty$). The results are given with the six values of Peclet number.

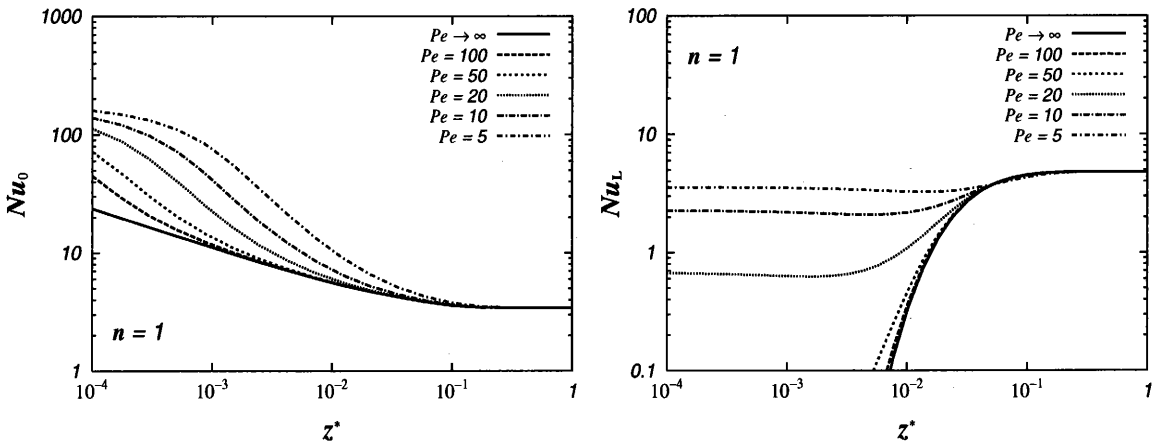

Fig.4-38 Nu at the walls for Case B, $U^* = 1$.
(Newtonian fluid, $n = 1$)

Pseudoplastic and dilatant fluids

In the below Nusselt numbers at the walls are shown for pseudoplastic and dilatant fluids. It is seen the qualitative behaviors of the heat transfer rate in terms of Nusselt number are similar to the Newtonian fluids that was discussed above. By comparing the figures in the same row in Fig.4-39, the effect of the flow index, n, on Nusselt number can be discerned and as expected from Eq.(4.14) no significant differences exist between them.

Discussion

Nu_0, Nusselt number at the upper, heated stationary wall ($T_0 > T_e$, $0 < z^*$)

Nu_0 is seen to be almost identical for the six Peclet numbers in the thermally fully developed region.

In the thermally developing region, Nu_0 decreases with an increase in Peclet number.

Nu_L, Nusselt number at the lower moving wall ($T_L = T_e$)

Including the axial heat conduction effect in the analysis causes an increase in the thermally developing region.

In the fully developed region, the values of Nu_L are almost identical for the six Peclet number.

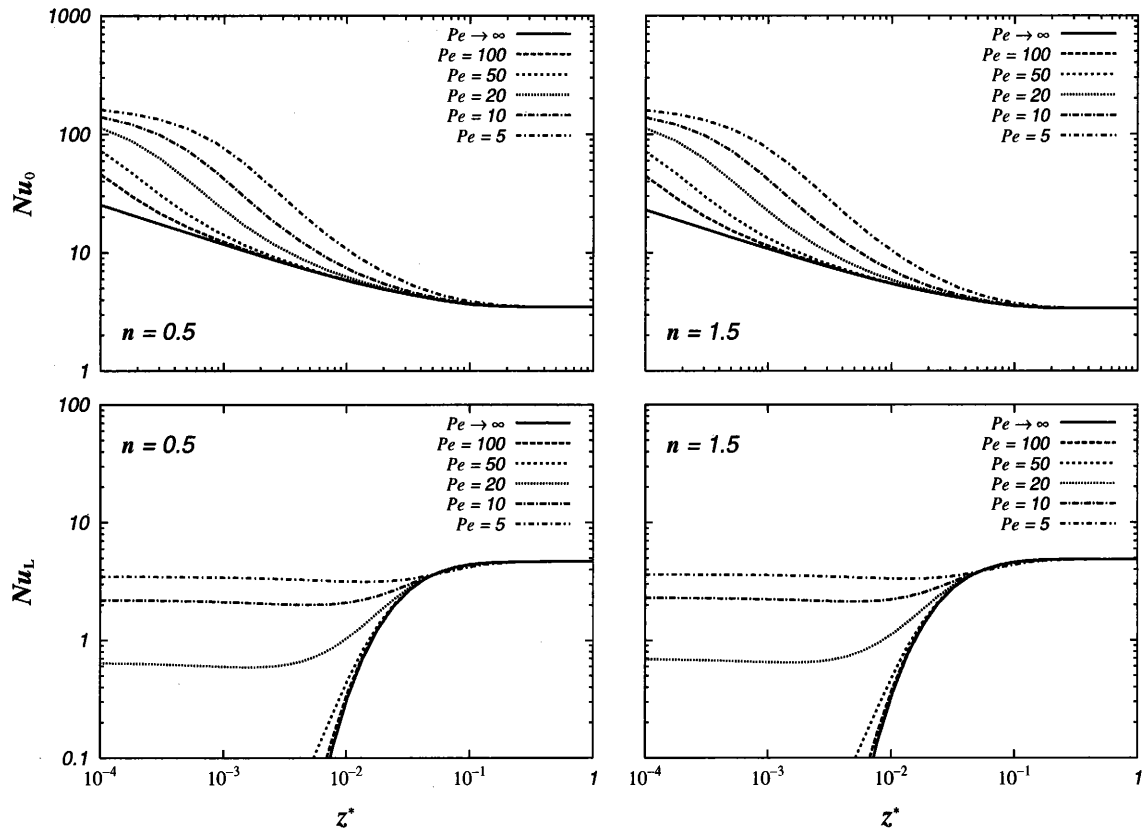

Fig.4-39 Nu at the walls for Case B, $U^* = 1$.
(pseudoplastic, $n = 0.5$ and dilatant, $n = 1.5$ fluids, $\beta = 1$)

4.5.2 The Second Kind Thermal Boundary Condition

(a) The Case of Moving Plate Heated

In the following figures the effect of fluid axial heat conduction combined with the moving wall velocity are shown for the second kind of thermal boundary condition. The computed results for Case A, in which the lower wall is heated constantly in $0 < z^*$ and the upper wall is insulated are illustrated first.

Newtonian fluid

In Fig.4-40 the fluid axial heat conduction effect on the axial development of temperatures at the walls, θ_0 and θ_L, and Nusselt number at the heated lower plate is portrayed for the Newtonian fluid. The presented figures are given in pair for comparison them with the relative velocity. The figures on the left side are for U^* = 0 and the other ones are for $U^* = 1$. The calculation results for the case of the

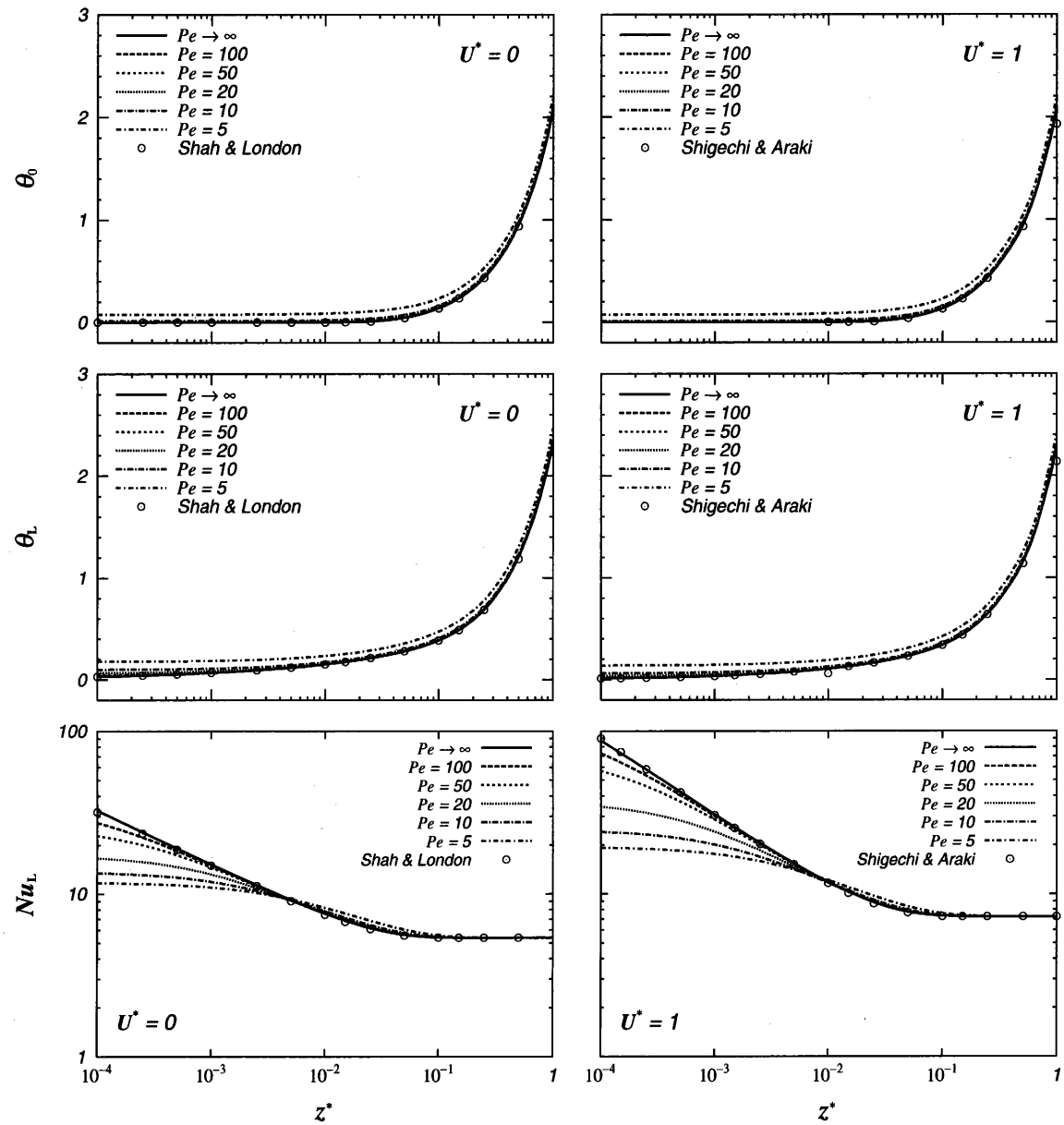

Fig.4-40 Wall temperatures and Nu for Case A, $U^* = 0$, 1.
(Newtonian fluid, $n = 1$)

neglected fluid axial heat conduction ($Pe \to \infty$) of the present study are compared with the predictions by [11] for stationary plates channel or for the Poiseuille flow ($U^* = 0$), and by [4] for the Poiseuille-Couette flow ($U^* = 1$), respectively. The circles show the results from [11] and [4]. Even at small values of z^*, it can be seen that the agreement is excellent. Since it was observed that the general qualitative behaviors of the axial development of the temperature profiles and Nusselt number at the plate are quite similar for the different fluids, Peclet number effects on the temperature development and on the Nusselt number at the heated plate, Nu_{L}, will

be discussed in more detail later at the end of this subsection.

Pseudoplastic fluid

Sample developing temperature profiles are presented to illustrate the fluid axial heat conduction effect on the developing temperature profiles in the below. The local development of temperature profiles during heating, from the lower wall (Case A), of a pseudoplastic fluid ($n = 0.5$ and $\beta = 1$) is shown in Fig.4-41. The upper two figures are for $U^* = 0$ and the two figures at the bottom are for $U^* = 1$. By comparing the figures in the same row one can observe the effect of the fluid axial heat conduction on the developing temperature distributions. If one compares the

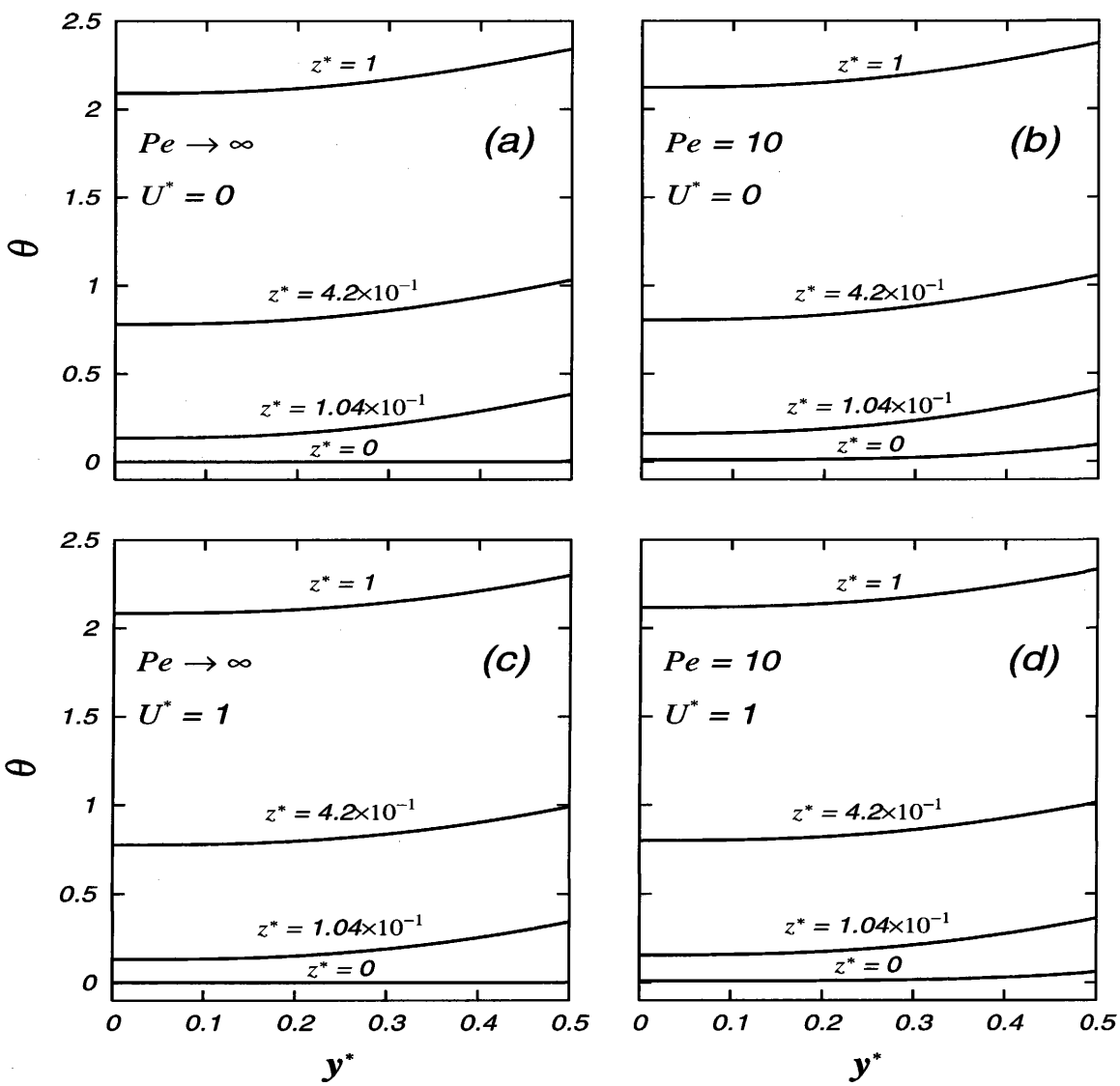

Fig.4-41 Developing temperature profiles for Case A, $U^* = 0$, 1.
(pseudoplastic fluid, $n = 0.5$, $\beta = 1$)

figures in the same column, then the relative velocity effect on the temperature distribution in the thermal entrance region is observed. $y^* = 0$ corresponds to the upper wall and $y^* = 0.5$ is the lower wall. At $z^* = 0$, there is a step change in heat flux at the lower wall. Figures 4-41(a) and 4-41(c) are for $Pe \to \infty$ and there at $z^* = 0$ the dimensionless fluid temperature is zero. But for $Pe = 10$, as it is seen in Figs.4-41(b) and 4-41(d) the fluid temperature at $z^* = 0$ deviates from zero near the heated lower wall or $y^* = 0.5$, even there is no heat flux from the wall. This increase is due to the contribution of the fluid axial heat conduction in the flowing fluid.

In order to study the fluid axial heat conduction effect, the heat transfer results are shown for a pseudoplastic fluid ($n = 0.5$ and $\beta = 1$) in Fig.4-42. The heat transfer results are displayed for the six values of Peclet number on these figures. Figure 4-42 displays the dimensionless bulk temperature and Nusselt number at the heated lower wall as functions of the axial distance z^*. The Peclet number is the parameter in these figures. In these figures the solid lines show the case of negligible

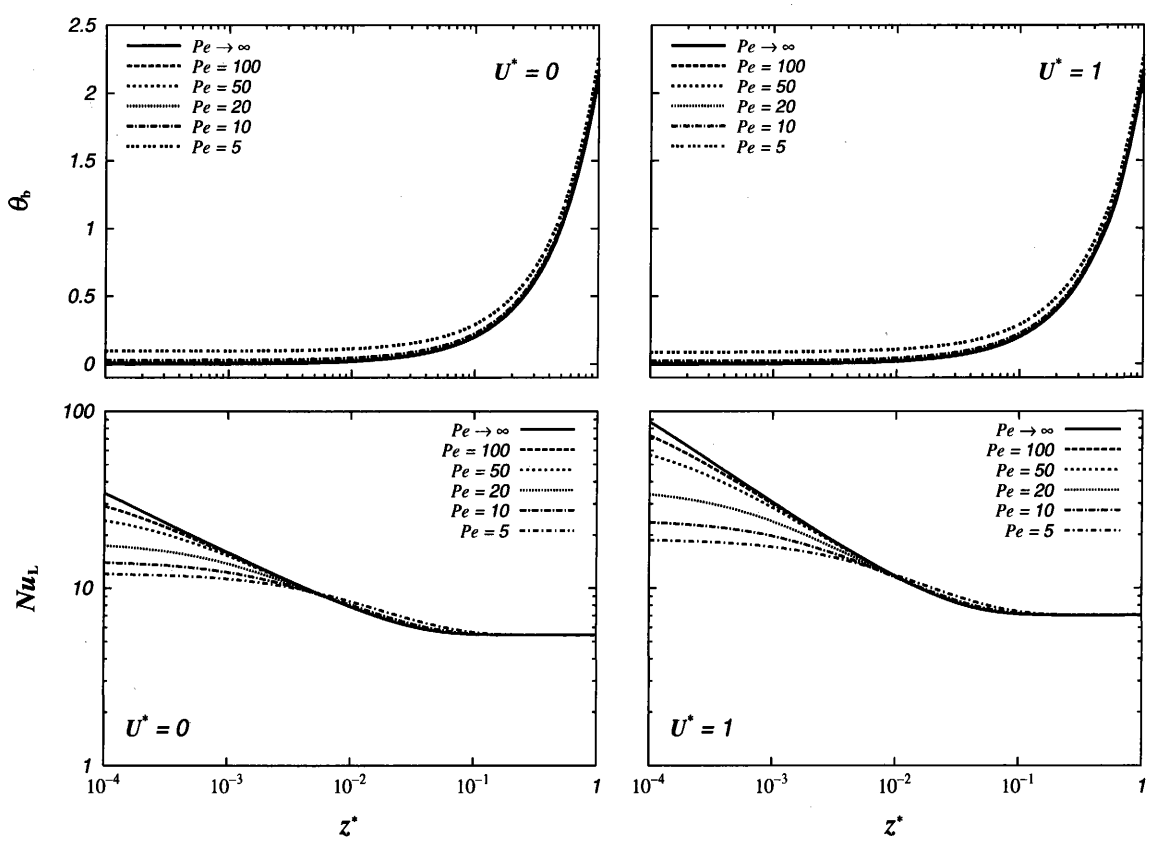

Fig.4-42 Bulk temperature and Nu for Case A, $U^* = 0$, 1.
(pseudoplastic fluid, $n = 0.5$, $\beta = 1$)

fluid axial heat conduction or $Pe \to \infty$. The way of illustration of the figures is given in the explanation for Fig.4-40. Scanning each row of the figures, the relative velocity effect is seen. The figures on the left side are for $U^* = 0$ or for the Poiseuille flow case and the other ones are for $U^* = 1$ or for the Poiseuille-Couette flow.

Dilatant fluid

The fluid axial heat conduction effect on the heat transfer for a dilatant fluid ($n = 1.5$ and $\beta = 1$) is shown in the following figures in the same way of illustration as done in Figs.4-40 and 4-42. It was noted the general qualitative behaviors are quite similar to those of the Newtonian and pseudoplastic fluids.

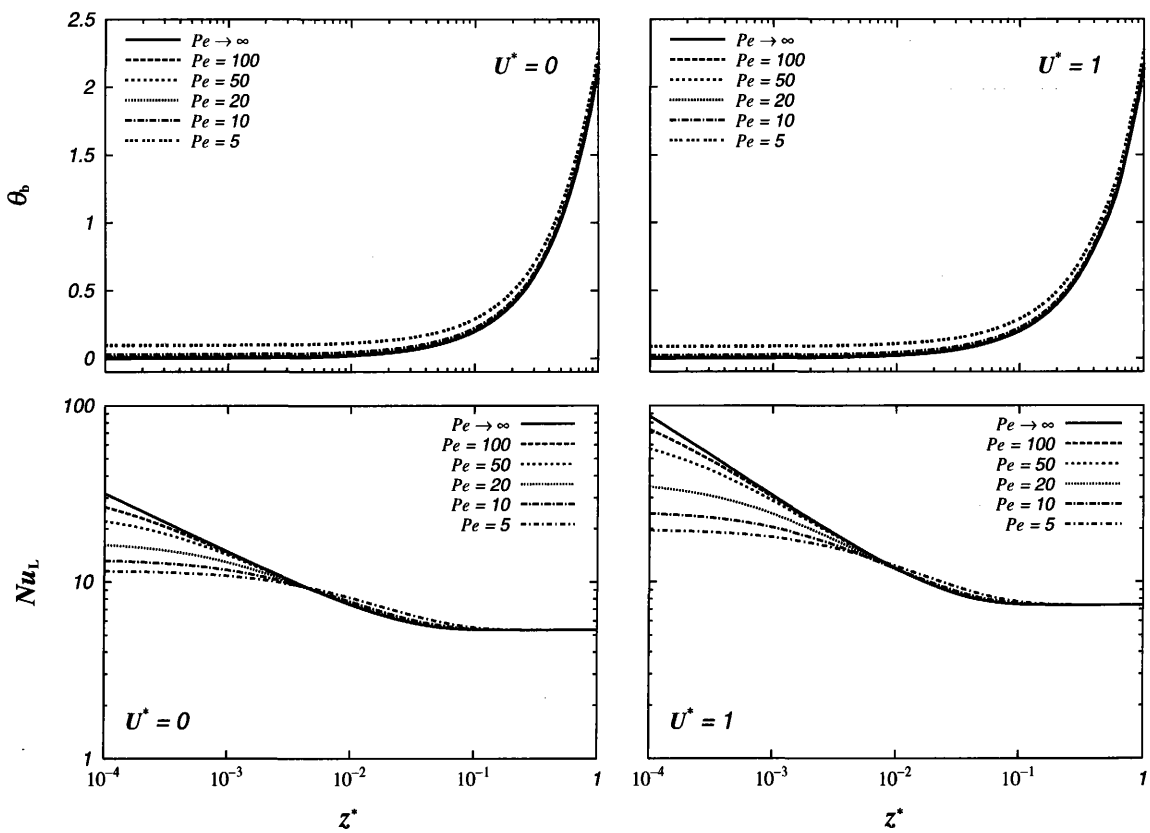

Fig.4-43 Bulk temperature and Nu for Case A, $U^* = 0$, 1.
(dilatant fluid, $n = 1.5$, $\beta = 1$)

Discussion

θ, temperature profile

- The local temperature profile is influenced by the fluid axial heat conduction only in the thermally developing range.

θ_b, bulk temperature

The dimensionless bulk temperature increases with decreasing Peclet number slightly in the thermally developing range, while they are almost identical in the fully developed region.

Bulk temperature is smaller for the case of moving lower wall ($U^* = 1$) than in the case of $U^* = 0$.

Nu_L, Nusselt number at the lower heated wall (q_L = const, $0 < z$)

Unlike the first kind T.B.C., the Nusselt number at the heated wall tends to decrease near $z^* = 0$ with a decrease in Pe. Nusselt number in the thermal entrance region remains almost constant if Pe is small. This trend was has been also seen for the first kind T.B.C.

It can be observed that the asymptotic Nusselt number values are identical regardless of the Peclet number values.

For a specified axial position with a given Peclet number, Nusselt number at the lower wall is larger for $U^* = 1$ than for $U^* = 0$.

(b) The Case of Stationary Plate Heated

The following figures illustrate the results for Case B, in which the lower wall is insulated and the upper wall is heated constantly in $0 < z^*$. Since the heat transfer study results of Case B for the Poiseuille flow or for $U^* = 0$ would not give some additional insights into the heat transfer (as the Nusselt number values at the upper wall for Case A are identical to those of the Nusselt numbers at the lower wall for Case B), only the results for $U^* = 1$ are presented. Also the axial development of the bulk temperature is not included in these figures.

Axial development of the Nusselt number at the wall is illustrated in Fig.4-44 for the Newtonian, pseudoplastic and dilatant fluids in the Poiseuille-Couette flow. The solid lines show the case of the negligible fluid axial heat conduction ($Pe \to \infty$). The results are given with the six values of Peclet number. By comparing these figures the effect of the flow index, n, on the Nusselt number can be discerned and no significant differences exist between them.

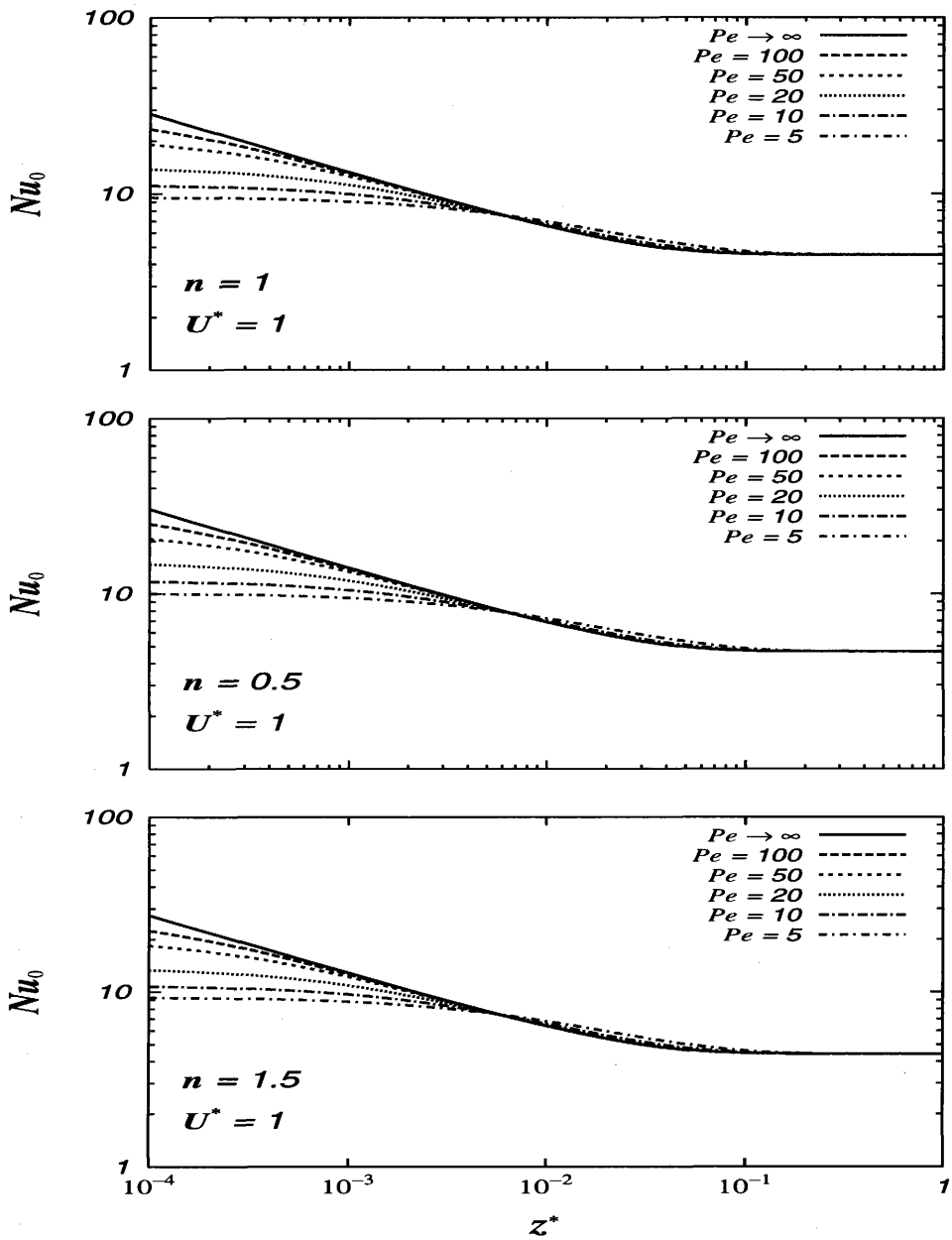

Fig.4-44 Nusselt numbers for Case B

Discussion

Nu_0, **Nusselt number at the upper heated wall** (q_0 = **const,** $0 < z$)

Nusselt number at the fixed upper wall decreases with a decrease in Peclet number in the thermally developing region.

4.6 Effects of Thermal Boundary Conditions

In this section various relevant results and figures have been discussed by comparing them for the two feasible thermal boundary conditions for the Poiseuille-Couette flow, that were examined in the present research. In the below, the essential heat transfer results of the present research work, namely, the axial development of the Nusselt number at the heated wall, Nu_{L}, are given for the thermal boundary conditions of the 1st kind and 2nd kind. From these figures one can discern all the considered effects on the heat transfer in the present research. The figures are displayed in four as a group. In every group of the figures, the effects of the thermal boundary conditions and the moving wall velocity are seen. The each column of the figures refers to the results of the 1st kind and 2nd kind thermal boundary conditions, respectively. The figures in the upper row show the results for the Poiseuille flow or $U^* = 0$, while the others are for the Poiseuille-Couette flow or $U^* = 1$. The remaining effects, such as the rheological parameters, the viscous dissipation and the fluid axial heat conduction are demonstrated separately in turn as a parameter in these figures.

The flow indices effect

The following results are for the special limiting case of negligible viscous dissipation ($Br = 0$) and fluid axial heat conduction ($Pe \rightarrow \infty$). If was found for the negligible viscous dissipation and fluid axial heat conduction case that

- minor difference is observed for the different fluid behaviors in the thermal entrance region if the heated wall is stationary ($U^* = 0$). However, there is no significant difference for different fluids in the thermally fully developed region and if the heated wall moves ($U^* = 1$).
- the Nusselt number at the heated wall is higher for the uniform wall heat flux condition (2nd kind T.B.C.) than that for the uniform wall temperature condition (1st kind T.B.C.).

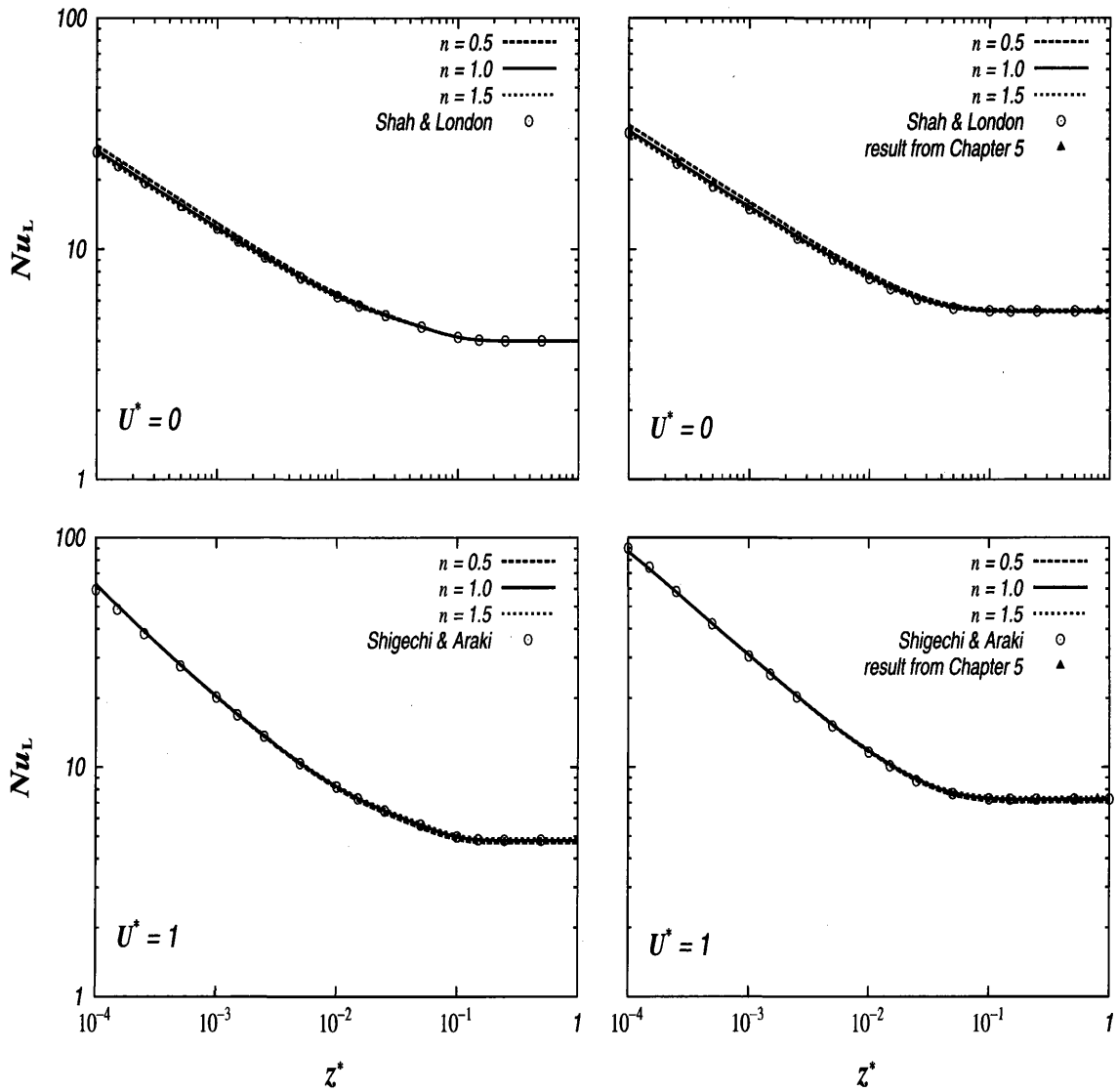

(1st kind T.B.C.) (2nd kind T.B.C.)

Fig.4-45 Effect of n on Nu_{L} ($Br = 0$, $Pe \to \infty$, $\beta = 1$)

Viscous dissipation effect

In the following figures, the attention is focused on the effect of the viscous dissipation on the heat transfer rate in terms of Nusselt number at the heated wall.

Pseudoplastic fluid

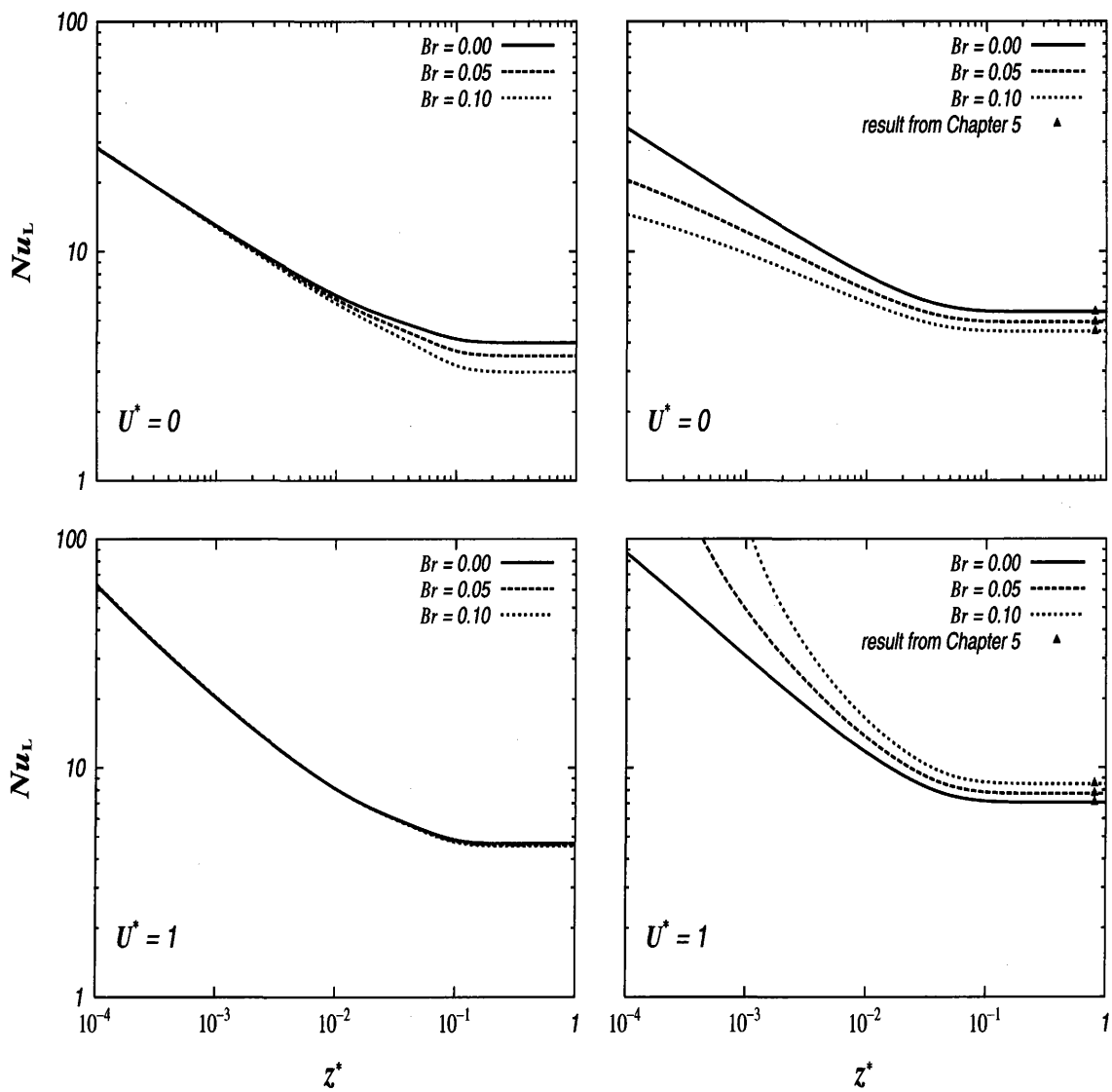

(1st kind T.B.C.) (2nd kind T.B.C.)

Fig.4-46 Effect of Br on Nu_{L} ($Pe \to \infty$, $n = 0.5$, $\beta = 1$)

- For the stationary walls case, the viscous dissipation causes a decrease in the Nusselt number at the heated wall in the thermally fully developed region for the 1st kind and 2nd kind thermal boundary conditions.

- For the 1st thermal boundary condition, if the moving wall ($U^* = 1$) is heated (at a constant temperature), the viscous dissipation effect is minor. However for the 2nd kind thermal boundary condition, if the moving wall ($U^* = 1$) is heated (at a constant heat flux), the viscous dissipation causes an increase in the Nusselt number at the heated wall.

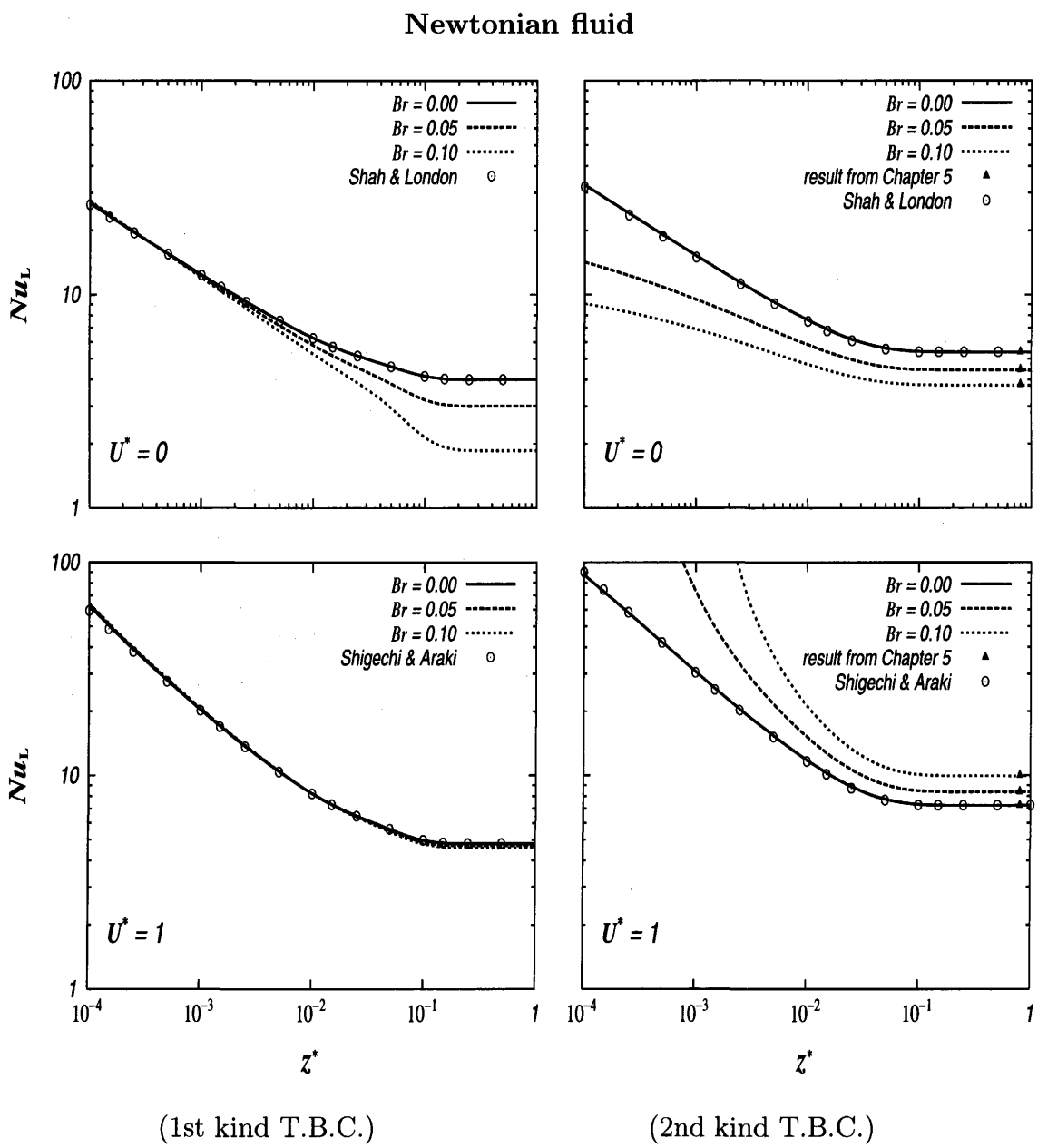

Fig.4-47 Effect of Br on Nu_{L} ($Pe \to \infty$, $n = 1$)

These results are for the Newtonian fluid. The trends are similar to those for the pseudoplastic fluids.

Dilatant fluid

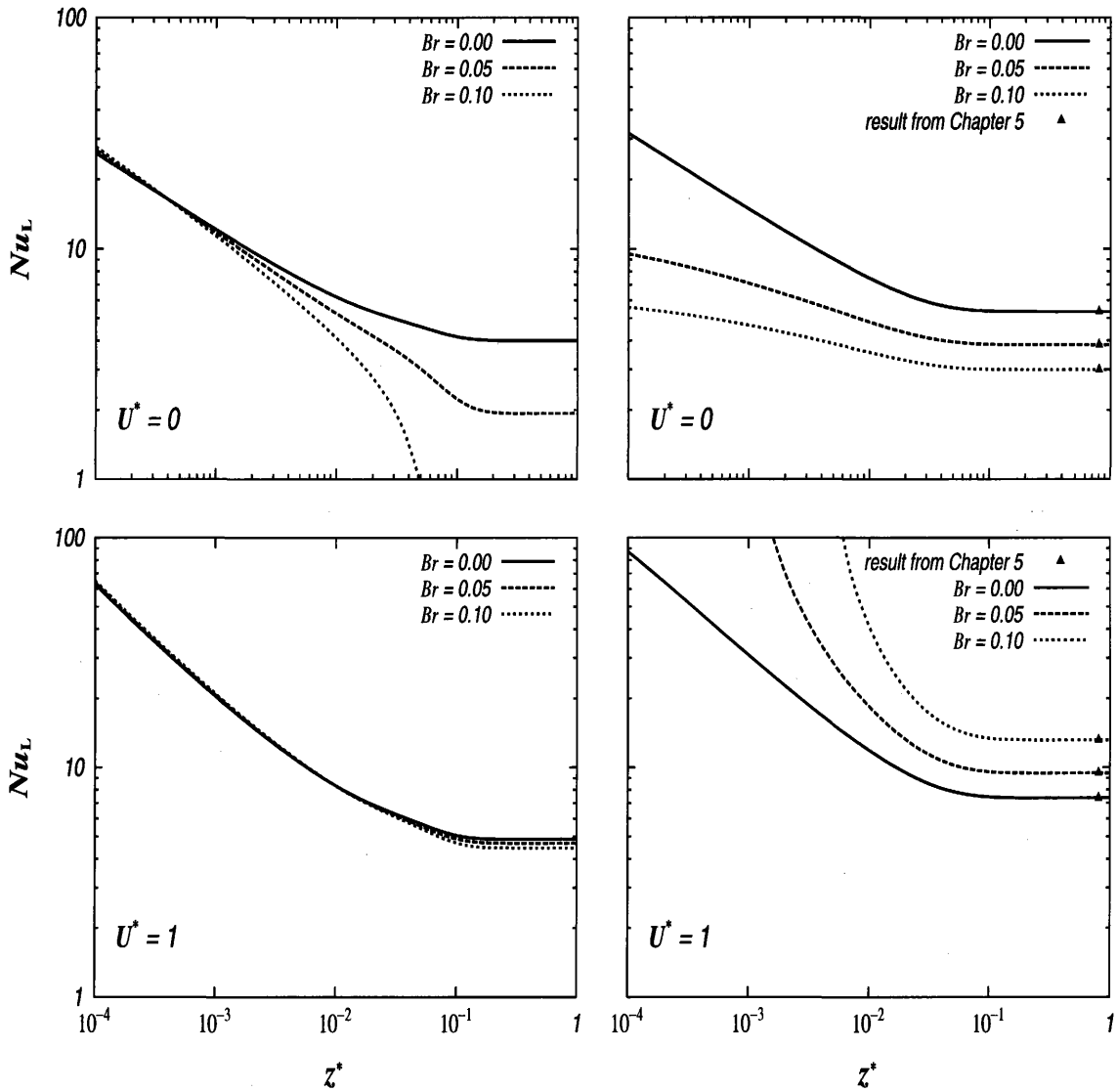

(1st kind T.B.C.) (2nd kind T.B.C.)

Fig.4-48 Effect of Br on Nu_{L} ($Pe \to \infty$, $n = 1.5$, $\beta = 1$)

These results are for the dilatant fluid. The trends are similar to those for the pseudo-plastic and Newtonian fluids. However, for the dilatant fluid the viscous dissipation effect is more pronounced.

Axial heat conduction effect

In the following figures, the attention is focused on the effect of the fluid axial heat conduction on the heat transfer rate in terms of Nusselt number at the heated wall.

Pseudoplastic fluid

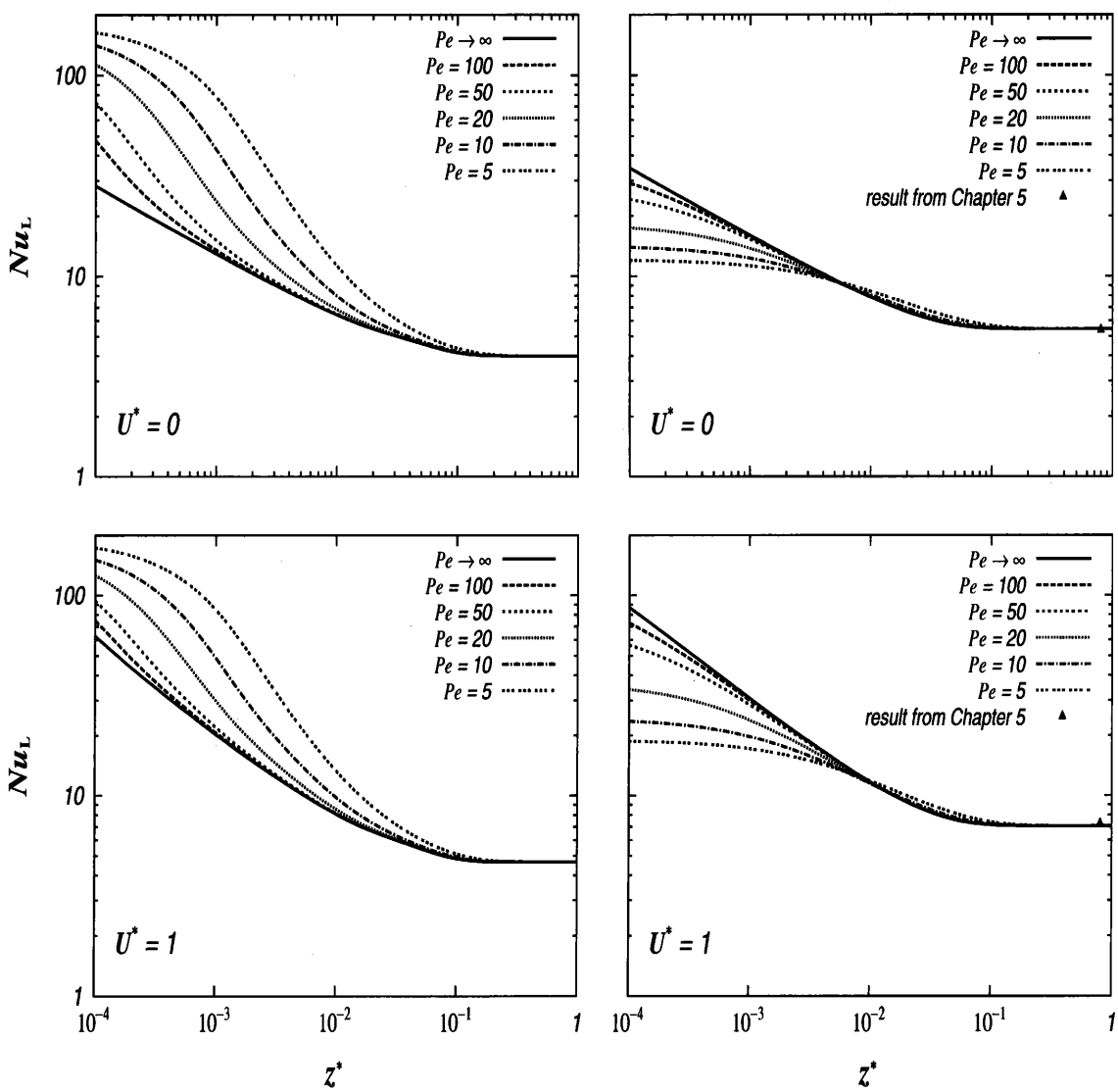

(1st kind T.B.C.) (2nd kind T.B.C.)

Fig.4-49 Effect of Pe on Nu_{L} ($Br = 0$, $n = 0.5$, $\beta = 1$)

- For the 1st kind thermal boundary condition, the fluid axial heat conduction causes an increase in Nusselt number at the heated wall in the thermally developing region whether the wall is stationary ($U^* = 0$) or moving ($U^* = 1$).

- For the 2nd kind thermal boundary condition, the fluid axial heat conduction causes a decrease in Nusselt number at the heated wall in the thermally developing region whether the wall is stationary ($U^* = 0$) or moving ($U^* = 1$).

Newtonian fluid

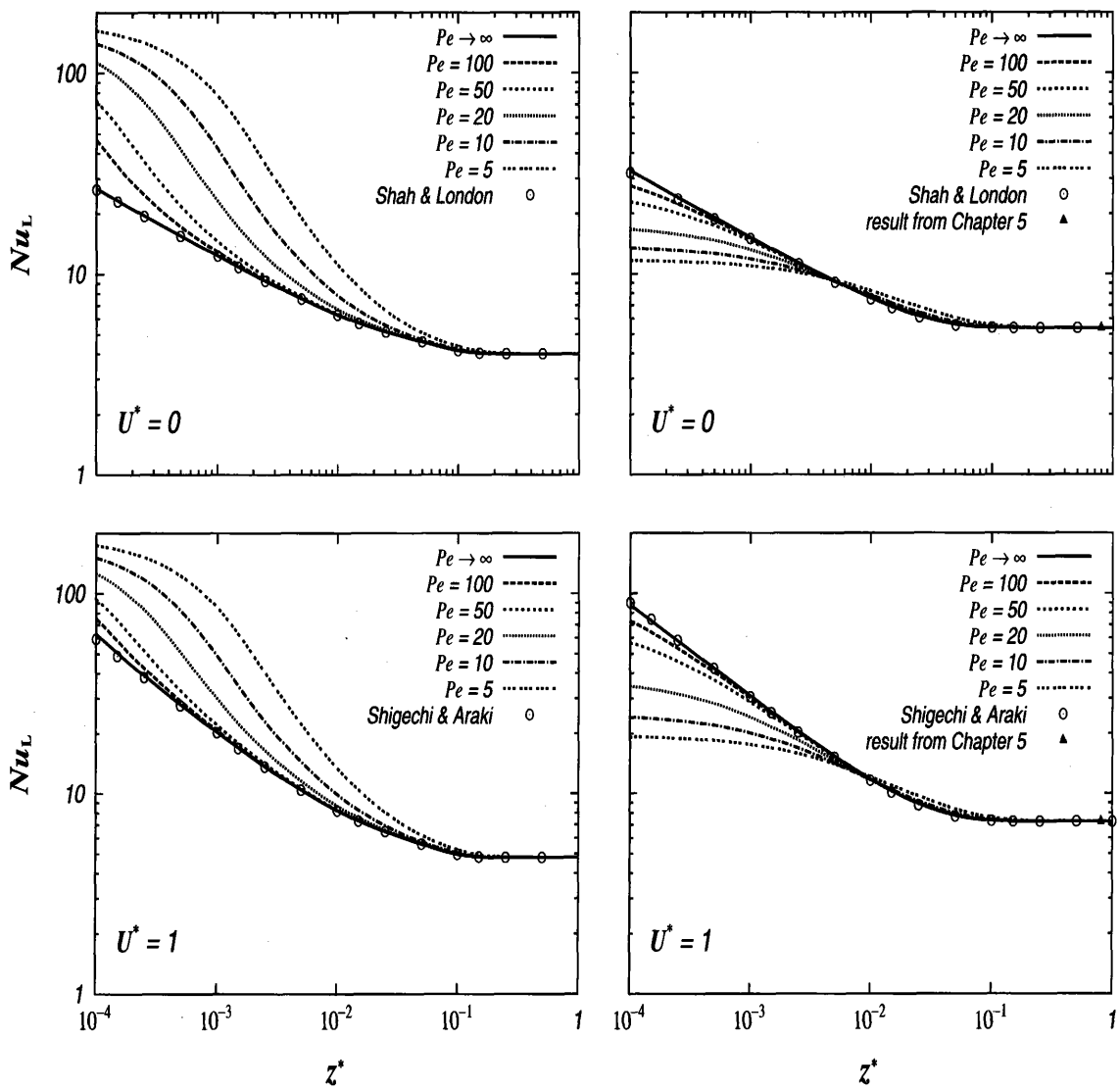

(1st kind T.B.C.) (2nd kind T.B.C.)

Fig.4-50 Effect of Pe on Nu_{L} ($Br = 0$, $n = 1$)

These results are for the Newtonian fluid. As it was discussed throughout this chapter, the trends are similar to those for the pseudoplastic fluids.

Dilatant fluid

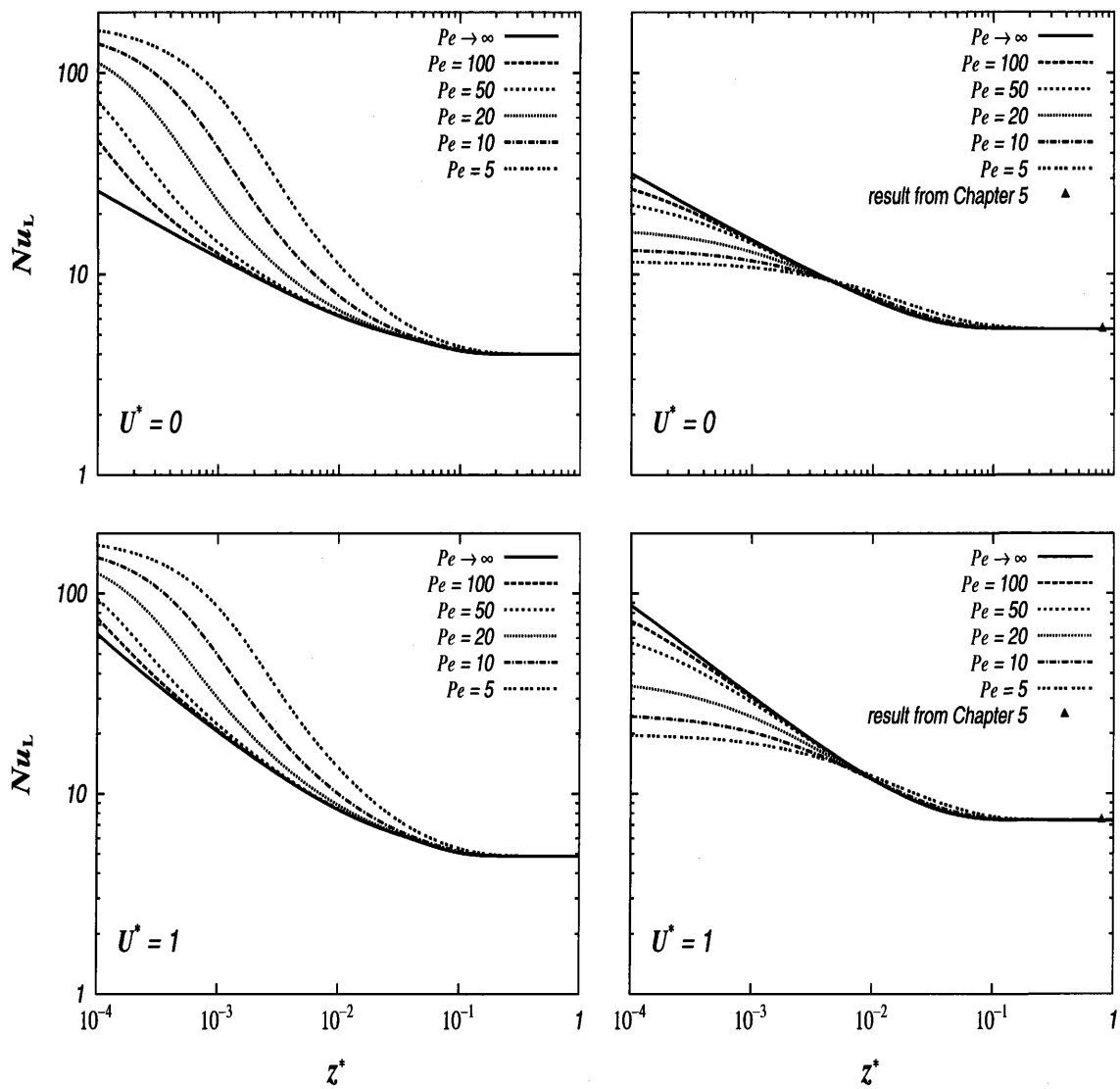

(1st kind T.B.C.) (2nd kind T.B.C.)

Fig.4-51 Effect of Pe on Nu_{L} ($Br = 0$, $n = 1.5$, $\beta = 1$)

These results are for the dilatant fluid. As it was discussed, the trends are similar to those for the pseudoplastic and Newtonian fluids.

Viscous dissipation and fluid axial heat conduction effects

In Figs.4-52 to 4-54, the attention is focused on the effects of the viscous dissipation and the fluid axial heat conduction on the heat transfer rate in terms of Nusselt number at the heated wall. The discussions of these results are given in Section 4.3.2 and Section 4.3.3.

Pseudoplastic fluid

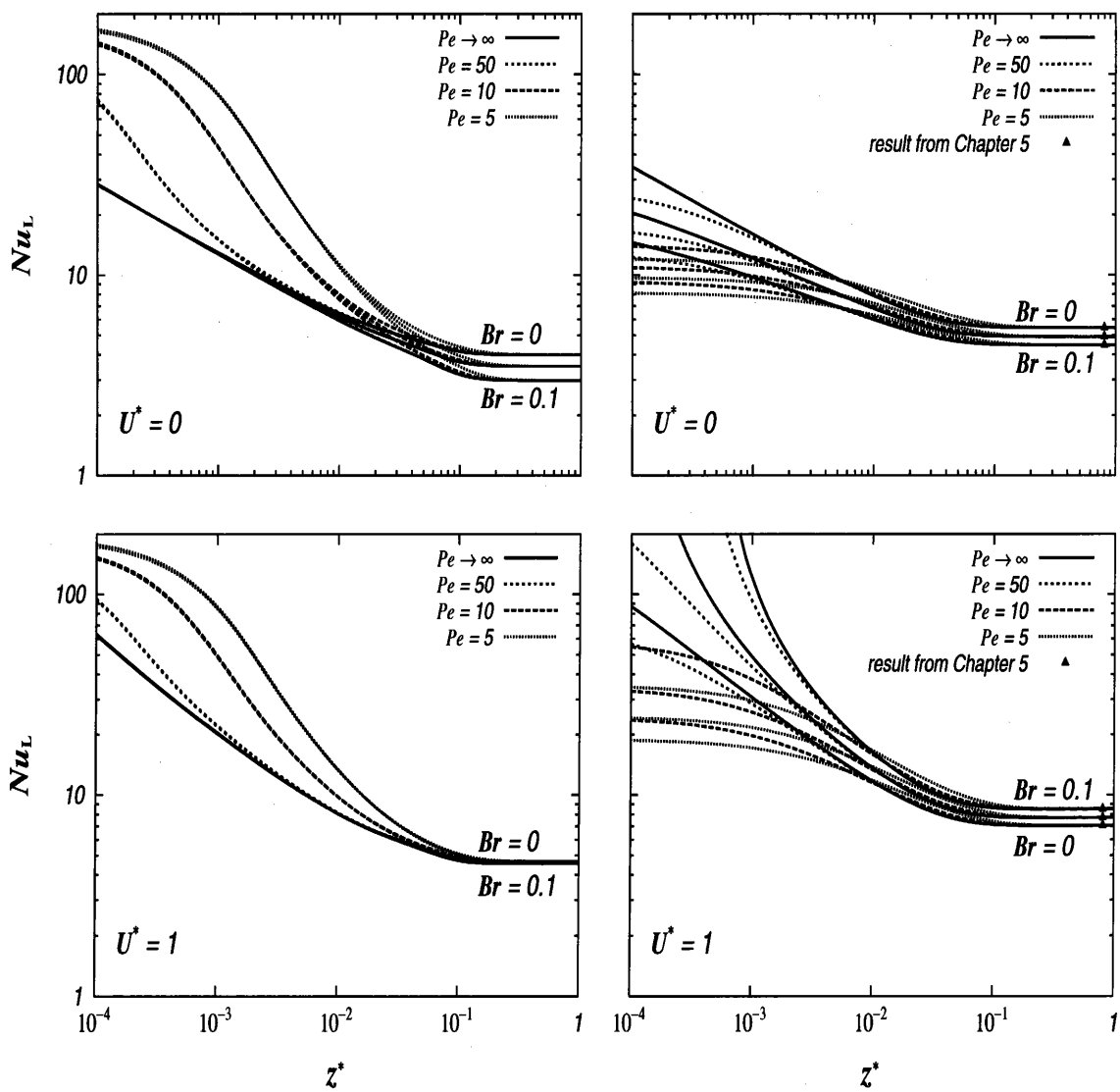

(1st kind T.B.C.) (2nd kind T.B.C.)

Fig.4-52 Effects of Br and Pe on Nu_{L} ($n = 0.5$, $\beta = 1$)

Newtonian fluid

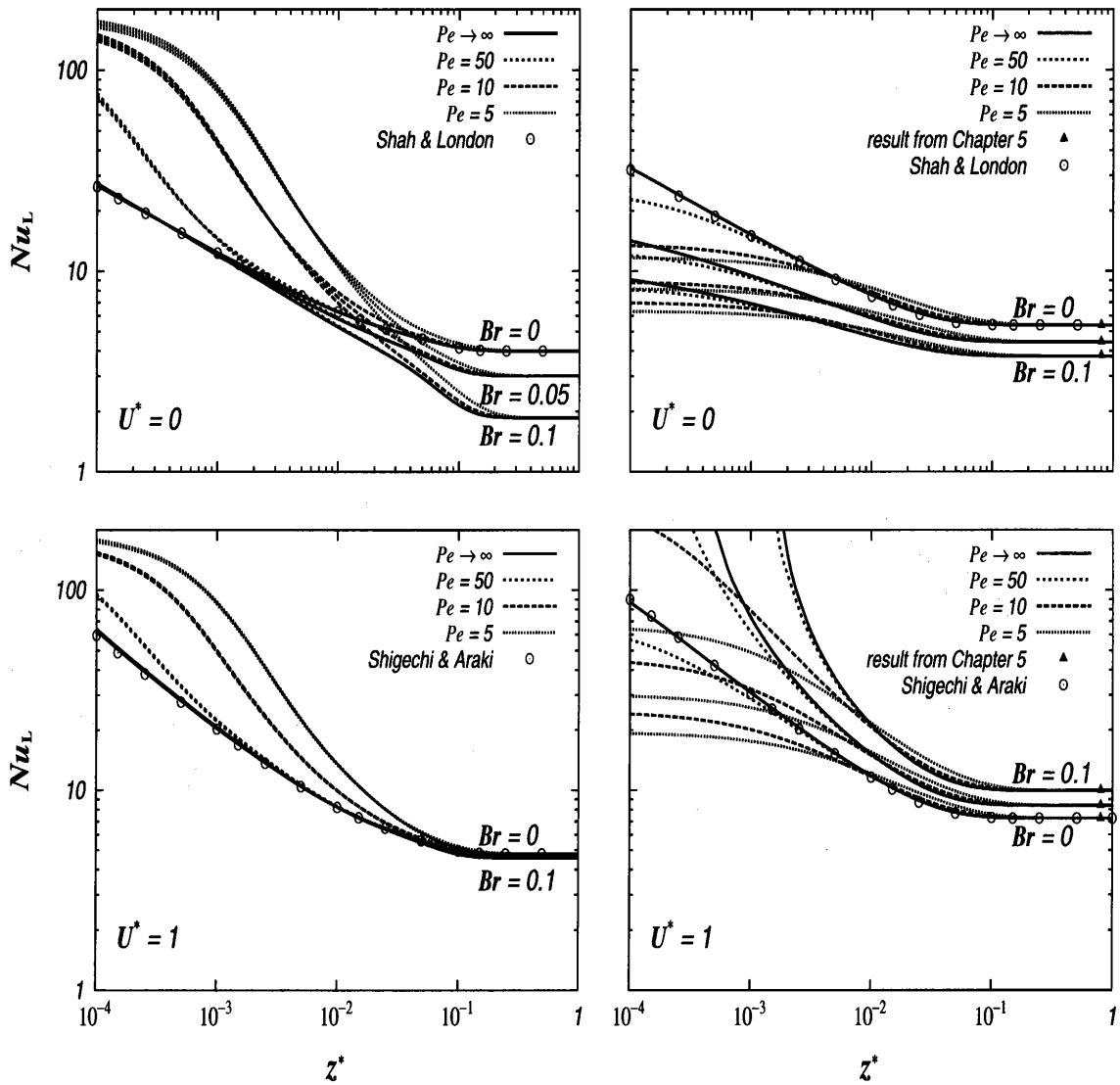

(1st kind T.B.C.) (2nd kind T.B.C.)

Fig.4-53 Effects of Br and Pe on Nu_{L} ($n = 1$)

These results are for the Newtonian fluid. As it was discussed throughout this chapter, the trends are similar to those for the pseudoplastic fluids.

Dilatant fluid

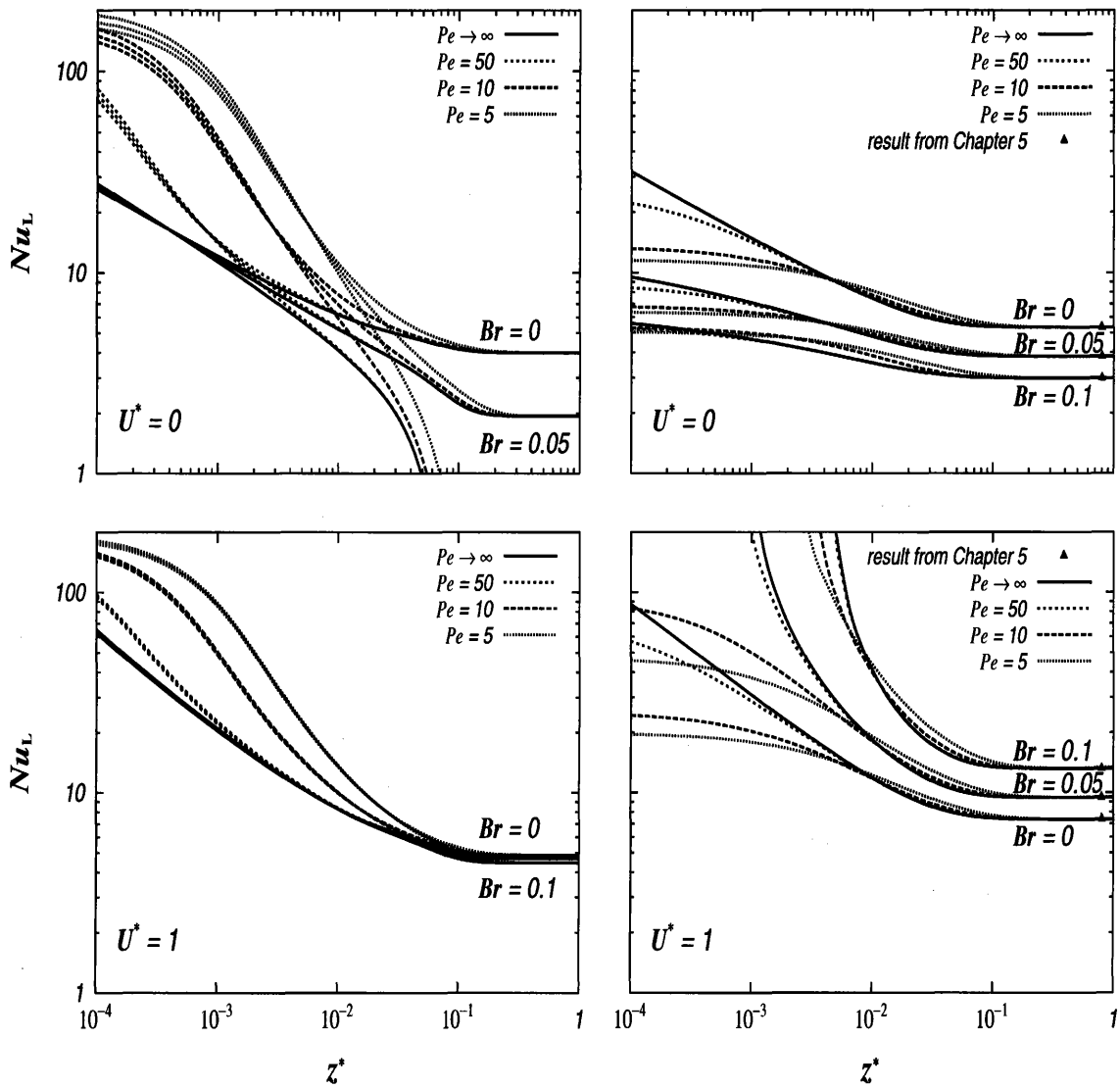

(1st kind T.B.C.) (2nd kind T.B.C.)

Fig.4-54 Effects of Br and Pe on Nu_{L} ($n = 1.5$, $\beta = 1$)

These results are for the dilatant fluid. As it was discussed throughout this chapter, the trends are similar to those for the pseudoplastic and Newtonian fluids. However, for the dilatant fluid the viscous dissipation effect is more pronounced for both the thermal boundary conditions.

4.7 Summary

The heat transfer for thermally developing plane Poiseuille-Couette flow of non-Newtonian fluids has been studied numerically with an emphasis on the effects of the viscous dissipation and of the fluid axial heat conduction. The heat transfer analysis dealing with the effects of fluid axial heat conduction and viscous dissipation is directed at the solution of the energy equation as an elliptic type problem for an infinite domain. In order to ascertain the accuracy of the numerical method and the proposed mesh system used in this work, several runs were made for the problem of the heat transfer with neglected fluid axial heat conduction and viscous dissipation in a Newtonian flow. The Nusselt number solutions corresponding to the limiting cases of $Pe \rightarrow \infty$ and $Br = 0$ show excellent agreement with those reported in [11] for $U^* = 0$ and in [4] for $U^* = 1$, who analyzed the heat transfer in the thermal entrance region of parallel-plates channel by neglecting viscous dissipation and fluid axial heat conduction for Newtonian fluids. This excellent agreement gives a considerable measure of reliability of the numerical method and the proposed mesh system in this work.

Temperature fields are obtained for (T) thermal boundary condition and for the first and second kinds of thermal boundary conditions and the computed variations are presented in graphical form for the different fluid behaviors. In order to show the effect of the moving plate velocity, the figures presenting the results are arranged in pairs of $U^* = 0$ and $U^* = 1$.

Having studied the heat transfer for the thermally developing plane Poiseuille-Couette flow of non-Newtonian fluids, the effects of the moving plate velocity, rheological parameters, viscous dissipation and fluid axial heat conduction on the developing temperature distributions and heat transfer rates were clarified. From the observation of the results the followings can be summarized.

- The inspection of the temperature profile development reveals that the fluid temperature increases at $z \leq 0$ due to the fluid axial heat conduction and due to viscous heating.

- The fluid axial heat conduction effect is negligible only at high Pe. For moderate values of Pe, the fluid axial heat conduction is important at the thermal entrance region.

- The response of the Newtonian fluid to viscous heating is more pronounced

than that of the pseudoplastic fluid but less remarkable than the dilatant fluid.

- For a specified axial position with a given Brinkman number and Peclet number, the Nusselt number at the lower wall for $U^* = 1$ is larger than the corresponding Nusselt number for $U^* = 0$.

Ⓣ T.B.C.

- The results indicate that for a given fluid, the asymptotic value of Nusselt number at the wall is a single value for the different non-zero values of Brinkman number.
- For zero Brinkman numbers, the asymptotic Nusselt numbers depends on the Peclet number values and with a decrease in Peclet number the asymptotic Nusselt numbers increase slightly.

The first kind T.B.C.

- Nusselt number at the heated wall increases if the fluid axial heat conduction is considerable.
- The effect of viscous dissipation on the Nusselt number at the moving plate is not important if the plate is maintained at a constant temperature different from the entering fluid temperature.
- Including the fluid axial heat conduction effect and viscous dissipation in the analyses results in higher values of Nusselt number at the stationary upper plate in the thermally developing region.

The second kind T.B.C.

- The viscous dissipation effect in heat transfer is different depending on U^*. For an aiding Poiseuille-Couette flow ($U^* = 1$), the Nusselt number at the moving plate decreases with an increase in Brinkman number.
- Nusselt number values at the fully developed region are identical regardless of Pe values and in the thermally developed region the Nusselt numbers decrease with an increase in Pe number.

As the results reveal, unlike the (T) and first kind T.B.C., for the second kind T.B.C., the effect of Peclet number on the fully developed Nusselt numbers vanish and become negligible. Also for the second T.B.C., the effect of Brinkman number is predominant and the role of viscous dissipation in heat transfer depends on the moving wall velocity, U^*. But for the first kind of T.B.C., the role of viscous dissipation in heat transfer was seen to be the same for both $U^* = 0$ and $U^* = 1$. Therefore in the next chapter a detailed study has been done for the fully developed heat transfer to plane Poiseuille-Couette flow by examining the second kind T.B.C. with an emphasis on viscous dissipation for a wide range of values of the moving wall. Throughout the next chapter, the effect of Peclet number will not be discussed, since it was found for the second kind T.B.C., the fluid axial heat conduction vanishes in the fully developed region.

Chapter 5

THERMALLY DEVELOPED POISEUILLE-COUETTE FLOW

The aim in this chapter is to clarify the viscous dissipation effect on the fully developed plane Poiseuille-Couette flow for a wide range of values of the moving wall.

This chapter provides the exact solutions for the Newtonian and power-law fluids in the fully developed plane Poiseuille-Couette flow. The solutions for modified power-law fluids in the fully developed plane Poiseuille-Couette flow have been obtained numerically. Inclusion of the analytical study for the Newtonian and power-law fluids was aimed to ascertain the accuracy of the finite difference method used for the modified power-law fluids.

5.1 Newtonian Fluid

The objective in this section is to obtain the exact solutions for Newtonian fluids in the fully developed Poiseuille-Couette flow including viscous dissipation effects. The passage is parallel-plates with the lower plate moving. The coordinate system and the fluid flow conditions applied in the analysis are given in Section 3.2. Under the assumptions that the Newtonian fluid in parallel-plates passage is incompressible, has constant properties (k, ρ, c_{p}, μ), the flow is fully developed, and negligible body forces and fluid axial heat conduction, the energy equation with thermally fully developed condition having the constant wall heat flux is written as

$$k\frac{\partial^2 T}{\partial y^2} + \mu\left(\frac{du}{dy}\right)^2 = \rho c_{\mathrm{p}} u \frac{dT_{\mathrm{b}}}{dz} \tag{5.1}$$

The inclusion of the viscous dissipation into the analysis amounts to adding a heat generation term (the second term in the left hand side) which is a parabolic function

of y coordinate. The following two types of the thermal boundary conditions are specified:

Case A (constant heat flux at the moving plate with the fixed plate insulated):

$$\begin{cases} k\dfrac{\partial T}{\partial y} = 0 \quad \text{at} \quad y = 0 \\ k\dfrac{\partial T}{\partial y} = q_{\mathrm{L}} \quad \text{at} \quad y = L \end{cases} \tag{5.2}$$

Case B (constant heat flux at the fixed plate with the moving plate insulated):

$$\begin{cases} -k\dfrac{\partial T}{\partial y} = q_0 \quad \text{at} \quad y = 0 \\ k\dfrac{\partial T}{\partial y} = 0 \quad \text{at} \quad y = L \end{cases} \tag{5.3}$$

dT_{b}/dz is evaluated from an energy balance as

$$\frac{dT_{\mathrm{b}}}{dz} = \frac{q_j}{\rho c_{\mathrm{p}} u_{\mathrm{m}} L}\left[1 + \frac{\int_0^L \mu \left(\dfrac{du}{dy}\right)^2 dy}{q_j}\right] \tag{5.4}$$

Substituting the above balance into Eq.(5.1) gives

$$k\frac{\partial^2 T}{\partial y^2} + \mu\left(\frac{du}{dy}\right)^2 = \frac{q_j}{L}\frac{u}{u_m}\left[1 + \frac{\int_0^L \mu \left(\dfrac{du}{dy}\right)^2 dy}{q_j}\right] \tag{5.5}$$

Introducing dimensionless temperature defined as

$$\theta \equiv \frac{Tk}{q_j D_{\mathrm{h}}} \tag{5.6}$$

the energy equation and the boundary conditions are expressed as

$$\frac{\partial^2 \theta}{\partial y^{*2}} = 2u^* + Br\left[\left\{\int_0^{\frac{1}{2}} \left(\frac{du^*}{dy^*}\right)^2 dy^*\right\} 2u^* - \left(\frac{du^*}{dy^*}\right)^2\right] \tag{5.7}$$

where

$$Br \equiv \left[\frac{\mu u_{\mathrm{m}}^2}{q_j D_{\mathrm{h}}}\right] \tag{5.8}$$

$j = \mathrm{L}$ for Case A and $j = 0$ for Case B

$$\textbf{Case A}: \begin{cases} \dfrac{\partial \theta}{\partial y^*} = 0 \quad \text{at} \quad y^* = 0 \\ \dfrac{\partial \theta}{\partial y^*} = 1 \quad \text{at} \quad y^* = \dfrac{1}{2} \end{cases} \tag{5.9}$$

$$\textbf{Case B}: \begin{cases} \dfrac{\partial \theta}{\partial y^*} = -1 \quad \text{at} \quad y^* = 0 \\ \dfrac{\partial \theta}{\partial y^*} = 0 \quad \text{at} \quad y^* = \dfrac{1}{2} \end{cases} \tag{5.10}$$

Nusselt number, Nu_j, is defined as

$$Nu_j \equiv \frac{[q_j/(T_j - T_\mathrm{b})]D_\mathrm{h}}{k} \tag{5.11}$$

where T_b is the bulk temperature defined as

$$T_\mathrm{b} \equiv \frac{\iint_A uTdA}{\iint_A udA} \tag{5.12}$$

In the dimensionless terms,

$$Nu_j \equiv \frac{1}{\theta_j - \theta_\mathrm{b}} \tag{5.13}$$

$(\theta_j - \theta_\mathrm{b})$ is calculated as

$$\theta_j - \theta_\mathrm{b} = 2\int_0^{\frac{1}{2}} u^* \left(\theta_j - \theta\right) dy^* \tag{5.14}$$

Solving Eq.(5.7) analytically together with Eq.(5.9) or Eq.(5.10), $\theta_j - \theta_\mathrm{b}$ has been obtained by applying the results for the velocity field (u^* and du^*/dy^*) of Newtonian fluids described in Section 3.3. The obtained results for Nu_L and Nu_0 are presented in Appendix B.1. The difference of the radial temperature and wall temperature are shown in Figs.5-1 and 5-2 for Cases A and B, respectively.

The Nusselt number at the heated wall is shown in Fig.5-3 as a function of the relative velocity, U^*, and Brinkman number, Br, as a parameter. It is seen that the fully developed Nusselt number at the heated wall depends on the relative velocity of the moving lower wall significantly. Br has different effect on Nusselt number depending on the relative velocity. The results for the Nusselt numbers are reported in Tables 2.1 and 2.2 in Appendix A.2. The detailed analysis and results are given also in references [80] and [81].

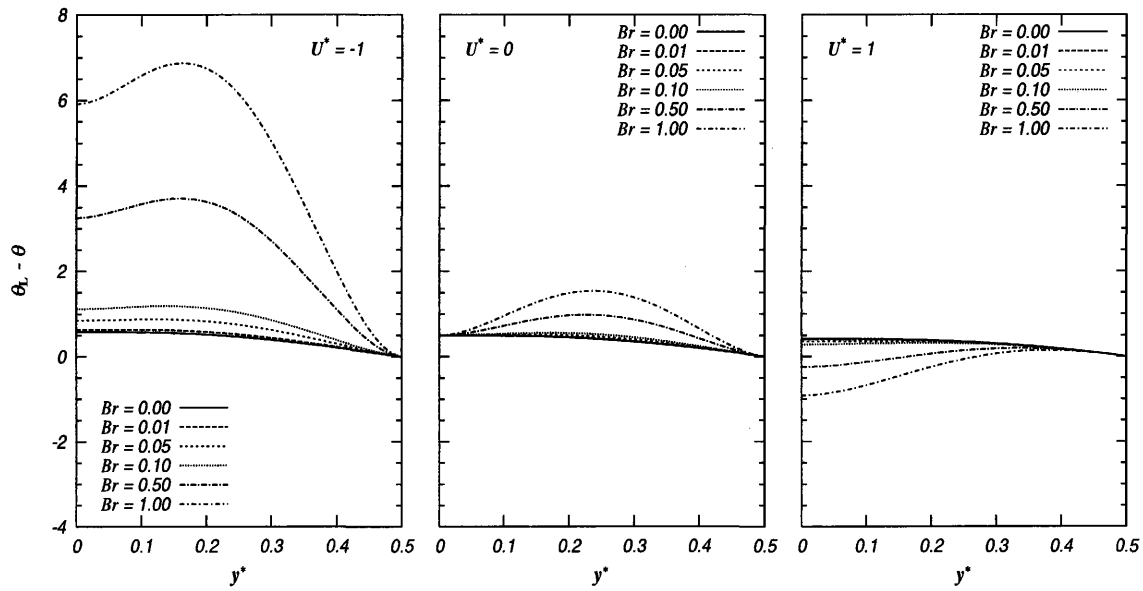

Fig.5-1 Dimensionless temperature difference, $\theta_{\mathrm{L}} - \theta$, for Case A

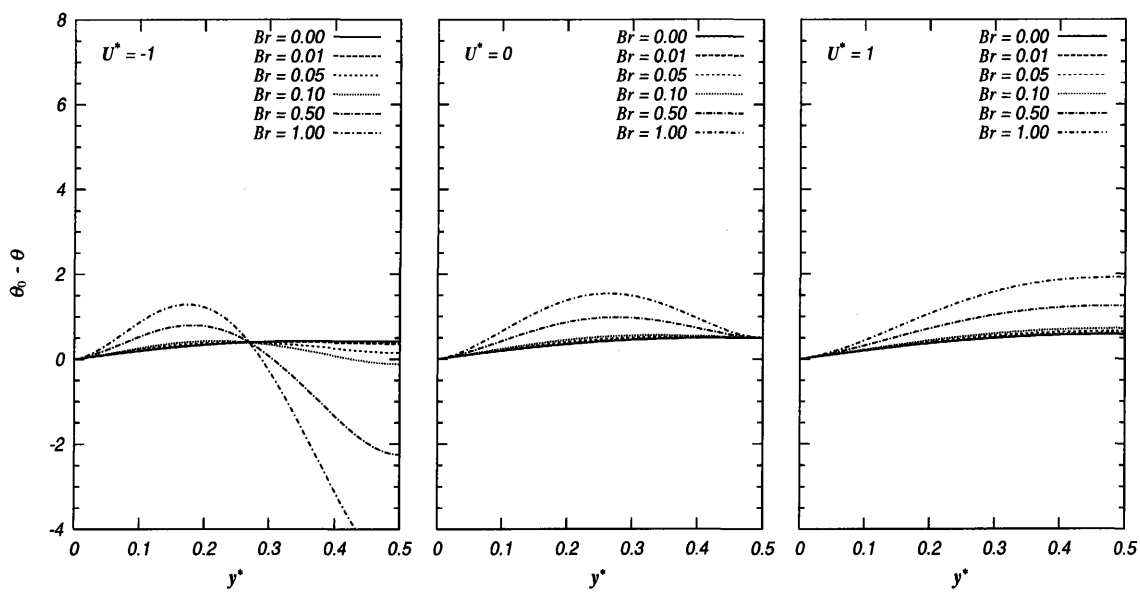

Fig.5-2 Dimensionless temperature difference, $\theta_0 - \theta$, for Case B

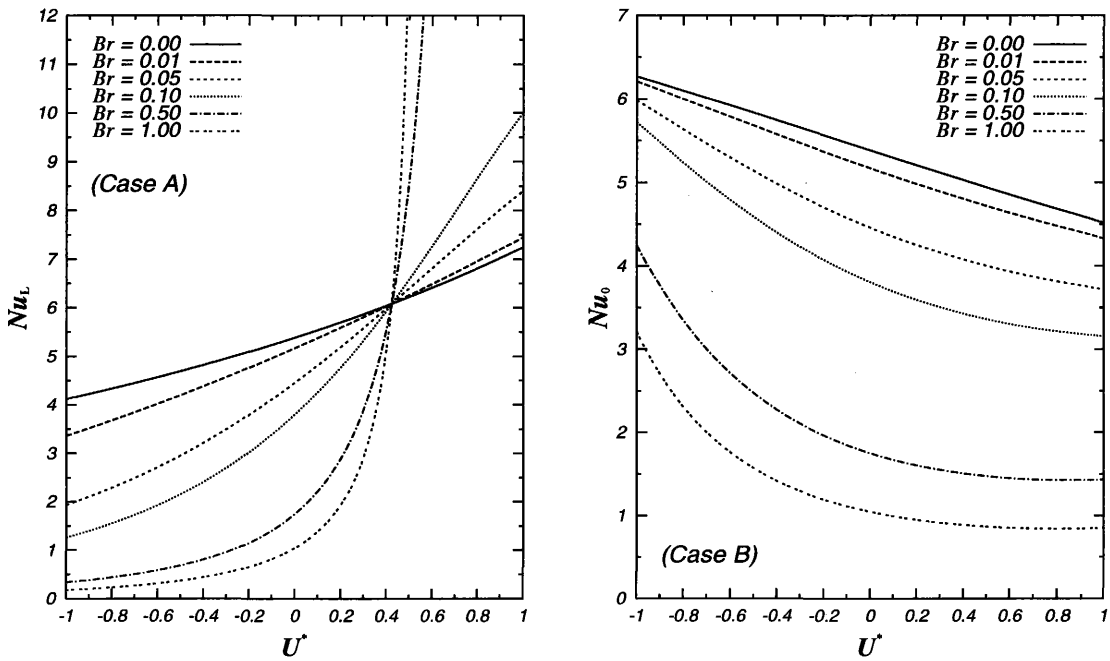

Fig.5-3 Nu vs U^* for Cases A and B.

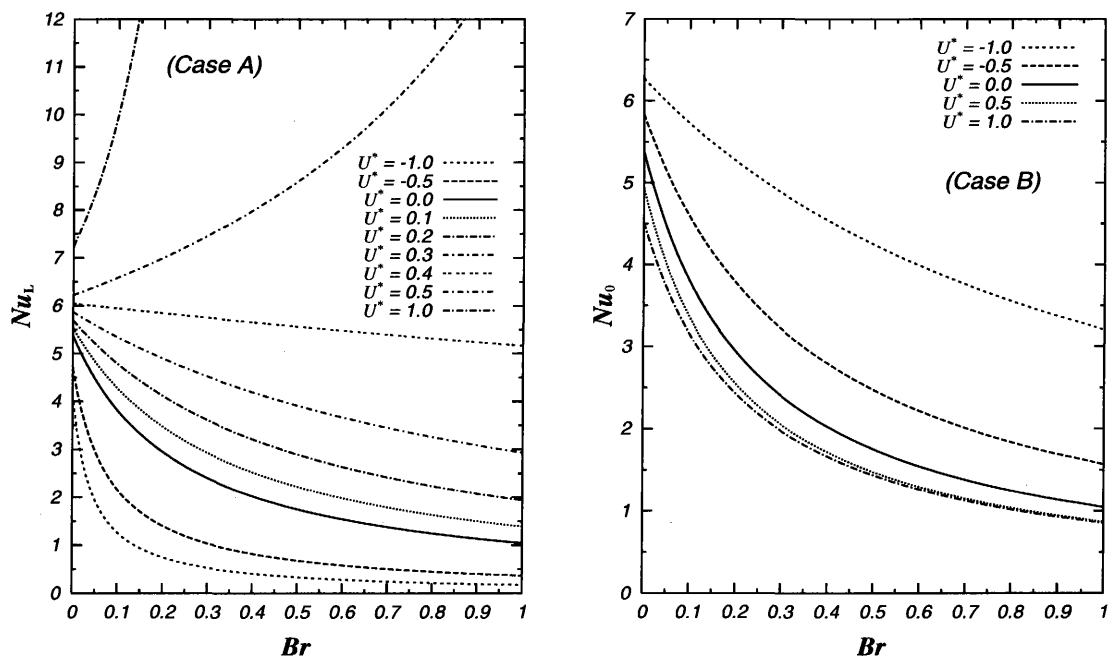

Fig.5-4 Nu vs Br for Cases A and B.

5.2 Non-Newtonian Fluid

5.2.1 Power-Law Model

In this section, by applying the power-law model to describe the fluid, the exact solutions for the fully developed temperature field in plane Poiseuille-Couette flow are obtained. Under the assumptions that the power-law fluid in parallel-plates is incompressible, has constant properties (k, ρ, c_{p}), the flow is fully developed, and negligible body forces and fluid axial heat conduction, the energy equation with constant heat flux condition is written as

$$k\frac{\partial^2 T}{\partial y^2} - \tau\left(\frac{du}{dy}\right) = \rho c_{\mathrm{p}} u \frac{dT_{\mathrm{b}}}{dz} \tag{5.15}$$

The following two types of the thermal boundary conditions are specified:

$$\textbf{Case A}: \quad \begin{cases} k\dfrac{\partial T}{\partial y} = 0 \quad \text{at} \quad y = 0 \\ k\dfrac{\partial T}{\partial y} = q_{\mathrm{L}} \quad \text{at} \quad y = L \end{cases} \tag{5.16}$$

$$\textbf{Case B}: \quad \begin{cases} -k\dfrac{\partial T}{\partial y} = q_0 \quad \text{at} \quad y = 0 \\ k\dfrac{\partial T}{\partial y} = 0 \quad \text{at} \quad y = L \end{cases} \tag{5.17}$$

The shear stress and the velocity field are given in Section 3.4.1. By introducing the relevant dimensionless quantities, $\theta = Tk/(q_j D_{\mathrm{h}})$, $u^* = u/u_{\mathrm{m}}$ and $y^* = y/D_{\mathrm{h}}$, the energy equation and the boundary conditions may be expressed in the dimensionless form as

$$\frac{\partial^2 \theta}{\partial {y^*}^2} = 2u^* + Br\left[\left\{\int_0^{\frac{1}{2}} \left|\frac{du^*}{dy^*}\right|^{n+1} dy^*\right\} 2u^* - \left|\frac{du^*}{dy^*}\right|^{n+1}\right] \tag{5.18}$$

$$\textbf{Case A}: \quad \begin{cases} \dfrac{\partial \theta}{\partial y^*} = 0 \quad \text{at} \quad y^* = 0 \\ \dfrac{\partial \theta}{\partial y^*} = 1 \quad \text{at} \quad y^* = \dfrac{1}{2} \end{cases} \tag{5.19}$$

$$\textbf{Case B}: \quad \begin{cases} \dfrac{\partial \theta}{\partial y^*} = -1 \quad \text{at} \quad y^* = 0 \\ \dfrac{\partial \theta}{\partial y^*} = 0 \quad \text{at} \quad y^* = \dfrac{1}{2} \end{cases} \tag{5.20}$$

Br is Brinkman number, defined as

$$Br \equiv \frac{m u_{\mathrm{m}}^{n+1}}{q_j D_{\mathrm{h}}^{n}} \tag{5.21}$$

where $j = \mathrm{L}$ for Case A and $j = 0$ for Case B.
The Nusselt number, Nu_j, is defined as

$$Nu_j \equiv \frac{[q_j/(T_j - T_{\mathrm{b}})]D_{\mathrm{h}}}{k} = \frac{1}{\theta_j - \theta_{\mathrm{b}}} \tag{5.22}$$

$(\theta_j - \theta_{\mathrm{b}})$ is calculated as

$$\theta_j - \theta_{\mathrm{b}} = 2 \int_0^{\frac{1}{2}} u^* \left(\theta_j - \theta\right) dy^* \tag{5.23}$$

Solving Eq.(5.18) together with Eq.(5.19) or Eq.(5.20), $\theta_j - \theta_{\mathrm{b}}$ is obtained. The equations for the dimensionless temperature difference are given by Eq.(B-7) and Eq.(B-14) in Appendix B.2.

In Figs.5-5 and 5-6, the Nusselt numbers at the heated walls are shown respectively for Case A and Case B as a function of Brinkman number for U^* -1, 0 and 1, and the flow index, n, as a parameter. The effect of flow index, n, on the Nusselt number is seen more strongly for Case A than Case B. It is seen from these figures that Nusselt numbers, Nu_{L}, change greatly depending on the values of Brinkman number, Br, and on the relative velocity of the moving plate, U^*, for Case A. Whereas for Case B the Nusselt number, Nu_0, decreases gradually with an increasing Brinkman number, Br. It is seen obviously from these figures that the role of the viscous dissipation on the heat transfer in the thermally developed region depends on the relative velocity. Nusselt number, Nu_{L}, increases with increasing relative velocity U^* for Case A. However, for Case B, Nusselt number, Nu_0, decreases with increasing relative velocity U^*. Incidentally, such behavior of the Nusselt numbers, Nu_{L} or Nu_0, is predicted by the temperature differences, $\theta_j - \theta_{\mathrm{b}}$, which is inversely proportional to the Nusselt number. The results for Nusselt numbers are reported in Tables 2.1 and 2.2 in Appendix A.2. The detailed analysis and results are given also in references [81], [91], [92] and [93].

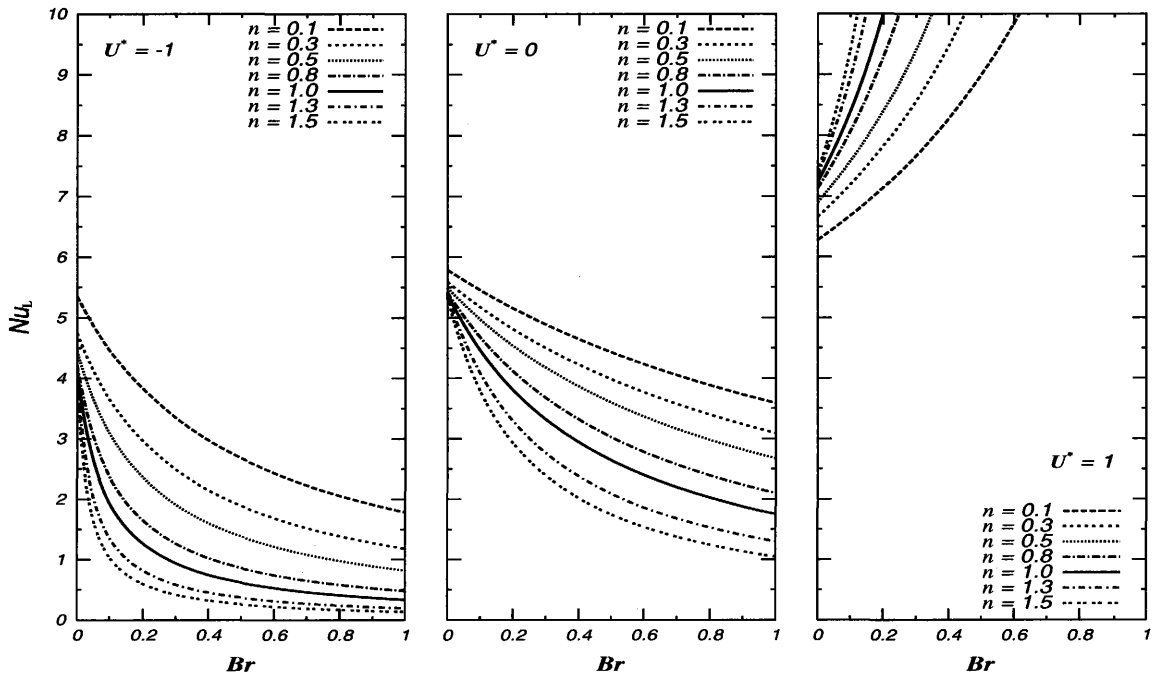

Fig.5-5 Nu vs Br for Case A (U^* = -1; 0 ; 1)

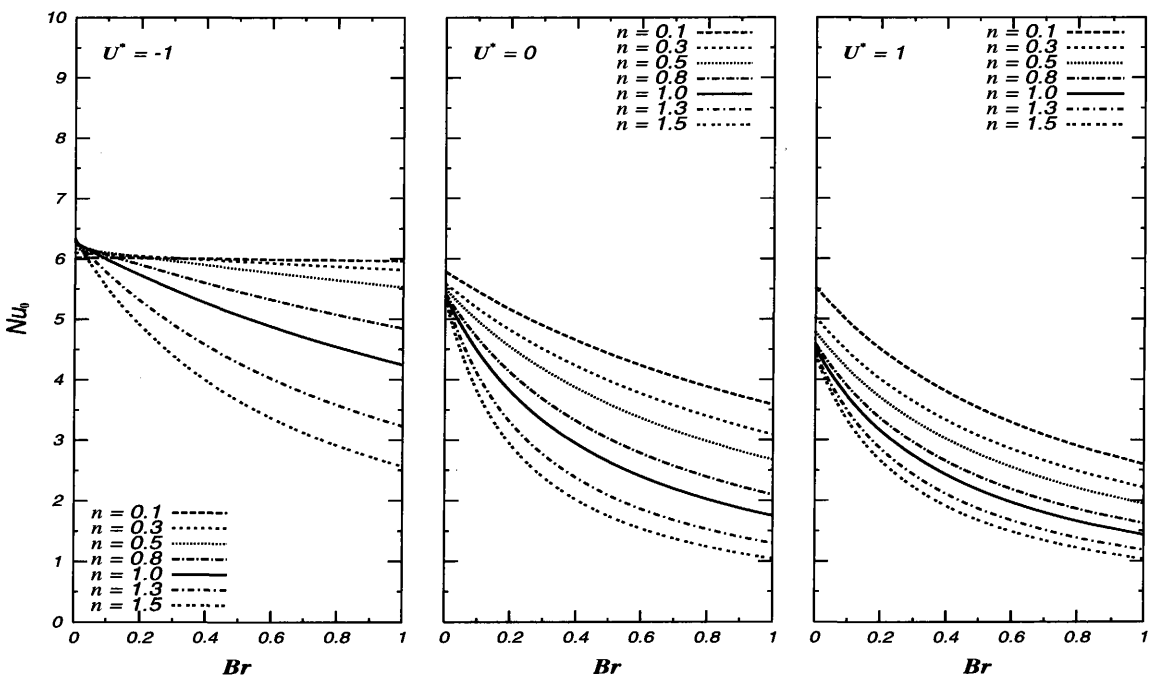

Fig.5-6 Nu vs Br for Case B (U^* = -1; 0; 1)

5.2.2 Modified Power-Law Model

In this section, the objective is to analyze the viscous dissipation effect on heat transfer in the fully developed plane Poiseuille-Couette flow of non-Newtonian fluids in which the shear stress is described by the modified power-law model. The advantage of applying the modified power-law model is discussed in Sections 3.1 and 3.4.2. Under the assumptions that the modified power-law fluid in parallel-plates is incompressible, has constant properties (k, ρ and c_p) and the flow is fully developed, the energy equation with the fully developed condition having constant wall heat flux is written as

$$k\frac{\partial^2 T}{\partial y^2} + \eta_a \left(\frac{du}{dy}\right)^2 = \rho c_\mathrm{p} u \frac{dT_\mathrm{b}}{dz}. \tag{5.24}$$

The following two types of the thermal boundary conditions are specified:

$$\textbf{Case A}: \quad \begin{cases} k\dfrac{\partial T}{\partial y} = 0 \quad \text{at} \quad y = 0 \\ k\dfrac{\partial T}{\partial y} = q_\mathrm{L} \quad \text{at} \quad y = L, \end{cases} \tag{5.25}$$

$$\textbf{Case B}: \quad \begin{cases} -k\dfrac{\partial T}{\partial y} = q_0 \quad \text{at} \quad y = 0 \\ k\dfrac{\partial T}{\partial y} = 0 \quad \text{at} \quad y = L \end{cases} \tag{5.26}$$

dT_b/dz in Eq.(5.24) is evaluated, from an energy balance, as

$$\frac{dT_\mathrm{b}}{dz} = \frac{q_j}{\rho c_\mathrm{p} u_\mathrm{m} L}\left[1 + \frac{\int_0^L \eta_a \left(\frac{du}{dy}\right)^2 dy}{q_j}\right] \tag{5.27}$$

Substitution of the above balance into Eq.(5.24) gives,

$$k\frac{\partial^2 T}{\partial y^2} + \eta_a \left(\frac{du}{dy}\right)^2 = \frac{2q_j u}{u_\mathrm{m} D_\mathrm{h}}\left[1 + \frac{\int_0^L \eta_a \left(\frac{du}{dy}\right)^2 dy}{q_j}\right] \tag{5.28}$$

By introducing the relevant dimensionless quantities, $\theta = Tk/(q_j D_\mathrm{h})$, $u^* = u/u_\mathrm{m}$, $y^* = y/D_\mathrm{h}$ and $z^* = z/(D_\mathrm{h} Pe)$, the above equation becomes

$$\frac{\partial^2 \theta}{\partial y^{*2}} = 2u^*\left(1 + \int_0^{0.5} V dy^*\right) - V \tag{5.29}$$

$$\textbf{Case A}: \quad \begin{cases} \dfrac{\partial \theta}{\partial y^*} = 0 \quad \text{at} \quad y^* = 0 \\ \dfrac{\partial \theta}{\partial y^*} = 1 \quad \text{at} \quad y^* = \dfrac{1}{2}, \end{cases} \tag{5.30}$$

$$\textbf{Case B}: \quad \begin{cases} \dfrac{\partial \theta}{\partial y^*} = -1 \quad \text{at} \quad y^* = 0 \\ \dfrac{\partial \theta}{\partial y^*} = 0 \quad \text{at} \quad y^* = \dfrac{1}{2} \end{cases} \tag{5.31}$$

where

$$V = Br\ \eta_a^* \left(\frac{du^*}{dy^*}\right)^2 \tag{5.32}$$

Brinkman number is

$$Br \equiv \frac{\eta\ u_{\mathrm{m}}^2}{D_{\mathrm{h}} q_j} \tag{5.33}$$

Nusselt number, Nu_j, is defined as

$$Nu_j \equiv \frac{[q_j/(T_j - T_{\mathrm{b}})]D_{\mathrm{h}}}{k} = \frac{1}{\theta_j - \theta_{\mathrm{b}}} \tag{5.34}$$

where dimensionless bulk temperature, θ_{b}, is defined as

$$\theta_{\mathrm{b}} \equiv T_{\mathrm{b}} k \big/ (q_j D_{\mathrm{h}}) \tag{5.35}$$

Temperature difference, $(\theta_j - \theta_{\mathrm{b}})$, is calculated as

$$\theta_j - \theta_{\mathrm{b}} = 2 \int_0^{1/2} u^* \left(\theta_j - \theta\right) dy^*. \tag{5.36}$$

Eq.(5.29) with Eqs.(5.30) and (5.31) has been solved by the finite difference method. Along the vertical axis, y^*, was divided evenly. The numerical values of the local Nusselt numbers that were calculated in this section are tabulated in Table 2.1 and 2.2 in Appendix A.2. To check the numerical method validity, the results corresponding to the Newtonian fluid and the power-law fluid are compared with the exact solutions obtained in the previous sections for the Newtonian and for the power-law fluids. Both solutions were in excellent agreement. Also to check the accuracy of the numerical solutions, our results for the Nusselt numbers corresponding to the Newtonian and power-law fluids for $Br = 0$ (negligible viscous dissipation) are compared with those presented by the previous researchers [11], [57], [76] and [94] in Tables 1.3 and 1.4 in Appendix A.1. The solutions are in excellent agreement within the error of 0.2%.

In the below some observations of the results for the different thermal boundary conditions are given.

Case A

In order to study the effect of the relative velocity and viscous dissipation on the heat transfer of different fluids, the calculation results for $(\theta - \theta_{\mathrm{b}})$ of Case A is shown in Fig.5-7 for U^* = -1, 0 and 1, and Brinkman number as a parameter. The

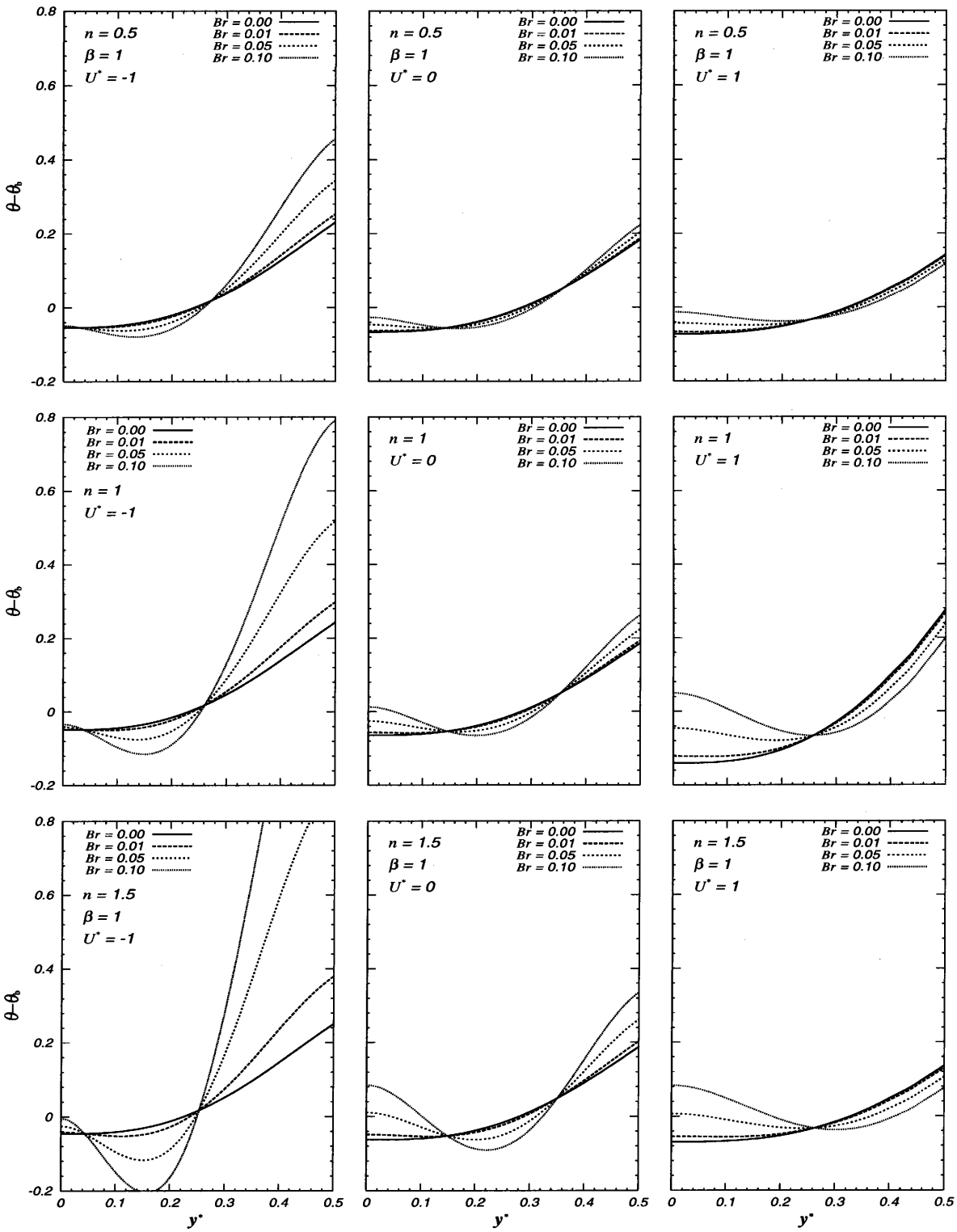

Fig.5-7 Dimensionless temperature difference for Case A

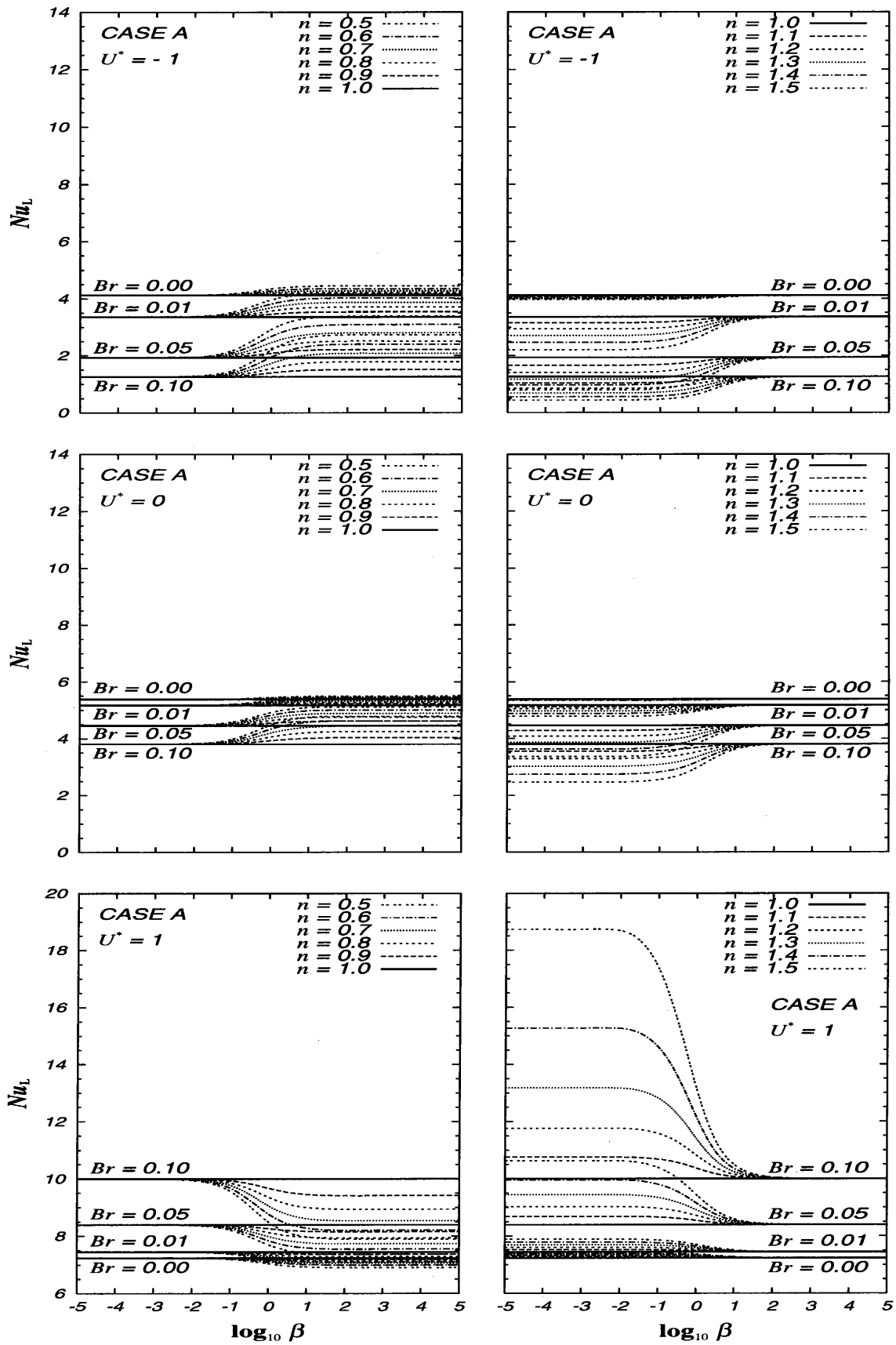

Fig.5-8 Nusselt numbers for Case A

case with U^* = -1 corresponds to an opposing flow, that is the plate moves to the opposite direction to the fluid flow. For $U^* = 0$, both of the plates are stationary. For $U^* = 1$, the flow is an aiding flow or the plate moves to the flow direction. In these figures the temperature difference, $(\theta - \theta_b)$, is shown as a function of dimensionless coordinate, y^*. The flow index n and dimensionless shear rate parameter β vary in these figures in a vertical direction having values of $n = 0.5$ and $\beta = 1$ in the first row, $n = 1$ in the second row and, $n = 1.5$ and $\beta = 1$ in the figures at the bottom. For U^* = -1 and $U^* = 0$, $(\theta - \theta_b)$ increases near the walls with an increase in Br and has a minimum value in the middle region of the channel. This is attributed to the heat generated by the viscous dissipation near the wall and large axial heat convection in the middle region as seen in Figs.3-12 and 3-13 (see Section 3.4.2). For the case of $U^* = 1$, $(\theta - \theta_b)$ increases with an increase in Br near the fixed wall. This is also owing to the heat generated by viscous dissipation near the fixed wall.

In Fig.5-8 the Nusselt number for Case A, Nu_L, is shown. Here Nusselt number at the heated wall is shown as a function of the dimensionless shear rate parameter, β. The relative velocity varies in these figures in a vertical direction having values -1, 0 and 1. The Brinkman number is the parameter on the curves having values 0, 0.01, 0.05 and 0.1. The left hand side figures show Nusselt number for the pseudoplastic fluids, while the right hand side ones are for the dilatant fluids. It can be observed in these figures that Nu_L decreases with an increase in Br for U^* = -1 and $U^* = 0$, but it increases with an increase in Br for $U^* = 1$. These behaviors of Nusselt numbers can be explained by the viscous dissipation effect on temperature difference $(\theta - \theta_b)$, as mentioned above.

Case B

In a similar means as done in Fig.5-7 the temperature differences, $(\theta - \theta_b)$, for Case B are shown in Fig.5-9. The figures in the middle column show the temperature difference for the case if the both plates are fixed, that is $U^* = 0$. The figures to the left correspond to the case of U^* = -1, that is an opposing flow and in such flows the plate moves to the opposite direction to the fluid flow. In opposing flows, it is seen that the temperature difference changes greatly with Br at the moving wall as it also was observed for Case A. But for Case B, this change is smaller than that for Case A. From these figures it can be observed that the effect of Br on the temperature difference is stronger for the dilatant fluid.

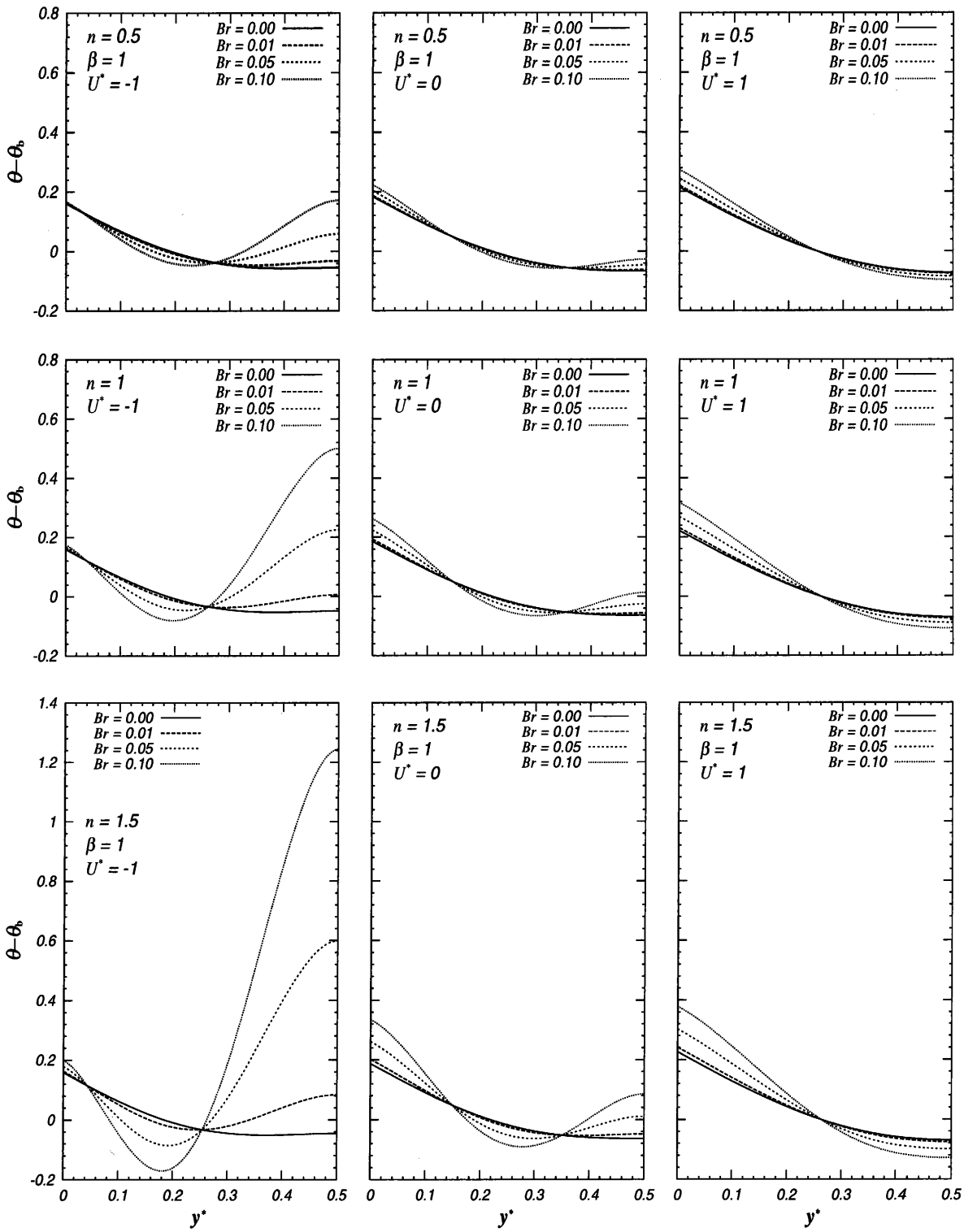

Fig.5-9 Dimensionless temperature difference for Case B

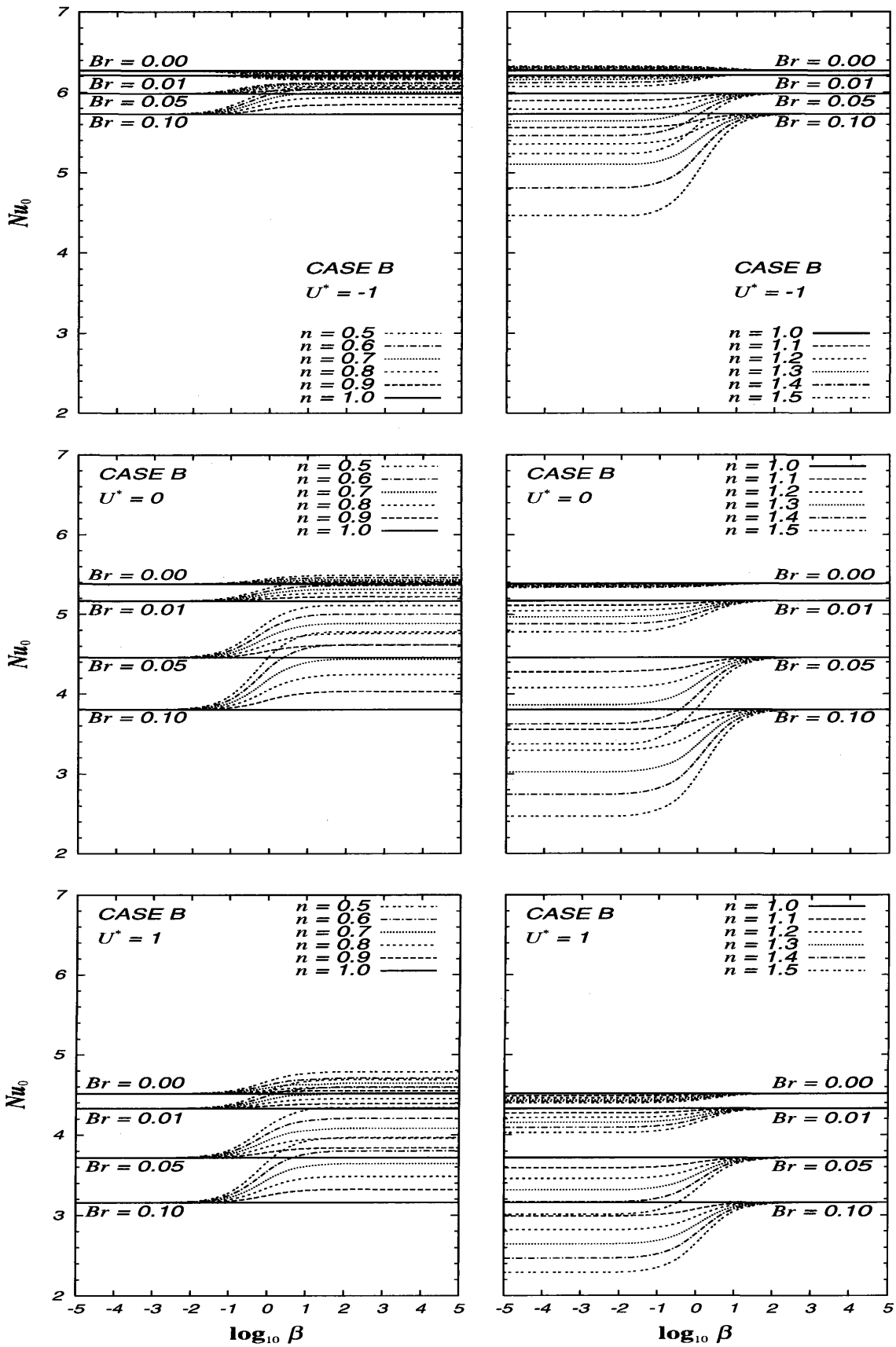

Fig.5-10 Nusselt numbers for Case B

In Fig.5-10, Nusselt number at the heated wall is shown for Case B. The means of depiction is same as done in Fig.5-8. Nu_0 decreases with an increase in Br for U^* = -1, 0 and 1. It is due to viscous dissipation near the walls. The bulk temperature always increases when viscous dissipation effects increase. With a decrease in relative velocity, U^*, the difference between the bulk temperature, θ_b, and the heated wall temperature, θ_0 (or the temperature difference at the heated wall) in Eq.(5.36) decreases and Nusselt number, Nu_0, increases. For the case of U^* = -1, it is seen that the relationship between Nu_0 and β is different for small values of Brinkman number ($Br = 0 \sim 0.01$) for both the pseudoplastic ($n < 1$) and dilatant ($1 < n$) fluids. It may be explained by how Br influences on the Nusselt number. It is seen from Fig.5-9, that for U^* = -1, the effect of Br on the difference between the bulk temperature and the heated wall temperature are slightly different from the cases of $U^* = 0$ and 1. For $U^* = 0$ and 1, Nusselt number, Nu_0, decreases with an increase flow index, n.

The detailed analysis and results are also given in references [83], [93] and [95] - [96].

5.3 Summary

The heat transfer for the thermally fully developed plane Poiseuille-Couette flow has been studied with the emphasis to the viscous dissipation effect. The heat transfer results have been obtained for the various values of the moving plate velocity and Brinkman number. The analytical method has been employed for all applicable situations and the exact solutions for the thermally developed flow of Newtonian and power-law fluids were acquired. For the modified power-law fluids the results were obtained by the numerical method.

The computed variations of the dimensionless temperature difference across the channel and Nusselt number are plotted in graphics and also tabulated. It was observed that, in the fully developed region the heat transfer rates in terms of Nusselt number at the heated wall depend on the relative velocity of the moving plate, the viscous dissipation degree and the boundary conditions.

The study showed that for equal conditions the following changes were observed in heating processes.

- The role of viscous dissipation in heat transfer depends on the relative velocity,

U^*.

- Heat transfer rate in terms of the Nusselt number at the heated moving wall (Case A) exhibits higher values with increasing Brinkman number for $U^* = 1$ and vice versa for $U^* = -1$.

- For the stationary wall heated case (Case B), Nusselt number decreases with an increase in Brinkman number for both aiding ($U^* > 0$) and opposing ($U^* < 0$) flows.

Chapter 6

CONCLUSIONS

This thesis deals with the study of the fluid flow and heat transfer for plane Poiseuille-Couette flow of non-Newtonian fluids. The research has yielded some new data that lead to a better understanding of the basic physical processes in heat transfer equipment associated with a moving surface. The aim of the present research was to provide a comprehensive treatment of the laminar heat transfer problems associated with moving boundary by clarifying the effects of viscous dissipation and fluid axial heat conduction.

Fluid Flow

The fluid flow analysis has been carried out for the non-Newtonian fluids in plane Poiseuille-Couette flow. The numerical study was performed for the steady, laminar, hydrodynamically fully developed flow of non-Newtonian fluids by employing the modified power-law model. In order to examine the numerically obtained results, the exact solutions for the plane Poiseuille-Couette flow of the Newtonian and power-law fluids were also obtained analytically for the wide range of the moving plate velocity.

The data on the flow fields of the plane Poiseuille-Couette flow of the modified power-law fluids have been obtained by solving the momentum equation. Wide range of parameters that exert the effect on the flow fields such as the relative velocity of the moving plate and the rheological parameters: the flow index and the dimensionless shear rate parameter were considered.

The behavior of the plotted velocity distribution across the channel implies the obvious distortion of the flow field due to the moving boundary. On comparing the predictions for the one wall moving case with those of the stationary walls case, I

found that the effect of the flow index on the fluid velocity field diminishes with an increase in the relative velocity of the moving wall if the fluid flows to the moving wall direction. If the fluid flows to the opposite direction of the moving wall, the fluid velocity profiles are strongly affected by the flow index. On account of the behavior of the curves for the friction factor, it is noted that the friction factor decreases with increasing values of the relative velocity.

Heat Transfer

The study for the heat transfer to the plane Poiseuille-Couette flow of non-Newtonian fluids with an emphasis to the effects of viscous dissipation and fluid axial heat conduction was directed at the numerical calculation of an elliptic type differential equation that governs the heat transfer problem. The proposed numerical method (the mesh system) was found to produce consistent results for thermally developing heat transfer problems.

The obtained solutions hopefully enable to evaluate the effects of the viscous dissipation and the fluid axial heat conduction quantitatively in a design problem related with heat transfer occurring in a system with a moving boundary.

It was found that the role of the viscous dissipation effect on heat transfer is completely different in a parallel plates channel depending on the surface movement for the case of one surface insulated with the other heated constantly. It is noteworthy that for different thermal boundary conditions, both the viscous dissipation and the fluid axial heat conduction show different effects in the forced convection. These results imply that at least in some cases, the analysis of laminar heat transfer associated with moving surface cannot be correctly performed by neglecting the effects of viscous dissipation and fluid axial heat conduction.

If, in order to neglect the effects of the viscous dissipation and the fluid axial heat conduction, Brinkman number is set to zero and Peclet number is set to infinity in the energy equation, then it was seen that the resulting analysis for the Newtonian fluid agrees excellently with that in references [11] and [4].

A comparison between the Nusselt numbers at the heated wall as the wall is being stationary and moving, shows that the Nusselt number value corresponding to the moving wall is larger. This was observed for the all considered boundary conditions and, for the cases of considerable and negligible effects of the viscous dissipation and fluid axial heat conduction, regardless the fluid unless the fluid flows to the moving

plate direction. A general conclusion that may be drawn from the study is the fact that, the heat transfer rate, expressed in terms of Nusselt number, at the moving heated surface is higher than at the stationary heated surface if the fluid flows to the same direction of the heated surface.

ACKNOWLEDGEMENT

I am grateful for a great deal of support in doing this research, but specially to my academic supervisor, Professor Toru SHIGECHI. I am gratefully acknowledge him for providing me the guidance and support at every stage of the research. He has been a constant source of encouragement and providing points and comments those were most essential for the research results I have obtained. He has took time to read and correct the significant parts of this thesis, as well as all other published papers.

I would like to express my sincere thanks to the members of the dissertation committee, Professor Yoshio KODAMA, Professor Masahiro ISHIDA and Associate Professor Satoru MOMOKI for giving their time to evaluate my thesis and suggesting valuable improvements.

I am also indebted to our laboratory research associate Mr. Takashi YAMADA. He helped in many things, including administrative matters of school.

I would like to thank to our laboratory technical officer Mr. Yoshitaka KUSUMOTO. He has always been kind.

It is with particular pleasure that I express my deeply-felt gratitude to the Japanese Ministry of Education, Culture, Sports, Science and Technology (Monbu Kagaku Sho) that made me able to study in Japan and financially supported to do this research.

My research could not have been completed without the assistance of many other individuals, undergraduate students, master and doctor students in our laboratory who created a very relaxed and happy environment for me to work in. I would also like to thank my many laboratory colleagues over the last 5 years who each supported my efforts in different ways.

I am also very grateful to my friends Mr. Maaninou NABIL (Morocco), Mr. Kazuhiro NAKAYAMA (Japan), Mr. Igor GILOWSKI (Poland), Mr. Jamal Tariq MAIN (Pakistan), Mr. Addepalli M.KRISHNA (India) and Mr. Akihiro NAKANO

(Japan) for having lots of fun together in Nagasaki.

I would like to offer special thanks to Mr. Nicolaas HART and his wife Kiyoko HART, Mr. Masanobu ITOH and his family, Associate Professor Keiko MORIYAMA, Mr. Keisuke OHBA and his family, and many others those have been sharing friendship and providing encouragement and hospitality.

Finally, and most importantly, I want to express my thanks and gratitude to my family members, my wife Odgerel JAMBAL, my son Bayasgalan GANBAT and Javkhlan GANBAT for their emotional support, patience, love and care. My special thanks are extended to my wife, for her continuous support and encouragement during all this effort and for her help on proofreading during the period of her busy study in doctor course. I would like to grasp this opportunity to express my sincere gratitude to my father Davaa TSERENCHUMBA and to my mother Maam SOSOR whose love, care and kindness are always in my memory.

APPENDICES

A. Tables

A.1 Comparisons with the Available Data

Table 1.1 Comparison of fRe_{M} for Newtonian fluids (U^* = -1, 0 and 1)

References	U^*		
	-1	0	1
Shah & London [11]^{an}	-	24.00	-
Etemad et al. [57]^{nu}	-	23.88	-
Capobianchi & Irvine [76]^{nu}	-	24.00	-
Shigechi & Lee [3]^{nu}	36.00	24.00	12.00
Present work	36.00	24.00	12.00

^{an} - Analytical solutions

^{nu} - Numerical results

Table 1.2 Comparison of fRe_{M} for power law fluids ($U^* = 0$)

n	Etemad et al. [57]^{nu}	Capobianchi & Irvine [76]^{nu}	Present work
0.5	7.99	8.00	8.00
0.6	-	10.02	10.02
0.7	-	12.51	12.50
0.8	-	15.57	15.57
0.9	-	19.34	19.34
1.0	23.88	24.00	24.00
1.1	-	29.74	29.75
1.2	-	36.83	36.84
1.3	-	45.57	45.58
1.4	-	56.35	56.37
1.5	-	69.65	69.67

^{nu} - Numerical results

Table 1.3 Comparison of Nusselt numbers for Newtonian fluids, $Br = 0$, (The 2nd kind T.B.C.)

References	Nusselt number	U^*		
		-1	0	1
Shah & London [11]^{an}	Nu_L	-	5.385	-
Etemad et al. [57]^{nu}	Nu_L	-	5.3856	-
Capobianchi & Irvine [76]^{nu}	Nu_L	-	5.387	-
Lungberg et al. [94]^{nu}	Nu_L	-	5.384	-
Shigechi & Lee [3]^{nu}	Nu_L	6.27	5.38	4.52
	Nu_0	4.12	5.38	7.24
Present work	Nu_L	6.269	5.385	4.516
	Nu_0	4.118	5.385	7.241

^{an} - Analytical solutions

^{nu} - Numerical results

Table 1.4 Comparison of Nusselt numbers for power law fluids, $U^* = 0$ and $Br = 0$, (The 2nd kind T.B.C.)

n	Capobianchi & Irvine [76]^{nu}	Present work
0.5	5.496	5.492
0.6	5.464	5.460
0.7	5.439	5.436
0.8	5.418	5.416
0.9	5.402	5.399
1.0	5.387	5.385
1.1	5.375	5.373
1.2	5.365	5.362
1.3	5.355	5.353
1.4	5.347	5.345
1.5	5.340	5.338

^{nu} - Numerical results

A.2 Numerical Values of Nusselt Numbers

Table 2.1 Fully developed Nusselt numbers for Case A (The second kind T.B.C.)

			Nu_L										
			n										
U^*	Br	Fluid	0.5	0.6	0.7	0.8	0.9	1.0	1.1	1.2	1.3	1.4	1.5
-1	0.00	N						4.118					
		MPL	4.343	4.270	4.215	4.173	4.141	4.118	4.096	4.071	4.046	4.020	3.996
		PL	4.450	4.353	4.276	4.214	4.162	4.118	4.080	4.048	4.019	3.994	3.972
	0.01	N						3.359					
		MPL	3.956	3.816	3.688	3.569	3.460	3.359	3.255	3.131	2.987	2.822	2.639
		PL	4.187	4.026	3.870	3.710	3.541	3.359	3.160	2.943	2.709	2.461	2.204
	0.05	N						1.934					
		MPL	2.917	2.677	2.457	2.260	2.086	1.934	1.787	1.627	1.459	1.288	1.119
		PL	3.387	3.095	2.804	2.510	2.219	1.934	1.661	1.407	1.176	0.971	0.793
	0.10	N						1.264					
		MPL	2.196	1.949	1.734	1.550	1.394	1.264	1.143	1.017	0.890	0.767	0.650
		PL	2.734	2.401	2.085	1.788	1.513	1.264	1.043	0.852	0.689	0.553	0.440
0	0.00	N						5.385					
		MPL	5.449	5.429	5.413	5.400	5.391	5.385	5.378	5.369	5.362	5.354	5.347
		PL	5.492	5.460	5.436	5.416	5.399	5.385	5.373	5.362	5.353	5.345	5.338
	0.01	N						5.170					
		MPL	5.333	5.295	5.261	5.228	5.198	5.170	5.140	5.104	5.062	5.013	4.956
		PL	5.411	5.362	5.316	5.270	5.222	5.170	5.112	5.046	4.970	4.882	4.781
	0.05	N						4.459					
		MPL	4.916	4.821	4.728	4.636	4.547	4.459	4.369	4.262	4.138	3.996	3.834
		PL	5.110	5.003	4.887	4.760	4.618	4.459	4.280	4.082	3.864	3.627	3.373
	0.10	N						3.804					
		MPL	4.477	4.336	4.197	4.061	3.931	3.804	3.680	3.533	3.369	3.187	2.989
		PL	4.779	4.616	4.440	4.246	4.034	3.804	3.557	3.295	3.023	2.744	2.465

N - Newtonian
PL - Power law
MPL - Modified power law ($\beta = 1$)

continued (Case A)

			Nu_L										
U^*	Br	Fluid	n										
			0.5	0.6	0.7	0.8	0.9	1.0	1.1	1.2	1.3	1.4	1.5
1	0.00	N	7.241										
		MPL	7.043	7.100	7.146	7.184	7.215	7.241	7.264	7.290	7.315	7.341	7.369
		PL	6.905	6.995	7.072	7.137	7.193	7.241	7.284	7.322	7.356	7.386	7.414
	0.01	N	7.447										
		MPL	7.166	7.238	7.301	7.355	7.403	7.447	7.488	7.536	7.587	7.644	7.707
		PL	6.993	7.100	7.196	7.284	7.366	7.447	7.527	7.609	7.696	7.788	7.890
	0.05	N	8.400										
		MPL	7.704	7.850	7.992	8.130	8.265	8.400	8.542	8.720	8.915	9.158	9.451
		PL	7.368	7.552	7.739	7.937	8.154	8.400	8.686	9.025	9.440	9.958	10.62
	0.10	N	10.00										
		MPL	8.502	8.778	9.064	9.362	9.674	10.00	10.37	10.83	11.41	12.17	13.18
		PL	7.899	8.204	8.544	8.939	9.413	10.00	10.75	11.76	13.17	15.28	18.73

N - Newtonian, PL - Power law, MPL - Modified power law ($\beta = 1$)

Table 2.2 Fully developed Nusselt numbers for Case B (The second kind T.B.C.)

			Nu_0										
U^*	Br	Fluid	n										
			0.5	0.6	0.7	0.8	0.9	1.0	1.1	1.2	1.3	1.4	1.5
-1	0.00	N	6.269										
		MPL	6.189	6.214	6.233	6.248	6.259	6.269	6.276	6.285	6.294	6.304	6.313
		PL	6.169	6.195	6.217	6.237	6.254	6.269	6.282	6.294	6.304	6.314	6.323
	0.01	N	6.209										
		MPL	6.171	6.189	6.201	6.208	6.210	6.209	6.207	6.202	6.193	6.178	6.156
		PL	6.159	6.180	6.195	6.206	6.211	6.209	6.201	6.186	6.160	6.123	6.071
	0.05	N	5.983										
		MPL	6.100	6.093	6.076	6.051	6.020	5.983	5.945	5.890	5.817	5.721	5.599
		PL	6.119	6.120	6.109	6.084	6.043	5.983	5.899	5.788	5.643	5.461	5.237
	0.10	N	5.722										
		MPL	6.014	5.977	5.927	5.866	5.799	5.722	5.648	5.543	5.408	5.236	5.029
		PL	6.070	6.047	6.004	5.939	5.847	5.722	5.560	5.357	5.107	4.811	4.469

N - Newtonian, PL - Power law, MPL - Modified power law ($\beta = 1$)

continued (Case B)

			Nu_0										
			n										
U^*	Br	Fluid	0.5	0.6	0.7	0.8	0.9	1.0	1.1	1.2	1.3	1.4	1.5
0	0.00	N						5.385					
		MPL	5.449	5.429	5.413	5.400	5.391	5.385	5.378	5.369	5.362	5.354	5.347
		PL	5.492	5.460	5.436	5.416	5.399	5.385	5.373	5.362	5.353	5.345	5.338
	0.01	N						5.170					
		MPL	5.333	5.295	5.261	5.228	5.198	5.170	5.140	5.104	5.062	5.013	4.956
		PL	5.411	5.362	5.316	5.270	5.222	5.170	5.112	5.046	4.970	4.882	4.781
	0.05	N						4.459					
		MPL	4.916	4.821	4.728	4.636	4.547	4.459	4.369	4.262	4.138	3.996	3.834
		PL	5.110	5.003	4.887	4.760	4.618	4.459	4.280	4.082	3.864	3.627	3.373
	0.10	N						3.804					
		MPL	4.477	4.336	4.197	4.061	3.931	3.804	3.680	3.533	3.369	3.187	2.989
		PL	4.779	4.616	4.440	4.246	4.034	3.804	3.557	3.295	3.023	2.744	2.465
1	0.00	N						4.516					
		MPL	4.667	4.622	4.586	4.557	4.534	4.516	4.499	4.482	4.463	4.446	4.428
		PL	4.787	4.708	4.645	4.594	4.552	4.516	4.486	4.460	4.437	4.417	4.399
	0.01	N						4.330					
		MPL	4.542	4.485	4.437	4.396	4.361	4.330	4.299	4.266	4.229	4.190	4.148
		PL	4.690	4.598	4.520	4.452	4.389	4.330	4.272	4.214	4.155	4.093	4.028
	0.05	N						3.717					
		MPL	4.103	4.012	3.929	3.853	3.783	3.717	3.651	3.577	3.495	3.407	3.310
		PL	4.339	4.207	4.083	3.962	3.841	3.717	3.588	3.454	3.314	3.166	3.012
	0.10	N						3.158					
		MPL	3.661	3.545	3.437	3.338	3.245	3.158	3.071	2.976	2.873	2.761	2.642
		PL	3.967	3.802	3.642	3.483	3.322	3.158	2.990	2.819	2.644	2.468	2.290

N - Newtonian
PL - Power law
MPL - Modified power law ($\beta = 1$)

B. Analytical Results

B.1 Heat Transfer of Newtonian Fluids (The second kind thermal boundary condition)

Nusselt numbers, Nu_{L} and Nu_0, for the Newtonian fluids.

Case A: constant heat flux at the moving plate with the stationary plate insulated

$$Nu_{\mathrm{L}} = \frac{70}{13\left(1 - \frac{11}{39}U^* + \frac{1}{39}U^{*2}\right) + 6Br\,(3 - U^*)^2\left(1 - \frac{23}{9}U^* + \frac{4}{9}U^{*2}\right)} \tag{B.1}$$

From Eq.(B.1), the following two limiting Nusselt numbers are obtained:

$$Nu_{\mathrm{L}} = \frac{70}{13\left(1 + \frac{54}{13}Br\right)} \qquad \text{for} \qquad U^* = 0 \tag{B.2}$$

$$Nu_{\mathrm{L}} = \frac{70}{13\left(1 - \frac{11}{39}U^* + \frac{1}{39}U^{*2}\right)} \qquad \text{for} \qquad Br = 0 \tag{B.3}$$

Case B: constant heat flux at the stationary plate with the moving plate insulated

$$Nu_0 = \frac{70}{13\left(1 + \frac{1}{6}U^* + \frac{1}{39}U^{*2}\right) + 6Br\,(3 - U^*)^2\left(1 + \frac{2}{3}U^*\right)^2} \tag{B.4}$$

From Eq.(B.4), the following two limiting Nusselt numbers are obtained:

$$Nu_0 = \frac{70}{13\left(1 + \frac{54}{13}Br\right)} \qquad \text{for} \qquad U^* = 0 \tag{B.5}$$

$$Nu_0 = \frac{70}{13\left(1 + \frac{1}{6}U^* + \frac{1}{39}U^{*2}\right)} \qquad \text{for} \qquad Br = 0 \tag{B.6}$$

B.2 Heat Transfer of Power Law Fluids (The second kind thermal boundary condition)

Nusselt numbers, Nu_{L} and Nu_0, for the power law fluids.

Case A with Pattern I

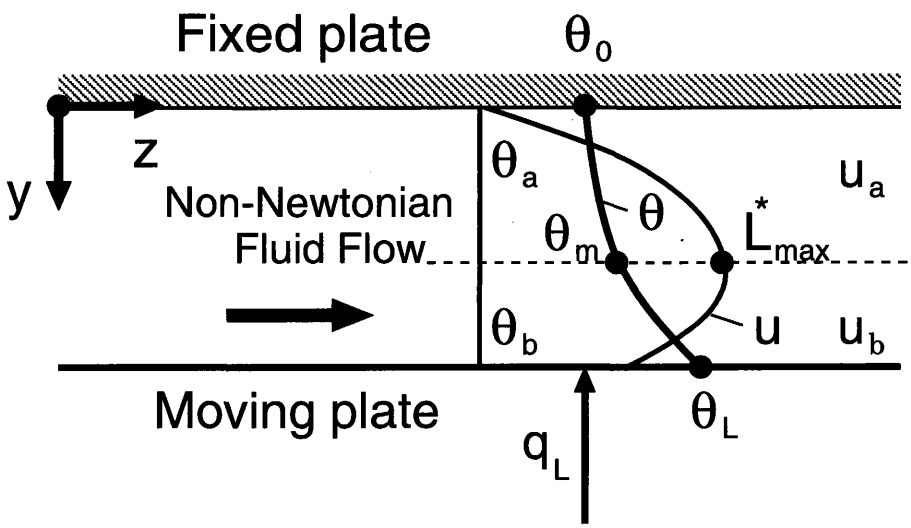

Fig.B-1 Physical model for Case A (Pattern I)

$$\theta_{\mathrm{L}} - \theta_{\mathrm{b}} = 2\int_0^{\frac{1}{2}} u^* \left(\theta_{\mathrm{L}} - \theta\right) dy^* = -2\left[\int_0^{L^*_{max}} u^*_a \left(\theta_a - \theta_{\mathrm{L}}\right) dy^* + \int_{L^*_{max}}^{\frac{1}{2}} u^*_b \left(\theta_b - \theta_{\mathrm{L}}\right) dy^*\right] \tag{B.7}$$

Integrating Eq.(B.7), we have

$$\theta_{\mathrm{L}} - \theta_{\mathrm{b}} = -2\left(\frac{n}{n+1}\right) F^{\frac{1}{n}} \left[S_{\mathrm{L1}} + S_{\mathrm{L2}}\right] \tag{B.8}$$

where S_{L1} and S_{L2} are

$$\begin{aligned} S_{\mathrm{L1}} &= -\left(\frac{n+1}{2n+1}\right)\left(\frac{1}{2} - L^*_{max}\right) L^{*\frac{2n+1}{n}}_{max} - \frac{1}{2}\left(\frac{1}{2} - L^*_{max}\right)^2 L^{*\frac{n+1}{n}}_{max} \\ &+ \frac{n^2}{(2n+1)(3n+1)}\left(\frac{1}{2} - L^*_{max}\right)^{\frac{3n+1}{n}} + 2F^{\frac{1}{n}} D_{\mathrm{L1}} \end{aligned} \tag{B.9}$$

$$S_{\mathrm{L2}} = 2BrF^{\frac{n+1}{n}}\left[\left\{\frac{1}{2} - \left(\frac{1}{2} - L^*_{max}\right) U^*\right\} D_{\mathrm{L1}} + \frac{D_{\mathrm{L2}}}{2}\right] \tag{B.10}$$

D_{L1} and D_{L2} are

$$
\begin{aligned}
D_{\mathrm{L1}} = & \left(\frac{n}{n+1}\right)\left[-\frac{(n+1)^2(9n+2)}{3(3n+1)(4n+1)(5n+2)}L_{max}^{*\frac{5n+2}{n}}\right. \\
& + \frac{1}{2}\left(\frac{n+1}{2n+1}\right)\left(\frac{1}{2}-L_{max}^{*}\right)^{2} L_{max}^{*\frac{3n+2}{n}} + \frac{1}{6}\left(\frac{1}{2}-L_{max}^{*}\right)^{3} L_{max}^{*\frac{2n+2}{n}} \\
& - \frac{n(n+1)}{(2n+1)(3n+1)}\left(\frac{1}{2}-L_{max}^{*}\right)^{\frac{3n+1}{n}} L_{max}^{*\frac{2n+1}{n}} \\
& - \frac{n\left(8n^2+5n+1\right)}{2(2n+1)(3n+1)(4n+1)}\left(\frac{1}{2}-L_{max}^{*}\right)^{\frac{4n+1}{n}} L_{max}^{*\frac{n+1}{n}} \\
& \left. + \frac{n^3}{(2n+1)(3n+1)(5n+2)}\left(\frac{1}{2}-L_{max}^{*}\right)^{\frac{5n+2}{n}}\right]
\end{aligned}
\tag{B.11}
$$

$$
\begin{aligned}
D_{\mathrm{L2}} = & \left(\frac{n}{2n+1}\right)\left[\frac{(n+1)(2n+1)(9n+2)}{2(3n+1)(4n+1)(5n+2)}L_{max}^{*\frac{5n+2}{n}}\right. \\
& - \left(\frac{n+1}{3n+1}\right)\left(\frac{1}{2}-L_{max}^{*}\right)^{\frac{3n+1}{n}} L_{max}^{*\frac{2n+1}{n}} \\
& - \frac{1}{2}\left(\frac{2n+1}{4n+1}\right)\left(\frac{1}{2}-L_{max}^{*}\right)^{\frac{4n+1}{n}} L_{max}^{*\frac{n+1}{n}} \\
& \left. + \frac{n^2}{(3n+1)(5n+2)}\left(\frac{1}{2}-L_{max}^{*}\right)^{\frac{5n+2}{n}}\right]
\end{aligned}
\tag{B.12}
$$

Nusselt number on the moving plate, Nu_{L}, is obtained as

$$
Nu_{\mathrm{L}} = \frac{1}{\theta_{\mathrm{L}} - \theta_{\mathrm{b}}} \tag{B.13}
$$

Case B with Pattern I

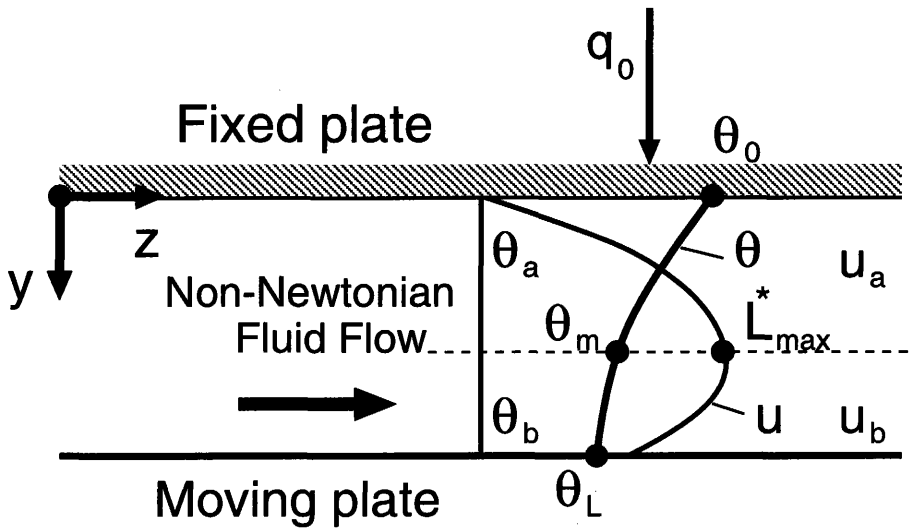

Fig.B-2 Physical model for Case B (Pattern I)

$$\theta_0 - \theta_b = 2\int_0^{\frac{1}{2}} u^*\left(\theta_0 - \theta\right) dy^* = -2\left[\int_0^{L^*_{max}} u^*_a\left(\theta_a - \theta_0\right) dy^* + \int_{L^*_{max}}^{\frac{1}{2}} u^*_b\left(\theta_b - \theta_0\right) dy^*\right] \quad \text{(B.14)}$$

Integrating Eq.(B.14), we have

$$\theta_0 - \theta_b = -2\left(\frac{n}{n+1}\right) F^{\frac{1}{n}}\left[S_{01} + S_{02}\right] \quad \text{(B.15)}$$

where S_{01} and S_{02} are

$$\begin{aligned} S_{01} &= -\frac{(n+1)(4n+1)}{2(2n+1)(3n+1)} L^{*\frac{3n+1}{n}}_{max} - \left(\frac{1}{2} - L^*_{max}\right) L^{*\frac{2n+1}{n}}_{max} \\ &+ \left(\frac{n}{2n+1}\right)\left(\frac{1}{2} - L^*_{max}\right)^{\frac{2n+1}{n}} L^*_{max} + 2F^{\frac{1}{n}} D_{01} \end{aligned} \quad \text{(B.16)}$$

$$S_{02} = 2BrF^{\frac{n+1}{n}}\left[\left\{\frac{1}{2} - \left(\frac{1}{2} - L^*_{max}\right) U^*\right\} D_{01} + \frac{D_{02}}{2}\right] \quad \text{(B.17)}$$

D_{01} and D_{01} are

$$\begin{aligned} D_{01} &= \left(\frac{n}{n+1}\right)\left[\frac{24n^4 + 61n^3 + 52n^2 + 17n + 2}{6(2n+1)(3n+1)(4n+1)(5n+2)} L^{*\frac{5n+2}{n}}_{max}\right. \\ &+ \frac{n+1}{2(3n+1)}\left(\frac{1}{2} - L^*_{max}\right) L^{*\frac{4n+2}{n}}_{max} - \frac{1}{3}\left(\frac{1}{2} - L^*_{max}\right)^3 L^{*\frac{2n+2}{n}}_{max} \\ &- \frac{n(n+1)}{2(2n+1)(3n+1)}\left(\frac{1}{2} - L^*_{max}\right)^{\frac{2n+1}{n}} L^{*\frac{3n+1}{n}}_{max} \end{aligned}$$

$$+ \frac{n(10n^2+7n+1)}{(2n+1)(3n+1)(4n+1)}\left(\frac{1}{2}-L^*_{max}\right)^{\frac{4n+1}{n}} L^{*\frac{n+1}{n}}_{max}$$

$$- \frac{2n^2}{(3n+1)(5n+2)}\left(\frac{1}{2}-L^*_{max}\right)^{\frac{5n+2}{n}}\Bigg] \tag{B.18}$$

$$D_{02} = \left(\frac{n}{2n+1}\right)\Bigg[-\frac{(22n^3+35n^2+15n+2)}{2(3n+1)(4n+1)(5n+2)} L^{*\frac{5n+2}{n}}_{max}$$

$$- \left(\frac{2n+1}{3n+1}\right)\left(\frac{1}{2}-L^*_{max}\right) L^{*\frac{4n+2}{n}}_{max}$$

$$+ \left(\frac{n}{3n+1}\right)\left(\frac{1}{2}-L^*_{max}\right)^{\frac{2n+1}{n}} L^{*\frac{3n+1}{n}}_{max}$$

$$+ \frac{10n^2+7n+1}{2(3n+1)(4n+1)}\left(\frac{1}{2}-L^*_{max}\right)^{\frac{4n+1}{n}} L^{*\frac{n+1}{n}}_{max}$$

$$- \frac{2n(2n+1)}{(3n+1)(5n+2)}\left(\frac{1}{2}-L^*_{max}\right)^{\frac{5n+2}{n}}\Bigg] \tag{B.19}$$

Nusselt number on the fixed plate, Nu_0, is obtained as

$$Nu_0 = \frac{1}{\theta_0 - \theta_b} \tag{B.20}$$

Bibliography

[1] T.Shigechi, N.Kawae and Y.Lee, *Turbulent fluid flow and heat transfer in concentric annuli with moving cores*, Int.J.Heat Mass Transfer, Vol.33, No.9, 2029-2037 (1990)

[2] Y.Lee and T.Shigechi, *Heat transfer in concentric annuli with moving cores -fully developed turbulent flow with arbitrarily prescribed heat flux*, Int.J.Heat Mass Transfer, Vol.35, No.12, 3488-3493 (1992)

[3] T.Shigechi, and Y.Lee, *An analysis on fully developed laminar fluid flow and heat transfer in concentric annuli with moving cores*, Int.J.Heat Mass Transfer, Vol.34, No.10, 2593-2601 (1991)

[4] T.Shigechi, K.Araki and Y.Lee, *Laminar heat transfer in the thermal entrance regions of concentric annuli with moving heated cores*, Trans. ASME, J.Heat Transfer, Vol.115, No.4, 1061-1064 (1993);
K.Araki, *Laminar heat transfer in annuli*, Department of Mechanical Systems Engineering, Nagasaki University, Master Thesis, (1991)

[5] T.Shigechi, S.Momoki and Y.Lee, *Fully developed laminar flow and heat transfer in an eccentric annulus with an axially moving core*, Trans. ASME, J.Heat Transfer, Vol.118, No.1, 205-209 (1996)

[6] R.P.Chhabra and J.F.Richardson, *Non-Newtonian Flow in the Process Industries*, Butterworth Heinemann, Oxford, (1999)

[7] S.Kakac, R.K.Shah and W.Aung, *Handbook of Single-Phase Convective Heat Transfer*, Wiley, New York, (1987)

[8] M.V.Karwe and Y.Jaluria, *Thermal transport from a heated moving surface*, Trans. ASME, J.Heat Transfer, Vol.108, 728-733 (1986)

[9] B.H.Kang, Y.Jaluria and M.V.Karwe, *Numerical simulation of conjugate transport from a continuous moving plate in materials processing*, Numerical Heat Transfer, Part A, Vol.19, 151-176 (1991)

[10] M.V.Karwe and Y.Jaluria, *Fluid flow and mixed convection transport from a moving plate in rolling and extrusion processes*, Trans. ASME, J.Heat Transfer, Vol.110, 655-661 (1988)

[11] R.K.Shah and A.L.London, *Laminar Flow Forced Convection in Ducts*, Advances in Heat Transfer, Supplement 1, Academic Press, New York, (1978)

[12] D.E.Bourne and H.Dixon, *The cooling of fibres in the formation process*, Int.J.Heat and Mass Transfer, Vol.24, 1323-1332 (1971)

[13] N.Afzal and I.S.Varshney, *The cooling of a low heat resistance stretching sheet moving through a fluid*, Wärme-und Stoffübertragung, Vol.14, 289-293 (1980)

[14] A.Moutsoglou and A.K.Bhattacharya, *Laminar and turbulent boundary layers on moving, nonisothermal continuous flat surfaces*, Trans. ASME, J.Heat Transfer, Vol.104, 707-714 (1982)

[15] T.A.Abdelhafez, *Skin friction and heat transfer on a continuous flat surface moving in a parallel free stream*, Int.J.Heat and Mass Transfer, Vol.28, No.6, 1234-1237 (1985)

[16] P.R.Chappidi and F.S.Gunnerson, *Analysis of heat and momentum transport along a moving surface*, Int.J.Heat and Mass Transfer, Vol.32, No.7, 1383-1386 (1989)

[17] M.V.Karwe and Y.Jaluria, *Experimental investigation of thermal transport from a heated moving plate*, Int.J.Heat and Mass Transfer, Vol.35, No.2, 493-511 (1992)

[18] M.V.A.Bianchi and R.Viskanta, *Momentum and heat transfer on a continuous flat surface moving in a parallel counterflow free stream*, Wärme-und Stoffübertragung, Vol.29, 89-94 (1993)

[19] P.Gospodinov and V.Roussinov, *Nonlinear instability during the isothermal draw of optical fibers*, Int.J.Multiphase Flow, Vol.19, No.6, 1153-1158 (1993)

[20] B.H.Kang, J.Yoo and Y.Jaluria, *Experimental study of the convective cooling of a heated continuously moving material*, Trans. ASME, J.Heat Transfer, Vol.116, 199-208 (1994)

[21] H.T.Lin and S.F.Huang, *Flow and heat transfer of plane surfaces moving in parallel and reversely to the free stream*, Int.J.Heat Mass Transfer, Vol.37, No.2, 333-336 (1994)

[22] S.R.Choudhury, Y.Jaluria, T.Vaskopulos and C.E.Polymeropoulos, *Forced convective cooling of optical fiber during drawing process*, Trans. ASME, J.Heat Transfer, Vol.116, 790-794 (1994)

[23] S.R.Choudhury and Y.Jaluria, *Analytical solution for the transient temperature distribution in a moving rod or plate of finite length with surface heat transfer*, Int.J.Heat and Mass Transfer, Vol.37, No.8, 1193-1205 (1994)

[24] T.Vaskopulos, C.Polymeropoulos and A.Zebib, *Cooling of optical fiber in aiding and opposing forced gas flow*, Int.J.Heat and Mass Transfer, Vol.38, No.11, 1933-1944 (1995)

[25] T.Sastrohartono, Y.Jaluria, M.Esseghir and V.Sernas, *A numerical and experimental study of three-dimensional transport in the channel of an extruder for polymetric materials*, Int.J.Heat and Mass Transfer, Vol.38, No.11, 1957-1973 (1995)

[26] R.Viskanta, *Heat Transfer From Continuously Moving Materials: An Overview of Selected Thermal Processing Problems*, in J.S. Lee, S.H. Chung and K.H. Kim (eds.), Transport Phenomena in Thermal Engineering, Begell House, Inc., New York, Vol.2, 779-788 (1993)

[27] A.S.El-Ariny and A.Aziz, *A Numerical solution of entrance region heat transfer in plane Couette flow*, Trans. ASME, J.Heat Transfer, Vol.98, No.3, 427-431 (1976)

[28] S.H.Lin, *Heat transfer to plane non-Newtonian Couette flow*, Int.J.Heat and Mass Transfer, Vol.22, No.7, 1117-1123 (1979)

[29] S.H.Lin and D.M.Hsieh, *Heat transfer to generalized Couette flow of a non-Newtonian fluid in annuli with moving inner cylinder*, Trans. ASME, J.Heat Transfer, Vol.102, No.4, 786-789 (1980)

[30] S.H.Lin, *Heat transfer to generalized non-Newtonian Couette flow in annuli with moving outer cylinder*, Int.J.Heat and Mass Transfer, Vol.35, No.11, 3069-3075 (1992)

[31] J.L.Hudson and S.G.Bankoff, *Heat transfer to a steady Couette flow with pressure gradient*, Chemical Engineering Science, Vol.20, 415-423 (1965)

[32] J.Šesták and F.Rieger, *Laminar heat transfer to a study Couette flow between parallel plates*, Int.J.Heat and Mass Transfer, Vol.12, No.1, 71-80 (1969)

[33] E.J.Davis and W.N.Gill, *The effects of axial conduction in the wall on heat transfer with laminar flow*, Int.J.Heat and Mass Transfer, Vol.13, No.3, 459-470 (1970)

[34] E.J.Davis, *Exact solutions for a class of heat and mass transfer problems*, The Canadian Journal of Chemical Engineering, Vol.51, 562-572 (1973)

[35] H.H.Winter, *The unsteady temperature field in plane Couette flow*, Int.J.Heat and Mass Transfer, Vol.14, No.8, 1203-1212 (1971)

[36] S.Bruin, *Temperature distributions in Couette flow with and without additional pressure gradient*, Int.J.Heat and Mass Transfer, Vol.15, No.3, 341-349 (1972)

[37] P.Payvar and P.Majumdar, *Heat transfer to flow between parallel plates of finite length induced by motion of one wall*, Proc. Fundamentals of forced convection heat transfer, HTD-Vol.210, ASME, 35-41 (1992)

[38] B.H.Kang and Y.Jaluria, *Heat transfer from continuously moving material in channel flow for thermal processing*, Journal of Thermophysics and Heat Transfer, Vol.8, No.3, 546-554 (1994)

[39] S.R.Choudhury and Y.Jaluria, *Forced convective heat transfer from a continuously moving cylindrical rod undergoung thermal processing*, Proc. Heat Transfer in Materials Processing, HTD-Vol.224, ASME, 43-50 (1992)

[40] A.Lawal and D.M.Kalyon, *Nonisothermal extrusion flow of viscoplastic fluids with wall slip*, Int.J.Heat and Mass Transfer, Vol.40, No.16, 3883-3897 (1997)

[41] S.Syrjälä, *Numerical study of fully developed non-Newtonian fluid flow and heat transfer in a rectangular channel with a moving wall*, J.Int.Comm.Heat and Mass Transfer, Vol.24, No1, 11-25 (1997)

[42] Y.Demirel, *Thermodynamic analysis of thermomechanical coupling in Couette flow*, Int.J.Heat and Mass Transfer, Vol.43, No.22, 4205-4212 (2000)

[43] C.A.Deavours, *An exact solution for the temperature distribution in parallel plate Poiseuille flow*, Trans. ASME, J.Heat Transfer, Vol.96, No.4, 489-495 (1974)

[44] R.C.LeCroy and A.H.Eraslan, *The solution of temperature development in the entrance region of an MHD Channel by the B.G.Galerkin Method*, Trans. ASME, J.Heat Transfer, Vol.91, No.2, 212-220 (1969)

[45] V.D.Dang, *Low Peclet number heat transfer for power law non-Newtonian fluid with heat generation*, Journal of Applied Polymer Science, Vol.23, 3077-3103 (1979)

[46] V.D.Dang, *Heat transfer of power law fluid at low Peclet number flow*, Trans. ASME, J.Heat Transfer, Vol.105, 542-549 (1983)

[47] C.T.Liou and F.S.Wang, *Solutions to the extended Graetz problem for a power-model fluid with viscous dissipation and different entrance boundary conditions*, Numerical Heat Transfer, Part A, Vol.17, 91-108 (1990)

[48] J.Lahjomri, A.Oubarra and A.Alemany, *Heat transfer by laminar Hartmann flow in thermal entrance region with a step change in wall temperatures: the Graetz problem extended*, Int.J.Heat and Mass Transfer, Vol.45, No.5, 1127-1148 (2002)

[49] T.Min, J.Y.Yoo and H.Choi, *Laminar convective heat transfer of a Bingham plastic in a circular pipe-I. Analytical approach-thermally fully developed flow and thermally developing flow (the Graetz problem extended)*, Int.J.Heat and Mass Transfer, Vol.40, No.13, 3025-3037 (1997)

[50] T.Min and J.Y.Yoo, *Laminar convective heat transfer of a Bingham plastic in a circular pipe with uniform wall heat flux: The Graetz problem extended*, Trans. ASME, J.Heat Transfer, Vol.121, 556-563 (1999)

[51] D.A.Nield, A.V.Kuznetsov and M.Xiong, *Thermally developing forced convection in a porous medium: parallel plate channel with walls at uniform temperature, with axial conduction and viscous dissipation effects*, Int.J.Heat and Mass Transfer, Vol.46, No.4, 643-651 (2003)

[52] D.Wei and Z.Zhang, *Decay estimates of heat transfer to melton polymer flow in pipes with viscous dissipation*, Electronic Journal of Differential Equations, Vol.2001, No.39, 1-14 (2001)

[53] C.L.Hwang, P.J.Knieper and L.T.Fan, *Effects of viscous dissipation on heat transfer parameters for flow between parallel plates*, Z.angew. Math.Phys., Vol.16, 599-610 (1965)

[54] J.Ou and K.C.Cheng, *Effects of pressure work and viscous dissipation on Graetz problem for gas flows in parallel-plate channels*, Wärme-und Stoffübertragung, Vol.6, 191-198 (1973)

[55] J.Vlachopoulos and C.K.J.Keung, *Heat transfer to a power-law fluid flowing between parallel plates*, AIChE J, Vol.18, No.6, 1272-1274 (1972)

[56] S.H.Lin and W.K.Hsu, *Heat transfer to power-law non-Newtonian flow between parallel plates*, Trans. ASME, J.Heat Transfer, Vol.102, No.2, 382-384 (1980)

[57] S.Gh.Etemad, A.S.Mujumdar and B.Huang, *Viscous dissipation effects in entrance region heat transfer for a power law fluid flowing between parallel plates*, Int.J.Heat and Fluid Flow, Vol.15, No.2, 122-131 (1994)

[58] R.M.Cotta and M.N.Özisik, *Laminar forced convection to non-Newtonian fluids in ducts with prescribed wall heat flux*, J.Int.Comm.Heat Mass Transfer, Vol.13, 325-334 (1986)

[59] R.M.Cotta and M.N.Özisik, *Laminar forced convection of power-law non-Newtonian fluids inside ducts*, Wärme-und Stoffübertragung, Vol.20, 211-218 (1986)

[60] A.Barlette, *Fully developed laminar forced convection in circular ducts for power-law fluids with viscous dissipation*, Int.J.Heat Mass Transfer, Vol.40, No.1, 15-26 (1997)

[61] T.V.Nguyen, *Laminar Heat transfer for thermally developing flow in ducts*, Int.J.Heat Mass Transfer, Vol.35, No.7, 1733-1741 (1992)

[62] A.S.Telles, E.M.Queiroz and G.E.Filho, *Solutions of the extended Graetz problem*, Int.J.Heat and Mass Transfer, Vol.44, No.2, 471-483 (2001)

[63] A.S.Jones, *Two-dimensional adiabatic forced convection at low Peclet number*, Appl.Sci.Res., Vol.25, 337-348 (1972)

[64] C.A.Deavours, *Laminar heat transfer in parallel plate flow*, Appl.Sci.Res., Vol.29, 69-76 (1974)

[65] H.C.Agrawal, *Heat transfer in laminar flow between parallel plates at small Peclet numbers*, Appl.Sci.Res., Sect.A, Vol.9, 177-189 (1960)

[66] S.Pahor and J.Strnad, *A note on heat tranfer in laminar flow through a gap*, Appl.Sci.Res., Sect.A, Vol.10, 81-84 (1961)

[67] F.W.Schmidt and B.Zeldin, *Laminar heat transfer in the entrance region of ducts*, Appl.Sci.Res., Vol.23, 73-94 (1970)

[68] C.J.Hsu, *An exact analysis of low Peclet number thermal entry region heat transfer in transversely nonuniform velocity fields*, AICh Journal, Vol.17, 732-740 (1971)

[69] Y.Taitel and A.Tamir, *Application of the integral method to flows with axial diffusion*, Int.J.Heat and Mass Transfer, Vol.15, 733-740 (1972)

[70] J.Lahjomri and A.Oubarra, *Analytical solution of the Graetz problem with axial conduction*, Trans. ASME, J.Heat Transfer, Vol.121, 1078-1083 (1999)

[71] B.Weigand, M.Kanzamar and H.Beer, *The extended Graetz problem with piecewise constant wall heat flux for pipe and channel flows*, Int.J.Heat and Mass Transfer, Vol.44, 3941-3952 (2001)

[72] S.Olek, *Heat transfer in duct flow of non-Newtonian fluids with axial conduction*, J.Int.Comm.Heat and Mass Transfer, Vol.25, No7, 929-938 (1998)

[73] R.B.Bird, W.E.Stewart and E.N.Lightfoot, *Transport phenomena*, New York, John Wiley & Sons, Inc., (1960)

[74] J.E.Dunleavy and S.Middleman, *Relation of shear behavior of solutions of polyisobutylene*, Trans. Soc. Rheol., Vol.10, 151-168 (1966)

[75] R.A.Brewster and T.F.Irvine, *Similitude considerations in laminar flow of modified power law fluids in circular ducts*, Wärme-und Stoffübertragung, Vol.21, 83-86 (1987)

[76] M.Capobianchi and T.F.Irvine, *Predictions of pressure drop and heat transfer in concentric annular ducts with modified power law fluids*, Wärme-und Stoffübertragung, Vol.27, 209-215 (1992)

[77] W.C.Luelf and L.C.Burmeister, *Viscous dissipation effect on pressure gradient for laminar flow of a non-Newtonian liquid through a duct of subfreezing wall temperature*, Trans. ASME, J.Heat Transfer, Vol.118, No.4, 973-977 (1996)

[78] H.W.Cox and C.W.Macosko, *Viscous dissipation in die flows*, AIChE J., Vol.20, No.4, 785-795 (1974)

[79] H.H.Winter, *Viscous dissipation in shear flows of molten polymers*, Advances in Heat Transfer, Academic Press, New York, Vol.13, 205-267 (1977)

[80] T.Shigechi, S.Momoki and G.Davaa, *Effect of viscous dissipation on fully developed heat transfer of plane Couette-Poiseuille laminar flow*, Reports of the Faculty of Engineering, Nagasaki University, Vol.29, No.53, 153-156 (1999)

[81] G.Davaa, *Fluid flow and heat transfer of non-Newtonian fluids in parallel-plates*, Department of Mechanical Systems Engineering, Nagasaki University, Master Thesis, (2000)

[82] G.Davaa, T.Shigechi and S.Momoki, *Plane Couette-Poiseuille flow of power-law non-Newtonian fluids*, Reports of the Faculty of Engineering, Nagasaki University, Vol.30, No.54, 29-36 (2000)

[83] G.Davaa, T.Shigechi S.Momoki and O.Jambal, *Fluid flow and heat transfer to modified power law fluids in plane Couette-Poiseuille laminar flow between parallel plates*, Reports of the Faculty of Engineering, Nagasaki University, Vol.31, No.57, 31-39 (2001)

[84] R.E.Lungberg, W.C.Reynolds and W.M.Kays, *Heat transfer with laminar flow in concentric annuli with constant and variable wall temperature with heat flux*, NASA Technical Note D-1972, Washington (1963)

[85] R.E.Fuller and M.R.Samuels, *Simultaneous development of the velocity and temperature fields in the entry region of an annulus*, Chemical Engineering Progress Symposium Series, Vol.67, No.113, 71-77 (1971)

[86] F.H.Verhoff and D.P.Fisher, *A numerical solution of the Graetz problem with axial conduction included*, Trans. ASME, Journal of Heat Transfer, Vol.95, 132-134 (1973)

[87] H.C.Ku and D.Hatziavramidis, *Chebyshev expansion methods for the solution of the extended Graetz problem*, Journal of Computational Physics, Vol.56, 495-512 (1984)

[88] A.Campo and J.C.Auguste, *Axial heat conduction in laminar pipe flows with nonlinear wall heat fluxes*, Int.J.Heat and Mass Transfer, Vol.21, 1597-1607 (1978)

[89] G.Davaa, T.Shigechi, S.Momoki and O.Jambal, *Effects of viscous dissipation and fluid axial heat conduction on laminar heat transfer in ducts with constant wall temperature (Part I: Parallel-plates duct)*, Reports of the Faculty of Engineering, Nagasaki University, Vol.33, No.61, 17-24 (2003)

[90] T.Shigechi, G.Davaa, S.Momoki and O.Jambal, *Laminar heat transfer with viscous dissipation and fluid axial heat conduction for modified power law fluids flowing in parallel plates with one plate moving*, JSME, International Journal, Series B, Vol.46, No.4, 1-10 (2003)

[91] G.Davaa, T.Shigechi and S.Momoki, *Effect of viscous dissipation on fully developed laminar heat transfer of power-law non-Newtonian fluids in plane Couette-Poiseuille flow*, Reports of the Faculty of Engineering, Nagasaki University, Vol.30, No.55, 97-104 (2000)

[92] G.Davaa, T.Shigechi, S.Momoki and T.Yamaguchi, *Heat transfer to power law fluids in plane Couette-Poiseuille laminar flow between parallel plates*, Proc. of the 4th JSME-KSME Thermal Engineering Conference, Vol.1, 481-486, (October 1-6, 2000), Kobe, JAPAN

[93] G.Davaa, T.Shigechi and S.Momoki, *Effect of viscous dissipation on fully developed heat transfer of non-Newtonian fluids in plane laminar Poiseuille-Couette flow*, International Communications in Heat and Mass Transfer, Vol.30, (2003) (in press)

[94] R.E.Lungberg, P.A.McCuen and W.C.Reynolds, *Heat transfer in annular passages. Hydrodynamically developed laminar flow with arbitrarily prescribed*

wall temperatures or heat fluxes, Int.J.Heat and Mass Transfer, Vol.6, 495-529 (1963)

[95] G.Davaa, T.Shigechi and S.Momoki, *Fully developed heat transfer of modified power-law fluids in plane laminar Couette-Poiseuille flow between parallel plates*, (in Japanese) Proc. of the 38th National Heat Transfer Symposium of Japan, Vol.I, 3-4, (May 23-25, 2001), Saitama, Japan

[96] G.Davaa, T.Shigechi, S.Momoki and O.Jambal, *Heat transfer to modified power law fluids in plane Couette-Poiseuille laminar flow between parallel plates with constant heat flux at the fixed wall*, Reports of the Faculty of Engineering, Nagasaki University, Vol.32, No.58, 75-82 (2002)